Effect of Frequency on Crack Propagation in CPVC and HDPE at different Temperatures

By

SHAIKH FARRUKH SAGHIR

A Thesis presented to the

DEANSHIP OF GRADUATE STUDIES

In Partial Fulfillment of the Requirements
for the degree

MASTER OF SCIENCE

IN

MECHANICAL ENGINEERING

KING FAHD UNIVERSITY
OF PETROLEUM AND MINERALS

Dhahran, Saudi Arabia

January 2004

KING FAHD UNIVERSITY OF PETROLEUM AND MINERALS
DHAHRAN 31261, SAUDI ARABIA

DEANSHIP OF GRADUATE STUDIES

This thesis, written by **SHAIKH FARRUKH SAGHIR** under the direction of his Thesis Advisor and approved by his Thesis Committee, has been presented to and accepted by the Dean of Graduate Studies, in partial fulfillment of the requirements for the degree of **MASTER OF SCIENCE IN MECHANICAL ENGINEERING.**

Thesis Committee

_____
Dr. Nesar Merah (Advisor)

_____
Dr. Zafarullah Khan (Member)

_____
Dr. Khaled Mezghani (Member)

_____
Dr. Faleh Al-.Sulaiman
Department Chairman

_____
Prof. Osama A. Jannadi
Dean of Graduate Studies

_____
Date

Dedicated to My Beloved Parents and Family Members whose constant prayers, sacrifice and inspiration led to this wonderful accomplishment

ACKNOWLEDGEMENTS

First and foremost, all praise to Allah *subhana-wa-ta'ala* for bestowing me with health, knowledge and patience to complete this work The Almighty, Who alone made this accomplishment possible. I seek His mercy, favor and forgiveness.

Acknowledgements are due to King Fahd University of Petroleum & Minerals for the support in carrying out this research.

I acknowledge, with deep gratitude and appreciation, the inspiration, encouragement, remarkable assistance and continuous support given to me by my thesis advisor, Dr. Nesar Merah. His guidance and assistance changed my thinking from pessimistic to optimistic one. I greatly appreciate dedication, attention and patience provided by him throughout the course of this study. Working with him was an opportunity of great learning and experience. Thanks are due to my thesis committee members, Dr. Zafarullah Khan and Dr. Khaled Mezghani for their constructive guidance, technical support and also for giving permissions to work in the advanced materials science lab (AMSL) and materials science lab (MSL) respectively.

I appreciate the assistance and encouragement received from Chairman ME Department, Dr. Faleh Al-Sulaiman for giving permission to work in after hours in the AMSL.

The technical support and help provided by Engr. Mr. Zainulabdeen in conducting experimental work in AMSL is highly appreciated. The sincere and untiring efforts by him in preparing the experimental program and set-ups utilized in this study are also

highly acknowledged. Both of us enriched every day spent at AMSL in a way which is difficult to encompass in words.

I owe very deep appreciations to Dr. Anwar Khaleel Shaikh, Director ME workshop and other staff of the ME workshop for their prompt and timely help and technical advice in specimen preparation. Thanks are also due to the laboratory personnel, Mr. Saleh Al-Abbas, Mr. Lateef Hashmi, Mr. Othman Al-Thubaiti, and Mr. Habib who assisted me in the experimental work and the Department Secretaries, Mr. Lateef and Mr.Jameel for their help and assistance.

Special thanks are due to my senior colleagues at the University, Sayyad Zahid, Mujtaba Hussain, Syed Imran, Salman Gaffar, Abdul Baseer, Ghulam Arshed, Jalal Shah, Omer Farooq, and Mohammad Ahsan who were always there to help me in my work. I am indebted to my friends Tayyab, Khusro, Iftikhar, Bilal, Hasan, Mujahid, Khaleel, Qaiyum, Basha, Saad, Gayazullah, Hafeez, Kabir, Khaleeq, Nazim, Jameel, Haseeb, Atif, Humayun and Samiullah for their encouragement and support throughout my stay at KFUPM. Notable mentions go to my friends at North Compound and Building 92 & 93. I am also thankful to all those who ever came to me for Da'waa and Tableegh.

Last but not the least I am grateful to my parents, brother, brother-in-law and sister for their extreme moral support, encouragement and patience during the course of my studies at KFUPM as well as throughout my academic career. No personal development can ever take place without the proper guidance of parents. This work is dedicated to my parents for their constant prayers and never ending love.

TABLE OF CONTENTS

LIST OF FIGURES

LIST OF TABLES

NOMENCLATURE

A	Paris power law coefficient (y-intercept on crack growth curve)
a	Crack length (m)
a_o	Initial crack length
a_f	Final crack length
B	Specimen thickness
da/dN	Crack growth rate (m/cycle)
E	Elastic modulus (MPa)
E_d	Dynamic elastic modulus (MPa)
e	Elongation (mm)
G	Shear modulus (MPa)
ΔH	Activation energy (KJ/mol)
ΔK	Stress intensity factor range (MPa$\sqrt{m}$)
m	Paris power law exponent (slope of crack growth curve)
N	Number of applied cycles (cycles)
N_i	Initiation life (cycles)
N_p	Propagation life (cycles)
N_f	Number of cycles to failure
r	Stress ratio ($\sigma_{min}/\sigma_{max}$)
R	Universal gas constant (8.32 J/K/mol)
T	Temperature (^oC or K)
W	Specimen width (m)
V	Activation volume (nm^3)
$\Delta\sigma$	Applied stress range (MPa)
σ_{min}	Minimum stress (MPa)
σ_{max}	Maximum Stress (MPa)
σ_m	Mean stress (MPa)
σ_a	Stress amplitude (MPa)

σ_{ys}	Yield strength (MPa)
σ_{yd}	Dynamic yield strength (MPa)
$\in$	Strain rate (s^{-1})
ε_y	Yield strain
ε_f	Fracture strain
τ	Shear stress (MPa)

LIST OF ABBREVATIONS

ABS	Acrylo butadiene styrene
COD	Crack opening displacement (m)
CPVC	Chlorinated poly vinylchloreide
CTOD	Crack tip opening displacement
FCG	Fatigue crack growth
FCP	Fatigue crack propagation
HDPE	High density polyethylene
HIPS	High impact polystyrene
PA	Poly acetal
PAS	Poly arylsulfone
PBT	Poly butylene terephthalate
PC	Poly carbonate
PE	Poly ethylene
PEEK	Poly etherether ketone
PEI	Poly etherimide
PEK-C	Phenol phthalein Poly ether ketone
PET	Poly ethylene terethphthalate
PMMA	Poly methylmethacrylate
POX	Poly oxy methylene
PP	Poly propylene
PPS	Poly phenylenesulfide
PS	Poly styrene
PSF	Poly sulfone
PVA	Poly vinylalcohol
PVC	Poly vinylchloride
T_g	Glass transition temperature
TPX	Poly 4-methyl-1-pentene
uPVC	unPlasticized PVC
LEFM	Linear Elastic Fracture Mechanics

THESIS ABSTRACT

NAME: **SHAIKH FARRUKH SAGHIR**

TITLE: **EFFECT OF FREQUENCY ON CRACK PROPAGATION IN CPVC AND HDPE AT DIFFERENT TEMPERATURES**

DEPARTMENT: **MECHANICAL ENGINEERING**

DATE: **6 JANAURY, 2004**

Since nowadays polymers are being used increasingly for load bearing industrial applications, understanding the fatigue process in these materials is very necessary and essential. For application of linear elastic fracture mechanics (LEFM) to polymers, it is necessary to recognize potential pitfalls caused by their viscoelastic behavior, i.e. stress-strain dependence on time (or frequency) and temperature. Due to their viscoelastic nature, the fatigue crack propagation (FCP) behavior of most polymers is sensitive to test variables such as cyclic frequency and temperature. In this study, Fatigue crack propagation in Cholorinated polyvinyl chloride (CPVC) pipefittings and high density polyethylene (HDPE) pipes are investigated over the frequency and temperature ranges of 0.1-10Hz and –10-70^{o}C, respectively. Monotonic tests are also performed on both materials for different temperatures, and their result shows decrease in yield stress with increase in temperature.

FCP tests were conducted on single edged notched specimens (SEN), prepared from CPVC pipefittings and HDPE pipes. A servo controlled electro hydraulic materials testing system was used for the fatigue testing. Crack growth was monitored optically by using the long distance traveling microscope with video camera system. The crack growth rate (da/dN) and stress intensity factor (ΔK) gave satisfactory correlation at all temperatures and frequencies. The fatigue crack growth resistance was found to increase with increasing frequency, and decrease with increasing temperature. Crazing was found to be the dominant fatigue mechanism, especially at (50^{o} C and 70^{o} C), while shear yielding was the dominant mechanism at (-10^{o}, 0^{o} and 23^{o} C). The da/dN-ΔK master curves for CPVC and HDPE were developed for different frequencies based on the modified mechanical properties at different temperatures. Microscopic examination of the fracture surfaces is also performed. Comparison of the fatigue surfaces obtained at different temperatures and frequencies gives useful information on the fatigue fracture mechanisms operative at these temperatures and frequencies.

MASTER OF SCIENCE DEGREE

KING FAHD UNIVERSITY OF PETROLEUM AND MINERALS

Dhahran, Saudi Arabia

رسالة الماجستير

الاسم : شيخ فرّخ صغير

العنوان: تأثير التردد على تقدم التشقق في (CPVC) و (HDPE) عند درجات حرارة مختلفة

قسم : الهندسة الميكانيكية

التاريخ: 6- يناير -2004

مع التزايد في استخدام البوليميرات في مجال تحمل الإجهادات في الصناعة, فان فهم عملية الحمل المتذبذب في هذه المواد امر هام وضروري. من ناحية تطبيقات ميكانيكا الكسر الخطي المرن للبولميرات(LEFM), فإنه من الضروري فهم المشاكل التي تنشأ بسبب السلوك اللزج المرن للمادة, الذي يعرف بأنه منحني الاجهاد-الإنفعال مع تغير الزمن, او التردد أو درجة الحرارة. بسبب الطبيعة اللزجة المرنة للبوليمرات, فان تقدم تشقق التعب(FCP) لمعظم البولميرات يكون حساس جدا لمتغيرات الفحص مثل التردد الدوري و درجة الحرارة. في هذه الدراسة, سيتم فحص تقدم تشقق التعبي وصلات الكلورايد البولي فينيل المكلور(CPVC) وأنابيب البولي إثيلين(DPEH) عالية الكثافة ضمن مجال التردد ودرجة الحرارة من 0.1-10هرتز و 10-70 درجة حرارة مئوية. أيضا أجريت عدة فحوصات على كلا المادتين لعدة درجات حرارة, و النتائج أظهرت تناقص في إجهاد الخضوع مع إزدياد الحرارة.

كماأجريت فحوصات(FCP) على حافة عينة محززة (SEM) حضرت من وصلات(CPVC) وأنابيب(HDPE). ايضا إستخدمت ألة فحص كهربائية هيدروليكية ذات تحكم سيرفو مخصص لفحص التعب و تمت مراقبة نمو التشقق بصريا باستخدام مكبر ذو انزياح مسافات طويلة مع الة تصوير فيديو. معدل نمو التشقق و عامل كثافة الإجهاد ($da/dN-\Delta K$) أعطيا نتائج متوافقة عند كل درجات الحرارة والترددات. في هذة الدراسة وجد ان مقاومة نمو تشقق التعب تزداد بازدياد التردد وتتناقص بازدياد درجة الحرارة. وقد ظهر أن اللدانة هي الية التعب السائدة, خاصة عند(50 و 70) درجة مئوية , بينما خضوع القص كان هو السائد عند (-10 و 23) درجة مئوية. منحنى ال $da/dN-\Delta K$ ل (CPVC) و (HDPE) طور من أجل ترددات مختلفة بالإعتماد على خواص ميكانيكية متغيرة عند درجات حرارة مختلفة. كما أجريت فحوصات مجهرية وتمت مقارنة سطح التعب الذي حصلنا عليه عند درجات حرارة وترددات مختلفة وأعطت معلومات مفيدة عن الية كسر التعب عند تلك الدرجات والترددات .

هذه الدراسة اعدت لنيل درجة الماجستير في العلوم
في جامعة الملك فهد للبترول والمعادن
الظهران 31261
المملكة العربية السعودية

CHAPTER 1

INTRODUCTION

1.1 Polymers

A polymer is a material whose molecules contain a very large number of atoms linked by covalent bonds, these molecules are in the form of long and flexible chains. Polymers consist mainly of identical or similar units joined together. The unit forming the repetitive pattern is called a "mer" or "monomer" (figure 1.1). Usually the biggest differences in polymer properties result from how the atoms and chains are linked together in space. Polymers that have a 1-D structure will have different properties than those that have either a 2-D or 3-D structure. There is a temperature, or range of temperatures, below which an amorphous polymer is in a glassy state and above which it is rubbery. This temperature is called the glass transition temperature, T_g, and it characterizes the amorphous phase. It is especially useful since all polymers are amorphous to some degree, they all have a T_g [1].

Polymers are a very important class of materials. Polymers occur naturally in the form of proteins, cellulose (plants), starch (food) and natural rubber. Engineering polymers, however, are usually synthetic polymers. The field of synthetic polymers or plastics is currently one of the fastest growing materials industries. The interest in engineering polymers is driven by their manufacturability, recyclability, mechanical

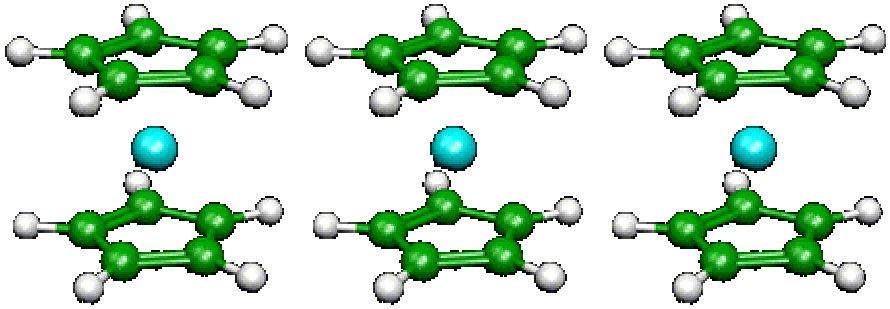

Figure 1.1 Mer or “Monomer”.

properties, and lower cost as compared to many alloys and ceramics. Also the macromolecular structure of synthetic polymers provides good biocompatibility and allows them to perform many biomimetic tasks that cannot be performed by other synthetic materials, which include drug delivery, use as grafts for arteries and veins and use in artificial tendons, ligaments and joints.

1.2 Chlorinated Polyvinyl Chloride (CPVC)

One of the important polymer Chlorinated Polyvinyl Chloride (CPVC) is produced by post chlorination of Polyvinyl chloride (PVC). It has been used in a variety of applications in a number of Industries. The objective of adding more chlorine to a PVC molecule is to raise the glass transition temperature (T_g) of the base resin from 95^o C to the 115-135 ^{o} C range. Chlorine also improves physical and mechanical properties of PVC [2]. The effect of chlorine addition on some physical and mechanical properties is shown in Table 1.1. Data for PVC is provided for comparison.

PVC belongs to the family of vinyl polymers (polymers made from vinyl monomers; that is small molecules containing carbon-carbon double bonds) and is produced by addition polymerization process. After the completion of the process, more chlorine is introduced into the bulk material. The chlorination of PVC is a free radical process, catalyzed by heat, ultraviolet radiation and radical initiators. Chlorine molecule Cl_2 splits into two free radicals $\{Cl^-\}$ under the application of energy. One free radical joins the PVC monomer by replacing one H atom to form CPVC. The other free radical combines with H atom to form HCl [3]. All the monomers in the PVC chain are not chlorinated, usually every fifth or sixth monomer is chlorinated. This done by controlling the quantity of chlorine.

Table 1.1 Physical and Mechanical properties of CPVC and PVC.

Property (@ 23 ^{o}C)	CPVC		PVC
	Irfan [8]	Data from Supplier	Data from Supplier
Yield Stress (MPa)	52	55	48
Elastic Modulus(GPa)	2.80	2.50	2.75
Poisson's Ratio	-	0.27	0.38
Compressive Strength (MPa)	-	70	66
Flexural Strength (MPa)	-	104	88
Impact Strength (ft-lb$_f$/in)	-	1.50	0.65
Max. Operating Temp. (^{o}C)	-	93	60
Glass Transition Temp. (^{o}C)	-	115-135	90
Specific Gravity	1.55	1.55	1.42

This is also desirable because high chlorine content deteriorates the mechanical properties of the product by making it brittle. For optimum results, Chlorine is kept up to 56.5% by weight.

CPVC offers a blend of corrosion resistance, mechanical strength and low installation cost for diverse applications including pulp and paper, metal treating, fertilizer production, ore benefaction, pollution control and wastewater treatment. Traditional applications of CPVC compound are hot and cold water distribution piping and fittings, as well as industrial pipe fittings and valves that can handle liquid chemicals. CPVC pipes can withstand pressures up to 1.40 MPa as compared to 0.95 MPa for PVC at 50^{o} C [2,4]. New technology has allowed the extrusion of CPVC into window glazing beads, cooling tower fill, automotive interior parts, waste-disposal devices, business machines covers, telecommunication equipment and appliance parts. A recent development is specialized CPVC pipe and fitting compounds for fire-sprinkler systems.

Major Applications of CPVC require service at non-ambient conditions. Thus, the investigation of temperature and frequency effects on the mechanical behavior of CPVC is very essential.

1.3 Polyethylene

High density polyethylene is produced by polymerization of ethylene in presence of Ziegler or Mettalocene catalyst under controlled temperature and pressure. The polyethylene molecule is based on a long chain of carbon atoms as shown in figure 1.2. Each ethylene molecule, as it adds on, contributes two more carbon atoms to the chain. Under the conditions of high pressure, the ethylene molecules did not add on in a regular fashion, and so put short branches in the chain, as shown in figure 1.3 [5].

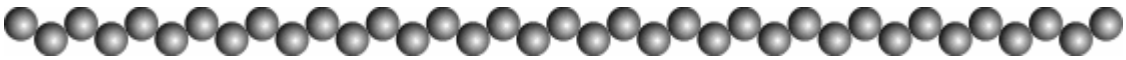

Figure 1.2 Long chain of atoms in polyethylene molecule.

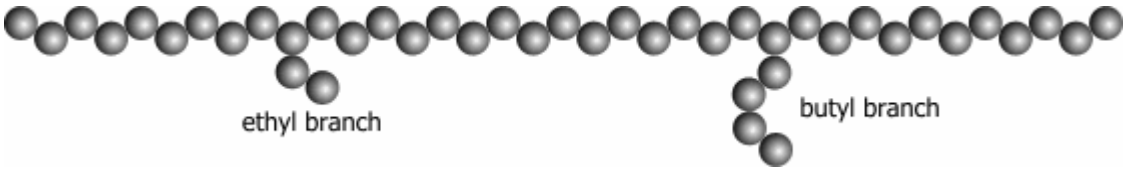

Figure 1.3 Branched chains of atoms in polyethylene molecule.

The HDPE pipes [6] has the following Mechanical and Thermal properties,

- Melt Flow ASTM D1238, 5 to 18 gm /10 min.
- Melting Temperature $T_{m,}$ 130 to 137^{o} C.
- Glass Transition T_{g}, -30^{o} C.
- Processing Temperature Range, 174.90 to 257.40^{o} C for injection molding, 174.9 to 275.15^{o} C for extrusion.
- Molding Pressure Range, 82.73 to 103.42 MPa.
- Compression Ratio, 2.
- Tensile Strength at Break, ASTM D638, 22.06 to 31.02 MPa.
- Elongation at break (%), ASTM D638, 10 to 1200 %.
- Tensile Yield Strength, ASTM D638, 26.20 to 33.09 MPa.
- Compressive Strength, ASTM D695, 18.61 to 24.82 MPa.
- Tensile Modulus, ASTM D638, 1068.68to 1089.37 MPa.

HDPE's pipes are inert to most organic and inorganic chemicals effluents, and have very good corrosion resistance. They are very durable and have a lifetime in the ranges of 50 years in normal working conditions. They are lightweight, hence their handling is easy and convenient and results in saving of transportation cost. Their flexibility makes laying of these pipes easy even on uneven surfaces. HDPE's pipes are tough and durable. They are resilient to withstand static and dynamic loads due to internal and external pressures. These pipes have smooth internal surfaces which ensure very low frictional losses resulting in energy saving up to 33%. HDPE's pipes are economical by almost 40% when compared with metal pipes, and marginally costlier than PVC.

Major Applications of HDPE require service at different loading and non-ambient conditions. Thus, the investigation of temperature and frequency effects on the mechanical behavior of HDPE is very essential.

1.4 Monotonic Properties of Polymers

The monotonic properties of any material are very important from the design point of view. The discussion of monotonic properties of polymers often contains two interrelated objectives. The first of these is to obtain an adequate macroscopic description of a particular facet of the polymer under consideration. The second objective is to seek an explanation of this behavior in molecular terms, which may include details of the chemical composition and physical structures. The present aims to establish a satisfactory macroscopic or phenomenological description of monotonic behavior involving the molecular interpretations.

In case of plastics, the monotonic properties might show large variation for small changes in environment and loading conditions. A plastic showing brittle behavior at room temperature may have elongation up to 300% just above the room temperature. Similarly another plastic specimen which shows considerable yielding at room temperature might behave brittle just below room temperature. Plastics fall in the category of viscoelastic materials (stress-strain dependence on time and temperature). These show time dependent mechanical behaviors such as creep and stress relaxation. The monotonic behavior also very much depends upon the material characteristics such as molecular weight, heat treatment, blending and additives like plasticizers and pigments.

The monotonic properties of most of the polymers are depend on the environment conditions, rate of application of load, amount of strain etc. A polymer can show all the features of a glassy brittle solid, an elastic rubber, or a viscous liquid depending upon the temperature. Many researchers have noted significant temperature dependence of mechanical properties of various polymers like PMMA, cellulose acetate, PVC, CPVC etc. The degree of dependence is related to the structure and crystallinity of the polymer.

Due to the dependence of mechanical properties on a large variety of parameters, it is difficult for the designer to select a certain material without knowing all these parameters. The mechanical properties like yield strength and elastic modulus are usually given as a range for plastics rather than a singular value. Thus, the accurate determination of mechanical properties of polymers with respect to environmental and material variables is of significant importance.

1.5 Fatigue in Polymers

Fatigue is a form of failure that occurs in structures subjected to dynamic and fluctuating stress. Under these circumstances it is possible for failure to occur at a stress level considerably lower than the tensile or yield stress for a static load. The process occurs by the initiation and propagation of cracks, and ordinarily the fracture surface is perpendicular to the direction of an applied tensile stress.

There are basically two approaches to evaluate fatigue behavior of a given material:

- **Total life approach:** This approach to fatigue design involve the characterization of total fatigue life to failure under controlled cyclic stress range (the S-N curve approach) or under controlled cyclic strain range (plastic or total).

- **Defect tolerant approach:** It entails presence of flaws in the material. The size of a preexisting flaw is generally determined from nondestructive flaw detection technique. The useful fatigue life is then defined as the number of fatigue cycles or time taken to propagate a dominant crack from this size to some critical dimension.

The fatigue properties of a material can be determined from laboratory simulation tests. The specimen is subjected to a series of tests involving stress cycling at relatively large maximum stress amplitude, usually of the order of two thirds of the static tensile strength, the number of cycles to failure is counted. This procedure is repeated on a number of specimens at progressively decreasing maximum stress amplitudes. Data are plotted as stress versus the logarithm of the number of cycles to failure for each of the specimens. The values of stress are normally taken as stress amplitudes. The higher the magnitude of the stress, the smaller the number of cycles the material is capable of sustaining before failure.

The process of fatigue failure is characterized by three distinct steps; Crack initiation, wherein a small crack forms at some point of high stress concentration; Crack propagation, during which this crack advances incrementally with each stress cycle; Final failure, it does not contribute to the total fatigue life as it concludes in fraction of seconds.

In spite of the need to understand fatigue in polymers, the sate of the art is not nearly as well advance as in the case of metals. The understanding of fatigue in polymers has been hindered by three major problems. First, the continuum mechanical approach to fracture does not itself described the atomic and molecular process. Second, the ultimate phenomenon of fracture, involves gross, irreversible and non-linear deformation related

to effects of molecular properties and polymer composition. Third, the precise nature of the competitive processes that are balanced out in fatigue and that gives rise to the especially damaging effect of intermittent loading is not precisely known. Thus three fundamentally different views of matter confront each other and require correlation and reconciliation [7].

Fatigue crack propagation (FCP) in polymers is affected by the environment and material irregularities. The use of polymers in non ambient conditions such as transportation systems for hot gas and fluids, liquid storage tanks, automobile engine parts has forced the designer to include the non ambient FCP behavior of polymers in design of components. One of the important tasks in the study of fatigue crack propagation is to achieve a satisfactory definition of crack growth resistance and then to correlate it with the macroscopic properties and morphological features of the material.

1.6 Present Study

The objectives of the present study are to investigate the effect of frequency on the fatigue crack growth properties of CPVC and HDPE at different temperatures. The effect of temperature on monotonic properties is also studied and is used to explain the fatigue crack growth at different temperatures. The frequencies and temperatures used in study are 0.1,1 and 10 Hz and -10, 0, 23, 50 and 70^{o} C.

The report is divided in six chapters. Chapter 1 gives introduction to the study which include basic information regarding polymers, CPVC, HDPE and mechanical properties of polymers. Chapter 2 describes the literature review that covers previous work done by researchers on monotonic and fatigue crack propagation in polymers. The experimental procedure adopted for specimen preparation and testing along with the

details of testing apparatus and results are provided in chapter 3. The results for monotonic tests performed on CPVC and HDPE are discussed in chapter 4, while chapter 5 contains the discussion of fatigue crack propagation test results. Finally, conclusions drawn from this study and recommendations for future work are given in chapter 6.

CHAPTER 2

LITERATURE REVIEW

This chapter describes the literature review which covers relevant previous and ongoing work done by different researchers on the monotonic and fatigue crack growth characteristics of polymers. First, the literature review regarding the effect of temperature on monotonic properties of polymers is presented in section 2.1. Then the effect of temperature and frequency on the fatigue crack propagation characteristics of polymers is discussed in section 2.2. At the end of the chapter the summary of the literature review and status of the present problem is discussed.

2.1 Monotonic Properties

The polymer chain length and its distribution, environmental conditions, rate of application of load, amount of strain are important molecular parameters in controlling the physical, mechanical and processing characteristics of polymers. Depending on molecular weight (MW) and its distribution (MWD), polymers can exist under a variety of formulations, each one with tailored properties for specific applications. The influence of MW and MWD on monotonic properties is clearly shown in Figure 2.1 [9].

Monotonic properties of polymers are discussed in terms of moduli. These are the proportionality constants between stress and strain, and represent the initial slope of the

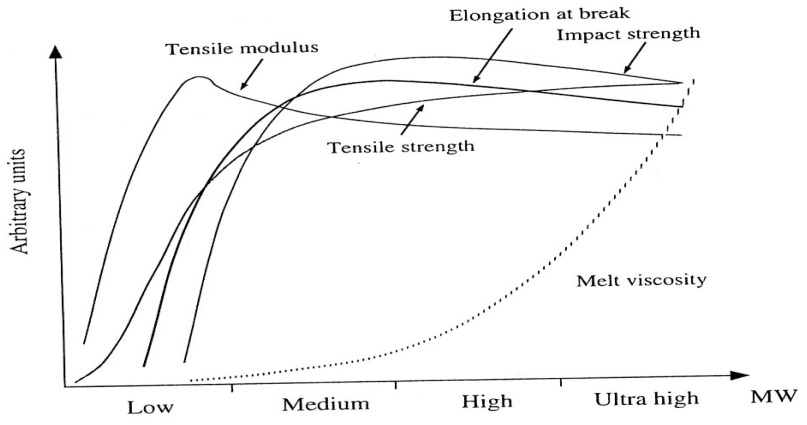

Figure 2.1 Effect of Molecular weight on the monotonic properties of polymers [9].

curves in figure 2.2 which illustrates the different modes of polymer failure. Not all polymers have all these failure modes, but most have two depending on temperature. It is also important to note that some polymers may have different failure modes for different modes of deformation. In general, all polymers at temperature significantly below their glass transition temperatures (T_g –T >100° C), undergo brittle fracture. In the region above the brittle fracture regime, but below T_g, polymers usually yield and undergo plastic deformation as the modulus decreases. This is illustrated in the hump that occurs in the stress-strain curves as shown in the figure 2.2. After a sufficient amount of strain the polymers chains begin to align in the strain direction and the modulus increases until the plastically deformed sample eventually breaks.

Deformation after the yield point may have various forms depending on the structure, mechanical and thermal history of the sample, such as shear yielding and cold drawing as depicted in figure 2.2. At an intermediate temperature between the brittle fracture and plastic deformation regimes many polymers undergo a non-catastrophic failure called crazing. Crazes may be observed visually as the whitening of the polymer, which occurs under stress. This whitening is caused by multiple reflections of light from polymer/void interfaces in the crazes. Crazes form perpendicular to the applied stress and consist of regions of polymer in which an incipient crack is bridged by highly oriented material in direction perpendicular to the direction of the crack. A schematic of craze is shown in Figure 2.3.

Thus due to the dependence of mechanical properties on a large variety of parameters, it is difficult for the designer to select a certain material without knowing all these parameters. The mechanical properties like yield strength and elastic modulus are

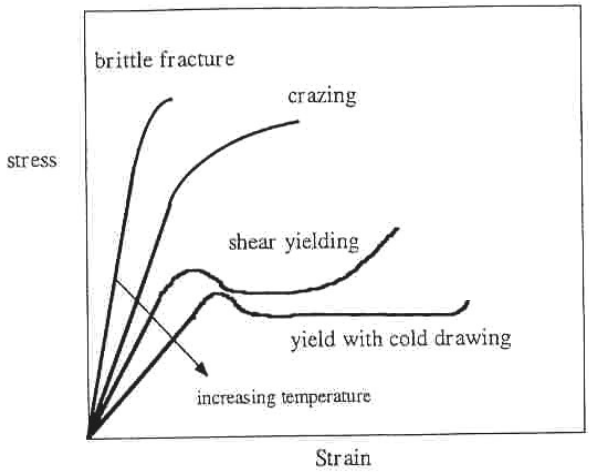

Figure 2.2 Schematic of some failure modes of polymers [9].

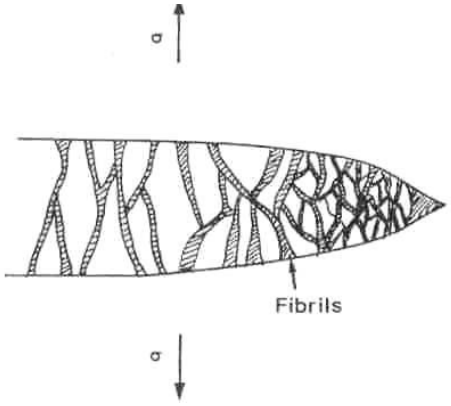

Figure 2.3 Schematic of a craze [9].

usually given as a range for plastics. Thus, the accurate determination of mechanical properties of polymers with respect to environment and material variables is very important.

2.1.1 Effect of Temperature on Monotonic Properties

Tordjeman et al [10] have studied the effect of temperature and strain rate on plastic and viscous elastic material behavior of PMMA and PMMA based random copolymers. Strain rate for the tensile tests on copolymers was $2x10^{-3}s^{-1}$, whereas it was varied from $5x10^{-3}$ to $3x10^{-1}$ s^{-1} for pure PMMA. The temperature range used was from -60^{o} C to T_g. Experiments performed below room temperature were less accurate because both types of samples become brittle below room temperature. The plastic softening amplitude SA was used to correlate the effects of strain rate and temperature on the stress strain behavior of the material. Their results are in accordance with the famous equation of Williams- Landel- Ferry WLF theory, i.e. an increase in strain rate is qualitatively equivalent to a decrease of temperature at fixed strain rate.

Bronnikov et al [11] investigated the thermal and mechanical properties of drawn polymers over a wide temperature range. They used Polyethylene tetrapythalte (PET), nylon 6, and nylon 610 for analysis. They have shown that mechanical properties of drawn polymers are directly related to the thermal expansion and have used this approach to show the temperature dependence of Young's modulus and yield stress over a wide temperature range. It is seen that Young's modulus and yield stress decrease with temperature increase.

Povolo et al [12] have studied the stress relaxation of PVC below yield point. The temperature dependence of elastic modulus is determined from measured stress-strain

curves. It has been shown that the elastic modulus varies linearly with the temperature. A relationship is proposed between the tensile modulus and the free volume which helps to explain the temperature dependence of the relaxation strength.

Che et al [13] have used fracture mechanics parameters, J-integral and crack tip opening displacement (CTOD) to determine the dependence of crack resistance behavior of PVC on specimen dimensions, specimen configuration and test conditions (temperature, strain rate) under monotonic loading. The temperature range investigated was from -40^{o} C to 60^{o} C. A strong temperature effect is observed. The crack initiation values in terms of J-integral show a maximum value at 23^{o} C, while the CTOD values, as well as the tearing moduli either in terms of the J-integral or of the CTOD concept, increase with increasing temperature.

Pal et al [14] investigated the mechanical properties of polyvinyl chloride based polymer blends intended for medical applications. The study was performed at room temperature and indicated that these blends could be investigated further for potential applications in medicine. They have proposed an equation for determining the mechanical properties. The values calculated are quite close to the experimental values for the blend system studied.

Han and co-workers [15] have analyzed the effect of rubber content and temperature on dynamic fracture behavior of ABS materials. The dynamic Young's modulas E_d and yield strength σ_{yd} tend to decrease with increasing temperature.

Hit and Gilbert [16] have studied tensile properties of PVC compounds at elevated temperatures. The temperature range used is from room temperature 23^{o} C to 180^{o} C. It was found that the relationships between elongation at break and stress at break for a

range of PVC compounds were almost independent of compound constituent and strain rate. Stress at break decreased steadily with increasing temperature, whereas elongation at break revealed a maximum between 80^{o} C and 90^{o} C and a minimum between 130^{o} C and 170^{o} C. This behavior is attributed to the presence of network crystallites, which start to break down at a temperature of 90^{o} C. Eventually there is sufficient destruction of network to enable viscous flow to occur.

Ye Lin et al [17] have reported effects of strain rate and temperature on fracture behavior of Ploy 4-methy-1-pentene (TPX) polymer. They used compact tension (CT) and single edge notch bending (SNEB) specimens. The results showed that the fracture behavior of TPX polymer was highly dependent on cross head rate and temperature.

Seitz [18] has developed the use of semi empirical and empirical relationships to estimate the mechanical properties of polymeric materials from their molecular structure. Based on these relationships properties can be calculated from only five basic molecular properties. They are molecular weight, Vander Wall volume, the length and number of rotational bonds in the repeat unit, as well as the T_g of the repeat unit. The temperature dependence of the properties like Young's modulus and Poisson's ratio was also given.

Merah, N. and Irfan [19] have investigated the effect of temperatures ranging from –10 to 70^{o} C on the mechanical properties of CPVC. They found that the yield strength and elastic modulus decrease linearly with temperature. Brittle fracture occurred at temperatures below room temperature while ductile fracture occurred at room temperature and temperatures above it. They observed the maximum elongation at break at 70^{o} C while the minimum at -10^{o} C. They also found considerable necking at 50^{o} C and 70^{o} C.

2.2 Fatigue Crack Propagation

2.2.1 Background

A schematic diagram showing the variation of load or stress with time is given in figure 2.4. Different parameters used to characterize the fluctuating stress cycle are also indicated in the figure. The stress amplitude alternates about a mean stress σ_m, defined as

$$\sigma_m = (\sigma_{max} + \sigma_{min})/2 \quad (2.1)$$

where σ_{max} and σ_{min} are the maximum and minimum stresses respectively. The stress amplitude σ_a is given as,

$$\sigma_a = (\sigma_{max} - \sigma_{min})/2 \quad (2.2)$$

The stress range $\Delta\sigma$ is defined as,

$$\Delta\sigma = \sigma_{max} - \sigma_{min} \quad (2.3)$$

The stress ratio R is just the ratio of minimum and maximum stresses

$$R = \frac{\sigma_{max}}{\sigma_{min}} \quad (2.4)$$

2.2.2 Kinetics of Fatigue Crack Propagation

The kinetics of fatigue crack propagation can be examined by simply measuring the change in crack length as a function of the total number of cycles. The fatigue crack growth rate per cycle (da/dN) is determined from the a-N curve at any value of the crack length by graphical procedures or by computation. For most specimen configurations, the crack growth rate increases with increasing crack length, thereby shortening the component life. The crack growth rate is also a function of stress level applied,

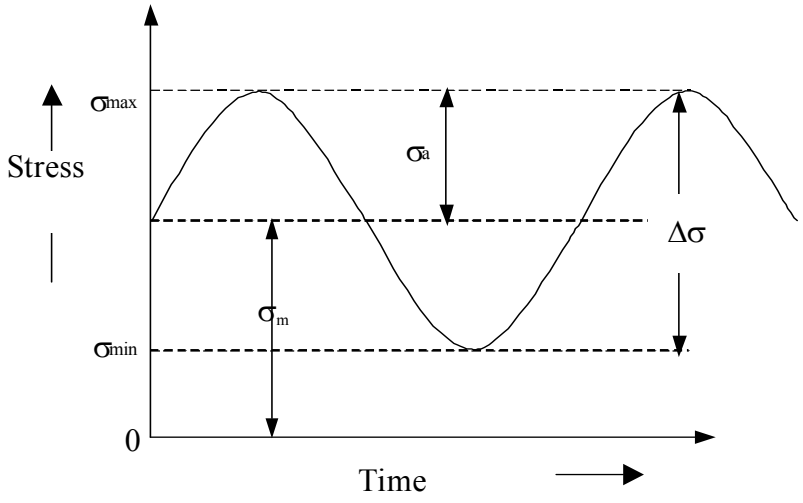

Figure 2.4 Variation of stress with time that accounts for fatigue failure.

$$da/dN \propto f(\Delta\sigma, a)$$

Numerous relations have been proposed to describe the fatigue crack growth (FCG) behavior of metallic and polymeric solids, based on empirical formulations and fracture mechanics principles. The most widely used and most general relationship was given by Paris and Erdogan [20]. Paris postulated that the stress intensity factor itself, a function of stress and crack length is a controlling factor in fatigue crack propagation process. This suggestion is totally consistent with the fact that the stress intensity factor controls the static fracture and environmental assisted cracking as well. The growth rate $(da/dN)a_{i,j,\ldots n}$ at any arbitrary crack length $a_{i,j,\ldots\ldots n}$ would correspond to respective values of $K_{i,j,\ldots\ldots n}$ for same fixed stress level. The key stress variable is the stress range ($\sigma_{max} - \sigma_{min}$) and so da/dN values are described in terms of stress intensity factor range ΔK with a relationship of the form

$$\frac{da}{dN} = A\Delta K^{m} \qquad (2.5)$$

where da/dN is the fatigue crack growth rate, ΔK the stress intensity factor range; $\Delta K = K_{max} - K_{min,}$ and A and m are constants depending on the material variables, environment, frequency of loading, test temperature and stress ratio.

The log-log plot of da/dN versus ΔK is a sigmoidal curve containing three distinct regions. At intermediate ΔK values, the curve is linear, but the crack growth deviates from the linear trend at high and low ΔK levels. In the former case, the crack growth accelerates as K_{max} approaches K_{crit}, the fracture toughness of the material. At the other

extreme, da/dN approaches zero at a threshold ΔK_{th}. The linear region of the log-log plot is usually described by equation 2.5.

In mode I loading principal load is applied normal to the crack plane and tends to open the crack. The mode I loading is shown in figure 2.5. The range of stress intensity factor in mode I loading is often denoted as ΔK_I. For simplicity ΔK_I will be written as ΔK throughout the text as only one mode of loading is dealt with here. The general expression for ΔK is

$$\Delta K = Y\Delta\sigma\sqrt{\pi a} \tag{2.6}$$

Where $\Delta\sigma$ is the applied stress or stress range, a is the crack length and Y is a geometry correction factor.

For a single edge notch (SEN) tensile plate specimen Y is given as:

$$Y(a/w) = 1.12 - 0.231(a/w) + 10.55(a/w)^2 - 21.72(a/w)^3 + 30.95(a/w)^4 \tag{2.7}$$

Where w is the width of the specimen. This relation is valid for $(a/w) \leq 0.60$.

2.2.3 Different Equations for Fatigue Crack Propagation

Following are empirical fatigue crack growth Equations formulated by different researchers for different regions in a typical da/dN vs. ΔK curve, some of them also include the effect of R value used in the experimentation.

(a) Forman (1967), proposed a relationship which is valid for regions I, II in a typical da/dN vs. ΔK curve,

$$\frac{da}{dN} = \frac{C\Delta K^m}{(1-R)K_{crit} - \Delta K} \text{ or } \quad \frac{da}{dN} = \frac{C\Delta K^{m-1}}{\frac{K_{crit}}{K_{\max}} - 1} \tag{2.8}$$

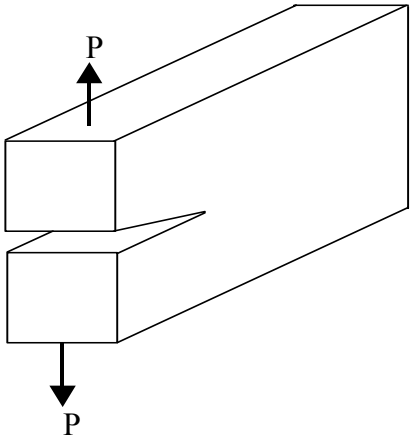

Figure 2.5 Loading in Mode I.

(b) Weertman's (1966), equation incorporates regions II, III in a typical da/dN vs. ΔK curve,

$$\frac{da}{dN} = \frac{C\Delta K^4}{K^2{}_{crit} - K_{\max}{}^2} \tag{2.9}$$

(c) Klesnil and Lukas (1972), proposed a da/dN vs. ΔK equation which applies for regions I, II in a typical da/dN vs. ΔK curve,

$$\frac{da}{dN} = C(\Delta K^m - \Delta K_{th}{}^m) \tag{2.10}$$

(d) Donahue (1972), proposed a relationship which is valid for regions I, II in a typical da/dN vs. ΔK curve,

$$\frac{da}{dN} = C(\Delta K - \Delta K_{th})^m \tag{2.11}$$

(e) Priddle's (1980), equation incorporates valid for regions I,II and III in a typical da/dN vs. ΔK curve,

$$\frac{da}{dN} = C\left(\frac{\Delta K - \Delta K_{th}}{K_{crit} - K_{\max}}\right)^m \tag{2.12}$$

(f) McEvily (1988), proposed a da/dN vs. ΔK equation which applies for regions I, II in a typical da/dN vs. ΔK curve,

$$\frac{da}{dN} = C\left(\Delta K - \Delta K_{th}\right)^2\left[1 + \frac{\Delta K}{K_{crit} - K_{\max}}\right] \tag{2.13}$$

Here C, m and K_{crit} are material constants. ΔK_{th} depends on material and R value. All these equations are valid for constant amplitude loading and in LEFM domain only. In our experimental program, we have done testing at a stress ratio of 0.2(no R value effect) and we are interested in the Paris region only hence we will be using equation 2.5 for our analysis purpose.

2.2.4 Crack Tip Plasticity

Linear elastic stress analysis of sharp cracks predicts infinite stresses at the crack tip. In real materials, however, stresses at the crack tip are finite because the crack tip radius must be finite. Inelastic material deformation such as plasticity in metals and crazing in polymers, lead to further relaxation of crack tip stresses.

The elastic analysis becomes increasingly inaccurate as the inelastic region at the crack tip grows. Some corrections to the linear elastic fracture mechanics are available when moderate crack tip yielding occurs. The Dugdale [21] or strip yield model is usually applied to determine the crack tip plasticity in polymers because it closely resembles the plastic zone shape observed in polymers. Figure 2.6 shows the strip yield model. The Dugdale plastic zone size is given by

$$\rho = \frac{\pi}{8}\left[\frac{K}{\sigma_{ys}}\right]^2 \tag{2.14}$$

where ρ is the plastic zone length, K is the stress intensity factor and σ_{ys} is the yield stress. This relation is valid for $\sigma <<< \sigma_{ys}$ and $\rho <<< a$.

2.2.5 Crack Closure

When a specimen is cyclically loaded between K_{max} and K_{min} the crack faces may be in contact for a certain portion of the cycle. This phenomenon is called crack closure as it does not contribute to the crack opening. Crack closure might be induced by plasticity, viscous fluid between the crack faces, crack face roughness or it can be transformation or oxide induced closure. Plasticity-induced closure results from residual stresses in the plastic wake. The residual stretch in the plastic wake causes the crack faces

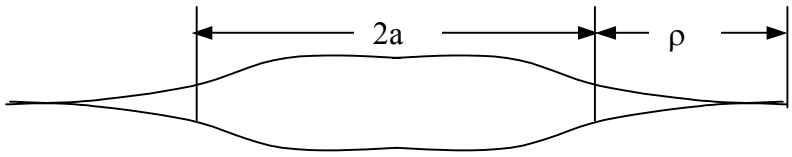

Figure 2.6 Schematic diagram for the strip yield model.

to close at a positive remote stress. Elber [22] postulated that crack closure decreased the fatigue crack growth rate by reducing the effective stress intensity range. The effective stress intensity range is defined (see figure 2.7) as

$$\Delta K_{eff} = K_{max} - K_{op} \tag{2.15}$$

where K_{op} is the stress intensity factor at which the crack opens. The effective stress intensity ratio U is given as;

$$U = \frac{\Delta K_{eff}}{\Delta K} \tag{2.16}$$

The stress intensity for crack closure is not a material constant but depends upon a number of factors. Elber measured the closure stress intensity in aluminum alloys and obtained the following simple empirical relationship.

$$U = 0.50 + 0.40R \tag{2.17}$$

2.2.6 Modified Paris Erdogan Equation

The Paris-Erdogan law (equation 2.7) is modified to include the plastic zone and crack closure effects. The modified Paris-Erdogan power law is given as;

$$\frac{da}{dN} = A\Delta K_{eff}^{m} \tag{2.18}$$

where

$$\Delta K_{eff} = \Delta\sigma(0.50 + 0.4R)\sqrt{\pi\left[a + \frac{\pi}{8}[\frac{K}{\sigma_{ys}}]^2\right]}f\left[\frac{a + \frac{\pi}{8}[\frac{K}{\sigma_{ys}}]^2}{w}\right] \tag{2.19}$$

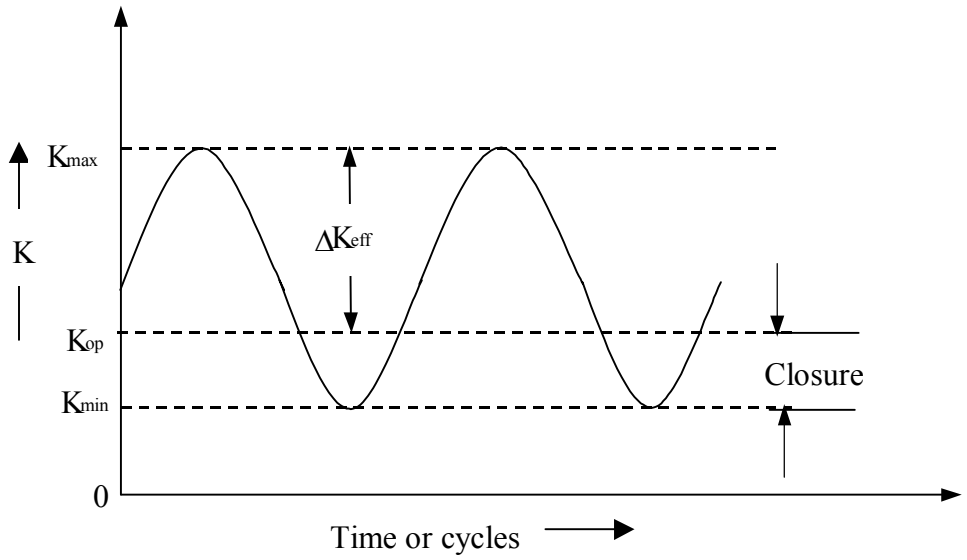

Figure 2.7 Definition of effective stress intensity range.

2.2.7 Factors Affecting Fatigue Crack propagation

When predictions of crack propagation have to be made, data should be available relevant to the conditions prevailing in the service. Such data may be hard to find. Fatigue crack propagation is affected by an endless number of parameters, and the circumstances during the test will seldom be the same as in service. The influence of the environment is the most conspicuous. Tests are usually not performed under controlled environmental conditions and part of the scatter in fatigue data may be attributed to this fact.

There is no concurrence of opinion as to the explanation of the influence of the environment on the rate of propagation of fatigue cracks. It is likely that different explanations will apply to different materials. Among the many factors that affect the crack propagation, the following should be taken into consideration for crack growth predictions, i.e.; thickness, type of product, heat treatment, cold deformation, temperature, manufacturer, batch to batch variations, environment, and frequency [23].

The effect of material thickness can be accounted for rather well, because the thickness of the component under consideration will be readily known. In sheets there is small but systematic effect of thickness on crack propagation. The effects appear to exist primarily before the fracture mode transition. Fatigue cracks in sheets always start as a tensile-mode crack perpendicular to the sheet surface. When the crack grows the size of the plastic zone increases and plane stress can finally develop. This causes the fatigue crack to change to single or double shear. Plane stress develops when the size of the plastic zone is in the order of the sheet thickness. Therefore, it is conceivable that the thickness effect is related to the fracture mode transition [24].

2.2.8 Fatigue Crack Propagation in Engineering Plastics

Hertzberg [7] reported about a growing number of studies concerning the FCP behavior of engineering plastics in his book. According to him, the FCP rates of polymers are strongly dependent on the magnitude of the stress intensity factor range, regardless of the polymer chemistry and molecular arrangement. Also, the data for amorphous, semi-crystalline, and rubber modified polymers have close correlations on plot of da/dN vs. ΔK, which is analogous to plots of data from metal alloys processing various crystal structures. Hertzberg [7] also found that plastics will exhibit superior or inferior FCP resistance as compared with metal alloys, depending on whether cycling is conducted under strain controlled or stress controlled conditions respectively.

Based on the results reported by Manson [25], Hertzberg [7] reported that superior FCP resistance is exhibited by semi crystalline polymers. Koo et al. [26] and Meinel & Peterlin [27] have also pointed out that crystalline polymers not only can dissipate energy when crystallites are deformed, but they can also apparently reform a crystalline structure that is extremely strong. This is further illustrated by Ramirez [28], he found that the remarkable superior FCP resistance of amorphous PET was related to strain-induced crystallization that took place within the plastic zone ahead of the crack tip. From this, Hertzberg [7] concluded that the percent crystallinity increased with increasing ΔK level (i.e. increasing plastic zone size).

According to Hertzberg [7] the greatest change in FCP resistance occurs when the molecular weight is modified. For example, Rimnac et al. [29] found a thousand fold decrease in FCP rates when the molecular weight (MW) of polyvinyl chloride was increased by little more than a factor of three. Similarly different researchers reported

major improvements in FCP resistance with increasing MW in the polyacetal, polycarbonate, polyethylene, nylon, and poly (methyl methacrylate). Using these Hertzberg [7] concluded that cyclic loading tends to disentangle existing molecular network, and these disentanglements are easier at low MW, along with positive contributions from enhanced orientation hardening with the higher MW species. Mitchel et al. [30] developed a theoretical model to show that the strong sensitivity of FCP rates to MW and molecular weight distribution is related to the fraction of molecules that can form effective entanglements network. According to Mitchel et al. [30] longer chains lead to the development of more fracture resistance entanglement networks.

2.2.9 Polymer FCP Frequency Sensitivity

Hertzberg [7] reported, one is faced with an interesting challenge when trying to explain the effect of test frequency on polymer fatigue performance. Although hysteretic heating arguments appear sufficient to explain a diminution of fatigue resistance with increasing cyclic frequency in unnotched polymer test samples, the fatigue resistance of several polymers in the notched condition is enhanced with increasing cyclic frequency. Hertzberg [7] used the results reproduced here in Figure 2.8 (a) to show the effect of frequency on FCP of PVC. Similar attenuation of FCP rates with increasing frequency has been reported in several other polymeric solids [7, 31, 32, 33, 34]. Other polymers such as polycarbonate (PC) and polysulfone (PSF), showed no apparent sensitivity of FCP rate to test frequency (figure 2.8 (b)).

- **Frequency Sensitivity at different temperatures**

Hertzberg and Manson [31] found an intriguing correlation between the relative FCP frequency sensitivity in polymers and the frequency of movement of main chain

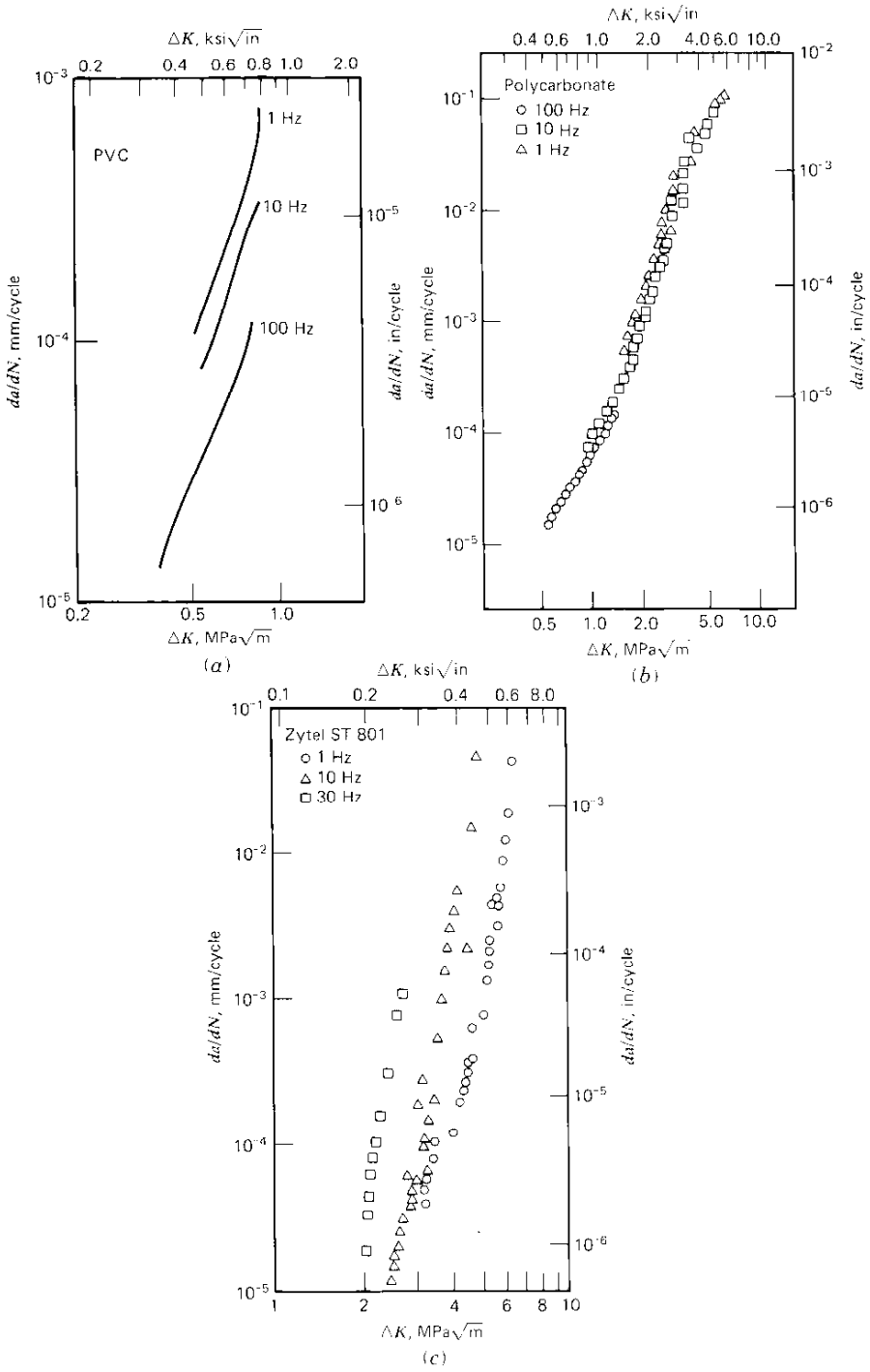

Figure 2.8 Effect of test frequency on fatigue crack growth rate, (a) PVC, (b) Polycarbonate, (c) impact-modified nylon 66. Crack growth can decrease, increase, or remain unchanged with increasing test frequency [7].

segments responsible for generating the β transition phase peak at room temperature. Data for several polymers are shown in (figure 2.9), as a function of frequency sensitivity factor FSF and frequency. FSF is defined as the multiple by which the FCP rate changes per decade change in test frequency, it has a value equal to 1.8 for PVC. Hertzberg [7] noted that the greatest frequency sensitivity is found in a material that revealed its β peak at a frequency comparable to the fatigue test frequency range. This resonance condition suggests the possibility that localized crack tip heating may be responsible for polymer FCP frequency sensitivity. According to Hertzberg [7], one may then speculate whether other materials that were not FCP frequency sensitive at room temperature might be made so at other temperatures, if the necessary segmental motion jump frequency were comparable to the fatigue test frequency range. Indeed this has been verified by Hertzberg and Manson [32,33] for PS and PSF under low temperature test conditions; conversely, the FCP response of PMMA was found to be less frequency sensitive at -50^{o} C than at room temperature, which is consistent with above hypothesis. Hertzberg et al [35] found that, the overall frequency sensitivity for all the engineering plastics tested has been shown to be dependent on $T-T_{\beta}$ (figure.2.10). This latter term represents the difference between the test temperature and the temperature corresponding to the β damping peak within the appropriate test frequency range. Experiments with PVC have confirmed a similar relation for fatigue tests conducted in the vicinity of the glass transition temperature T_g.

Since β peak represents a region of maximum loss of compliance, associated with considerable damping and energy dissipation, hysteretic heating should occur along with a localized temperature rise. In precracked samples utilized in FCP experiments, the

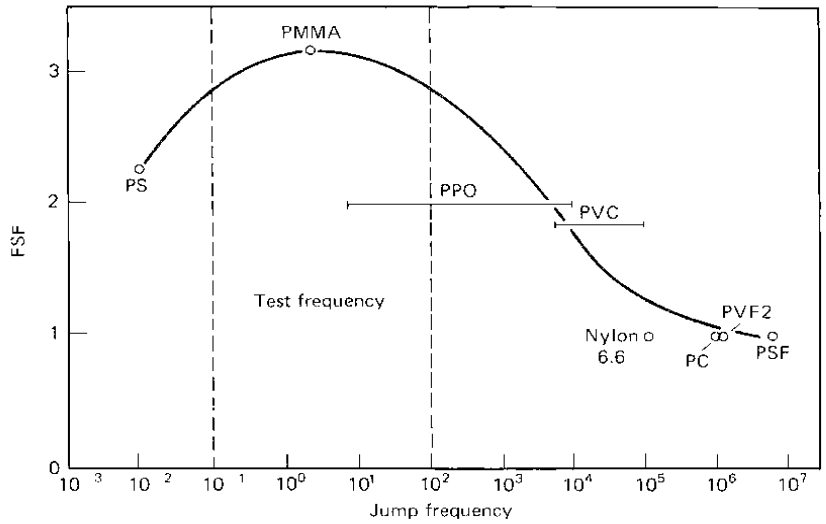

Figure 2.9 Relation between FCP frequency sensitivity and the room temperature jump frequency for several polymers [7].

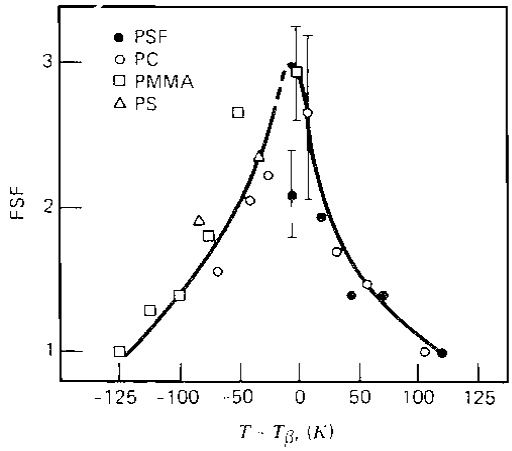

Figure 2.10 Frequency sensitivity factor (FSF) relative to normalized β-transition temperature $T-T_\beta$ [7].

maximum heat rise is restricted to the plastic zone near the crack tip; the bulk of the specimen experiences lower cyclic stresses and remains essentially at ambient temperatures. When the temperature increases, yielding processes in the vicinity of the crack tip are enhanced and lead to an increase in the crack tip radius. A larger radius of curvature at the crack tip should result in a lower effective ΔK; fatigue crack growth rates should decrease accordingly with increasing test frequency. On the other hand, if the amount of specimen heating becomes generalized rather than localized, higher FCP rates would be expected at high test frequencies. This special condition was found to exist in impact modified nylon 66, a material possessing a high degree of internal damping (fig. 2.8c). Hertzberg and Manson [36,37] measured temperatures with an infrared microscope and thermocouples and found increase in crack tip temperatures along with substantial heating throughout the specimen's unbroken ligament [36,37]. Such major temperature rises in the specimen decrease the specimen stiffness and enhance damage accumulation. It is seen that the antipodal behavior of rubber-toughened nylon 66 with that of PMMA, PVC, or polystyrene reflects a different balance between gross hysteretic heating (which lowers the elastic modulus overall) and localized crack tip heating (which involves crack tip blunting). Lang [38] found that materials like PC and PSF, which do not reveal FCP rate frequency sensitivity over a large ΔK range at room temperature, exhibited no significant localized crack tip heating.

2.2.10 Effect of Temperature on FCP

Yeh and Huang [39] investigated the fatigue fracture behavior of the notched polyethylene terephthalate (PET) at temperatures from their beta transition temperature to their glass transition temperatures. Detailed characterization on the morphology of the

notch roots showed that crack tip during crack propagation became dull with increasing testing temperature. The failure cycle of these samples increased with increasing temperatures until it reached the glass transition temperatures T_g of PET polymers, and most of this increase in failure cycle is due to the increased time consumed in the initiation period. On the other hand, the initial crack growth rate increases significantly and failure cycles of these samples decreased dramatically as the temperature increased well above the glass transition temperature. They explained this interesting temperature dependence of fatigue behavior by change in the molecular motion of PET polymers.

Massa and Laurent [40] studied the rapid crack propagation of a medium density polyethylene used to extrude pipes for gas distribution for cracked ring specimens and charpy specimens, over a wide temperature range of -100^{o} C to 20^{o} C. They found that in cracked ring specimens, the fracture toughness K_{IC} gradually and linearly decreases between -100^{o} C and -45^{o} C, and above -45^{o} C a transition in the slope occurs, and linear fracture mechanics concepts are no more valid, they defined this temperature as transition temperature. For charpy specimens they got the same variation of fracture toughness with a slightly higher transition temperature equal to -20^{o} C.

Zhuang and Donoghuue [41] demonstrated how experimental and numerical simulation techniques can be successfully integrated to solve the complex crack propagation events in the pipelines, as it is not necessary to perform any full scale tests, their approach is highly cost effective. They concluded that the toughness almost doubles as the temperature rises by 10^{o} C, and consistent with other material trends. Thus, the material value of the fracture toughness is greater at higher temperatures. This also indicates that the critical pressure increases when operating at higher temperatures. The

reason for this is that the ductility of the pipe material is increased when temperature increases. These data are fully consistent with charpy data with the transition temperature typically in the range 0^{o} C to 10^{o} C.

Norman and Xici [42] studied the critical temperature for rapid crack propagation in 11 polyethylene (PE) 200 mm diameter gas pipes each with different resins. They found the plane stress fracture energy (PSFE) in thin charpy impact specimens of the resin is correlated with the critical temperature for rapid crack propagation. The higher the PSFE, the lower the critical temperature. This result was related to the observation that the PSFE decreases as the temperature decreases.

Martin and Gerberich [43] have examined the temperature effects on fatigue crack propagation in Polycarbonate. Fatigue crack growth properties were measured in the temperature range of -173^{o} C to 100^{o} C and were analyzed using the fracture mechanics approach. Fatigue behavior was found to be related to the fracture toughness of the material. There is a linear relationship between $(\Delta K)_{da/dN}$ and K_{IC} over the temperature range studied. The interrelationship between ΔK, K_{IC} and slope of FCG curve 'm' allowed crack propagation velocities to be predicted from the fracture toughness data. A minimum in both $(\Delta K)_{da/dN}$ and K_{IC} is found at -50^{o} C meaning that the material is least tough at this temperature.

Mai and Willium [44] have conducted fatigue tests on polystyrene in air at different mean stress conditions over the temperature range -60^{o} C to 60^{o} C using notched specimens at a frequency of 0.15Hz. The data was presented on a conventional da/dN versus log ΔK plot to determine the Paris power law parameters and how these varied with mean stress and temperature. Considerable variations were noted but no useful

pattern could be discovered. The data was also analyzed using the continuum mechanics of the crack tip based on the Dugdale's line plastic zone model. It was found that crazing occurred giving a sharp change in crack tip stresses which was also reflected in da/dN versus ΔK plot.

Wann et al [45] have studied the fatigue behavior of Poly arylsulfone (PAS) over a temperature range of -175^{o} C to 120^{o} C. Both fatigue crack propagation and fracture toughness tests were run. Fracture toughness and fatigue crack growth resistance were found to vary similarly with temperature (increase), with minima being observed near -50^{o} C. The slope m of da/dN versus ΔK curve varied from 2.60 to 13.20, being minimum near -50^{o} C.

Kasakevich, Moet and Chudnovsky [46] presents a comparative analysis of crack propagation in high density polyethylene (HDPE) under fatigue and creep loading conditions. Their analysis is focused on the issue of mechanistic similarity between creep and fatigue failure in HDPE. Demonstration of such similarity is a crucial step in establishing the validity of fatigue as an accelerated laboratory test for long-term field failure under creep conditions. The crack layer approach is utilized by the authors as an analytical tool for their investigation.

Kasakevich, Moet and Chudnovsky [47] studied the Fatigue Crack Propagation in high density polyethylene (HDPE) and observed that it occurs with an accompanying layer of damage ahead of the crack tip. They used the crack layer theory for their investigation. They observed that the kinetic behavior of HDPE under fatigue consists of three regions: initial acceleration, constant crack speed, and reacceleration to failure. They noticed that within the first two regions, crack propagation appears 'brittle', while

in the third region ‘ductile’ behavior is found. They concluded that two damage mechanisms are responsible for HDPE failure: formation of fibrillated voids and yielding. Both mechanisms are present throughout the entire lifetime of the crack, but the former dominates the ‘brittle’ crack propagation region, while the latter is more prominent in the ‘ductile’.

Sehanobish, Chudnovsky and Moet [48] conducted the low stress fatigue crack propagation (FCP) experiments on HDPE to understand the phenomenon of brittle fatigue crack propagation in this polymer. They found crack propagation in HDPE was preceded and surrounded by a layer of damage. They identified three stages of FCP kinetics in HDPE each stage is associated with a specific pattern in damaged evolution.

Sehanobish, Chudnovsky & Moet [49] found that rate of fatigue crack propagation (FCP) in high density polyethylene is a nonmonotonic function of the energy release rate. They noticed from microscopic observations a single craze-like active zone preceding the crack during the initial crack acceleration and crack deceleration is associated with a circular active zone, finally ultimate failure occurs by crack reacceleration preceded by large scale yielding through an elongated damage zone accompanied by large scale deformation.

Bucknall and Dumpleton [50] have performed the Fatigue crack growth measurements on two grades of HDPE of density 940 and 958 kg/m^3, and on one transparent grade of toughned poly(methyl methacrylate) PMMA and examine the relationships between crack growth rate da/dN and stress intensity factor K. They found in both grades of HDPE, prolonged cycling is necessary to initiate a crack from a razor notch. They conclude that Paris plots of log(da/dN) against log ΔK are linear provided (a)

that the loading pattern applied to the specimen remains constant, and (b) that growth has taken place for a sufficient period to eliminate the effects of previous loading history.

Chudnovsky, Sehanobish and Wu [51] have performed the durability analysis of HDPE pipes, which involves defect characterization, crack initiation and propagation mechanism, and long term performance prediction. They analyzed the initiation and propagation mechanisms in HDPE by some accelerated tests and compared with that observed in the long-term hydrostatic pressure test.

Parsons, stepnov, Hiltner and Baer [52] studied the effects of frequency and R-ratio on the kinetics of stepwise crack propagation in fatigue and creep of HDPE. They proposed a model relating crack growth rate to stress intensity factor parameters and applied strain rate considering the total crack growth rate to consist of contributions from creep and fatigue loading components. The creep contribution in fatigue test was calculated from the sinusoidal loading curve and the known dependence of creep crack growth on stress intensity factor in HDPE.

Irfan and Merah [53] have studied the effect of temperature ranging from -10^{o} C to 70^{o} C on fatigue crack growth behavior of CPVC. They found that FCG increases with temperature increase. Two different fatigue mechanisms were identified to be operative in different temperature ranges; at high temperatures (23^{o} C to 70^{o} C) crazing was found to be the dominant fatigue mechanism while at low temperature (-10^{o} C to 23^{o} C) shear yielding was the dominant fatigue mechanism. The above transition occurs near the room temperature. Their results are supported by fractographic analysis.

2.2.11 Effect of Frequency on FCP

Ramsteiner and Armbrust [54] studied the fatigue crack propagation rate in PMMA and rubber modified polypropylene for two frequencies 1 and 10 Hz. They found slightly higher rate of crack propagation at 1 Hz (for ΔK greater than and equal to 0.6 MPa$\sqrt{m}$). They concluded that, at high frequency of loading, material deforms plastically and thus the rate of crack propagation is reduced.

Allard and others [55] tested the edge notched samples of Polypropylene (PP) and high density polyethylene (HDPE) containing different mica concentrations in mode I tensile loading. In HDPE mica reduces FCP rates resulting in a higher resistance to fatigue crack propagation. The effect of test frequency on the unfilled polymers and 10 percent mica concentrations by weight in both polymers has been studied. They found that an increase in the test frequency has no significant effect on FCP rates for both raw and mica reinforced PP. Whereas unfilled and mica-filled HDPE show 2.5 to 16 times decrease in FCP rates with increasing frequency.

Hwang and Manson [56] studied the epoxies containing epoxy-terminated butadiene acrylonitrile rubber (ETBN) or amino-terminated butadiene acrylonitrile rubber (ATBN) in terms of FCP resistance and toughening mechanisms. Rubber incorporation in these polymers improves both impact and FCP resistance, but results in slightly lower Young's modulus, as rubber induced shear yielding of the epoxy matrix. They found that with increasing cyclic loading frequency there is a decrease in fatigue resistance for both neat and rubber-toughened epoxies due to strain rate effects, which results in decreasing plastic zone size at the crack tip and consequently result in less FCP resistance.

Hertzberg [7] has reported pronounced decrease in FCP rates with increasing test frequency for a given ΔK level in PVC and several other polymeric materials. The reason for the above is reported to be localized heating at the crack tip, which causes temperature increase which enhanced yielding processes in the vicinity of the crack tip and lead to an increase in crack tip radius, and thus results in lower effective ΔK, and consequently lower fatigue growth rates.

Hakeem and Culver [57] studied the fatigue crack propagation in HDPE in terms of stress cracking properties. They found dependence of crack growth rate on test frequency, amplitude and level of stress intensity factor. They concluded that increase in frequency is expected to cause an increase in the resistance to cyclic crack propagation, due to the increase in the modulus, yield strength and fracture toughness of the material.

Parsons, Stepnov, Hiltner and Baer [58] characterized the effects of frequency and R-ratio on the kinetics of step-wise crack propagation in fatigue and creep of high density polyethylene. They found that at low enough frequency 0.01, a fatigue test might behave like a creep test; i.e. fracture is completely controlled by a creep process even though the load is cycled, and thus we have to superimpose fatigue and creep components for getting total crack growth.

Bureau M. and Dickson J. [59] studied the fatigue crack propagation behavior of polystyrene (PS) and 95/5 PS/HDPE blends at different cyclic frequencies. They found an increase in FCP with decreasing frequency. According to them the time available during each cycle for the craze to deform non-elastically is the most important factor, at high frequencies this time is shorter where as at lower frequencies this time is longer. They concluded that an increase in FCP with decreasing frequency was associated with a

decrease in the time-dependent deformation in the fracture process zone slightly ahead of the crack tip.

From above we may conclude that the effect of frequency on FCP is basically linked with the size of the plastic zone size near the crack tip, and its size at high or low frequencies results in the decrease or increase of FCP. Different researchers have given three major reasons for variation of plastic zone size with frequency. Ramsteiner et al [54], Bureau et al [58] and Parsons et al [59] reported that time available during each fatigue cycle for craze to deform non elastically is the most important factor, at high frequencies due to very less time available, plastic deformation occurred near the crack tip, thus molecules have no time to disentangle and thus the rate of crack propagation is reduced. Hakeem and Culver [57] concluded that increase in frequency result in increase in yield stress near the crack tip and results in enlarged plastic zone, that consequently cause a decrease in FCP. Hertzberg [7] found that increase in frequency results in an increase in the crack tip temperature. This temperature rise cause the enlargement of the plastic zone size near the crack tip and hence a decrease in FCP.

2.2.12 Effect of Temperature and Frequency on FCP

Cheng and manson [60] have investigated the effects of temperature and frequency on fatigue crack propagation rates for PMMA. They reported that the FCP rate increases with increasing test temperature and decreasing cycle frequency. The crack growth is near a maximum at 80^{o} C and 10 Hz. Also the above conditions lie in the saddle between T_{β} and T_{g}. They selected PMMA as a model system to test the Michel-Manson equation [61],

$$\frac{da}{dN} = \tau_0^{-1} \frac{C}{\nu}\left[\frac{-E_a+\sigma_{y,m}V}{RT}\right]\left[\frac{(\Delta K - \Delta K_{th})^4}{\sigma_{ys}\left(K_c^{\,2} - K_{\max}^{\,2}\right)}\right]^m \qquad \textbf{(2.20)}$$

where τ_0, C, m are constants, ν is frequency, E_a is activation energy, $\sigma_{y,m}$= 0.55xyield strength, V is activation volume, R is the gas constant, ΔK and ΔK_{th} are the applied stress intensity range and threshold range, σ_{ys} is the yield strength, K_c is the fracture toughness, and $K_{\max}$ is the stress intensity factor at maximum cyclic load. It is seen that when the test temperature reaches the glass transition region, the failure mechanism changes and the material becomes more fatigue resistant while simultaneously softening.

Kim and Wang [62] studied the fatigue crack growth in a commercial grade acrylonitrile butadiene styrene (ABS) over the temperature and frequency ranges of 10-70^o C and 0.01-10 Hz. They refined a model developed by Mitchel [61] for the effects of temperature and frequency on the FCG rates. This refined model accurately predicts the FCG rates in ABS. The refined model is given by

$$\frac{da}{dN} = \nu^{-nm} C \exp\left[-\frac{\Delta H_{th} - \gamma \log \Delta K}{RT}\right] \qquad \textbf{(2.21)}$$

where, n, m, γ, and C are constants; ν, the frequency of loading; ΔH_{th}, the apparent activation energy independent of ΔK or the apparent activation energy at unit ΔK; R, the gas constant and T, the absolute temperature. They recognized three different types of fatigue fracture surface, the first type is characterized by discontinuous growth bands; the second, by a rather smooth surface; and the last, by a rougher surface relative to the second. The transition between the first and second types were found to be dependent on temperature and frequency as well, whereas the transition between the second and last

types was found to be dependent only on temperature. They linked these findings with crazing.

Kim and Wang [63] modeled the temperature and frequency effects on fatigue crack growth rate of uPVC. They used stress intensity factor biased Arrhenius equation and Michel-Manson [61] model to present there model which accurately predicts the FCG of uPVC. Basically they refined their model for ABS [62] by incorporating a reference frequency ν_r,

$$\frac{da}{dN} = \left(\frac{\nu}{\nu_r} \right)^{-nm} B \exp\left[-\frac{\Delta H_{th} - \gamma \log \Delta K}{RT} \right] \qquad \textbf{(2.22)}$$

The temperature and frequency effects on fatigue crack growth in uPVC were studied over a temperature range 15-55^{o} C and a frequency range 0.01-10 Hz. It was found that the FCP rates increase with increasing test temperature and decreasing cycle frequency.

Radon and Culver [64] investigated the effect of frequency and temperature in polymethyl methacrylate and polycarbonate. They found that the cyclic crack growth decreased with decreasing temperature and increasing frequency. According to them changes in frequency expected to produce a distinct effect in polymers on account of their strain rate sensitivity. They used a parameter viscous energy loss W_V, for characterizing the frequency effects in polymers, which is a function of the loss modulus ($E^{/}$, the imaginary component of the complex modulus) which in turn is a function of frequency. Thus increasing loss factor may greatly affect the amount of viscoelastic energy absorbed per cycle and the decreasing yield strength will lead to the enlargement of the deformed zone around the crack tip and result in lower FCP rates.

From the literature survey it can be concluded that no work was reported on frequency effects on FCG properties of CPVC and HDPE at different temperatures in

open literature, but PVC and PE and their compounds which are closely related to CPVC and HDPE have been studied extensively. The effect of temperature on FCG in polymers has been studied comprehensively by several researchers, but the data available was not self consistent since different materials were examined that possessed different viscoelastic and deformation characteristics. On the basis of the literature, survey it can be concluded that the effect of frequency and temperature on FCG properties of CPVC and HDPE is an open area for research and the results of the study will be a useful addition to the existing literature.

CHAPTER 3

EXPERIMENTAL PROCEDURE AND RESULTS

In this chapter specimen preparation procedure, experimental setup details and test results are presented. The experimental program is divided into the following parts; first part describes the procedure adopted for preparation of specimens for tensile and FCG testing programs from four inch CPVC sockets and HDPE pipes, second part consists of setting up of testing apparatus, third part explains the procedure for studying and analyzing fracture surface morphology of fatigue fractured specimens using SEM. The Section 3.3 describes the conditions at which the various tests were performed. Finally, the results from both the monotonic and fatigue crack growth testing programs are presented.

3.1 Specimen Preparation

- **CPVC**

The specimens for monotonic and fatigue crack growth testing programs were prepared from commercially available four inch injection molded couplings manufactured by Epson. The schematic drawing and photograph of the coupling is shown in figure 3.1 (a) and (b), respectively. Rings 50 mm wide were cut from the sides of the couplings as shown in figure 3.2 and slit into two equal parts. After heating for 20

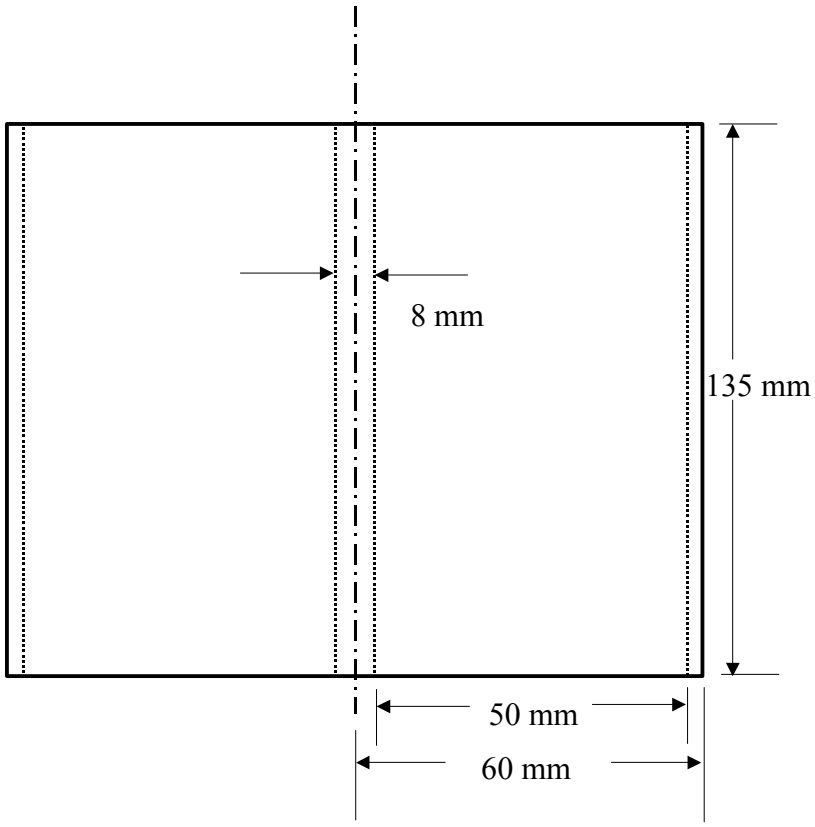

(a)

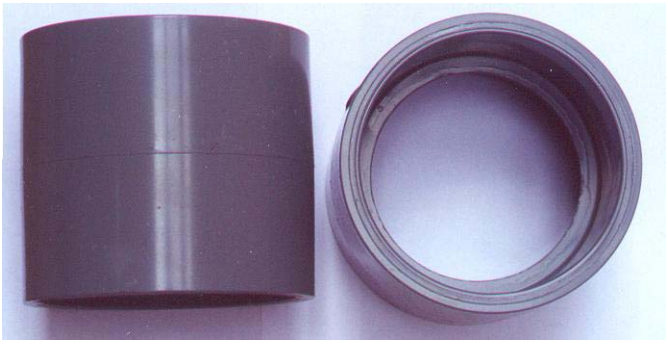

(b)

Figure 3.1 The Schematic diagram (a) and photograph (b) of 4-inch CPVC coupling.

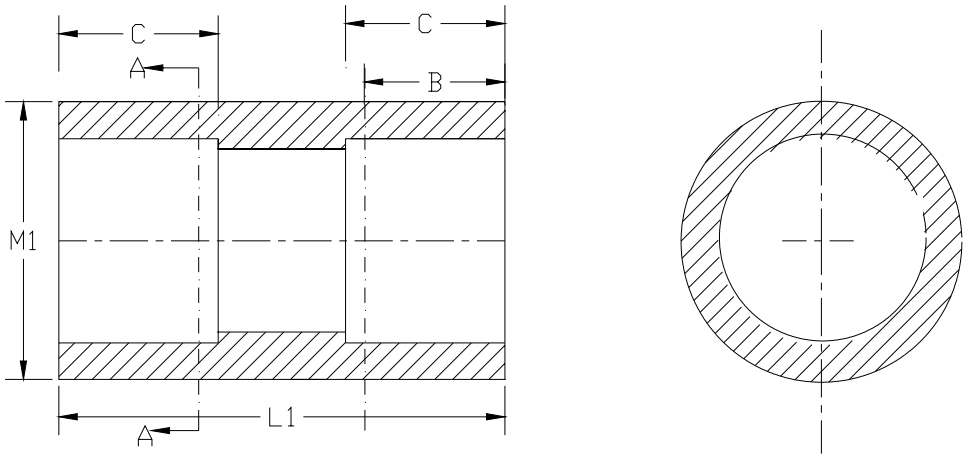

Figure 3.2 Rings of width equal to B (50 mm) were cut from CPVC coupling, C=50, M1=120, L1=135 mm.

minutes at 105^{o} C in an electric oven, the rings were straightened in a specially designed mold (see figure 3.3). Same procedure as that adapted by Irfan [8] was employed here as shown in figure 3.4.

The specimens for fatigue crack growth and tensile tests were machined from the straightened plates. Coolants were used during machining processes to avoid any thermal degradation of material. The tensile test specimens were prepared according to the ASTM D638 Standard method of test for tensile properties of plastics [66]. The fatigue specimens are produced with the dimensions of 40x180x9.4 mm^3. A sharp razor balde was used to make a through thickness 1 mm deep notch manually in all fatigue crack growth test specimens. Figure 3.5 and 3.6 show the schematic diagram and photograph of tensile and fatigue crack propagation specimens respectively. The direction of propagation of crack is shown in figure 3.7. The couplings are cut in the way that plane of cutting coincides with the weldline. (Figure 3.8); the weldline is cut out of the specimen.

- **HDPE**

The specimens for monotonic and fatigue crack growth testing programs were prepared from commercially available four inch diameter pipes manufactured by Al-Wassel. These pipes are manufactured by extrusion. Several additives are also added to improve their mechanical properties. The schematic drawing and photograph of the pipe is shown in figure 3.9. Rings 50 mm wide were cut from the pipes as shown in figure 3.10 and slit into two equal parts. After heating for 60 minutes at 100^{o} C in an electric oven, the rings were straightened in a specially designed mold (see figure 3.3). Due to the presence of additives in the HDPE pipes, these samples when taken out from the

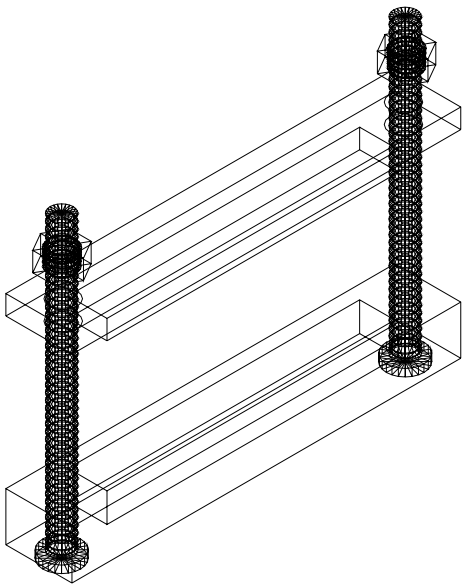

Figure 3.3 Specially designed mold for straightening Specimens.

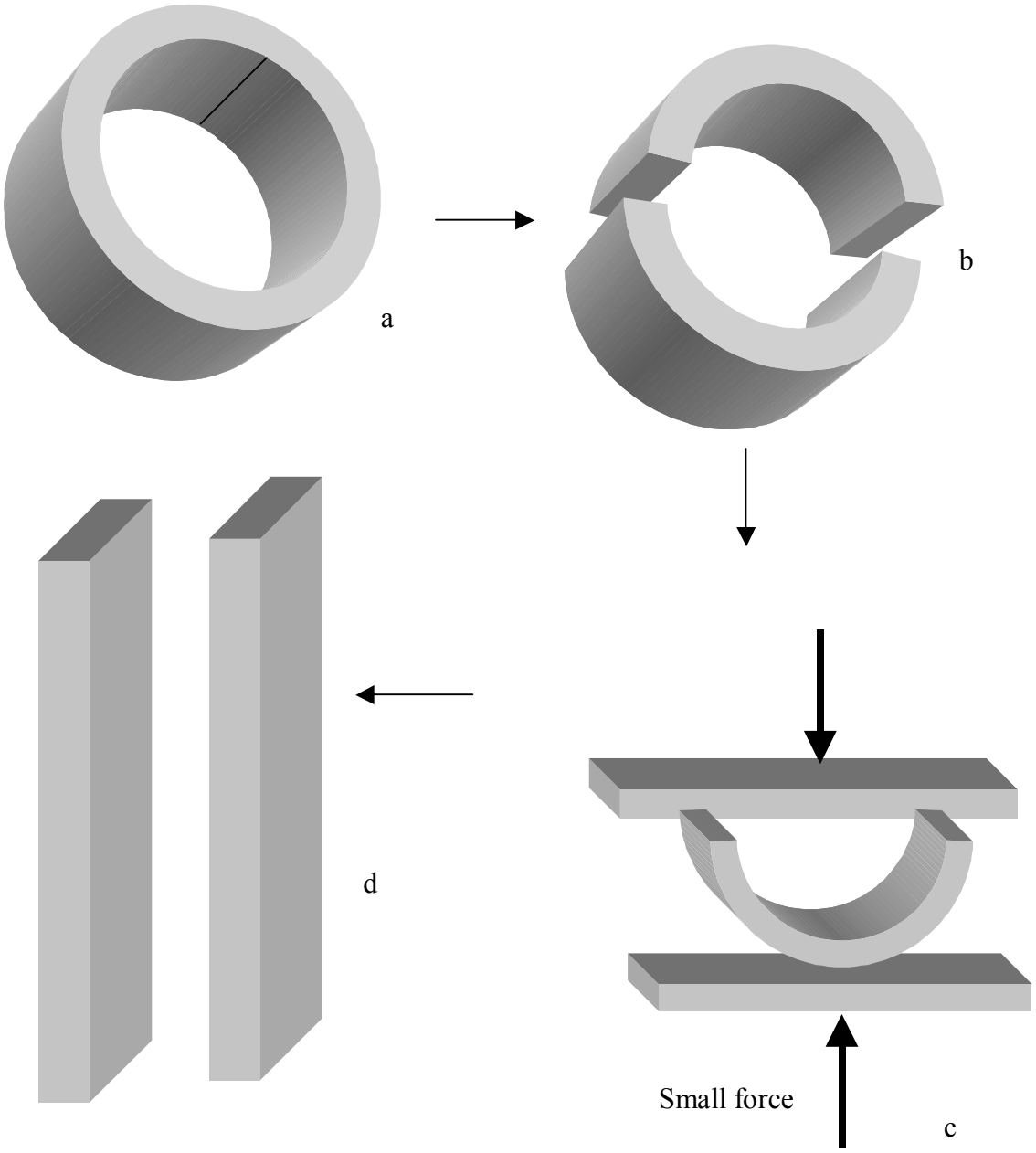

Figure 3.4 Procedure for making flat plates from rings (a) The ring cut from coupling, (b) ring cut into two parts, (c) the half ring is heated at 105^{o} C and straightened between plates and (d) flat plates.

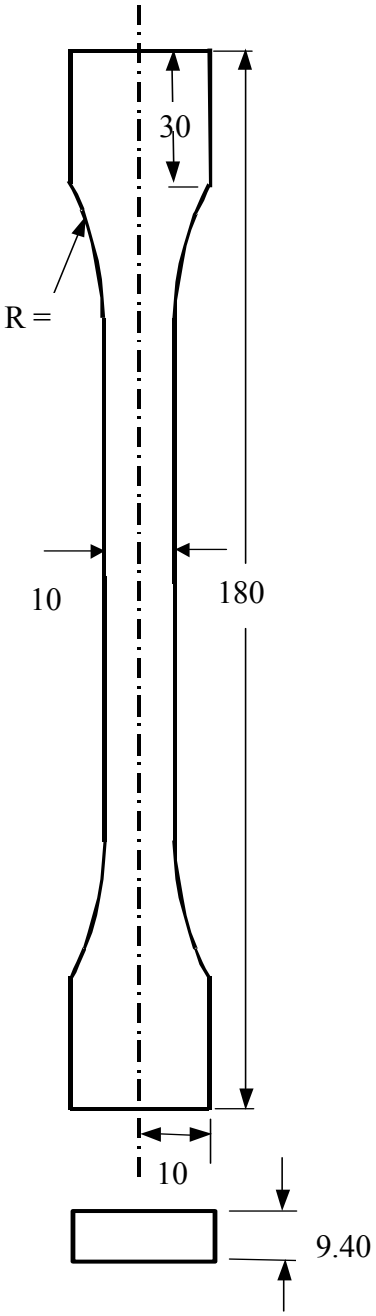

Figure 3.5 Schematic diagram and photograph of the tensile specimen used in the study.

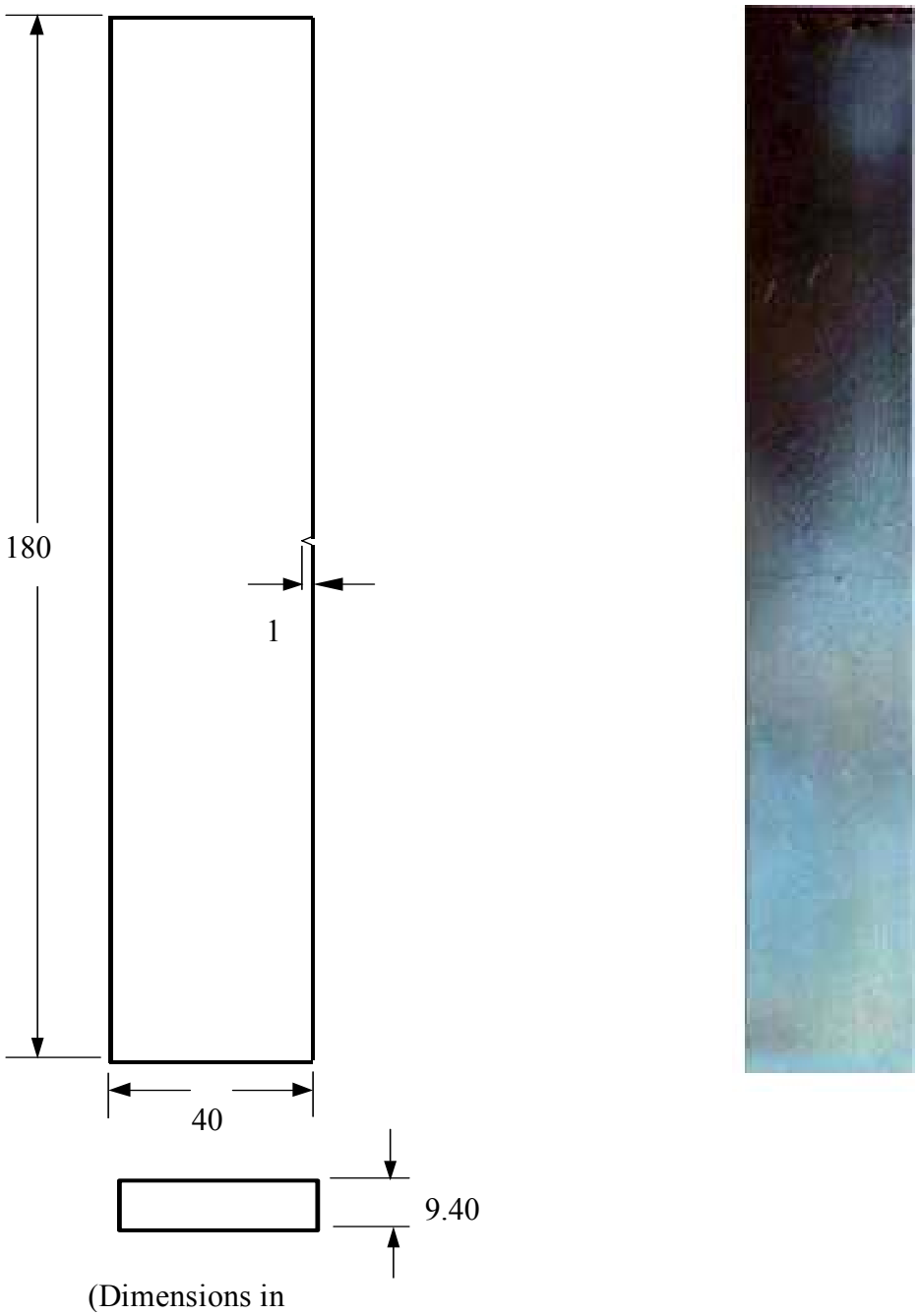

Figure 3.6 Schematic diagram and photograph of the SEN fatigue crack specimens used in this study.

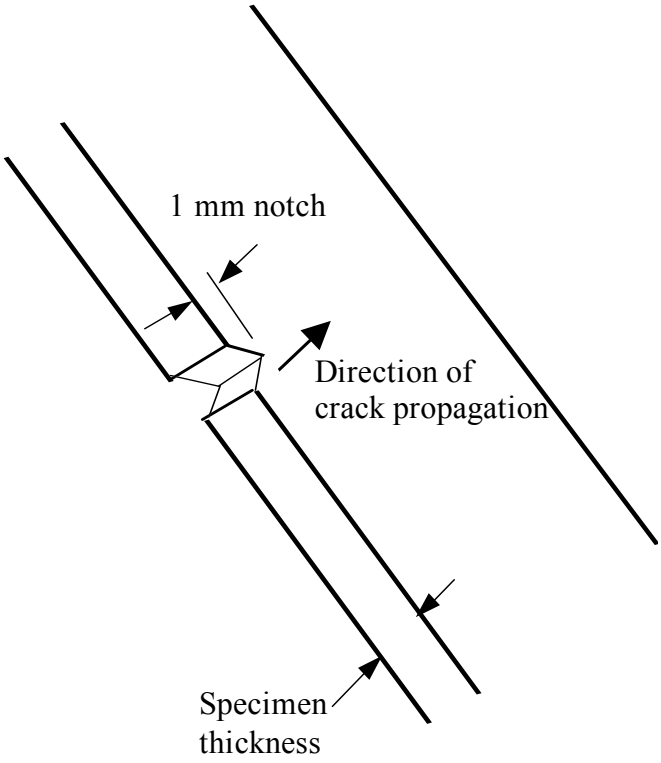

Figure 3.7 Notch orientation in specimens.

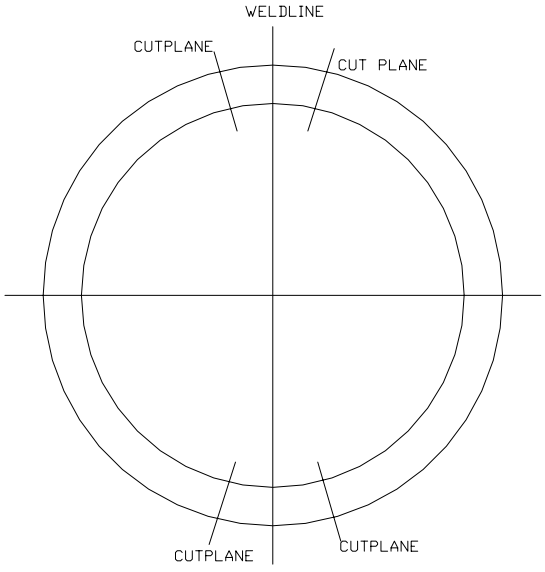

Figure 3.8 CPVC rings are cut at a plane, which is passing through the weldline.

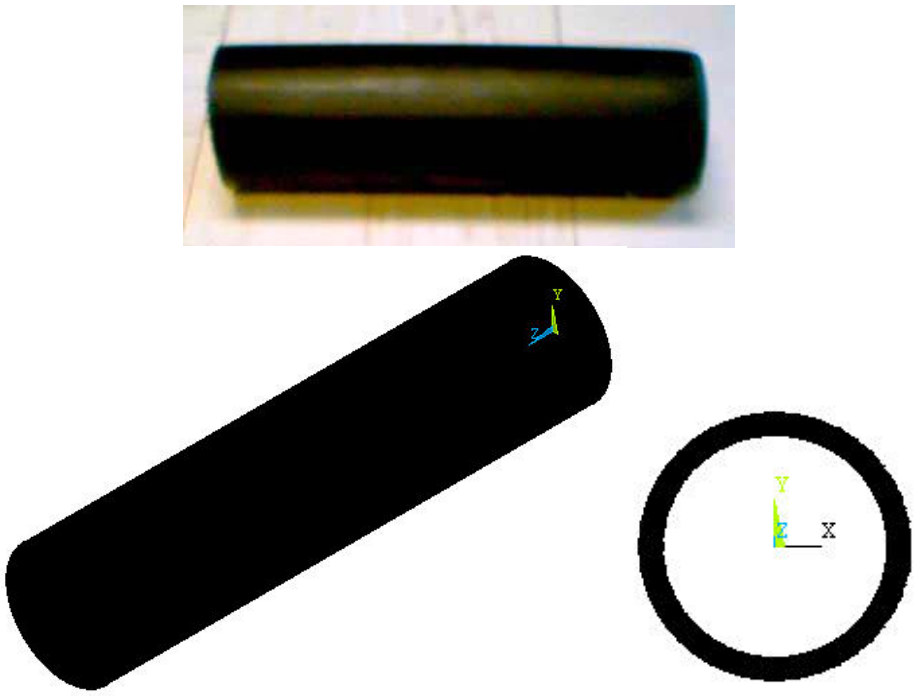

Figure 3.9 HDPE pipe used for making test specimens.

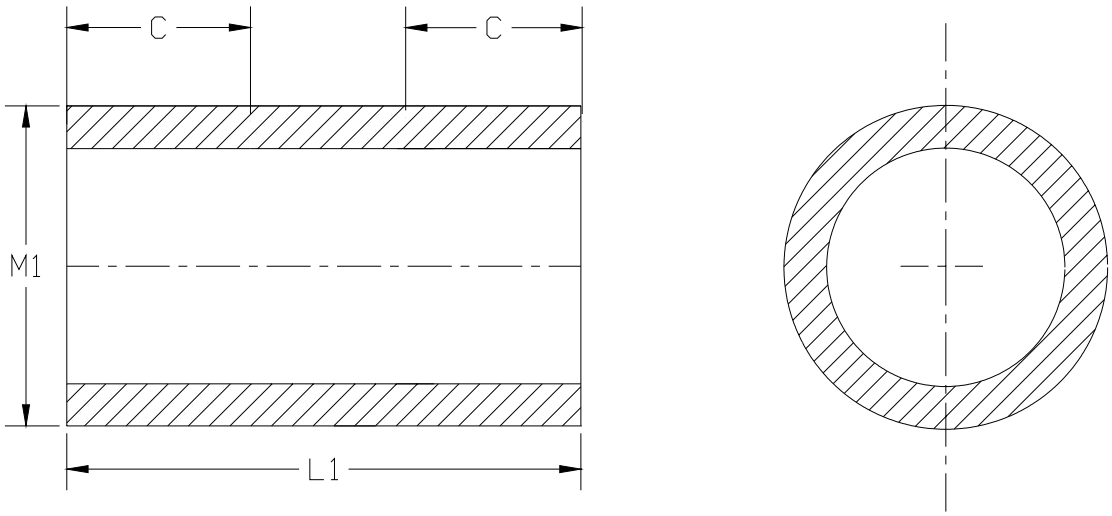

Figure 3.10 Rings of width equal to C (40 mm) were cut from HDPE pipes, M1=120, L1=135 mm.

specially designed mould they were not completely straight. To have the straightened sample the time for heating was increased to 120 minutes, but still desired specimen shape is not obtained. Hence, the temperature for heating was increased in steps of 10^{o} C keeping time for heating constant (60 minutes). A check for specimen's straightness is done at the end of each step. Finally, at 130^{o} C we get the desired straightened specimens ready for testing.

3.2 Testing Apparatus

The testing apparatus used in the present study included Instron 8501 material testing machine, traveling microscope, video recording system, environmental chambers and a scanning electron microscope.

3.2.1 Instron 8501

The Instron 8501 machine was used to perform the tensile and fatigue tests. It is a closed loop servo-hydraulic single axis fatigue testing system. The main controlling modes of the system are strain (±10 %), load (±100 kN) and position (±75 mm) with a frequency range from 0 to 200 Hz. The controlling limits can be viewed on the digital control panel any time during the test along with all other test variables (e.g. maximum/minimum limits of each cycle or the safety limits set or number of cycles or elapsed time etc.). The photograph of testing frame is shown in figure 3.11.

The machine is equipped with a hydraulically actuated self-aligning gripping system. To ensure the vertical alignment of the specimen specially machined inserts were used during the tests. Any pre-loading induced during clamping was adjusted to zero prior to testing by the re-calibration of the load cell after clamping.

Figure 3.11 Photograph of testing frame with environmental chamber and crack monitoring system.

The tensile tests were carried out in position control mode. The Instron Series IX machine control, data acquisition and analysis software for material testing was used. A PC, interfaced with the testing frame was used for test data acquisition. The software provides position and corresponding load of the test with a constant position increment till fracture at the ultimate tensile strength which is logged along with the final position before fracture. The fatigue tests were performed in load control mode. The sine wave with a frequency of 0.1,1 and 10 Hz was used for cyclic loading.

3.2.2 Traveling Microscope and Video Recording Equipment

A Questar QM-100 microscope with a working range of 15-45 cm and resolution of 0.1 mm was used to observe the crack initiation and growth during the fatigue crack propagation tests. The microscope is mounted on a movable stand having both horizontal and vertical movements. Penlight focusing arrangement is used for accurate location and focus of the crack. A digital meter (Questar ZE 5-KA) is interfaced with the microscope, which displays the horizontal and vertical movements of the microscope. This meter was used to measure the crack extension (Δa). Crack lengths of 0.01 mm can be measured using this meter.

Due to the long duration of some tests, especially at low temperatures, a video recording system was employed to record the tests. This system consists of an industrial video camera (magnification x 10) and a 24 hour video recorder. The video camera was placed at a distance of 15 cm from the specimen. The recording equipment was calibrated before starting the actual tests. After the completion of the test, video recordings were played back to measure the crack lengths. The fatigue cycles were recorded with a help of a built-in digital timer in the recording system.

3.2.3 Environmental Chambers

Two environmental chambers designed and fabricated by Irfan [8], were used for conducting monotonic and fatigue tests in non-ambient environments.

The high temperature environmental chamber was designed to maintain temperatures up to 150^{o} C for extended periods of time. It was made from Plexiglas and insulated with glass wool embedded in aluminum foil. The second chamber for low temperature testing was also made from Plexiglas. It is a double walled chamber with glass wool and insulating foam filled between the two walls. The details of the design were reported in the work of Irfan [8]. A window (30x60 mm^2) was designed to allow video camera crack detection and measurement. The environmental chamber is shown mounted in testing machine in figure 3.11.

3.2.4 Scanning Electron Microscope

The fracture surface morphology of the failed specimens was studied using a Joel JSM scanning electron microscope. The magnification range available is 35x to 300,000x. The excitation potential can be varied between 1 to 50 kV. To suppress charging and increasing electron emission, gold coating of the fracture surface was done. This process provided very fine uniform coating of a conducting material (i.e. gold), so that the surface after coating was an exact replica of the underlying material. The coating was done by vacuum depositing in several stages provided by rotary and diffusion pumps of Joel Fine Coat Ion Sputter JFC-1100 with a vacuum of 0.1 Torr at1-1.5 kV. The time and amperage were selected with the constraint of the coat thickness and the specimen surface area.

After the fatigue test, fractured samples were stored in the decicator to protect the fracture surface from any atmospheric contamination. The specimens were reduced to the appropriate size (for mounting on SEM) by Buehler Isomet^{TM} low speed saw using a diamond wafer, in order to eliminate the possibility of inducing any post fatigue damage near the fractured surface.

3.3 Testing Program

- **CPVC**

The fatigue crack propagation tests on CPVC single edge notch plate specimens were conducted at –10, 0, 23, 50 and 70^{o} C for three frequencies i.e. 0.1, 1 and 10 Hz. A stress ratio, R of 0.2, and two stress ranges ($\Delta\sigma$) 13.30 and 11 MPa were used for FCP tests. Two to three tests were run at each condition. The mean stress was taken to be about 20 % of the yield strength of CPVC in order to keep σ_{max} below 50 % of σ_{ys} to avoid elasto-plastic behavior. The monotonic tests for same CPVC material being used in this study were conducted earlier by Merah and Irfan [19].

- **HDPE**

The monotonic tests on HDPE specimens were conducted at a strain rate of $6x10^{-4}$ s^{-1} (cross head speed of 5 mm/min) at –10, 0, 23, and 50^{o} C. The fatigue crack propagation tests on HDPE single edge notch plate specimens were also conducted at –10 and 0^{o} C for frequencies of 0.1, 1 and 10 Hz. Stress ratio, R equal to 0.2, and two stress ranges ($\Delta\sigma$) 9.0 and 8.0 MPa was used for FCP tests.

3.4 Results

The monotonic tests on HDPE specimens were conducted at –10, 0, 23 and 50^{o} C. As described earlier the load-elongation curves were obtained using a PC interfaced with the testing frame. The load-elongation curves for HDPE at 23^{o} C is shown in figure 3.12. The load-elongation curves for HDPE and CPVC [19] at different test temperatures are shown in figure 3.13 and 3.14. Table 3.1 provides the results of the monotonic tests carried out on HDPE specimens. The complete analysis and determination of stress-strain curves is presented in chapter 4. The results of monotonic tests on CPVC [19] and HDPE were used for the development of Master curves for FCP at different temperatures for a given frequency.

The fatigue crack propagation tests on CPVC and HDPE single edge notch plate specimens were conducted at (–10, 0, 23, 50 and 70^{o} C) and (-10 and 0^{o} C) respectively, for frequencies equal to 0.1, 1 and 10 Hz.

It had been found from the fatigue propagation tests performed on HDPE corresponding to 0.1 Hz test frequency at different temperatures that crack propagation did not start even after very long times (approximately one week) of testing. Hence, we do not have any fatigue crack growth data for these tests.

As mentioned in section 3.2.2, in the present study an industrial video camera was used for crack growth monitoring. Table 3.2 show the a-N table for CPVC fatigued at 70^{o} C and 0.1 frequency. Crack propagation data from the fatigue crack propagation tests on HDPE at 0^{o} C are given in table 3.3 for test frequency equal to 10 Hz. These tables are the samples from the FCP test results. Similar tables were used to develop a-N curves. The detailed analysis and discussion of these results are provided in chapter 5.

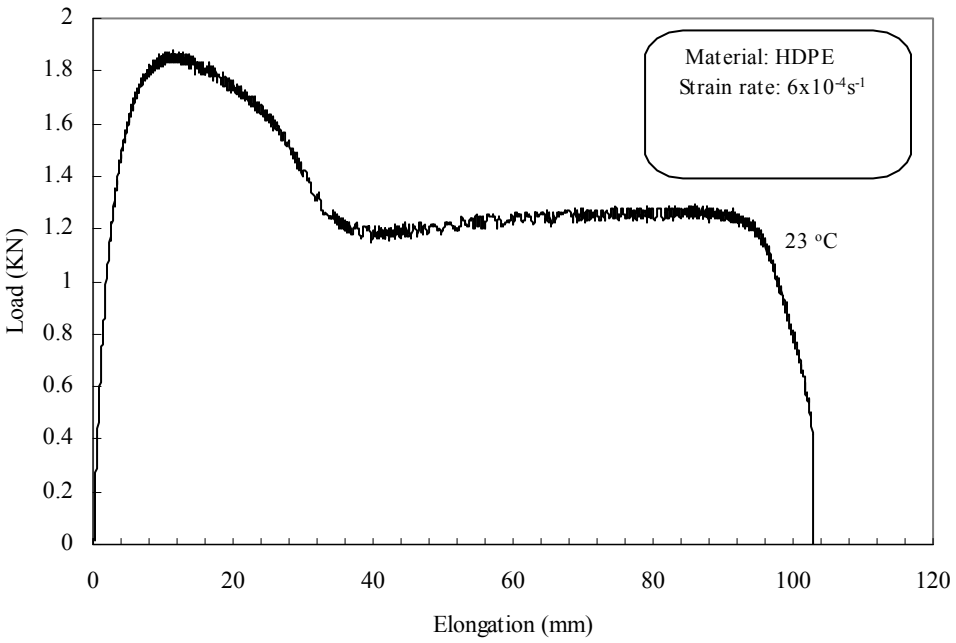

Figure 3.12 Load-elongation curves for HDPE at 23° C temperatures.

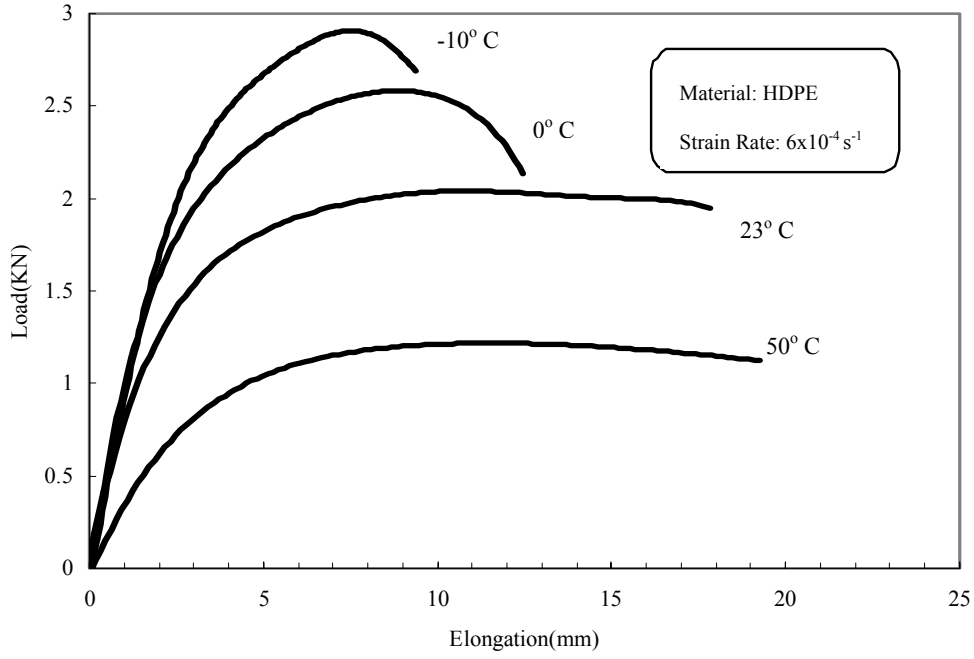

Figure 3.13 Load-elongation curves for HDPE at different test temperatures.

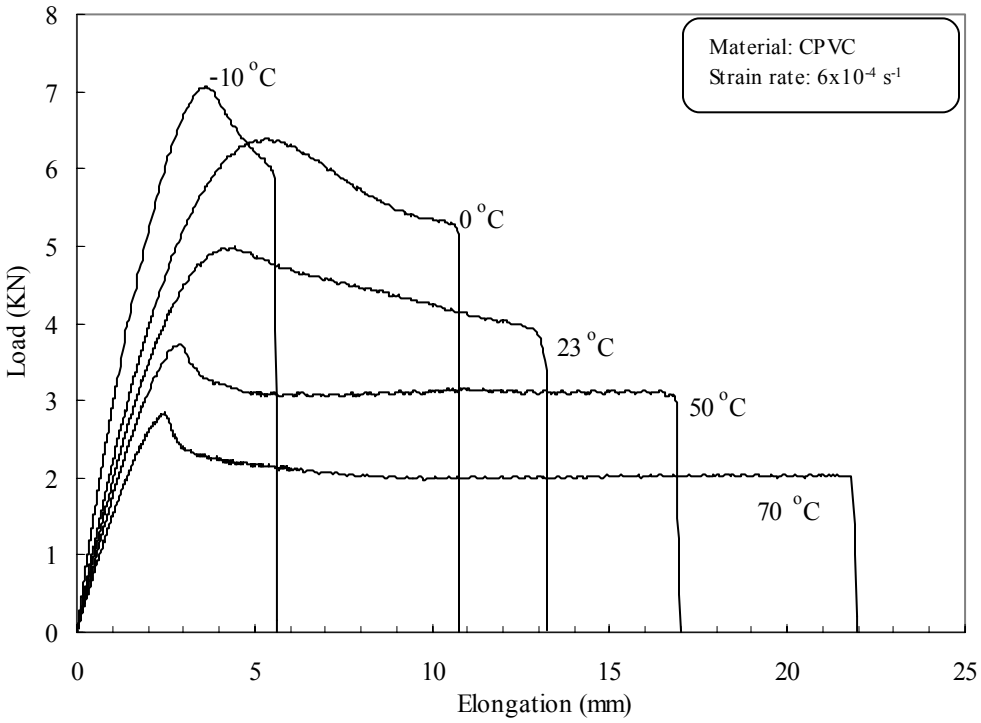

Figure 3.14 Load-elongation curves for CPVC [19] at different test temperatures.

Table 3.1 Results of monotonic tests performed on HDPE specimens.

Serial No.	Yield Strength (MPa)	Elastic Modulus (MPa)
-10° C		
1	32.61	1032.00
2	31.79	1038.5
Average	**32.20**	**1035.25**
0° C		
3	29.49	923.25
4	30.00	925.35
Average	**29.74**	**924.30**
23° C		
5	23.85	670.3
6	23.27	665.10
Average	**23.56**	**667.7**
50° C		
7	14.21	291.95
8	14.55	287.35
Average	14.38	289.65

Table 3.2 Crack propagation data obtained from fatigue crack propagation test on CPVC at 70^{o} C and 0.1 Hz.

Crack length 'a'	No. of cycles 'N'	Crack length 'a'	No. of cycles 'N'
0	0	1.648	538
0.994	401	1.701	544
0.989	407	1.772	550
1.014	413	1.877	555
1.038	419	1.946	561
1.035	424	2.030	567
1.057	430	2.111	572
1.097	436	2.217	578
1.119	441	2.323	584
1.116	447	2.455	590
1.140	453	2.576	595
1.166	458	2.709	601
1.160	464	2.922	607
1.151	470	3.168	612
1.199	476	3.386	618
1.249	481	3.597	624
1.243	487	3.888	629
1.261	493	4.227	635
1.316	498	4.625	641
1.374	504	5.161	647
1.404	510	5.643	652
1.426	515	6.175	658
1.475	521	7.005	664
1.534	527	8.070	669
1.555	533	9.484	675

Table 3.3 Crack propagation data obtained from fatigue crack propagation test on HDPE at 0^{o} C and 10 Hz.

Crack length 'a'	No. of cycles'N'	Crack length 'a'	No. of cycles 'N'
0	0	1.424	475975
0.400	303175	1.530	483175
0.460	310375	1.648	490375
0.507	317575	1.757	497575
0.538	324775	1.841	504775
0.558	331975	1.966	511975
0.579	339175	2.116	519175
0.592	346375	2.267	526375
0.586	353575	2.386	533575
0.587	360775	2.535	540775
0.583	367975	2.754	547975
0.584	375175	2.903	555175
0.596	382375	3.097	562375
0.628	389575	3.303	569575
0.664	396775	3.510	576775
0.703	403975	3.710	583975
0.747	411175	3.978	591175
0.810	418375	4.301	598375
0.884	425575	4.645	605575
0.963	432775	5.109	612775
1.038	439975	5.467	619975
1.113	447175	5.894	627175
1.188	454375	6.547	634375
1.260	461575	7.603	641575
1.336	468775	10.519	648775

CHAPTER 4

EFFECT OF TEMPERATURE ON MONOTONIC PROPERTIES

4.1 Introduction

In this chapter the effect of temperature on the monotonic properties of HDPE is discussed. Tensile test specimens were designed and prepared according to the ASTM D638 Standard [67]. Tensile tests were performed at –10, 0, 23 and 50^{o} C on the different specimens at a crosshead speed of 5 mm/min (strain rate $6x10^{-4}$ s^{-1}). The data derived from tensile tests is important from practical point of view; providing information on the elastic modulus, yield and fracture strengths. This information is essential for material selection during design of engineering components. Furthermore, it is used in the present study to explain the effect of temperature on fatigue crack resistance and to develop FCP master curves.

Due to the dependence of mechanical properties on a large variety of parameters, it is difficult for the designer to select a certain material without knowing all these parameters. The mechanical properties like yield strength and elastic modulus are usually given as a range for plastics. Thus the accurate determination of mechanical properties of polymers with respect to environment and material variables is very important. A polymer can show all the features of a glassy brittle solid or an elastic rubber or a viscous

liquid depending on the temperature. Many researchers have shown temperature dependence of mechanical properties of different polymers like PMMA, cellulose acetate, PVC, etc. The degree of dependence is related to the structure and crystallinity of the polymer.

In the present study, it is observed that the stress strain properties of HDPE are sensitive to temperature. Figure 4.1 shows the stress-strain curves for HDPE at 23^{o} C. Figure 4.2 shows the stress-strain curves for HDPE at different temperatures. Several features of these curves are worth noting; increasing the temperature produces, a decrease in elastic modulus and a reduction in tensile strength.

The monotonic tests for same CPVC material being used in this study were conducted earlier by Merah and Irfan [19]. Their results are used in our study to explain the temperature effect on the FCP in the CPVC material. Figure 4.3 shows the stress-strain curves for CPVC [19] at different temperatures. The effect of temperature on the main tensile properties such as yield stress, elongation and elastic modulus is discussed in detail in the following sections.

4.2 Effect of Temperature on Yield Strength

A normal tensile test on a polymer produces a stress-strain curve similar to that of a metal. As the strain is increased, the material passes through a recoverable elastic region, which in contrast to metals is usually non-linear. The slope of the curve decreases until it reaches a peak value in stress, which can be used to define the yield stress, σ_{ys}. Strictly speaking, the yield point of the material should be described as the point at which permanent set takes place. This is very difficult to define in polymers, as in polymers

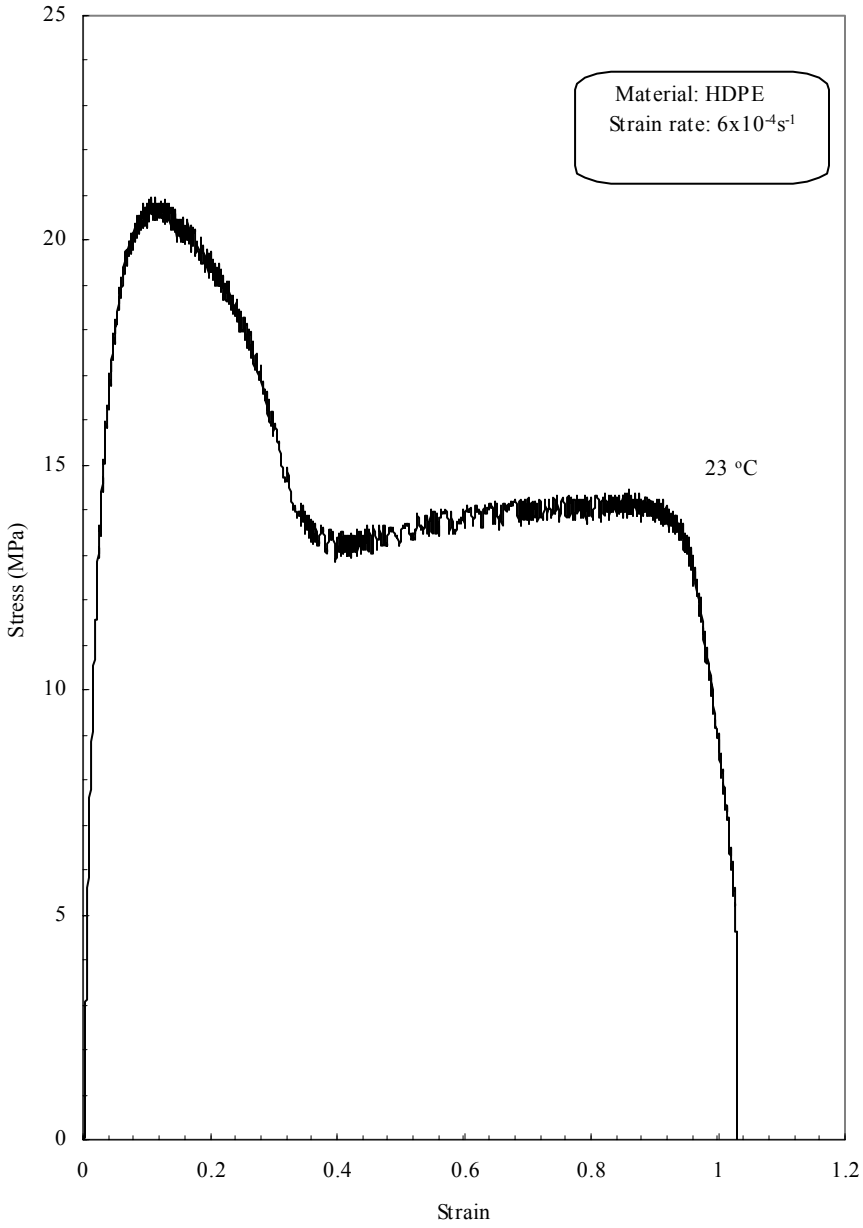

Figure 4.1 Stress strain curves for HDPE at 23^{o} C temperatures

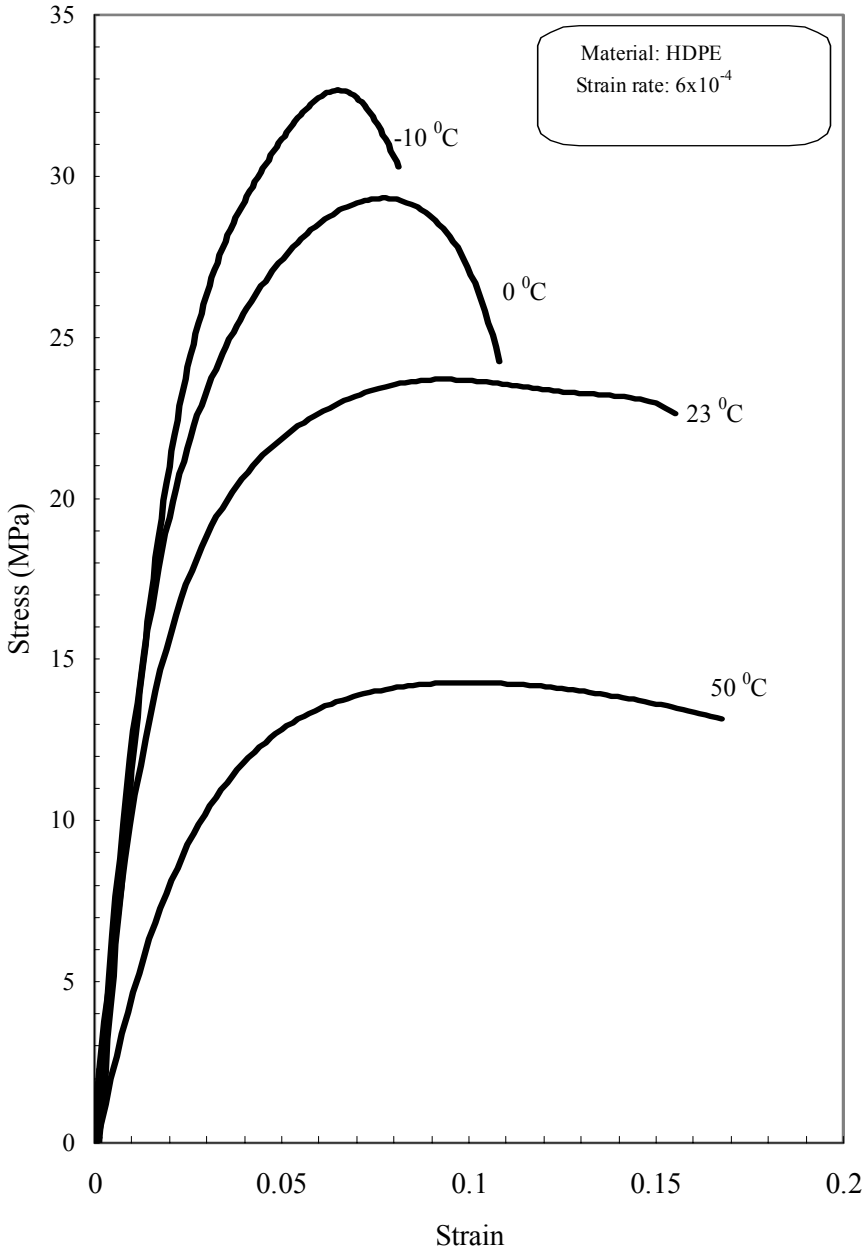

Figure 4.2 Stress strain curves for HDPE at different temperatures

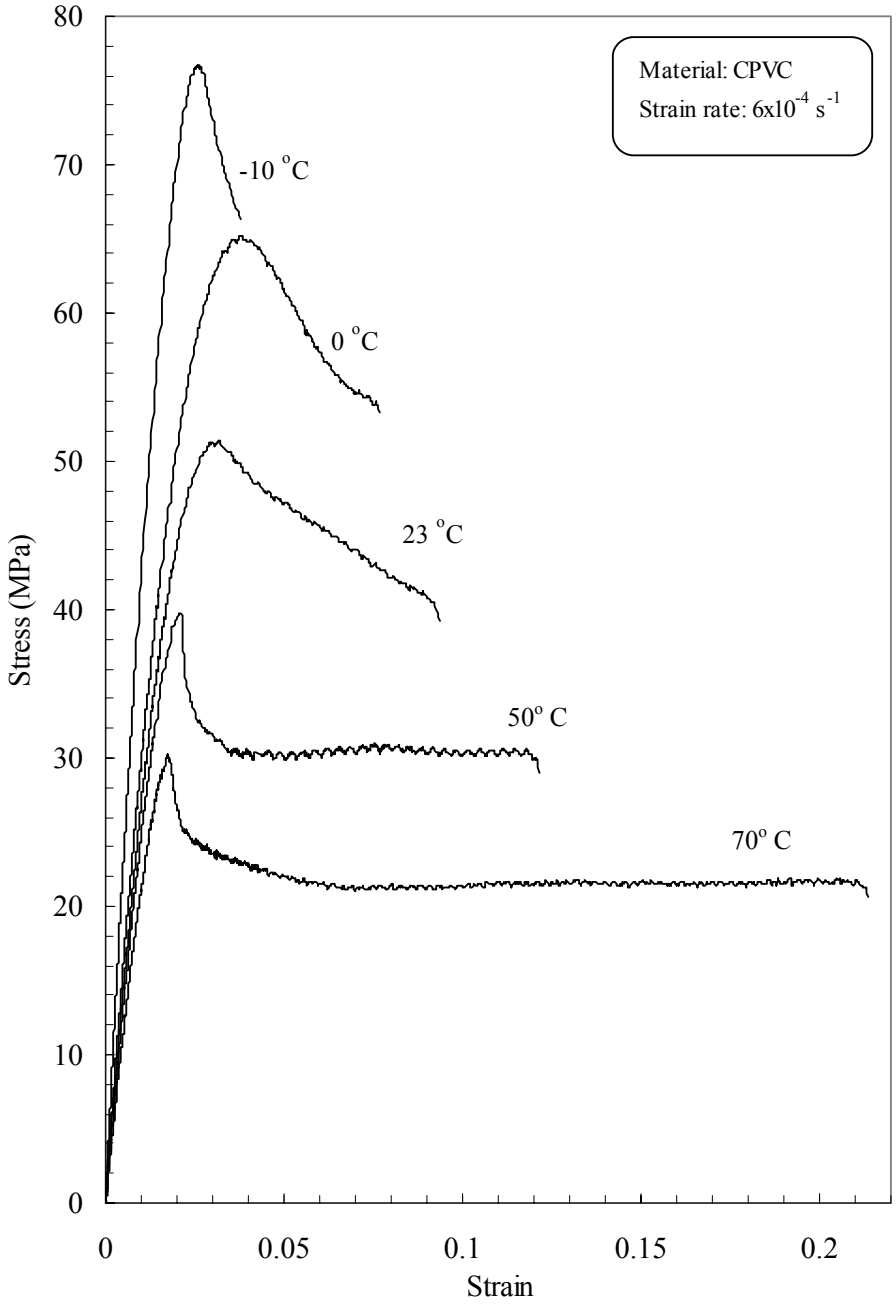

Figure 4.3 Stress strain curves for CPVC at different temperatures [19]

there is no clear distinction between elastic recoverable deformation and plastic irrecoverable deformation.

In case of polymers yield coincides with the observation of a maximum load in the load-elongation curve. The yield stress then can be defined as the true stress at the maximum observed load. Because this stress is achieved at comparatively low elongation of the sample it is often adequate to use the engineering definition of the yield stress at the maximum observed load divided by the initial cross section area.

The temperature dependence of yield stress for different polymers has been studied by many researchers. Povolo et al [12] shown that there is a linear dependence of yield stress with temperature for PVC. Similar results are given by Che et al [13] and Hit and Gilbert [16] for PVC in the temperature range (-60^o to 60^o C) and (23^o to 180^o C) respectively.

The variation of yield stress with temperature for HDPE is shown in figure 4.4. The value of yield stress at each temperature (Table 4.1) is the average value of all the tests done at that condition. It can be seen that the yield stress varies linearly in the temperature range –10 to 50^o C. The slope of the linear regression line for HDPE is –0.2987, with a linear correlation coefficient of 0.9948. The linear dependence of yield stress with temperature for HDPE can be expressed as;

$$\sigma_{ys} = 111.3 - 0.2987T \qquad \text{for } -10^o\text{ C} \le T \le 50^o\text{ C} \qquad (4.1)$$

Irfan and Merah [19] have investigated the effect of temperature on CPVC in the temperature range of -10^o to 70^o C. Their results are reproduced in figure 4.5. The linear dependence of yield strength with temperature for CPVC, was described by

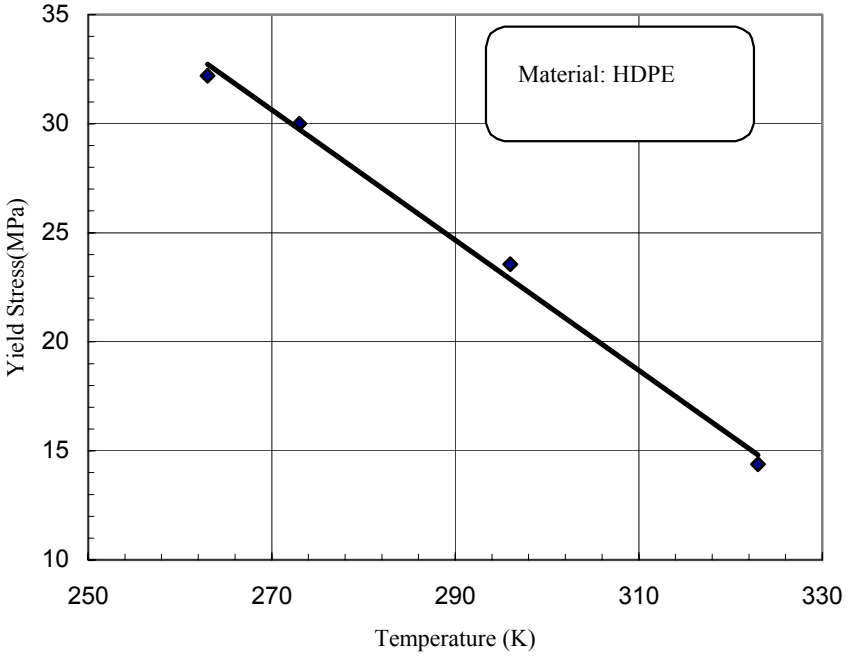

Figure 4.4 Variation of yield stress with temperature for HDPE.

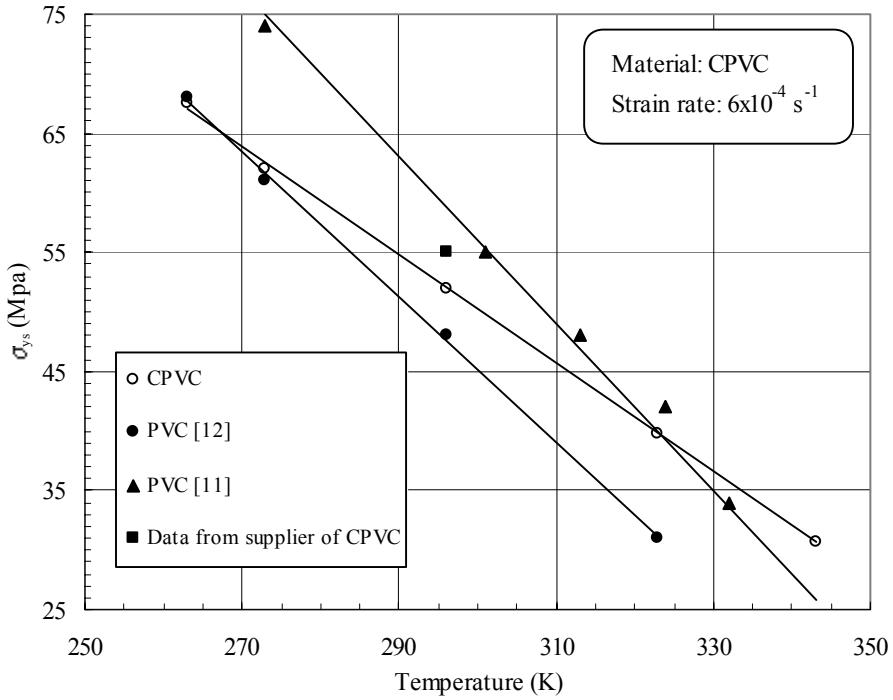

Figure 4.5 Variation of yield stress with temperature for CPVC [19]

Table 4.1 Yield Stress and Elastic Modulus of HDPE at different temperatures.

Temperature	**Yield Stress (MPa)**	**Elastic Modulus (MPa)**
-10	32.20	1035.25
0	30.00	924.30
23	23.56	667.7
50	14.38	289.65

$$\sigma_{ys} = 187 - 0.456T \qquad \text{for } -10^{o}\,C \le T \le 70^{o}\,C \qquad (4.2)$$

By comparing both HDPE and CPVC results it can be concluded that the yield stress of CPVC is more sensitive to temperature (the slope being 1.5 times higher).

Eyring theory of viscosity [68] very well defined the temperature and the strain rate dependence of the yield behavior of polymers. For temperatures below the glass transition temperature of the polymer, the yield stress is as follows:

$$\frac{\sigma_{ys}}{T} = \frac{R}{V}\sinh^{-1}\left[\frac{\in}{2A_{\in}}\exp\left(\frac{\Delta H}{RT}\right)\right] \qquad (4.3)$$

Where R is the universal gas constant, V is the activation volume also known as the Eyring flow volume; for PVC it is 8.60 nm^3 [68], $\in$ is the strain rate, ΔH is the activation energy and $A_{\in}$ is a material constant. At the yield in glassy polymers, high stresses are encountered, hence equation (4.3) can be approximated, assuming sinh (x) = exp (x) / 2 (i.e. for large x) as;

$$\frac{\sigma_{ys}}{T} = \frac{\Delta H}{VT} + \frac{R}{V}\ln\left(\frac{\in}{A_{\in}}\right) \qquad (4.4)$$

In the above Eyring Model, ΔH, V, R, $\in$, $A_{\in}$ are constant for a given material, for tests conducted at constant strain rates. Thus, the above model predicts a linear relationship between yield stress and temperature. The results in figure 4.4 and 4.5 confirm this linear relationship for HDPE and CPVC [19] in this study.

4.3 Effect of Temperature on Modulus of Elasticity

Modulus of elasticity or tensile modulus is the ratio of stress to strain within the elastic region of the stress-strain curve (prior to the yield point). According to Hooke's law the modulus of elasticity is defined as

$$E = \sigma / \varepsilon \quad (4.5)$$

Modulus of elasticity can be also defined as the slope of the tangent to the part of the stress-strain curve which lies in the limit of proportionality. The variation in elastic modulus with temperature for HDPE is shown in figure 4.6. It can be observed that, in the present temperature range, E decreases linearly with increasing temperature.

Povolo et al [12] have also reported linear dependence of E with temperature for PVC. Povolo et al [12] expressed the modulus of elasticity as a function of temperature, in the following form

$$E(T) = E_o - \xi T \quad (4.6)$$

The values of Slope, ξ and intercept, E_o obtained for PVC by Povolo are (13.30 ± 0.7 GPa) and (34 ± 2 MPa/K) respectively.

A linear regression is done on the elastic modulus values of HDPE (figure 4.6) with a correlation coefficient of 0.9963. From this regression analysis the values of E_o and ξ for HDPE are found to be 4.304 GPa and 12.38 MPa/K respectively. Irfan and Merah [19] also reported that E increased with decreasing temperature for CPVC from -10^o C to 70^o C. The variation in elastic modulus with temperature for CPVC obtained by them is shown in figure 4.7. The values of E_o and ξ for CPVC were found to be 6.53 GPa and 12.40 MPa/K respectively. The value of the slopes ξ of E-T curves for CPVC and HDPE are the same; the stiffness of these materials is same. By comparing both HDPE and CPVC results it can be concluded that the modulus of elasticity of CPVC is more sensitive to temperature (the slope being 1.5 times higher).

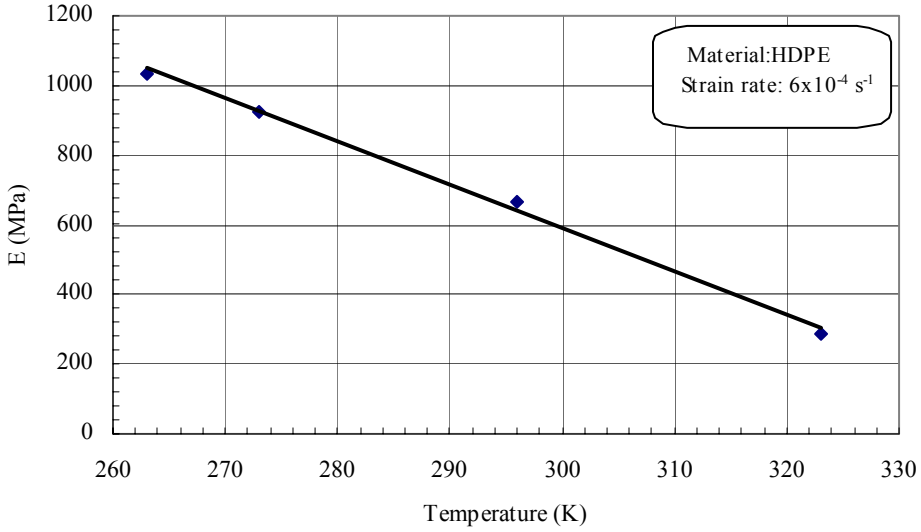

Figure 4.6 Variation of elastic modulus with temperature for HDPE.

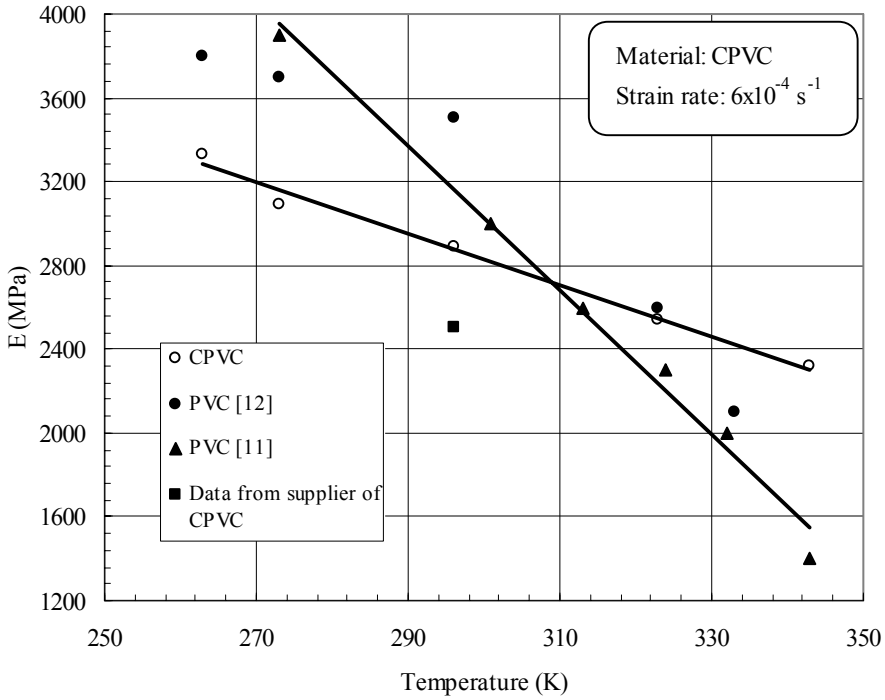

Figure 4.7 Variation of elastic modulus with temperature for CPVC [19]

4.4 Relationship between Elastic Modulus and Yield Stress

Elastic modulus and yield stress are linearly related to each other. Hence, any variable that affects elastic modulus will also going to affect the yield stress. Argon et al [69] derived the theories relating elastic modulus to yield stress over a wide temperature range. These theories show excellent agreement with Argon's experimental results but their analytical form is too complex to be applied to practical situations. Kitagawa [70] in 1977 has expanded and generalized Argon's theory to arrive at a relationship between shear stress (τ) and shear modulus (G) which can be represented by a power law relation of the form,

$$\frac{T_o \tau}{T \tau_o} = \left[\frac{T_o G}{T G_o} \right]^n \tag{4.7}$$

Here T_o is the reference temperature, the values τ_o and G_o are of shear yield stress and shear modulus at some T_o (conveniently taken as the ambient temperature), and n is a temperature independent exponent.

The tensile modulus and yield stress are converted into the corresponding shear modulus and shear yield stress for using Kitagawa's relationship. This can be done using the following equations of solid mechanics:

$$G(T) = \left[\frac{E(T)}{2(1+\nu)} \right] \tag{4.8}$$

$$\tau(T) = \left[\frac{\sigma_{ys}(T)}{\sqrt{3}} \right] \tag{4.9}$$

Here ν is the Poisson's ratio (ratio of the strain in the z direction over the strain in the x direction when a specimen is pulled in tension uniaxially in the z direction).

Kitagawa in agreement with Argon showed that a relation of the form of equation 4.7 held over a wide range of temperature for most polymers. He also found that the exponent, n had a unique value of 1.63 for all amorphous polymers, and between 0.80 and 0.90 for semi-crystalline polymers.

Figure 4.8 is a log–log plot according to equation 4.7 for the values of τ and G obtained for HDPE tested over temperature range –10 to 50^{o}. The value of Poisson's ratio was assumed constant (equal to 0.46 [72]) over the temperature range of interest. The line drawn on the graph has a slope of 0.5484 and all the points fall very close to this line with a coefficient of regression of 0.9995. The obtained value of slope is less than that for semi-crystalline polymers (a polymer that is neither all crystalline in nature, nor is it amorphous in nature.) because of presence of additives in the HDPE pipe chosen for testing. Irfan and Merah [19] have also used Kitagawa's model in their study of CPVC, they reported the value of exponent n equal to 1.69.

4.5 Effect of Temperature on Elongation Yield Strain and Necking

4.5.1 Elongation

The stress-strain curves for polymers tested over a wide temperature range show three different mechanical behavior [68]. First one is brittle fracture which is characterized by no yield point, a region of Hookean behavior at low strains. Second is yield behavior characterized by a maximum in the stress-strain curve followed by yielding deformation, which is usually associated with crazing or shear banding and usually ductile failure. Third, one is rubber-like behavior- characterized by the absence of a yield point maximum but exhibiting a plateau in an engineering stress-strain curve.

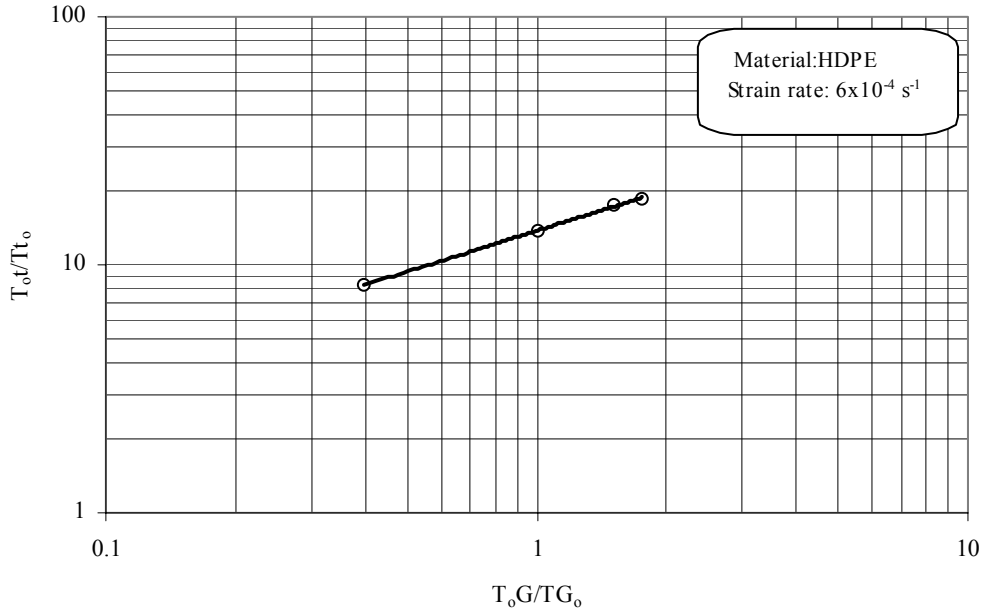

Figure 4.8 Relationship between τ and G for HDPE.

Rubbery behavior is usually present when temperatures are higher than the glass transition temperature.

From the tests conducted on HDPE over the temperature range -10 to 50^{o} C, yield behavior is observed to present at all temperatures. This is evident from figure 4.2. Ductile fracture occurs with a definite yield point characterized by a maximum in the stress-strain curve and considerable plastic deformation, which is usually associated with crazing.

4.5.2 Yield Strain

Yield strain is defined as the ratio of yield stress to modulus of elasticity, i.e.

$$\varepsilon_y = \frac{\sigma_{ys}}{E} \tag{4.10}$$

Figure 4.9 shows the variation of yield strain (denoted by ε_y) with temperature. The yield strain remains fairly constant for the temperature range studied. Similar results are given by Povolo et al [12] and Irfan and Merah [19] for PVC and CPVC respectively.

4.5.3 Necking

As with metals, polymers can show localized necking after yield. Necking is first observed as a local reduction in cross sectional area and corresponds to the drop in load observed at the yield point. If the neck is stable, the load will remain at a steady value and the neck will traverse the length of the specimen. The mechanisms of necking start with either a local reduction in cross sectional area or a local fluctuation in material properties which allows yielding to take place in a small element. Deformation will continue within this element because it has a lower effective stiffness and the local stress is higher.

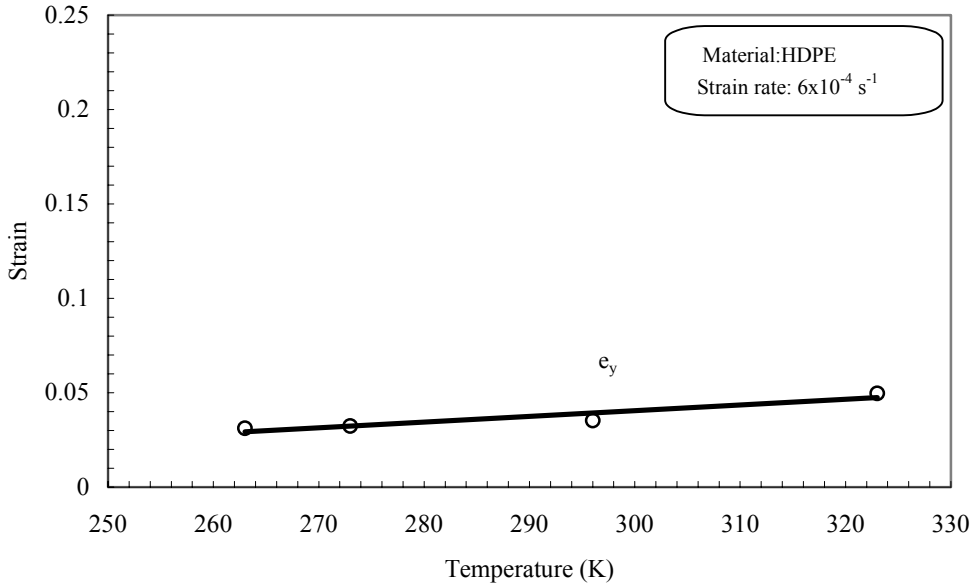

Figure 4.9 Variation of yield strain with temperature for HDPE.

In the case of HDPE it can be seen that considerable necking occurs at all tests temperatures (-10 to 50^{o} C). The neck starts to form at the point where the cross sectional area of the specimen is minimum. Once the whole cross section has yielded, the neck travels along the length of the specimen at constant load until fracture occurs.

4.6 Development of FCG Master Curves using Monotonic Properties

The technique of developing FCG master curves using the monotonic properties is based upon the dependence of monotonic properties on the temperature as can be seen in figures 4.2- 4.6. The monotonic properties influence the FCG properties of CPVC as well as HDPE. As a lower value of yield stress results in a high value of crack tip opening displacement (CTOD), which will introduce blunting of the crack tip, which is expected to lower the crack propagation rate. In order to know this effect da/dN is plotted in terms of the modified stress intensity factors. The stress intensity factors are modified by CTOD (which describes the crack tip condition in elastic plastic materials and is used as a fracture criterion). The detailed analysis and discussion of the development of these master curve s are provided in chapter 5.

CHAPTER 5

EFFECT OF TEMPERATURE AND FREQUENCY ON FATIGUE CRACK GROWTH PROPERTIES

5.1 Introduction

In this chapter the results concerning the effect of temperature and frequency on the fatigue crack growth properties of CPVC and HDPE are discussed. This chapter consists of four main sections. The first section deals with temperature and frequency effects on a-N curves for CPVC and HDPE. The second deals with the characterization of fatigue crack propagation rate in CPVC and HDPE. The third section concentrates on the development of da/dN-ΔK master curves, and the last section presents the fractographic analysis of failed specimens.

Fatigue tests were carried out at –10, 0, 23, 50 and 70^{o} C for CPVC and at –10 and 0^{o} C for HDPE. FCP tests were performed at the frequencies of 0.1, 1 and 10 Hz, on single edge notched plate specimens. The tests were performed under a stress ratio R (σ_{min} / σ_{max}) of 0.20. Stress ranges ($\Delta\sigma$) of 13.30 and 11.00 MPa were used for CPVC and 9.0 and 8.0 MPa for HDPE. The maximum stress was kept below 50 % of the yield stress to avoid large plastic deformations.

5.2 a-N Curves

The fatigue failure is characterized by three distinct processes; (1) crack initiation, where a small crack forms at some point of high stress concentration; (2) crack propagation, during which this crack advances incrementally with each stress cycle; and (3) final failure, which occurs very rapidly once the advancing crack has reached a critical size. The fatigue life N_f, i.e., the total number of cycles to failure, is taken as the sum of the number of cycles for crack initiation N_i and crack propagation N_p.

The contribution of the final failure step to the total fatigue life is insignificant, since it occurs so rapidly. Relative proportions to the total life of N_i and N_p depend on the particular material, specimen or component geometry and shape and test conditions. For the FCG testing program in this study, 1 mm deep notch was manually introduced in all specimens with a sharp blade. Since the notch is sharp thus the initiation period is expected small and does not need consideration. The present study will concentrate on the crack propagation period of the life and its characteristics.

Any crack propagation study requires an accurate detection and measurement of crack length. Many monitoring techniques have been employed for crack measurement these include, compliance measurement, acoustic emission detectors, eddy current technique, electro-potential measurements and the use of a calibrated traveling microscope. Most of the data generated for polymeric solids have been based on traveling microscope readings [43, 44, 45 and 73], but other techniques like conductive surface grid printed on specimen surface [62, 63], cathetometer [64] and compliance technique [65,74] have also been used for crack measurement in polymers. In this study a video

camera was used for crack growth monitoring. The data was plotted as discrete points on the a-N plot and a curve was manually fitted to this data.

- **CPVC**

Figure 5.1 shows the a-N curve for CPVC at 23^{o} C and 0.1 Hz. It is observed that initially the curve is approximately flat and the crack growth is very slow. The crack grows only up to 0.50 mm for 3,300 cycles, which is due to the initial threshold resistance provided by CPVC material. Once the crack has grown to about 3-4 mm it takes about 1000 cycles for the crack to travel to the final length a_f of 15.5 mm. Similarly in a-N curve for CPVC at 23 ^{o}C and 1 Hz the crack grows only up to 0.90 mm for 6,600 cycles. Again in a-N curve for CPVC at 23^{o} C and 10 Hz the crack grows only up to 0.6 mm for 12,300 cycles. These observations are true for all the tests.

- **HDPE**

Figure 5.2 illustrates the variation of crack length a with number of cycles N for HDPE at 0^{o} C and 10 Hz. Initially the crack growth is very slow. It took more than 300,000 cycles to initiate the crack and propagate it to 0.50 mm. This is due to the absence of sharp enough notch in HDPE specimens. Once the crack has grown to about 3-4 mm it takes only 90700 cycles for the crack to travel to the final length a_f of 10.2 mm. Similarly in a-N curve for HDPE at -10^{o} C and 10 Hz the crack grows only up to 0.70 mm for more than 450,000 cycles.

5.2.1 Effect of Temperature on a-N Curves

The crack growth in almost all the polymers is sensitive to the environmental conditions. Figures 5.3, 5.4 and 5.5 show representative a-N curves for CPVC at different temperatures for the frequencies of 0.1, 1, and 10 Hz respectively. It can be seen that the

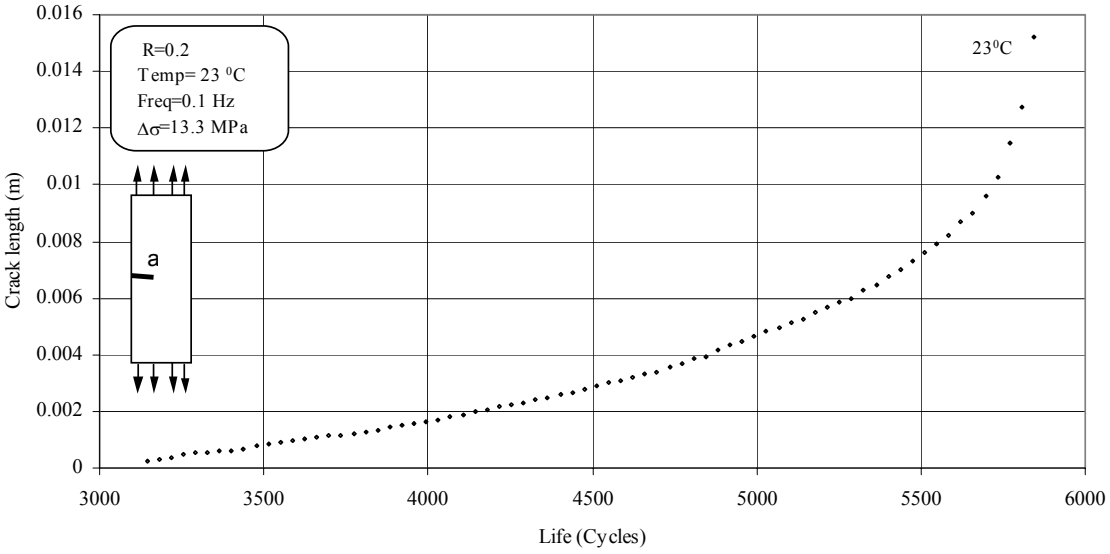

Figure 5.1 a-N curve for CPVC at 0.1 Hz and 23° C.

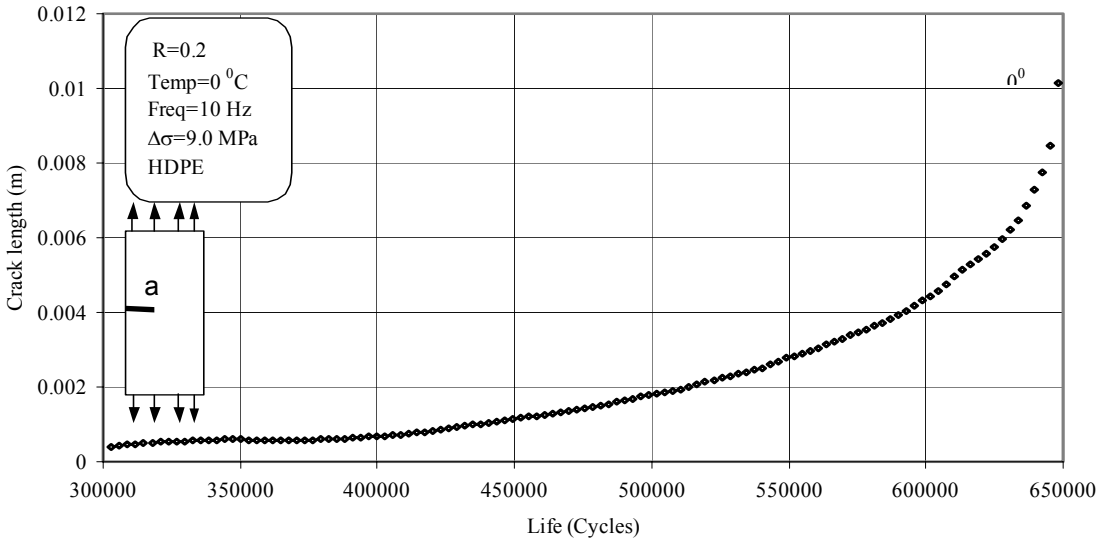

Figure 5.2 a-N curve for HDPE at 10 Hz and 0° C.

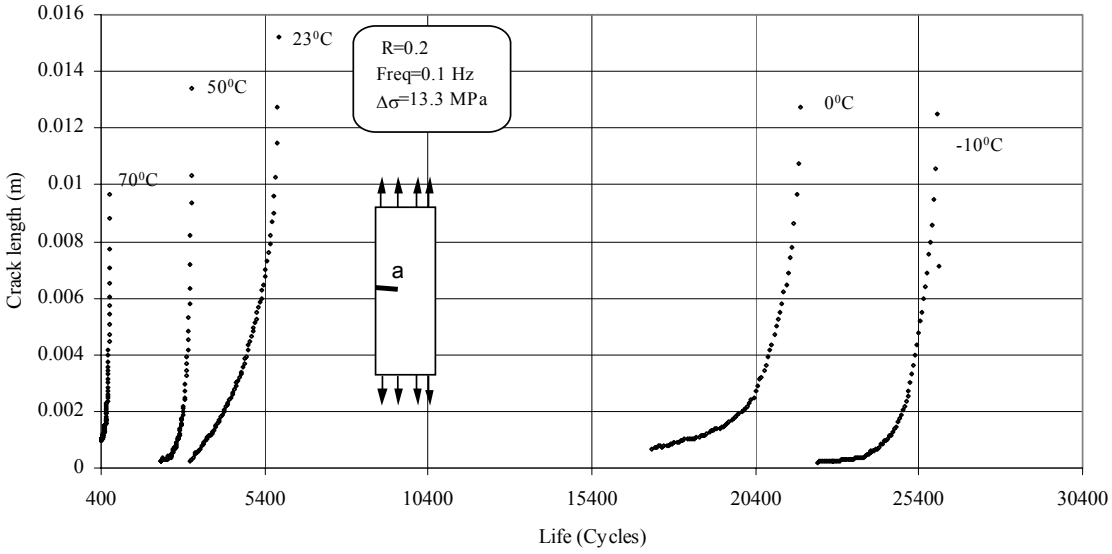

Figure 5.3 a-N curve for CPVC at 0.1 Hz and different temperatures.

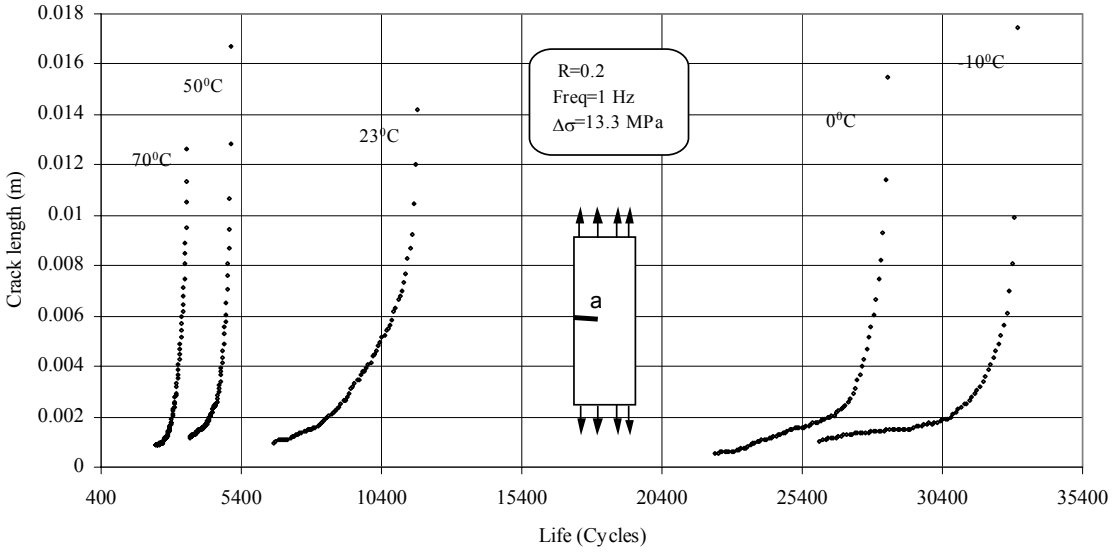

Figure 5.4 a-N curve for CPVC at 1 Hz and different temperatures.

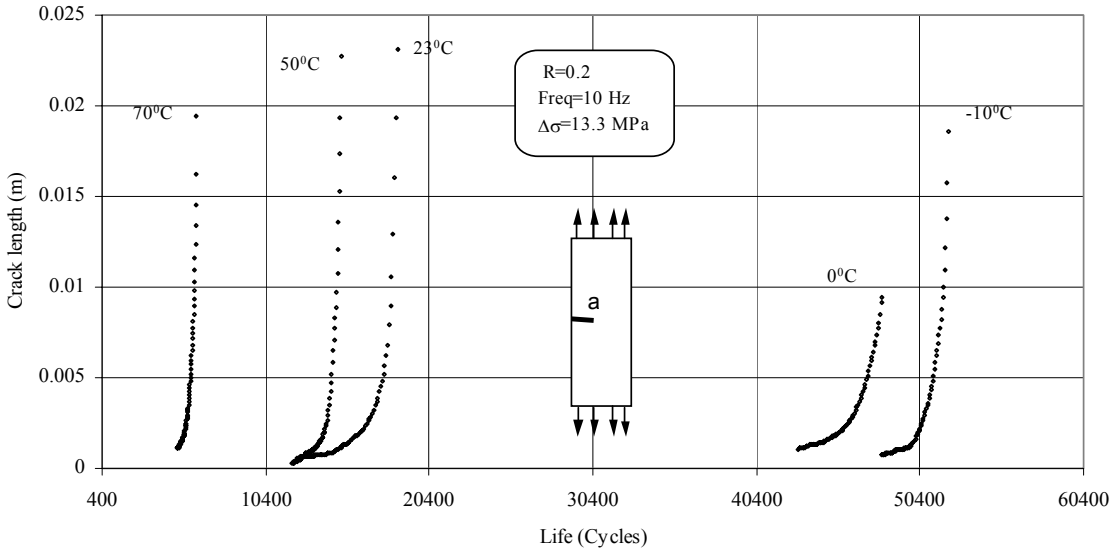

Figure 5.5 a-N curve for CPVC at 10 Hz and different temperatures.

fatigue life (N_f) decreases drastically with increase in temperature for all the frequencies. At high temperatures i.e. 23, 50 and 70^o C large size of craze zones are observed near the crack tip. Also comparably large crack tip opening displacements (CTOD) were observed at high temperatures. At –10^o C and 1 Hz the total life is 33,068 cycles while at 70^o C and 1 Hz, it reduces to only 3473 cycles. The reduction in life is due to the loss of strength in the material. At high temperatures the disentanglement of the molecular chains becomes easier due to the temperature induced molecular vibrations. Whereas at low temperatures the chains are tightly packed and strongly held so it takes a larger number of cycles to disentangle them. It can be inferred from the a-N curves that the propagation life of CPVC specimens varies with temperature. The propagation life does not decrease much in going from -10 to 0^o C for all three frequencies. The difference in propagation lives at -10 and 0^o C is around 2205 cycles, which is expected as the fracture mechanisms remain the same for these temperatures.

A comparison of a-N curves for HDPE at 0^o C and -10^o C for the frequencies of 1 and 10 Hz are shown in Figures 5.6 and 5.7. Fatigue life (N_f) decreases with increase in temperature. For example at 1 Hz frequency the specimen life is 80,100 cycles at -10^o C, it reduces to 65,700 cycles at 0^o C. It is expected that at -10^o C the material is more brittle than at 0^o C. It can be inferred from the a-N curves that the propagation life of HDPE specimens decreases with increasing temperature.

5.2.2 Effect of Frequency on a-N Curves

Polymers are sensitive to the frequency of loading due to their viscoelastic nature. Figures 5.8-5.12 show representative a-N curves for CPVC at different frequencies for the temperatures of –10, 0, 23, 50 and 70^o C. Fatigue life (N_f) decreases drastically with

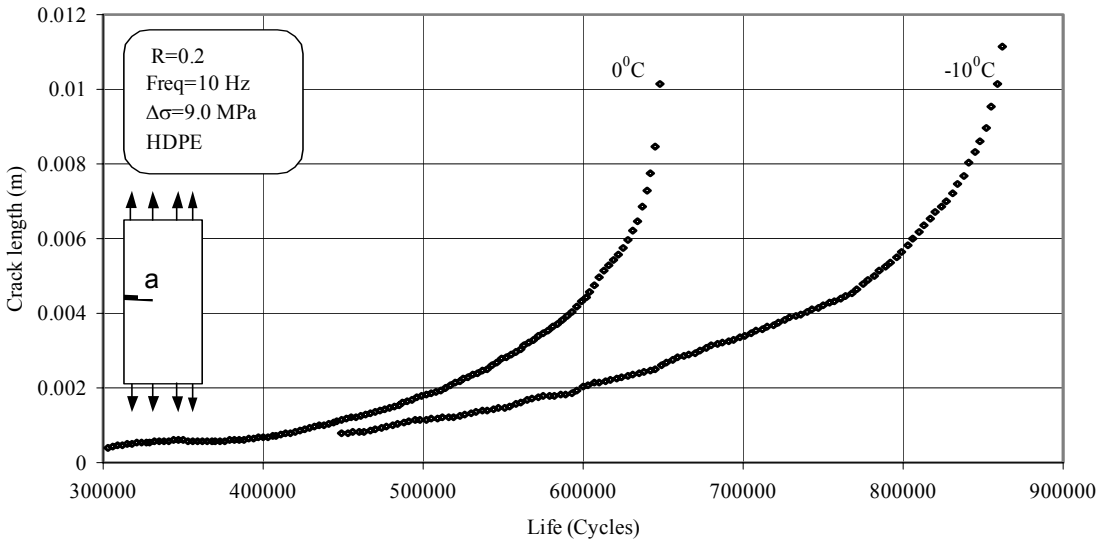

Figure 5.6 a-N curve for HDPE at 10 Hz and different temperatures.

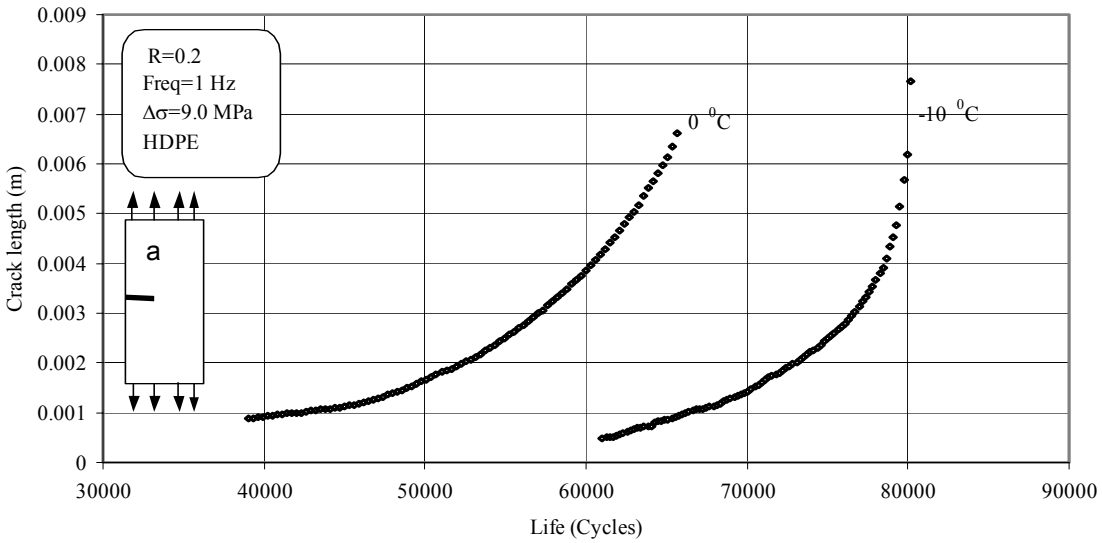

Figure 5.7 a-N curve for HDPE at 1 Hz and different temperatures.

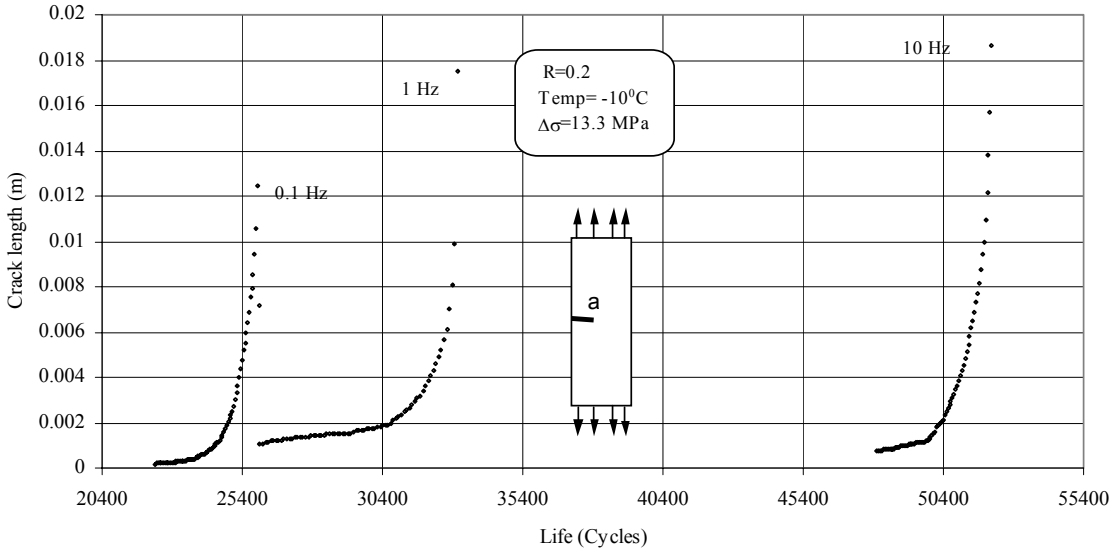

Figure 5.8 a-N curve for CPVC at -10° C and different frequencies.

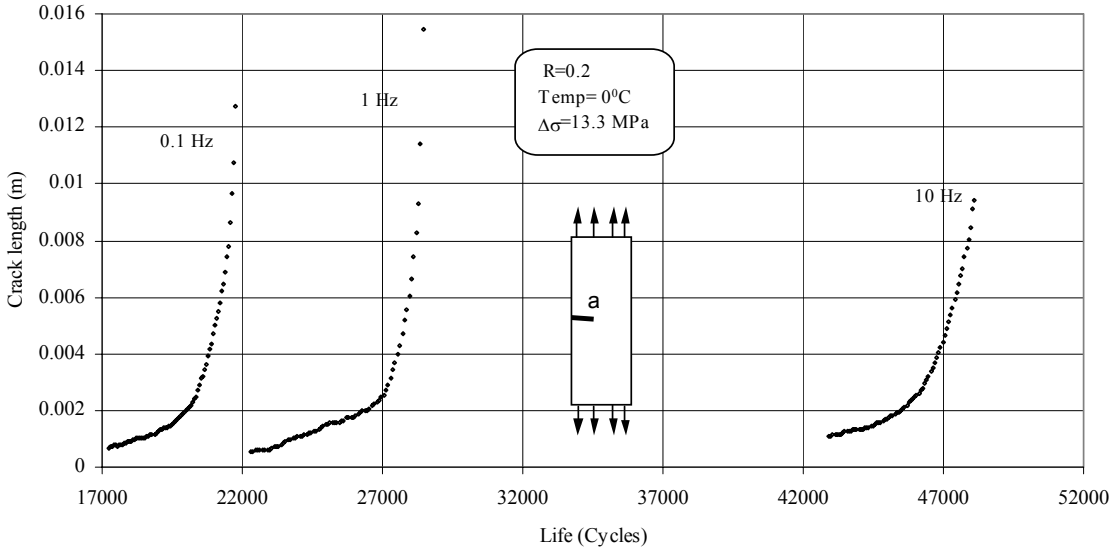

Figure 5.9 a-N curve for CPVC at 0° C and different frequencies.

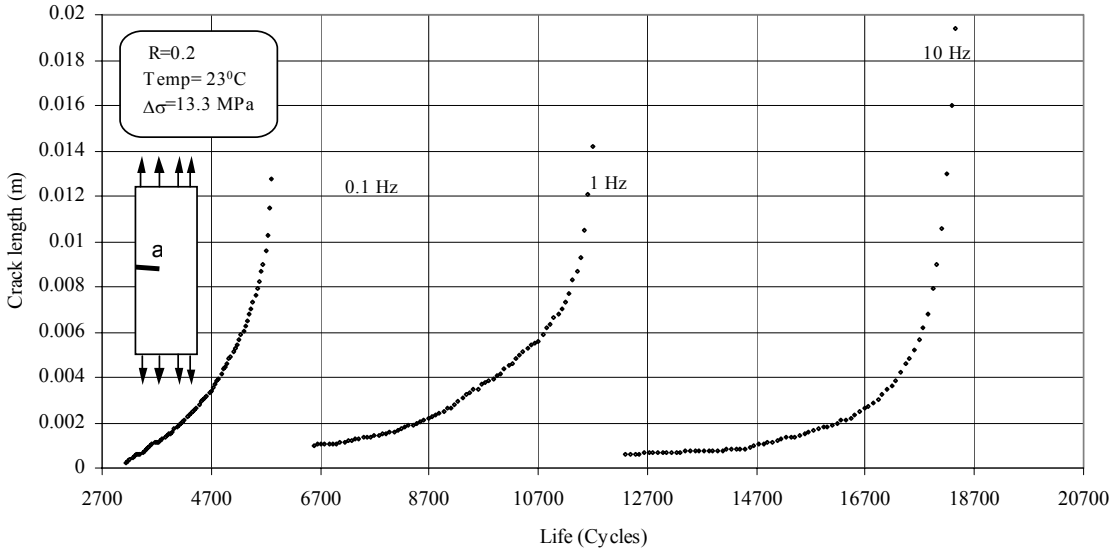

Figure 5.10 a-N curve for CPVC at 23° C and different frequencies.

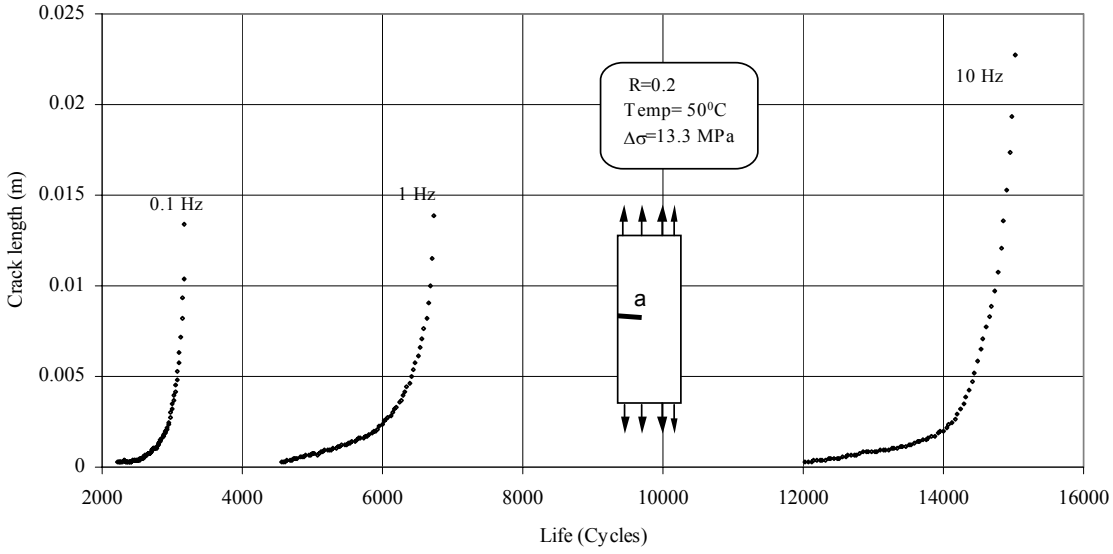

Figure 5.11 a-N curve for CPVC at 50° C Hz and different frequencies.

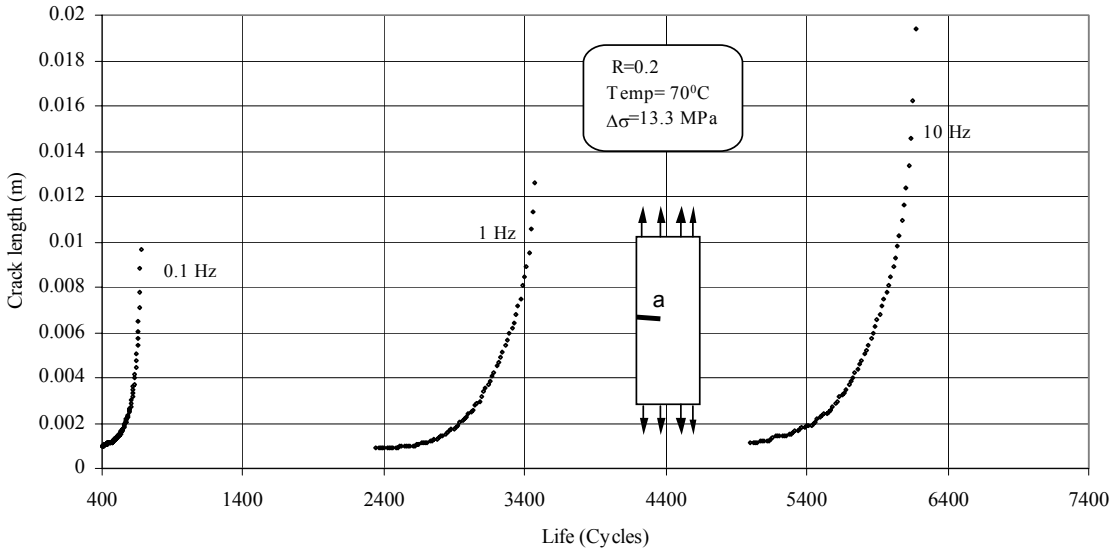

Figure 5.12 a-N curve for CPVC at 70° C Hz and different frequencies.

decreasing frequency for high temperatures (50^{o} C and 70^{o} C). At 10 Hz and 70^{o} C the average specimen life is 6168 cycles while at 0.1 Hz and 70^{o} C, it reduces to only 675 cycles. As at low frequencies the magnitude of chain disentanglements and chain slippage in each cycle is larger because of large period of time involved. The propagation life does not decrease much in going from 10 to 0.1 Hz for temperatures –10 and 0^{o} C, as chain disentanglements and chain slippage occurring at these temperatures are limited, so their magnitude is independent of time they get in every fatigue cycle.

a-N curves for HDPE at different frequencies for –10 and 0^{o} C are shown in Figure 5.13 and 5.14. Fatigue life (N_f) decreases drastically with decrease in frequency for both temperatures. At 10 Hz and 0^{o} C the average life for specimen is 64,8300 cycles while at 1 Hz and 0^{o} C, it reduces to only 65,700 cycles. As at high frequencies there is less time for chain disentanglements and chain slippage in every cycle which results in larger number of cycles to failure. It can be inferred from the a-N curves that the propagation life of HDPE specimens decreases with decreasing frequency.

5.3 Fatigue Crack Propagation Characteristics in CPVC and HDPE

In this section, the results of FCP tests on CPVC and HDPE are discussed. At least three tests are performed at each test condition to ensure the repetition of the results. Data scattering is a common phenomenon in fatigue crack propagation results. The main reason behind data scattering comes from errors in the optical crack measurements.

- **CPVC**

The fatigue crack propagation in CPVC is presented in the form of da/dN vs ΔK plots. The fatigue crack growth da/dN is obtained using slopes of points on a-N curves. These slopes are calculated using seven point difference polynomial technique. Figure

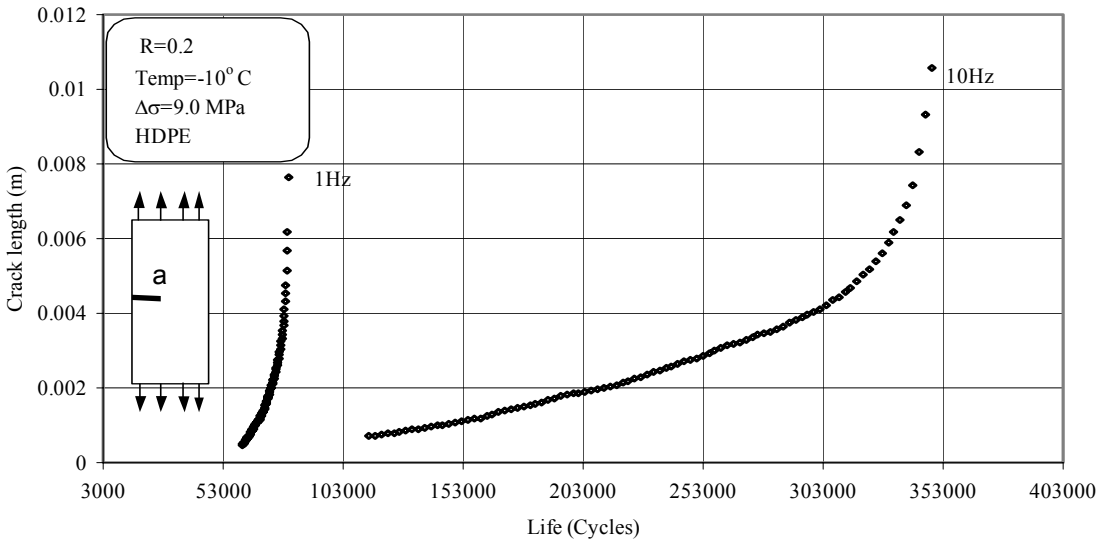

Figure 5.13 a-N curve for HDPE at -10° C Hz and different frequencies.

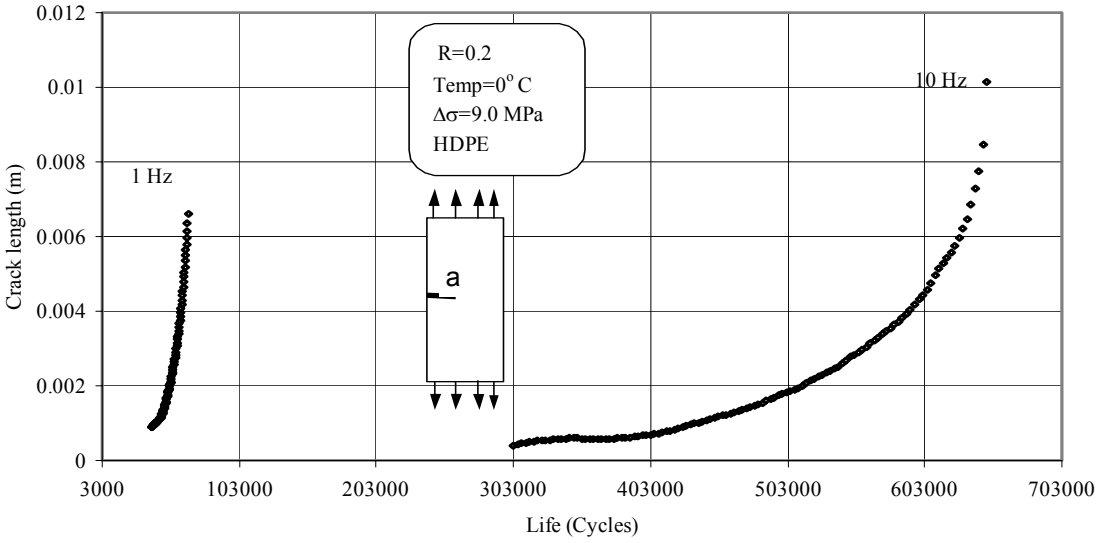

Figure 5.14 a-N curve for HDPE at 0° C Hz and different frequencies.

5.15 shows the FCP characteristic curve for CPVC at 23° C and 1 Hz. The linear portion of the curve which represents the stable crack propagation (known as the Paris region) is from ΔK = 0.8 to 3.1 MPa$\sqrt{m}$, corresponding to da/dN = 6.0×10^{-7} m/cycle to 8.2×10^{-6} m/cycle, respectively. Kim et al [63] have studied the fatigue crack characteristics in uPVC. They reported ΔK values varying from 0.84 to 2.05 MPa$\sqrt{m}$ with a corresponding variation in da/dN from 4×10^{-8} to 5.2×10^{-7} m/cycle. Maddox [65] has studied fatigue crack propagation in uPVC water pipes at room temperature. He reported a variation of ΔK from 0.25 to 2.10 MPa$\sqrt{m}$ for a corresponding growth rate variation of 4×10^{-10} to 9×10^{-8} m/cycle. The power law parameters m and A for CPVC at 23° C and 1 Hz found in the present study and for CPVC by Irfan [53], and for uPVC by Kim [63] and Maddox [65] are given below;

	Present study	Irfan [53]	Kim [63]	Maddox [65]
m	2.39	2.22	2.89	2.54
A ($\times 10^{-7}$)	9.0	8.32	0.65	0.14

Hertzberg and Manson [7] found that for PVC at room temperature the value of ΔK lied between 0.40 to 1.10 MPa$\sqrt{m}$ with da/dN varying from 1.30×10^{-5} to 1.15×10^{-4} m/cycle. The values of m and A were 2.15 and 9.4×10^{-5}, respectively. The above comparisons show that the values of exponent m obtained for CPVC in the present study are close to those of uPVC and PVC, but A is higher by a factor of more than ten suggesting that injection molded CPVC pipe fitting material has a lower crack propagation resistance. This may be due to two factors; lower molecular weight in injection molded parts and brittleness induced by the presence of more chlorine in CPVC.

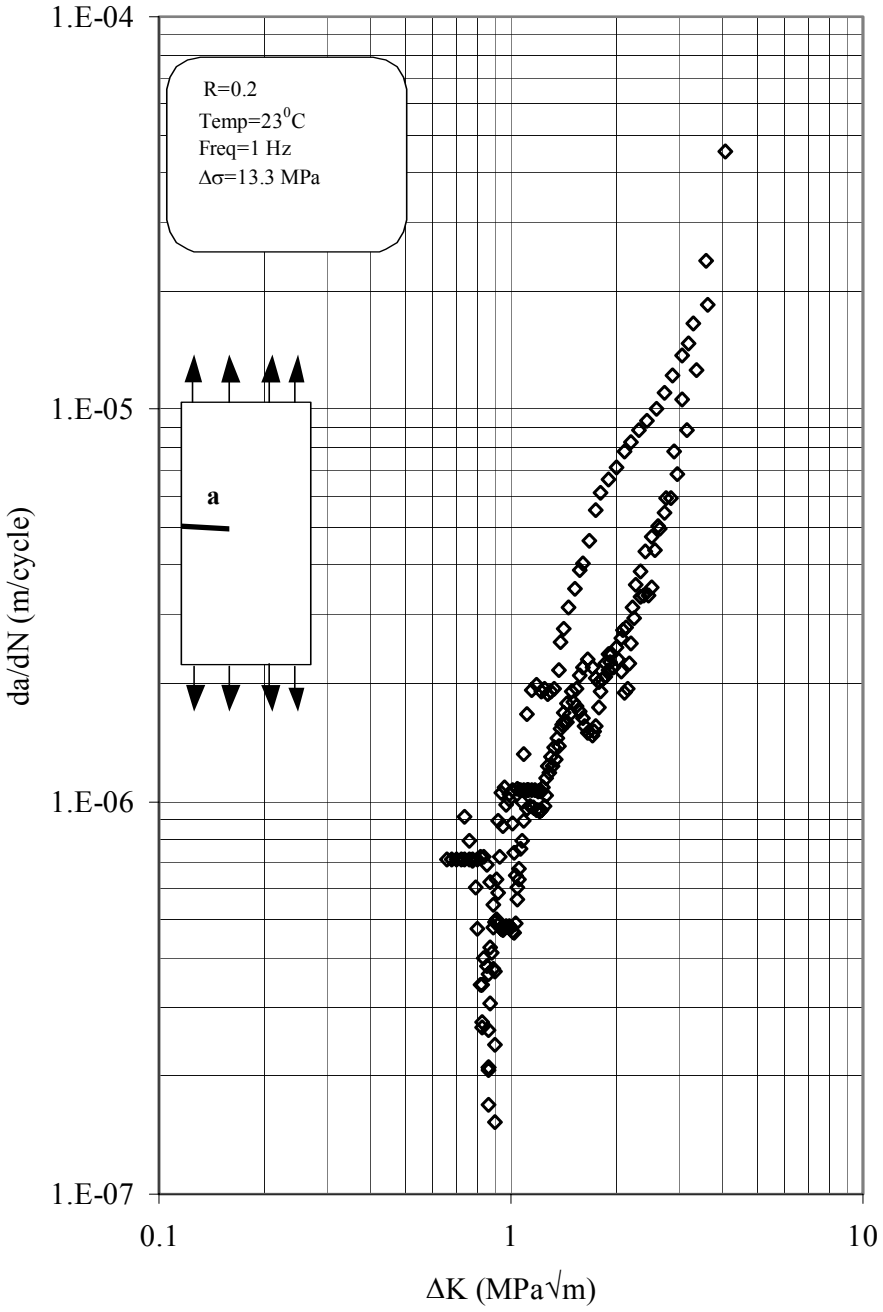

Figure 5.15 da/dN-ΔK curve for CPVC at 1 Hz and 23° C.

Fatigue crack propagation tests were also performed at stress range $\Delta\sigma$ = 11 MPa for 1 and 10 Hz at 70° C to determine if there is any effect of stress on da/dN–ΔK curve, and the result show as expected that a unique curve can be drawn through all the data points. The fatigue crack growth curves at $\Delta\sigma$ = 11 and 13.30 MPa at 1 Hz and 70° C, and 10 Hz and 50° C are shown in figure 5.16 and 5.17. It can be seen that all of the data fall within a band size of 2.0 on da/dN from the curve representing the paris region for these conditions. These curves can be represented by the following equations:

(a) CPVC, 70° C-1Hz:($\Delta\sigma$ = 11,13.30 MPa) $$\frac{da}{dN} = 5.00x10^{-6}\Delta K^{2.40} \qquad (5.1)$$

(b) CPVC,50° C-10Hz:($\Delta\sigma$ = 11,13.30 MPa) $$\frac{da}{dN} = 1.65x10^{-6}\Delta K^{2.26} \qquad (5.2)$$

- **HDPE**

Again, fatigue crack propagation (FCP) in HDPE is presented in the form of da/dN vs ΔK plots. Figure 5.18 shows the FCP characteristic curve for HDPE at 0° C and 10 Hz. The linear portion of the curve which represents the crack propagation is from ΔK = 0.4 to 1.40 MPa$\sqrt{m}$, corresponding to da/dN = $5.00x10^{-9}$ m/cycle to $1.00x10^{-7}$ m/cycle respectively. Bucknall and Dumpleton [50] have performed the fatigue crack growth measurements on two grades of HDPE. They reported a variation of ΔK from 0.4 to 0.8 MPa$\sqrt{m}$ for a corresponding growth rate variation of $3x10^{-9}$ to $8x10^{-8}$ m/cycle for R=0.1 and frequency of 2 Hz. Hakeem and Culver [57] studied the fatigue crack propagation in HDPE, they reported a variation of ΔK from 1.24 to 1.64 MPa$\sqrt{m}$ for a corresponding growth rate variation of $2.3x10^{-9}$ to $2.7x10^{-8}$ m/cycle for R=0.3 and frequency of 5 Hz. Bureau M. and Dickson J. [59] studied the fatigue crack propagation behavior of polystyrene (PS) and 95/5 PS/HDPE blends. They reported ΔK values varying from 0.27

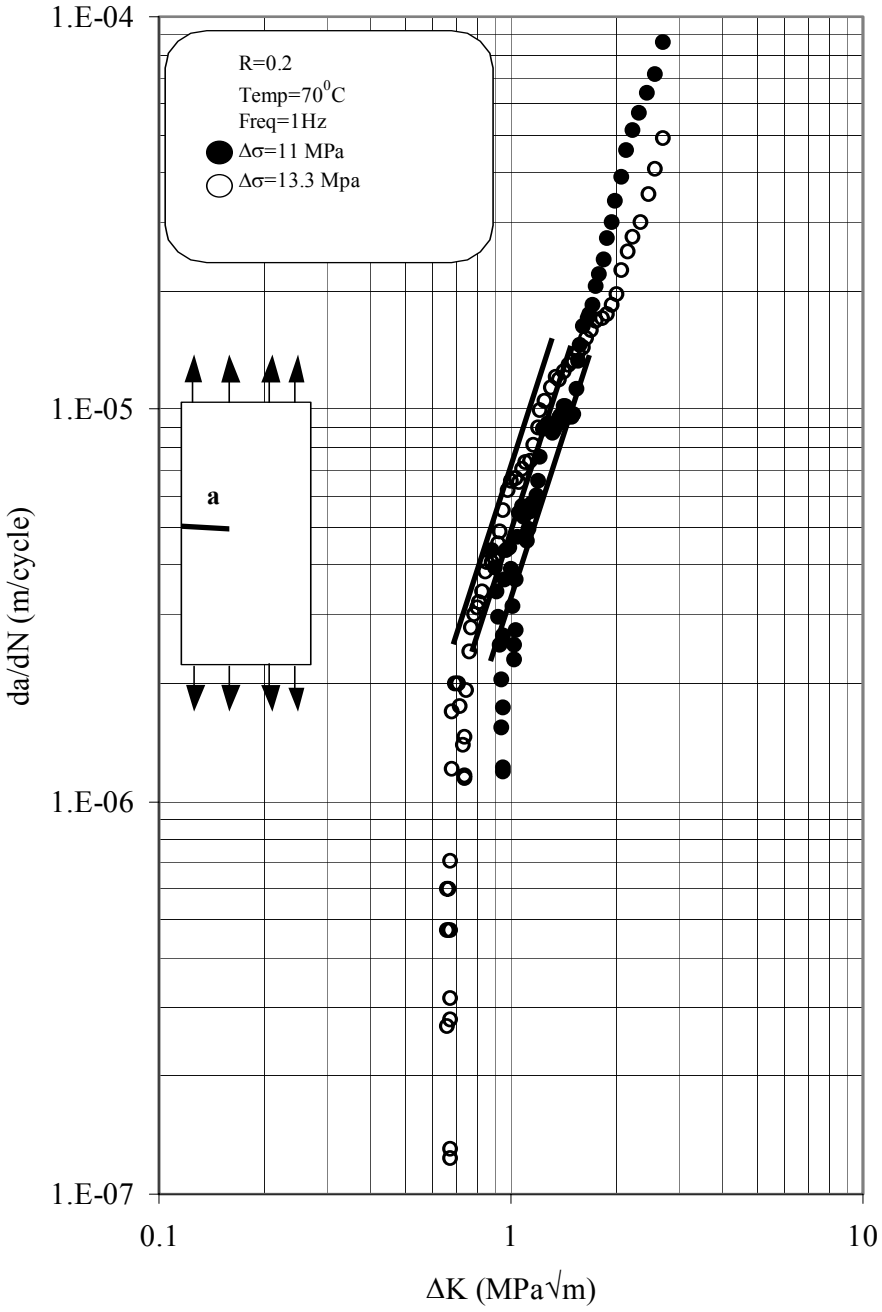

Figure 5.16 Fatigue crack growth curves for CPVC at $\Delta\sigma$= 11 and 13.30 MPa at 1 Hz and 70° C.

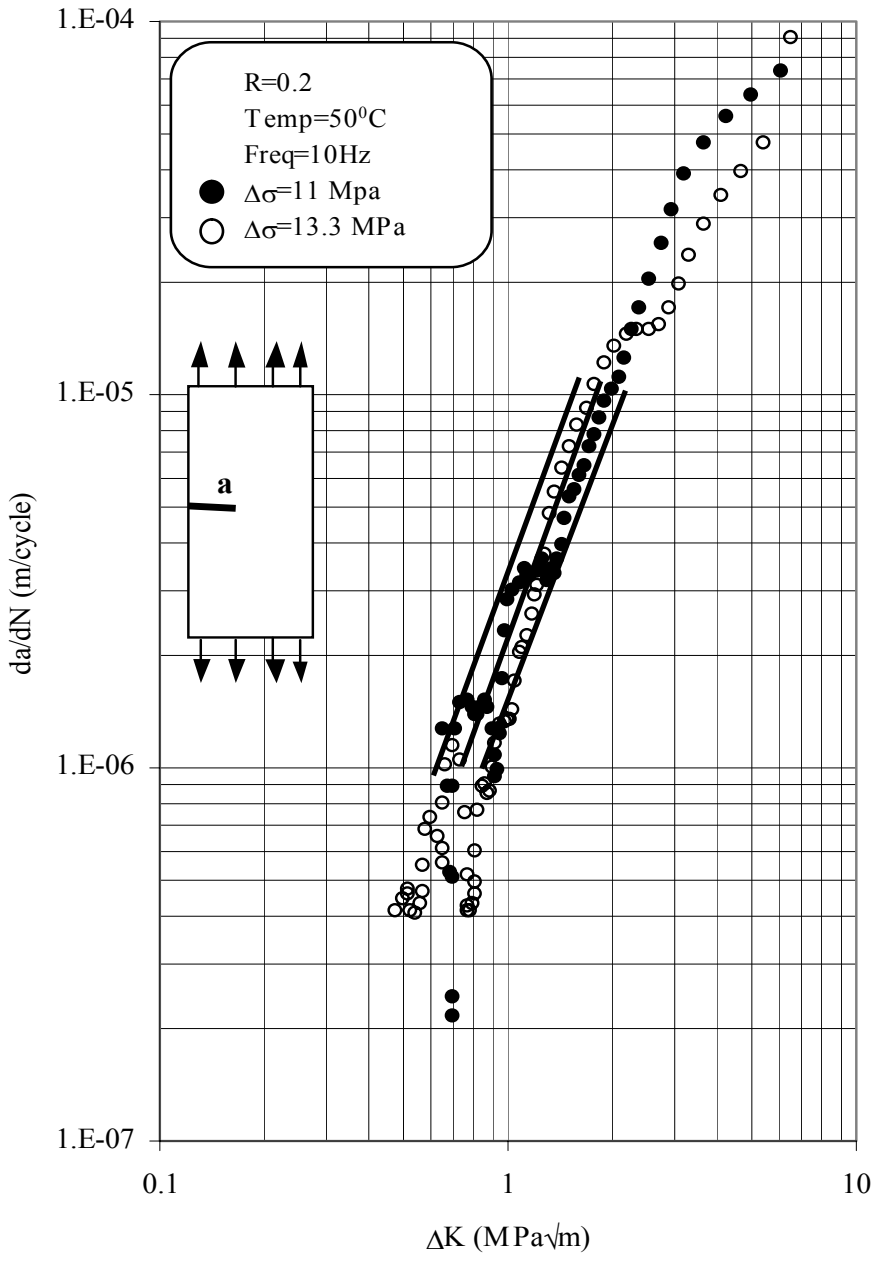

Figure 5.17 Fatigue crack growth curves for CPVC at $\Delta\sigma$= 11 and 13.30 MPa at 10 Hz and 50° C.

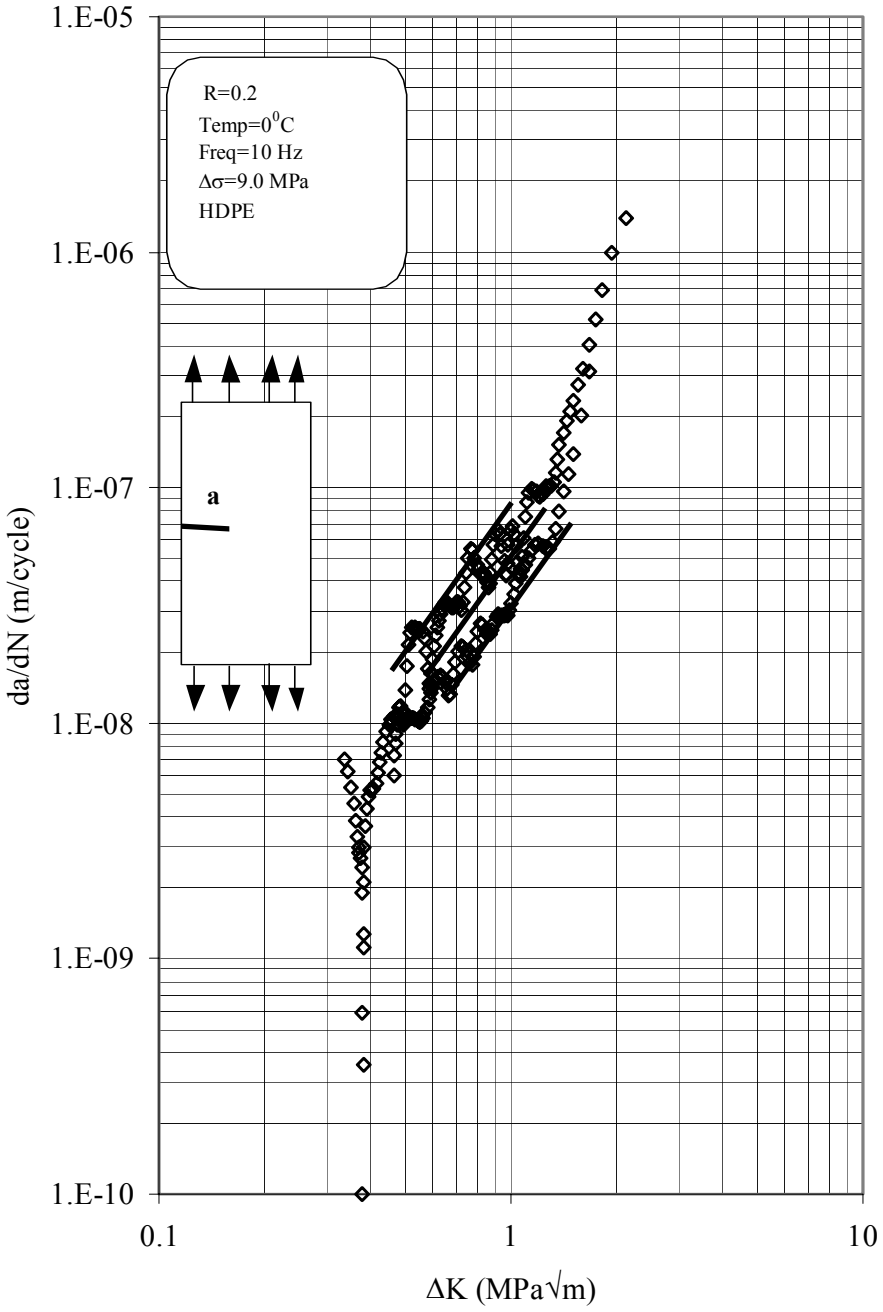

Figure 5.18 da/dN-ΔK curve for HDPE at 10 Hz and 0^o C.

to 1.15 MPa√m with a corresponding variation in da/dN from $3x10^{-8}$ to $1.2x10^{-6}$ mm/cycle for R=0.1 and frequency of 2 Hz.

Fatigue crack propagation tests were also performed at stress range $\Delta\sigma$ = 8.0 MPa at 10 Hz and for 0^{o} C and -10^{o} C to determine if there is any effect of stress on da/dN–ΔK curve. It was found that the da/dN-ΔK curve for HDPE is unique within the experimental scatter and as expected no $\Delta\sigma$ effect was observed at both temperatures. The fatigue crack growth curves at $\Delta\sigma$ = 8.0 and 9.0 MPa for 0^{o} C and -10^{o} C at a frequency of 10 Hz are shown in figure 5.19 and figure 5.20. It can be seen that all of the data fall within a band size of 2.0 on da/dN from the curve representing the paris region for these conditions. These curves can be represented by the following equations:

(a) HDPE, 0^{o} C-10Hz: ($\Delta\sigma$ = 8.0,9.0 MPa) $$\frac{da}{dN} = 4.00x10^{-8}\Delta K^{2.14} \qquad (5.3)$$

(b) HDPE, -10^{o} C-10Hz: ($\Delta\sigma$ = 8.0,9.0 MPa) $$\frac{da}{dN} = 2.00x10^{-8}\Delta K^{2.02} \qquad (5.4)$$

5.3.1 Effect of Temperature on FCP rate of CPVC

The effect of test temperature on fatigue crack growth in CPVC is analyzed by using the Paris and Erdogan [75] law given by equation 2.7. The representative fatigue crack propagation data for all temperatures and frequencies studied are illustrated in figures 5.21 to 5.34.

Data scattering in figure 5.27, which shows the da/dN-ΔK curve for 23^{o} C and 0.1 Hz, is caused due to variation in temperature and humidity during the testing as the tests at 23^{o} C are not performed inside controlled temperature chamber, also 0.1 Hz frequency tests take long periods (nearly 48 hours) for completion.

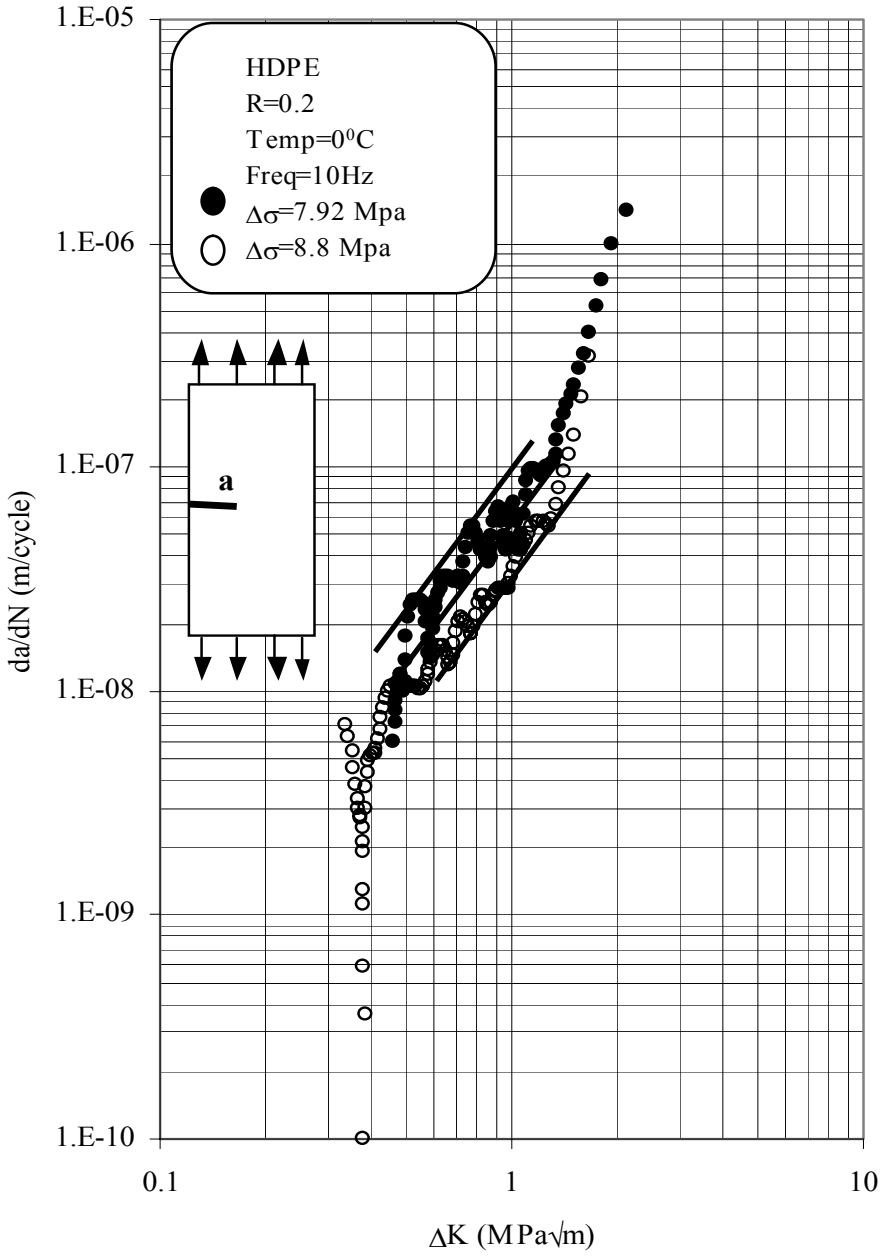

Figure 5.19 Fatigue crack growth curves for HDPE at $\Delta\sigma$ = 8.0 and 9.0 MPa at 10 Hz and 0^{o} C.

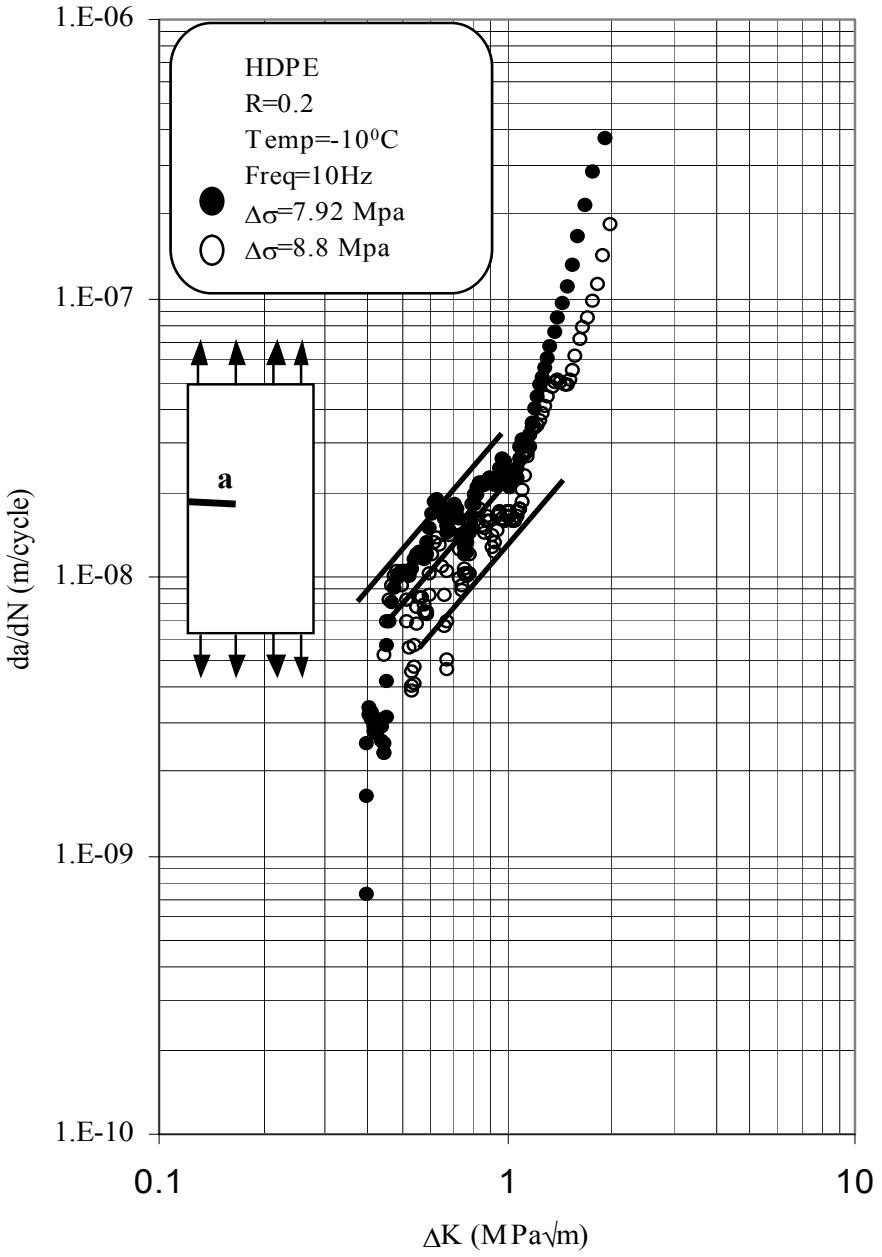

Figure 5.20 Fatigue crack growth curves for HDPE at $\Delta\sigma$= 8.0 and 9.0 MPa at 10 Hz and -10^{o} C.

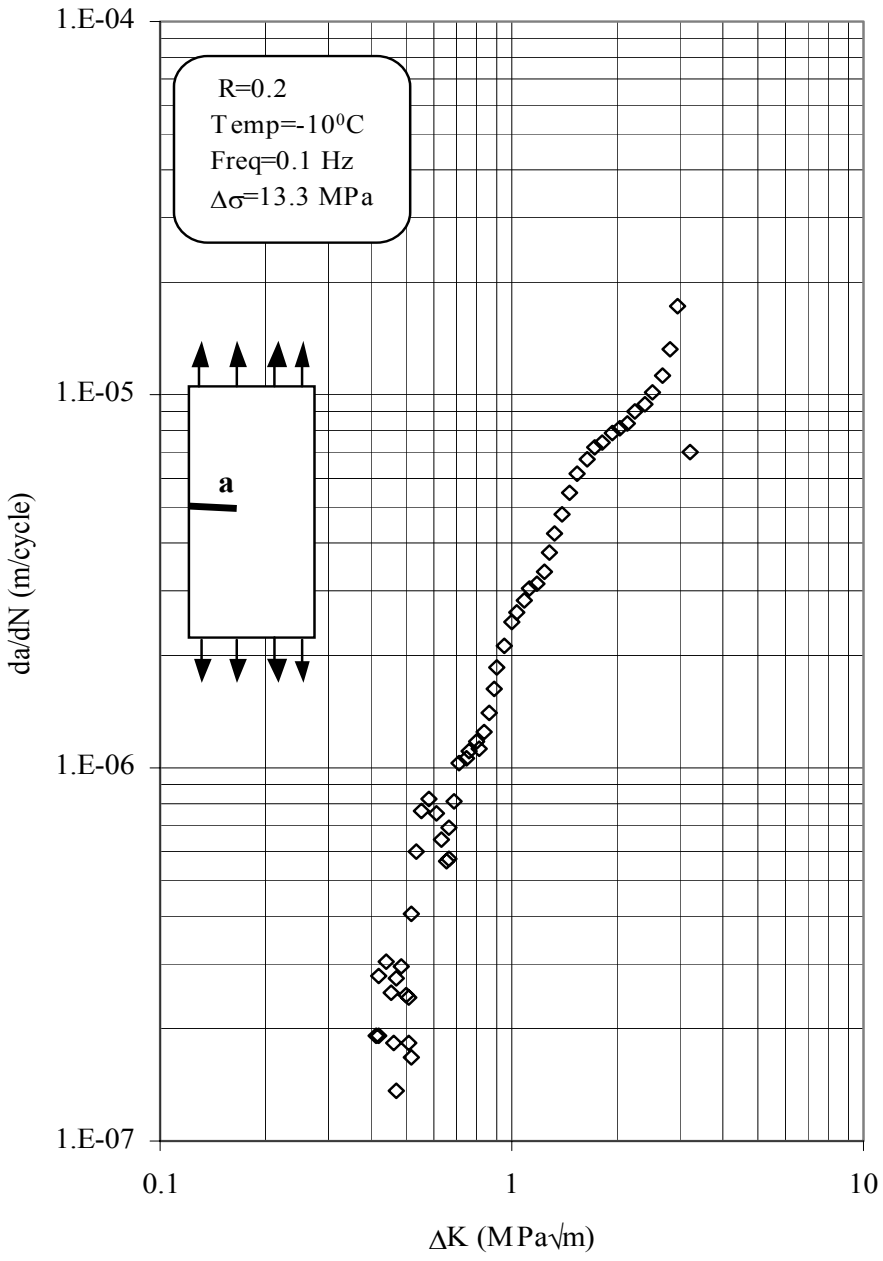

Figure 5.21 da/dN-ΔK curve for CPVC at 0.1 Hz and -10° C.

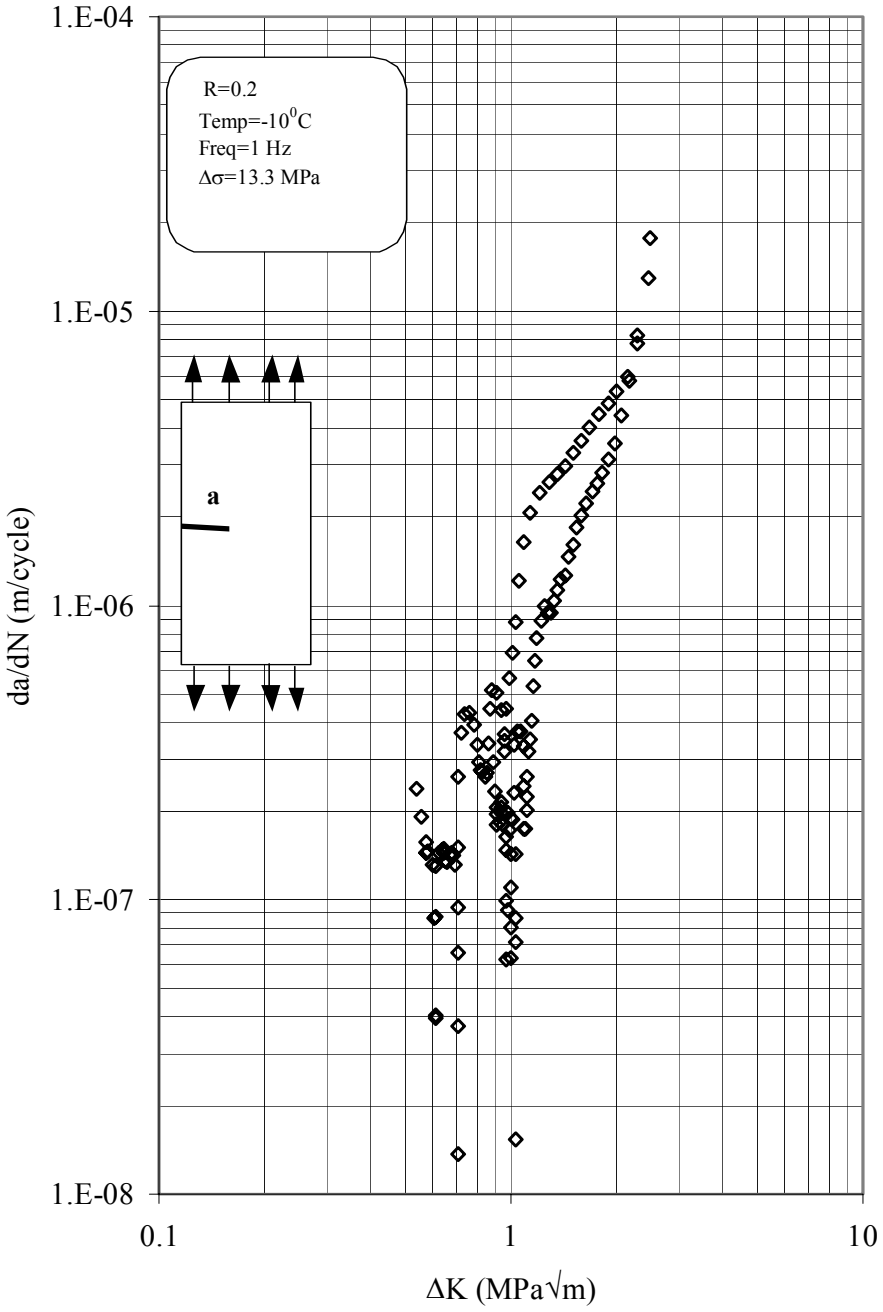

Figure 5.22 da/dN-ΔK curve for CPVC at 1 Hz and -10^o C.

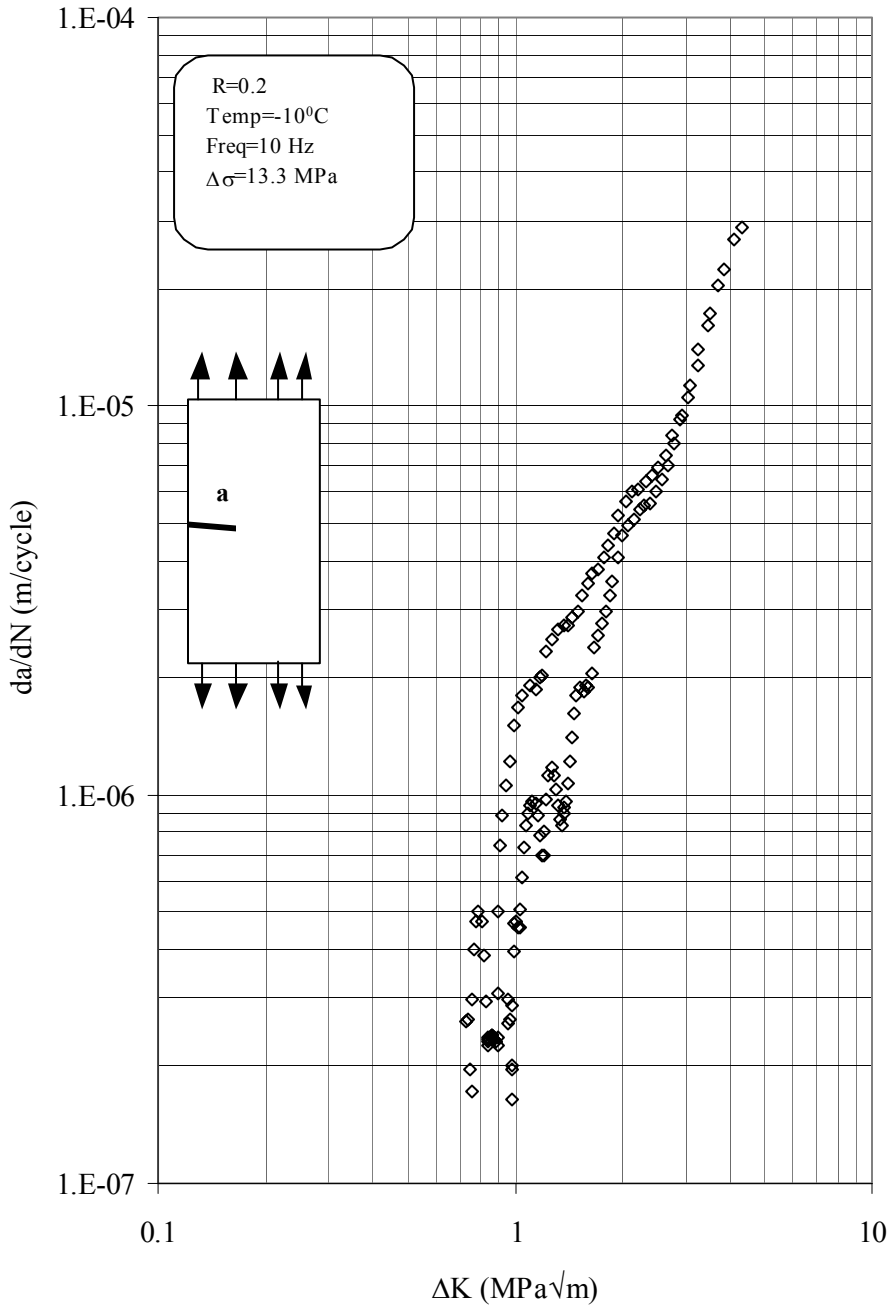

Figure 5.23 da/dN-ΔK curve for CPVC at 10 Hz and -10° C.

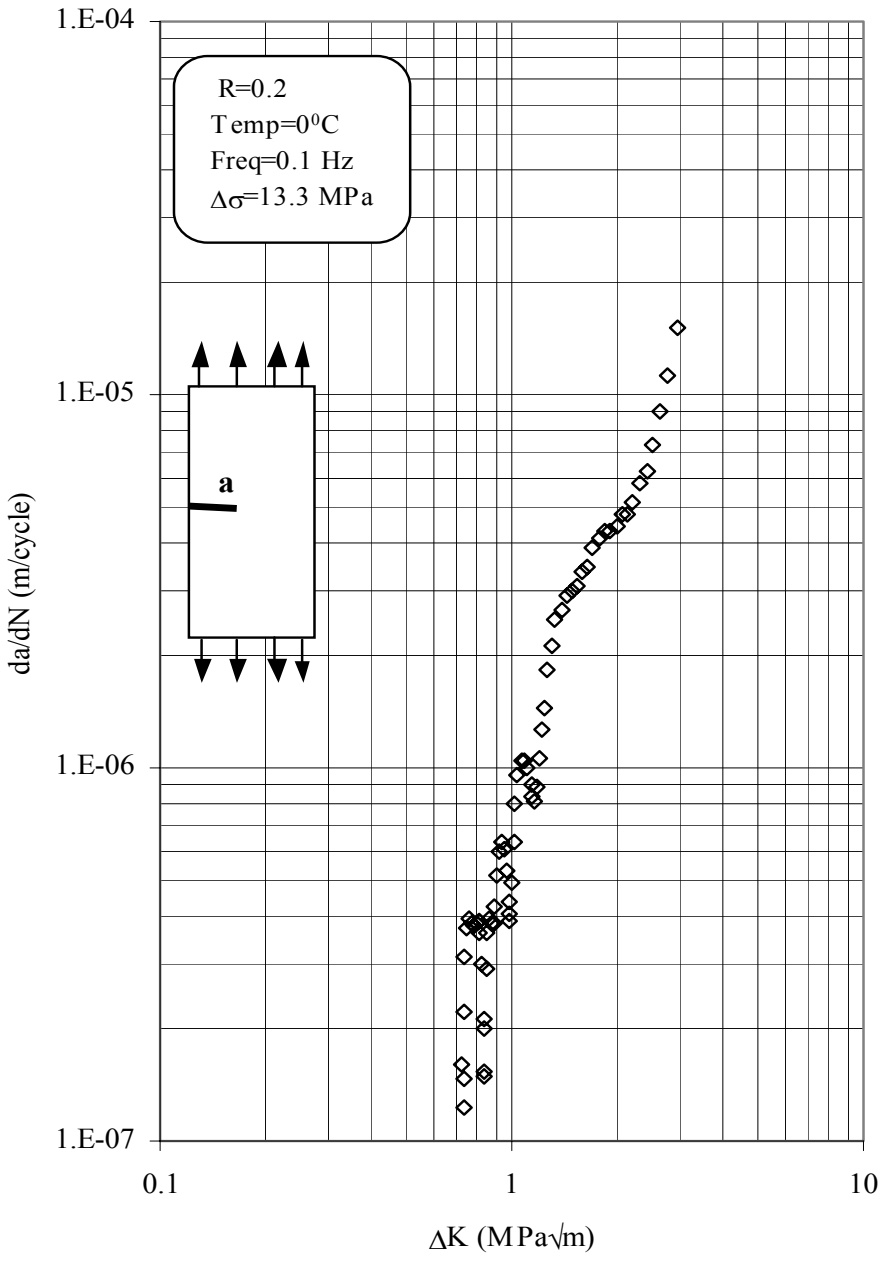

Figure 5.24 da/dN-ΔK curve for CPVC at 0.1 Hz and 0° C.

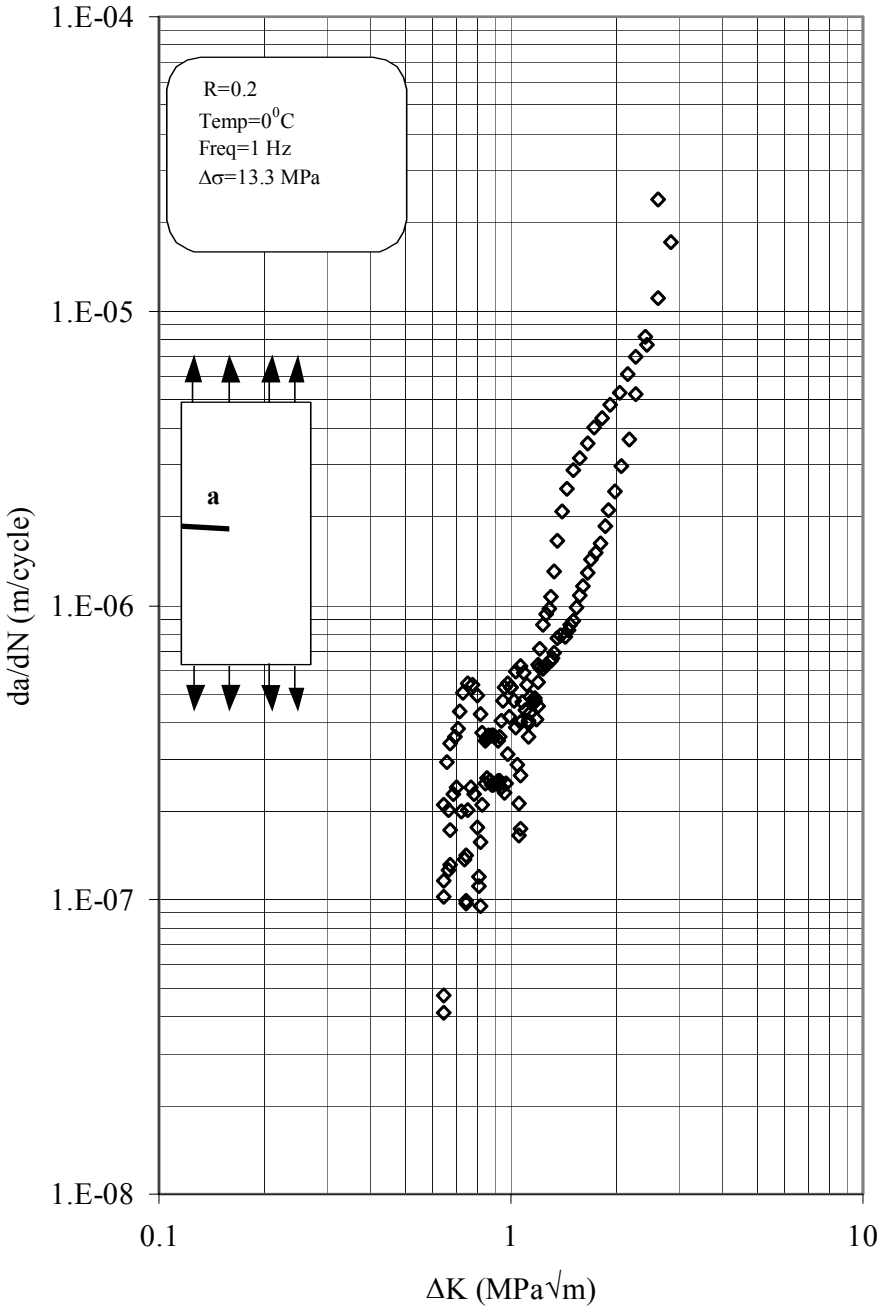

Figure 5.25 da/dN-ΔK curve for CPVC at 1 Hz and 0^o C.

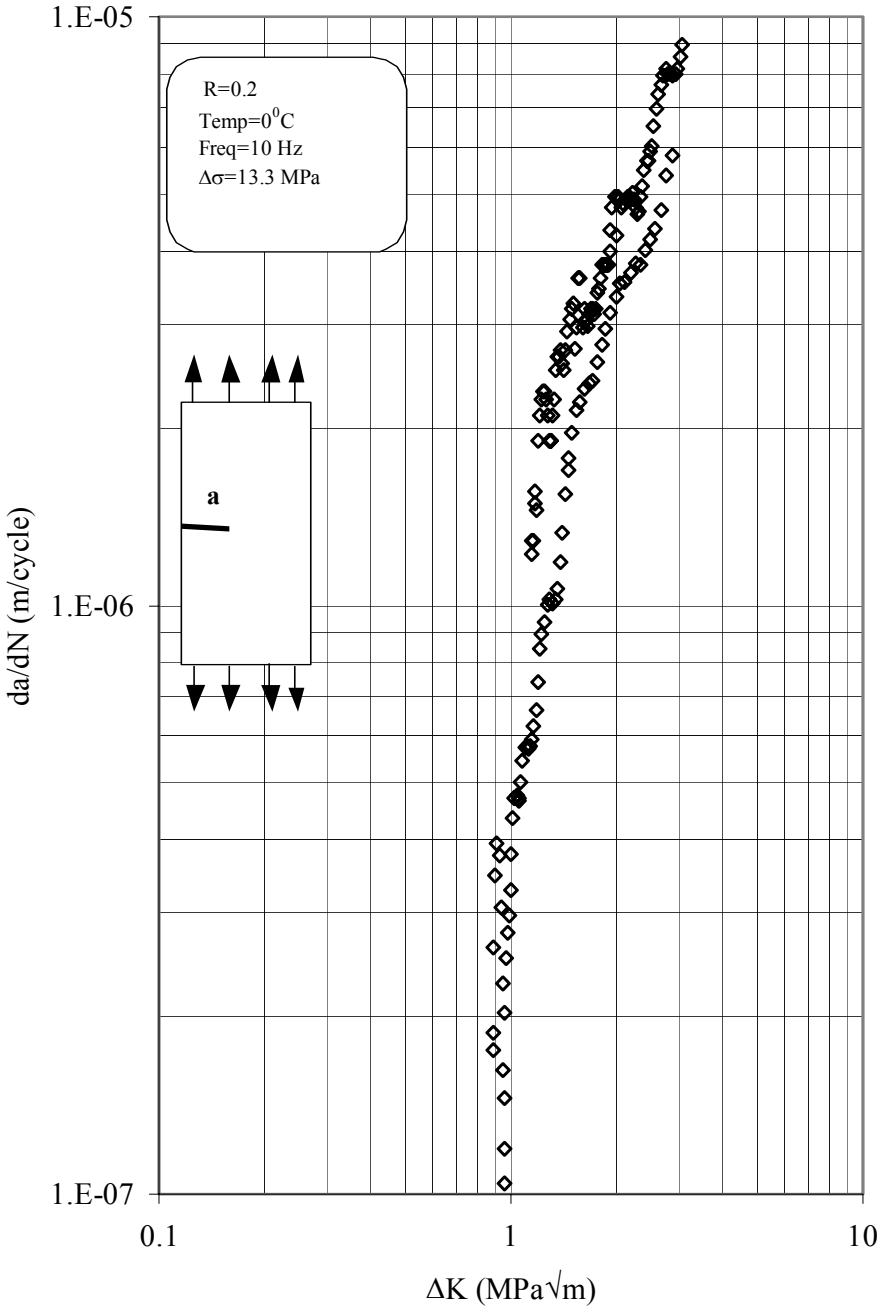

Figure 5.26 da/dN-ΔK curve for CPVC at 10 Hz and 0^o C.

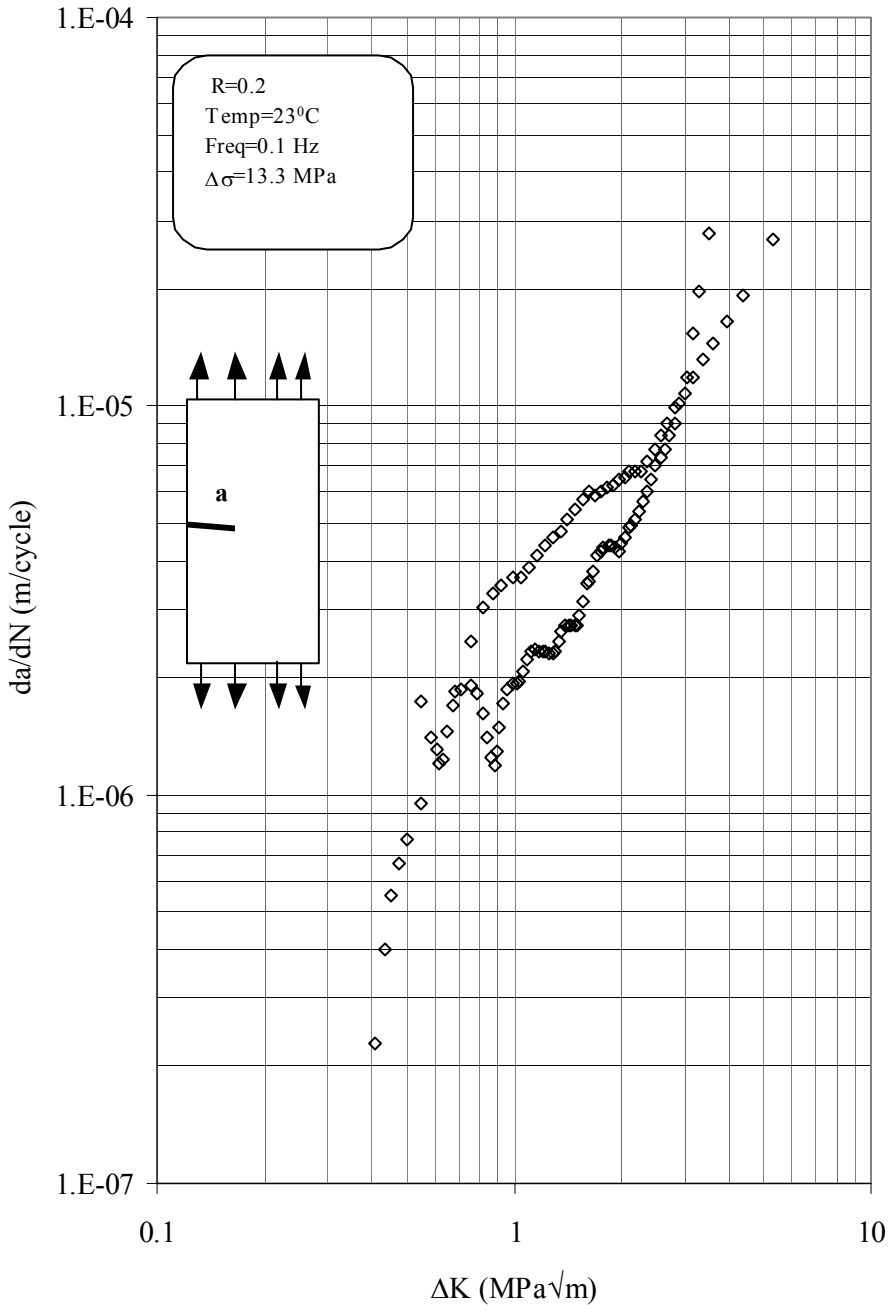

Figure 5.27 da/dN-ΔK curve for CPVC at 0.1 Hz and 23° C.

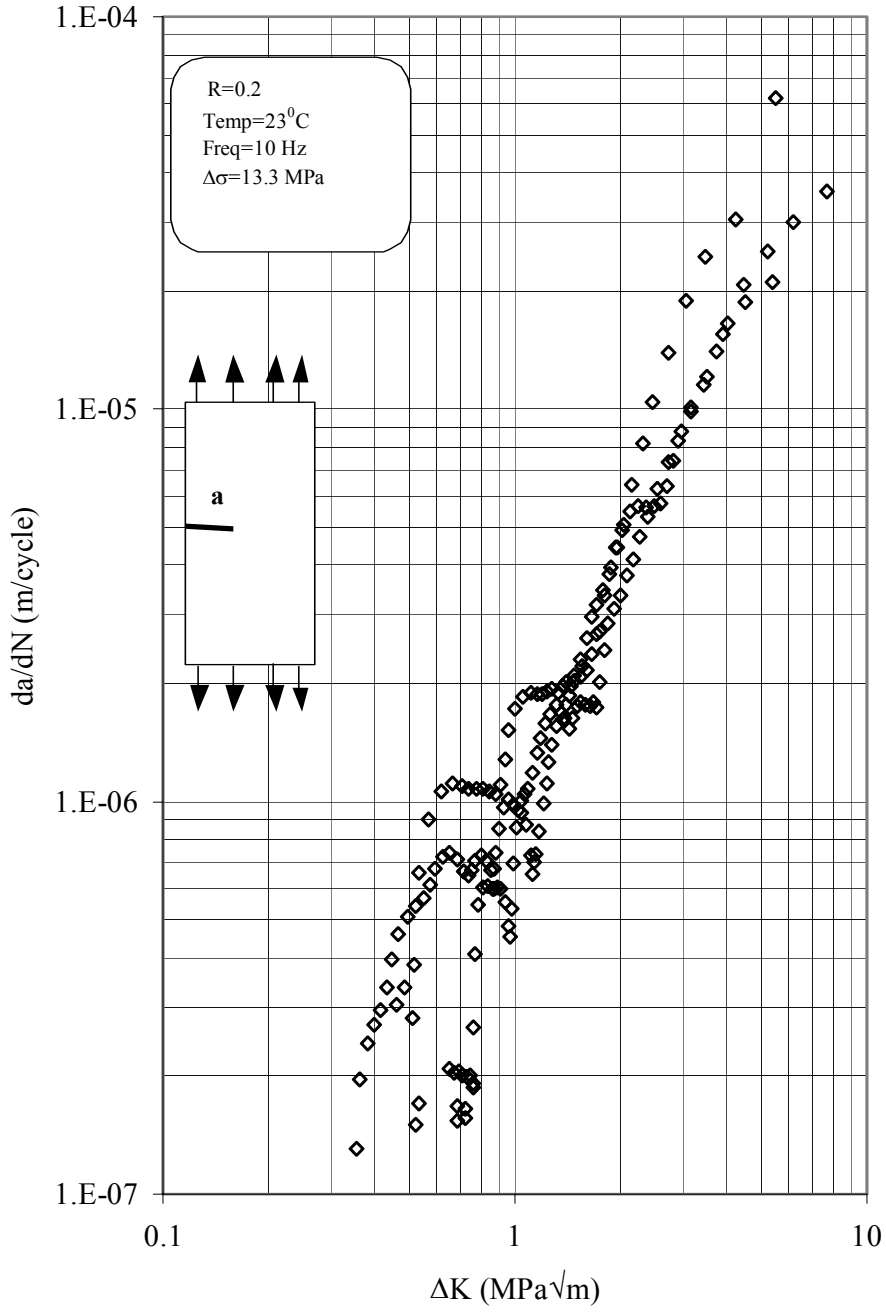

Figure 5.28 da/dN-ΔK curve for CPVC at 10 Hz and 23° C.

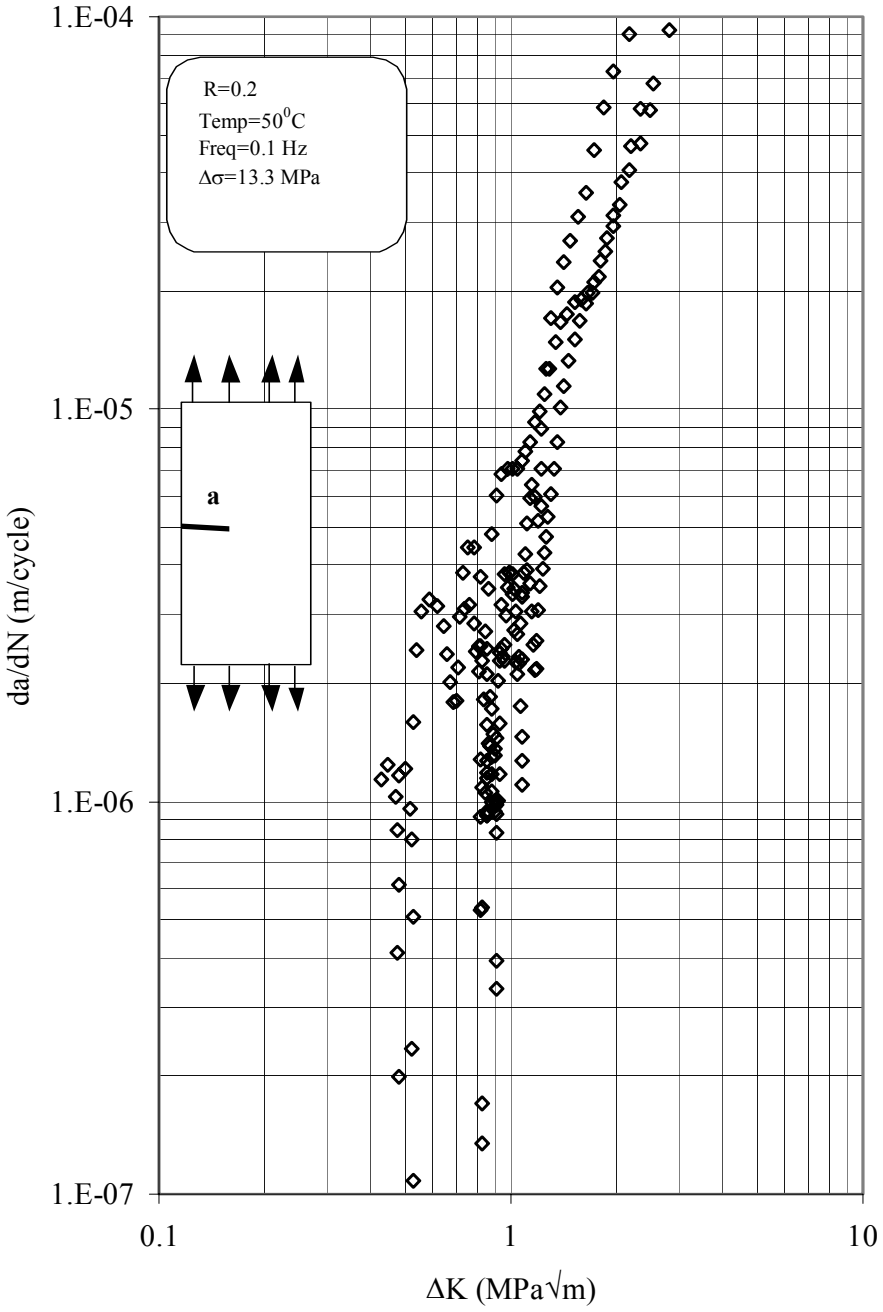

Figure 5.29 da/dN-ΔK curve for CPVC at 0.1 Hz and 50° C.

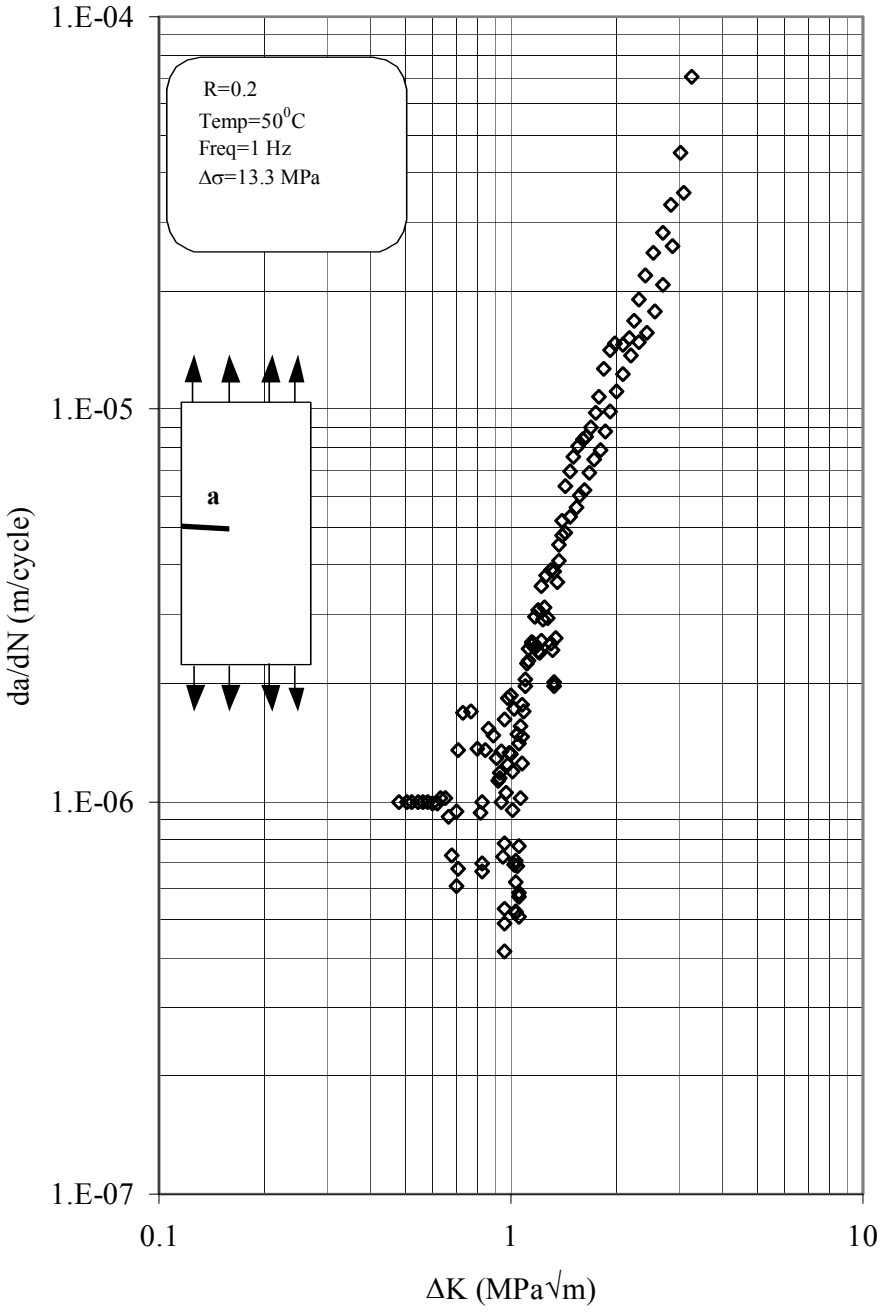

Figure 5.30 da/dN-ΔK curve for CPVC at 1 Hz and 50° C.

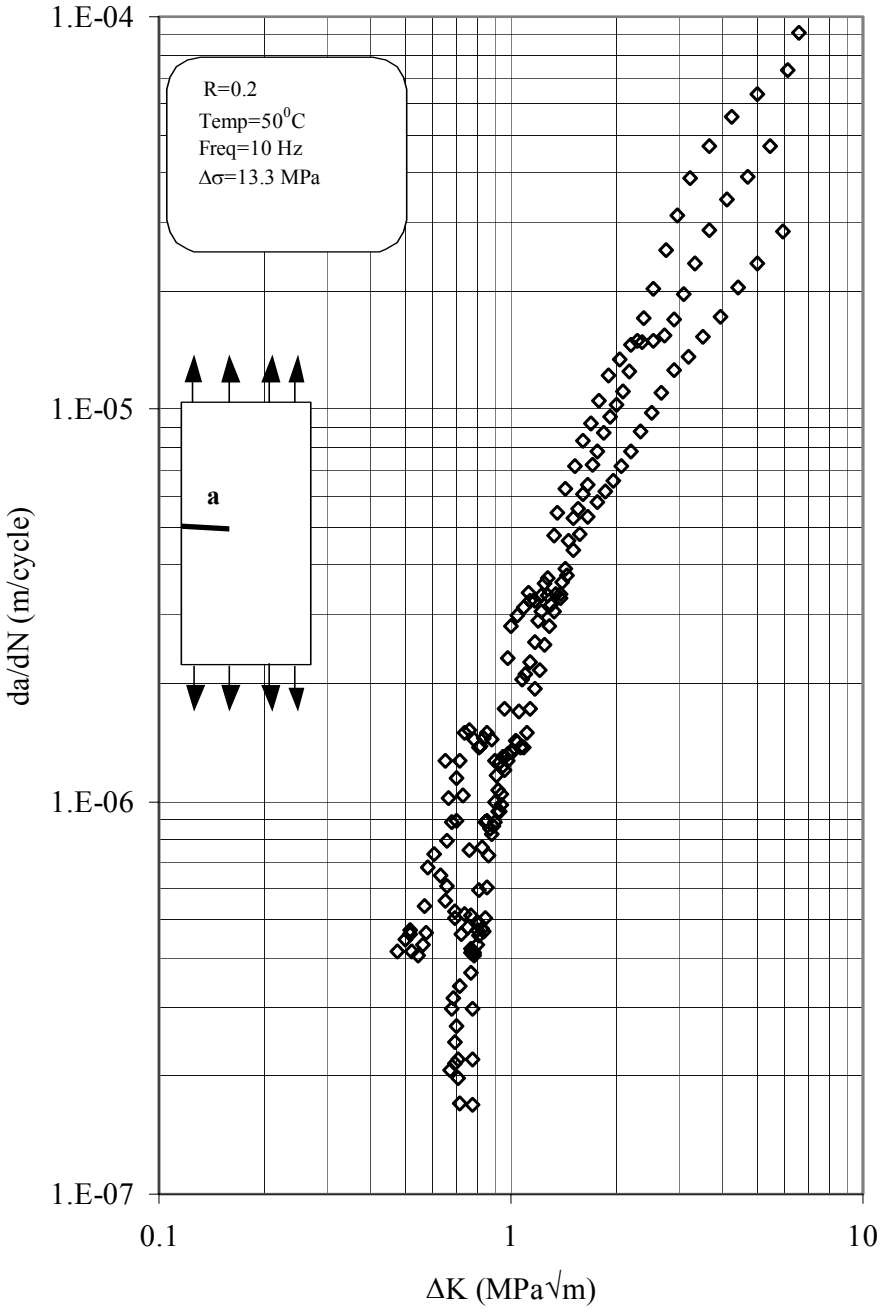

Figure 5.31 da/dN-ΔK curve for CPVC at 10 Hz and 50° C.

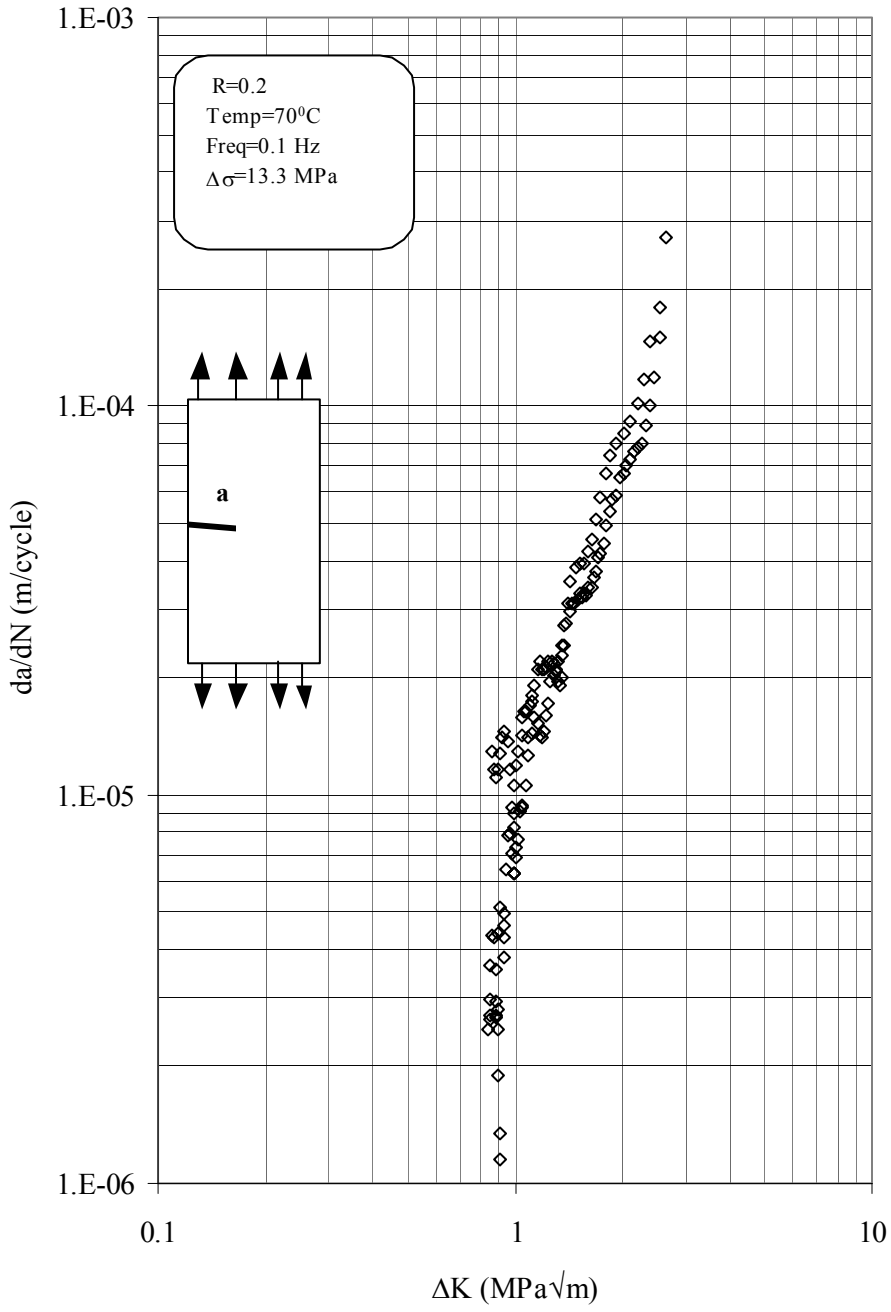

Figure 5.32 da/dN-ΔK curve for CPVC at 0.1 Hz and 70° C.

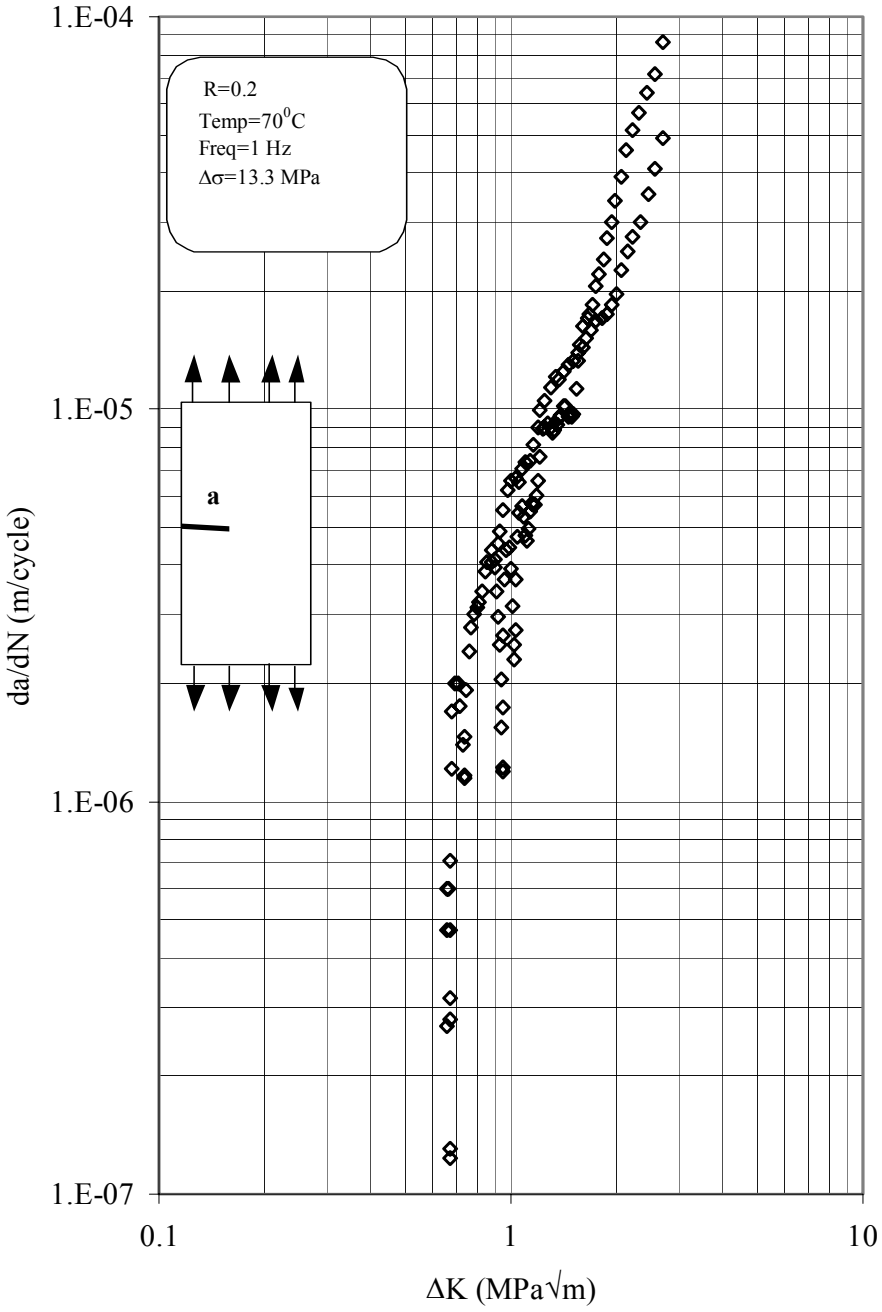

Figure 5.33 da/dN-ΔK curve for CPVC at 1 Hz and 70° C.

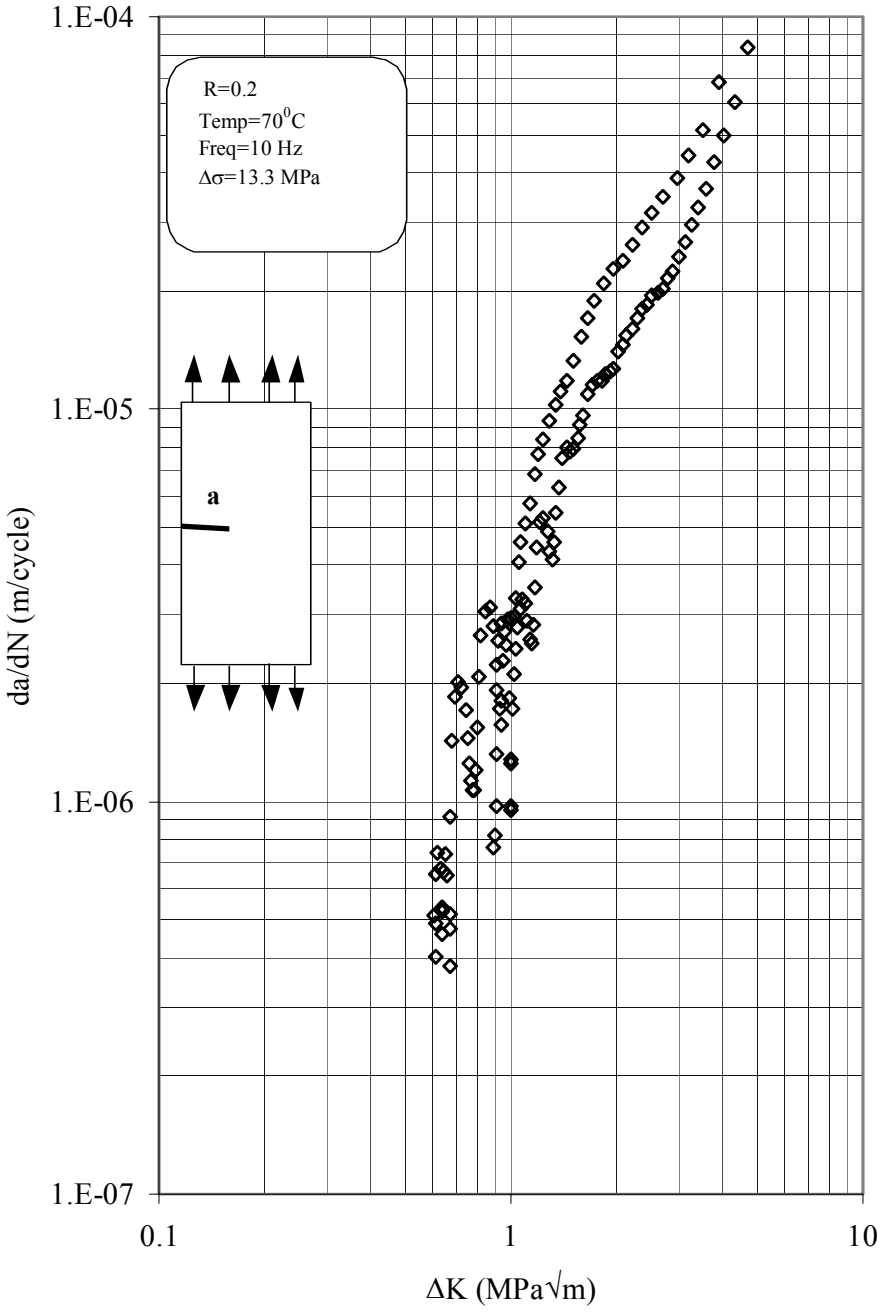

Figure 5.34 da/dN-ΔK curve for CPVC at 10 Hz and 70° C.

The effect of temperature on crack growth rate can be better illustrated by using the representative best fit curves on all the test data at each frequency, as shown in figure 5.35 to 5.37. These curves can be represented by the following equations:

(a) CPVC, -10° C-0.1Hz $$\frac{da}{dN} = 2.14x10^{-6}\Delta K^{2.63} \quad (5.5)$$

(b) CPVC, -10° C-1Hz $$\frac{da}{dN} = 5.37x10^{-7}\Delta K^{2.60} \quad (5.6)$$

(c) CPVC, -10° C-10Hz $$\frac{da}{dN} = 6.45x10^{-7}\Delta K^{2.42} \quad (5.7)$$

(d) CPVC, 0° C-0.1Hz $$\frac{da}{dN} = 1.12x10^{-6}\Delta K^{2.11} \quad (5.8)$$

(e) CPVC, 0° C-1Hz $$\frac{da}{dN} = 6.54x10^{-7}\Delta K^{2.55} \quad (5.9)$$

(f) CPVC, 0° C-10Hz $$\frac{da}{dN} = 5.00x10^{-7}\Delta K^{2.89} \quad (5.10)$$

(g) CPVC, 23° C-0.1Hz $$\frac{da}{dN} = 1.00x10^{-6}\Delta K^{2.00} \quad (5.11)$$

(h) CPVC, 23° C-1Hz $$\frac{da}{dN} = 9.00x10^{-7}\Delta K^{2.39} \quad (5.12)$$

(i) CPVC, 23° C-10Hz $$\frac{da}{dN} = 8.00x10^{-7}\Delta K^{2.29} \quad (5.13)$$

(j) CPVC, 50° C-0.1Hz $$\frac{da}{dN} = 6.00x10^{-6}\Delta K^{2.57} \quad (5.14)$$

(k) CPVC, 50° C-1Hz $$\frac{da}{dN} = 2.00x10^{-6}\Delta K^{2.46} \quad (5.15)$$

(l) CPVC, 50° C-10Hz $$\frac{da}{dN} = 1.65x10^{-6}\Delta K^{2.26} \quad (5.16)$$

(m) CPVC, 70° C-0.1Hz $$\frac{da}{dN} = 1.00x10^{-5}\Delta K^{2.80} \quad (5.17)$$

(n) CPVC, 70° C-1Hz $$\frac{da}{dN} = 5.00x10^{-6}\Delta K^{2.40} \quad (5.18)$$

(o) CPVC, 70° C-10Hz $$\frac{da}{dN} = 3.82x10^{-6}\Delta K^{2.02} \quad (5.19)$$

Results obtained illustrate two important points. First, for a given ΔK, crack growth rate da/dN increases with increasing temperature, (except for 0.1 Hz where -10° C is above 0° C and 23° C, which may be due to some problem associated with this test due to long period of testing involved in it). For example, at ΔK = 1.0 MPa√m and 1 Hz, da/dN = 0.57, 0.7, 1.0, 2.0 and 5.0 μm/cycle for T = -10, 0 23, 50 and 70° C, respectively. Second, the value of intercept A of the fatigue curves increases with increase in temperature. A higher value of intercept A signifies less resistant provided to the crack propagation. For a frequency of 1 Hz the value of A is dependent on temperature ranging from a value of $5x10^{-6}$ at 70° C to $5.37x10^{-7}$ at –10° C. The average values of m and A at all test temperatures and frequencies for CPVC are given in table 5.1. Also, the variation of m and A with temperature at frequency of 1 Hz is shown graphically in figures 5.38 and 5.39 respectively. The values of m and A obtained by Kim et al [63] for uPVC at room temperature are also plotted in these figures for comparison. It has been seen that value of slope m of the fatigue curves are constant with variations in the temperature. Martin and Gerberich [43] and, Mai and Williams [44] have found that the variation of m values with temperature for PC and polystyrene respectively, did not follow a linear pattern. Whereas Radon and Culver [64] have shown that the slopes of

Table 5.1 Constants m and A for CPVC at different frequencies and temperature in the Paris equation (da/dN in m/cycle and ΔK in MPa√m)

Temperature (^{o}C)	Frequency (Hz)	Exponent m	Parameter A
-10 ^{o}C	**0.1**	2.633359	2.149×10^{-06}
	1	2.609423	5.37×10^{-07}
	10	2.427453	6.457×10^{-07}
0 ^{o}C	**0.1**	2.118562	1.123x-10^{-06}
	1	2.555418	6.545×10^{-07}
	10	2.898244	5.000×10^{-07}
23 ^{o}C	**0.1**	2	1.00×10^{-06}
	1	2.3979	9.00×10^{-07}
	10	2.292	8.00×10^{-07}
50 ^{o}C	**0.1**	2.5702	6.00×10^{-06}
	1	2.465	2.00×10^{-06}
	10	2.2665	1.65×10^{-06}
70 ^{o}C	**0.1**	2.8074	1.00×10^{-05}
	1	2.4022	5.00×10^{-06}
	10	2.0205	3.82×10^{-06}

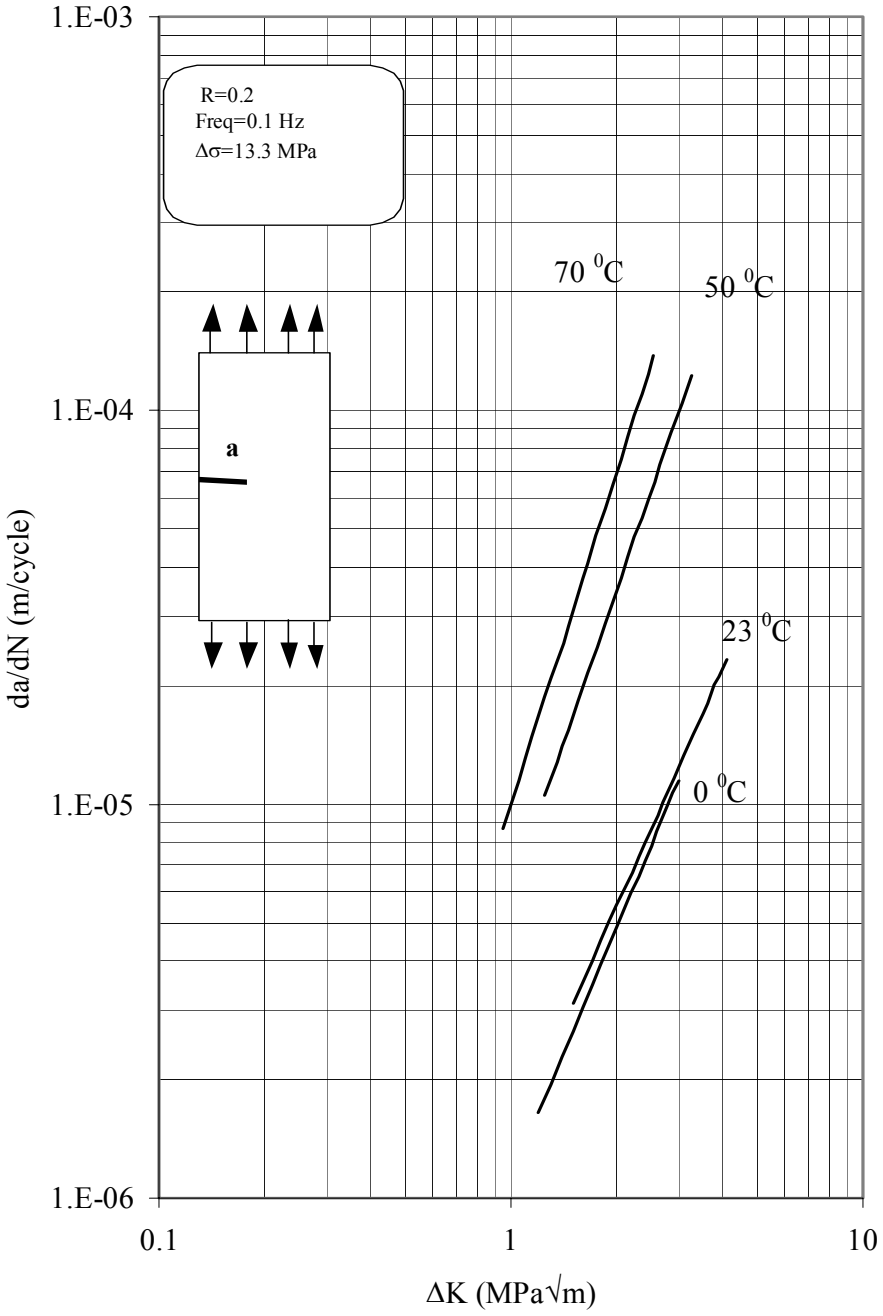

Figure 5.35 Fatigue crack growth rates at different temperatures for CPVC at 0.1 Hz.

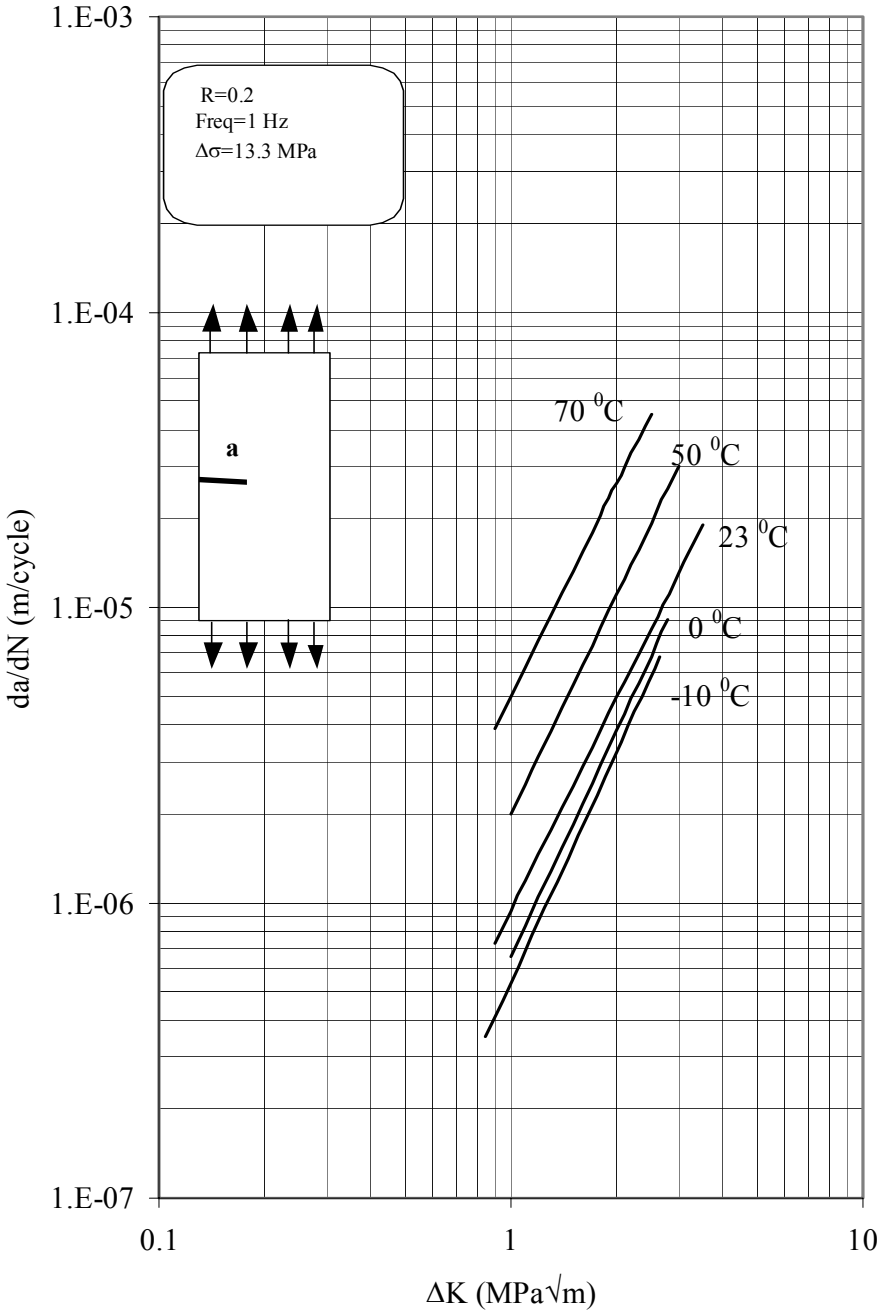

Figure 5.36 Fatigue crack growth rates at different temperatures for CPVC at 1 Hz.

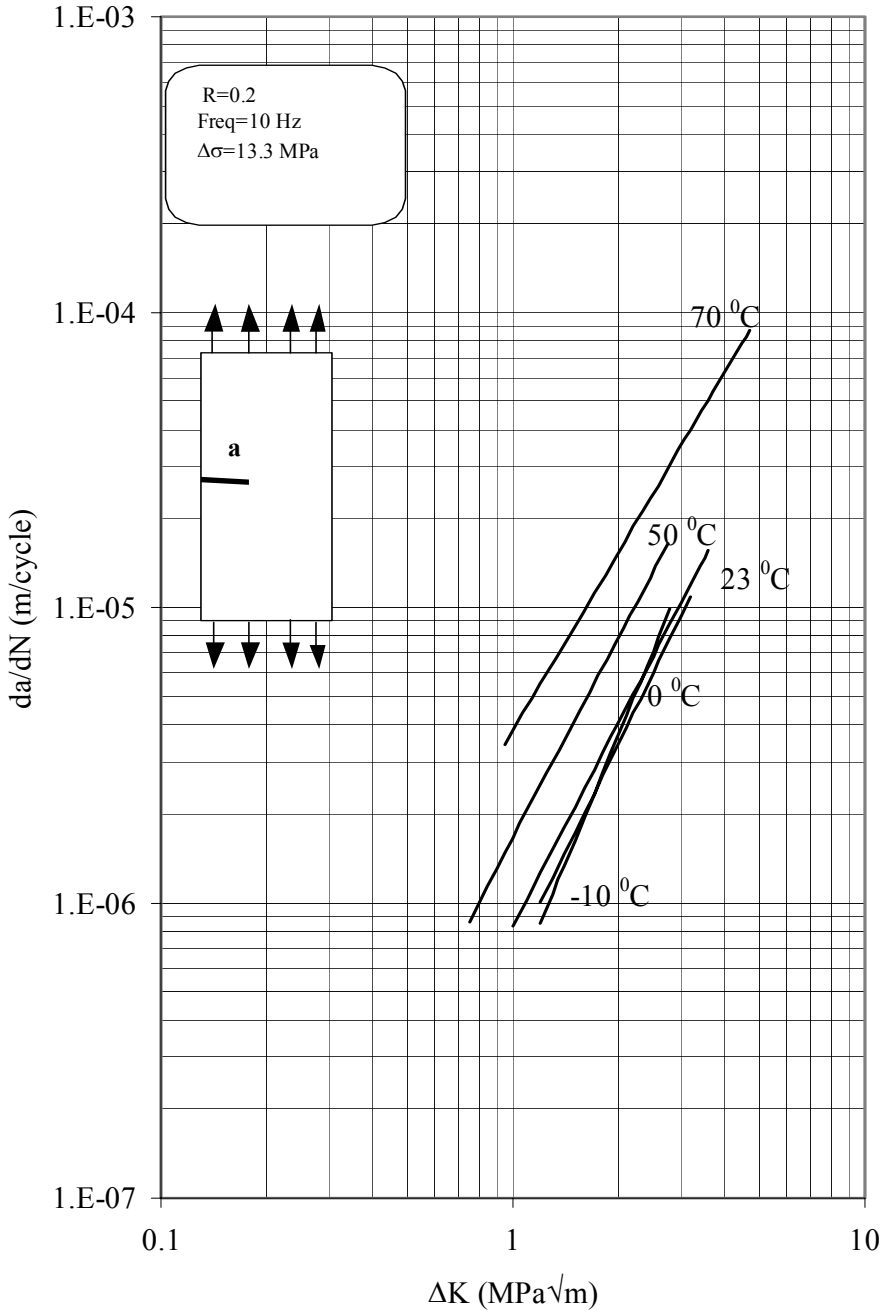

Figure 5.37 Fatigue crack growth rates at different temperatures for CPVC at 10 Hz.

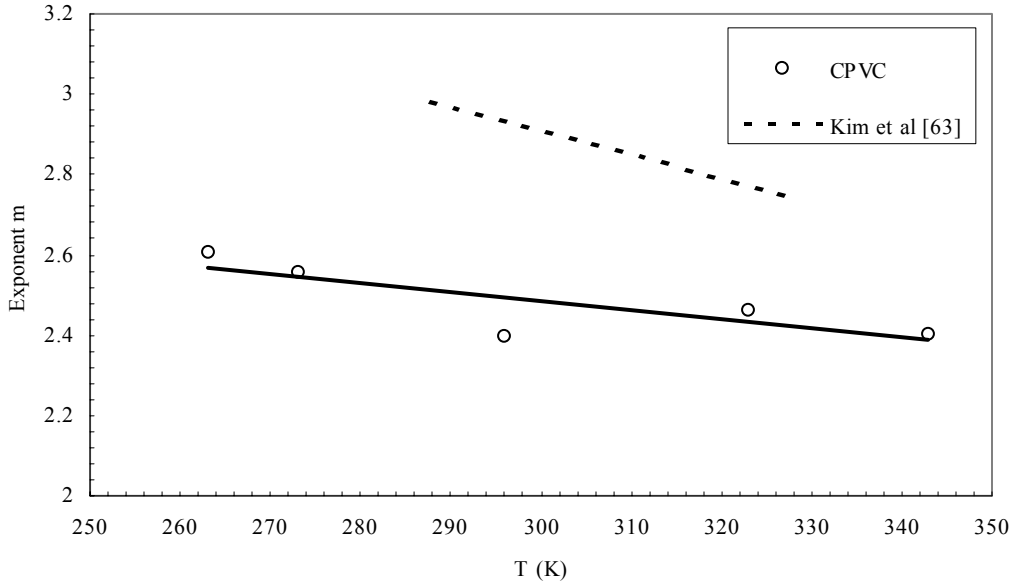

Figure 5.38 Variation of m with temperature for CPVC at 1 Hz.

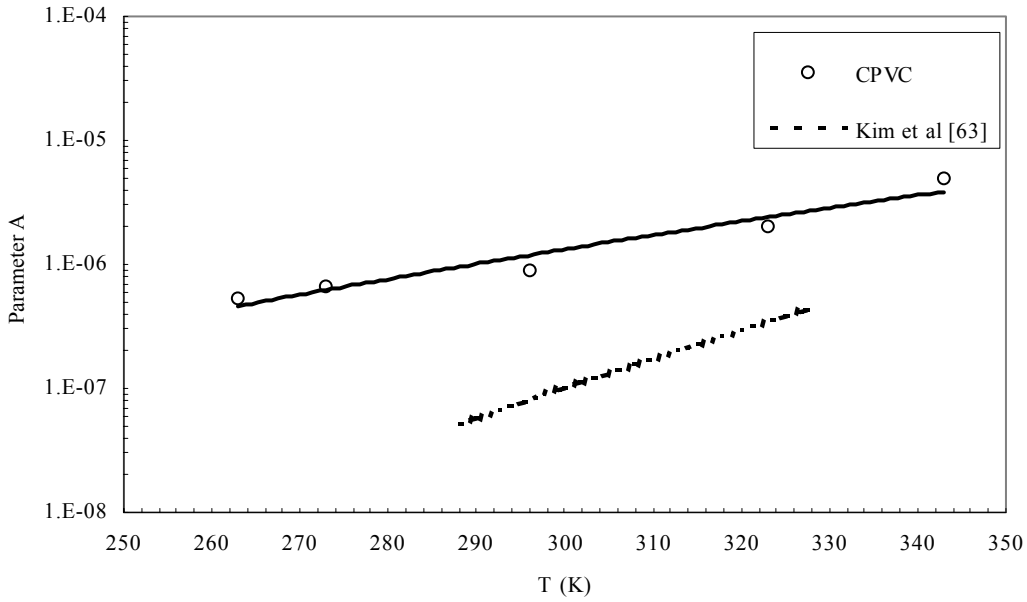

Figure 5.39 Variation of A with temperature for CPVC at 1 Hz.

fatigue crack propagation curves do not change with temperature for PMMA and had a constant value equal to 2.7 for a temperature range of -60^{o} C to 27^{o} C.

The effect of sub room temperature at all frequencies is almost insignificant especially at high ΔK values. This may be due to the brittleness of the material at these temperatures. Material usually fails by shear and no craze zone were present at these temperatures.

Fatigue crack propagation in CPVC at high temperatures is characterized by the formation of plastic zone or crazing. Crazing is a highly localized deformation phenomenon that leads to the formation of voids (cavitations). On the macroscopic level, crazing appears as a stress-whitened region, due to low refractive index. The craze zone was observed to form perpendicular to the maximum applied principal normal stress. Fracture occurred in a craze when individual fibrils rupture. This process can be unstable if, when a fibril fails, the redistributed stress is sufficient to rupture one or more neighboring fibrils.

Irfan and Merah [53] measured the plastic zone size using traveling microscope and video recording equipment from the fatigue crack growth tests for CPVC. They plotted the craze length as a function of temperature for crack lengths of 5 and 10 mm. Figure 5.40 shows the variation of craze length with temperature. It is observed that the craze length increases with increase in temperature, thus showing more plasticity at high temperatures.

Irfan and Merah [53] plotted the craze length as function of crack length (Figure 5.41). The plastic zone was observed to increase with increasing crack length at all test temperatures, which is in accordance with Dugdale's [21] strip yield model.

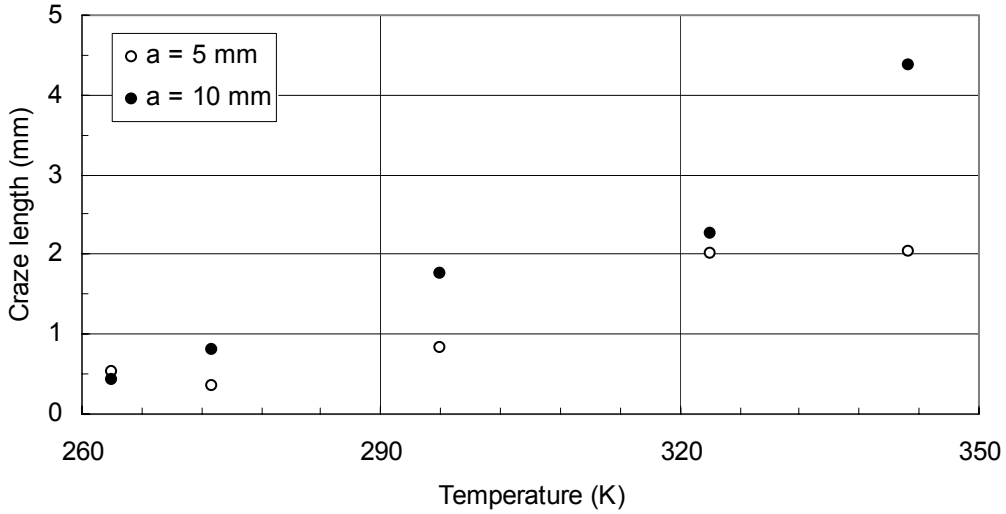

Figure 5.40 Craze length as a function of temperature at crack lengths of 5 and 10 mm [53].

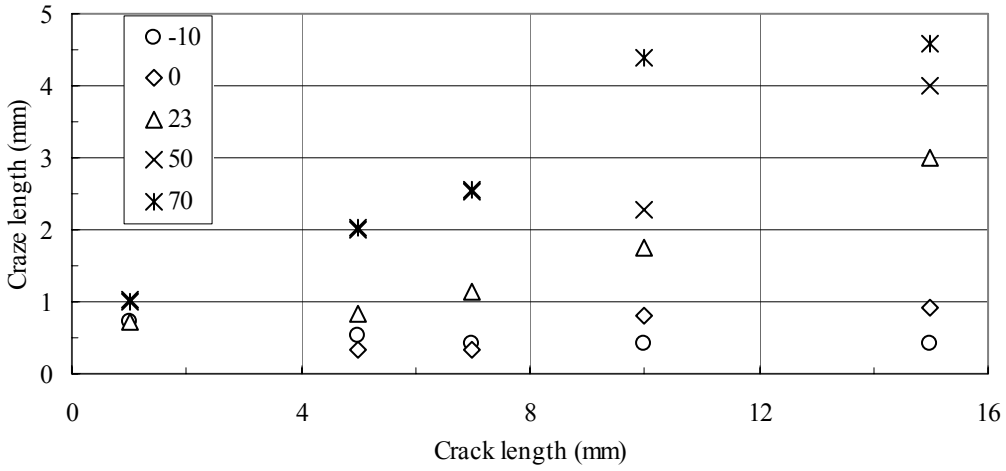

Figure 5.41 Craze length as a function of crack length at all test temperatures [53].

At low temperatures shear yielding is the dominant fracture mechanism involved. Shear yielding mechanism involves the sliding of molecules with respect to one another when subjected to a critical shear stress. Crazing and shear yielding are competing mechanisms, the dominant yielding behavior depends upon molecular structure, stress state and temperature [7]. Kim et al [62] have studied the effect of temperature on FCG in uPVC. They reported that crazing is the dominant fracture mechanism at high temperature while shear yielding is dominant at low temperatures. They [62] have shown that a transition from one mechanism to the other occurs around 23^{o} C for uPVC. They [62] used a plot of ln a_T against 1/T to determine the change in fracture mechanisms where ln a_T is defined as;

$$\ln a_T = (da/dN)_r / (da/dN) \tag{5.20}$$

Where r indicated the da/dN value at a reference temperature for a given ΔK, conveniently taken as 23^{o} C. Kim et al [62] found that the change in the slope of the line indicates a change in the fracture mechanism involved. The slope of the line is a measure of the activation energy. Thus different values of activation energy are associated with different fracture mechanisms. This method is applied to the fatigue crack growth rates at different temperatures in CPVC to determine if any transition point occurs for fracture mechanisms in CPVC. Figures 5.42 (a), 5.42 (b) and 5.42 (c) show the plot of ln a_T against 1/T at ΔK= 1.0 MPa$\sqrt{m}$ for CPVC at frequencies of 0.1, 1 and 10 Hz, respectively. Clearly, there are two straight lines obtained at frequency of 1 Hz with a transition around 44^{o} C. Irfan and Merah [53] also reported transition in the range of

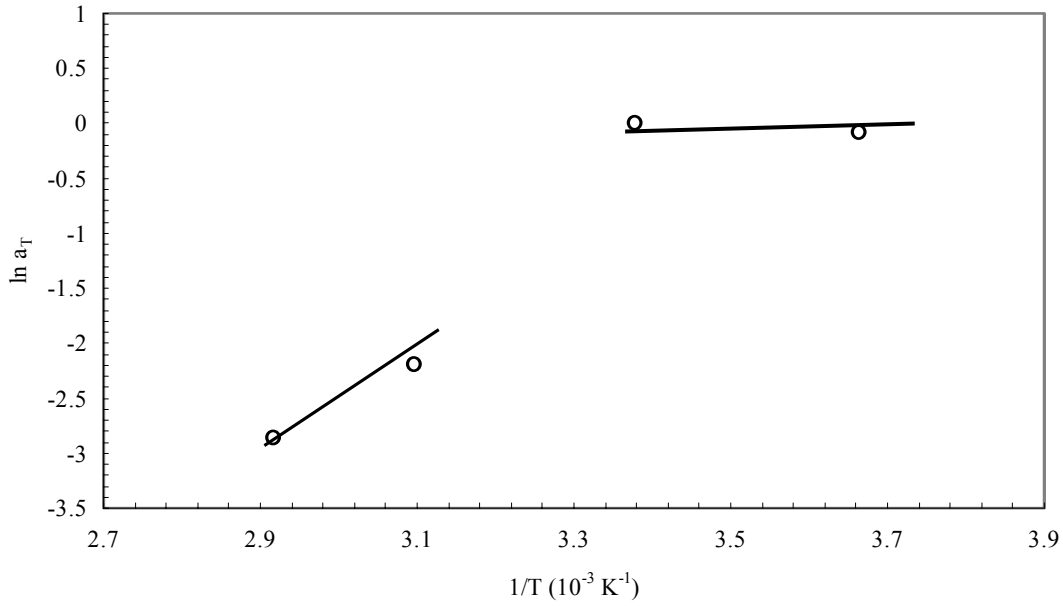

Figure 5.42 (a) Plot of ln a_T at ΔK=1.0 MPa√m for CPVC at 0.1 Hz.

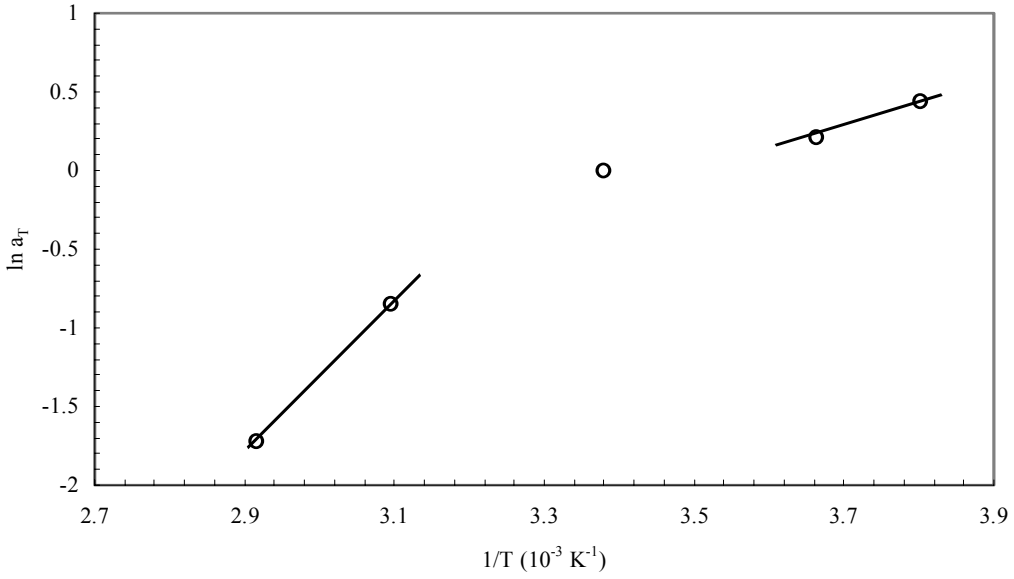

Figure 5.42 (b) Plot of ln a_T at ΔK=1.0 MPa√m for CPVC at 1 Hz.

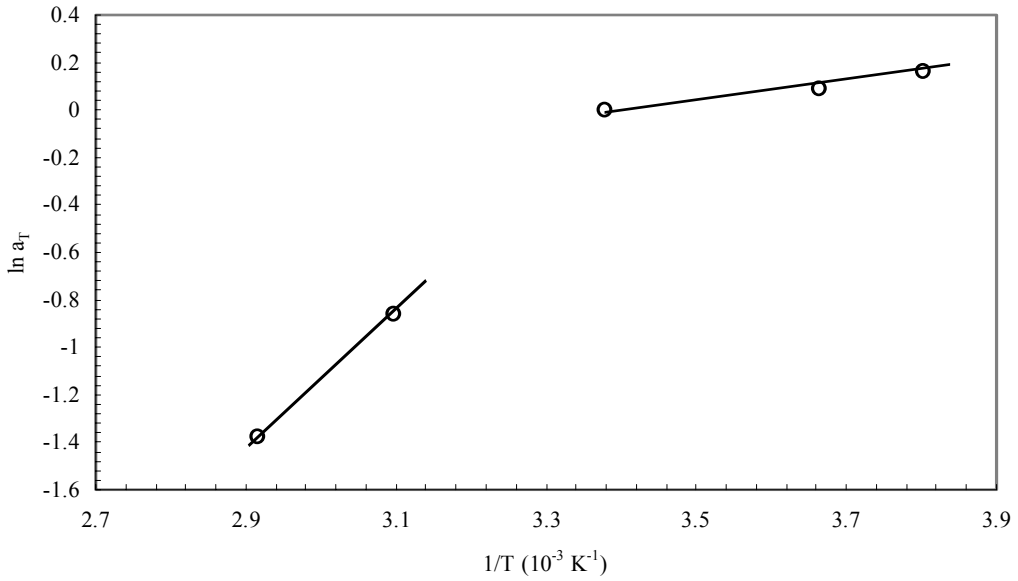

Figure 5.42 (c) Plot of $\ln a_T$ at ΔK=1.0 MPa$\sqrt{m}$ for CPVC at 10 Hz.

23 - 50^{o} C for frequency of 1 Hz. The different slopes of these lines indicate two ΔH (activation energy) values for two separate cyclic fatigue mechanisms.

To confirm this prediction fracture surface of the fatigued specimen were examined. The details of the fracture surface analysis are discussed in section 5.5.

5.3.2 Effect of Temperature on FCP rate of HDPE

The effect of test temperature on fatigue crack growth in HDPE is examined assuming principles of linear elastic fracture mechanics. The representative fatigue crack propagation data for temperatures -10 and 0^{o} C at frequencies equal to 1 and 10 Hz are shown in figures 5.43 – 5.45.

In figures 5.43 and 5.45, there is data scattering in the initial stages of FCP. This data scattering is due to the absence of perfectly sharp notch tip, as the initial notch is made manually using a sharp razor blade. The blunted tip acts as an overload and results in retarding effect on the FCP. Once the crack grows through the plastic zone created by overload resumption of normal crack propagation takes place.

The effect of temperature on crack growth rate can be better illustrated by using the representative best fit curves on all the test data as shown in figure 5.46 and 5.47. These curves can be represented by the following equations:

(a) HDPE, -10^{o} C-1Hz $$\frac{da}{dN} = 2.00x10^{-7}\Delta K^{2.17} \quad (5.21)$$

(b) HDPE, -10^{o} C-10Hz $$\frac{da}{dN} = 2.00x10^{-8}\Delta K^{2.02} \quad (5.22)$$

(c) HDPE, 0^{o} C-1Hz $$\frac{da}{dN} = 3.00x10^{-7}\Delta K^{1.90} \quad (5.23)$$

(d) HDPE, 0^{o} C-10Hz $$\frac{da}{dN} = 4.00x10^{-8}\,\Delta K^{2.14} \qquad (5.24)$$

Results obtained illustrate a number of important points. For instance, for a given ΔK, crack growth rate da/dN increases with increasing temperature. For example, at ΔK = 1.0 MPa√m and 10 Hz, da/dN = $2.40x10^{-8}$ and 3.861 x 10^{-8} m/cycle for T = -10 and 0^{o} C, respectively. Also, the intercept A of the fatigue curves change with temperature. The value of A is 2.22 $x10^{-8}$ at -10^{o} C and 4.86 $x10^{-8}$ at $–0^{o}$ C and 10 Hz frequency. The average values of m and A at all test temperatures and frequencies for HDPE are given in table 5.2. Also, the variation of m and A with temperature for frequency equal to 10Hz is shown graphically in figures 5.48 and 5.49 respectively. It has been seen that value of slope m of the fatigue curves are constant with variations in the temperature.

Fatigue crack propagation in HDPE at -10 and 0^{o} C temperatures is characterized by phenomenon of crazing. Craze constituted expanded material containing oriented fibrils interspersed with small-interconnected voids. The combination of fibrils (extended across the craze thickness) and interconnected microvoids contributes toward an overall weakening of the material, though the craze is capable of supporting some reduced stress relative to that of the uncrazed matrix. The growth of craze occurs by extension of the craze tip into uncrazed material. Because of its intrinsic weakness the craze is an ideal path for crack propagation. Crack breakdown mechanisms include chain slippage and disentanglements, rupture of primary bonds within the molecular entanglements and detachment at the craze matrix interface.

Parsons et al [52] found step-wise crack propagation mechanism in HDPE developed due to crazing. Bureau M. and Dickson J. [59] also found fracture of crazes are responsible for fatigue crack propagation in these materials. Similarly Bucknall and

Table 5.2 Constants m and A for HDPE at temperature in the Paris equation (da/dN in m/cycle and ΔK in MPa√m)

Temperature (^{o}C)	**Frequency (Hz)**	**Exponent m**	**Parameter A**
-10 ^{o}C	**1**	2.1761	$2x10^{-07}$
	10	2.0294	$2x10^{-08}$
0 ^{o}C	**1**	1.9031	$3x10^{-07}$
	10	2.1470	$4x10^{-08}$

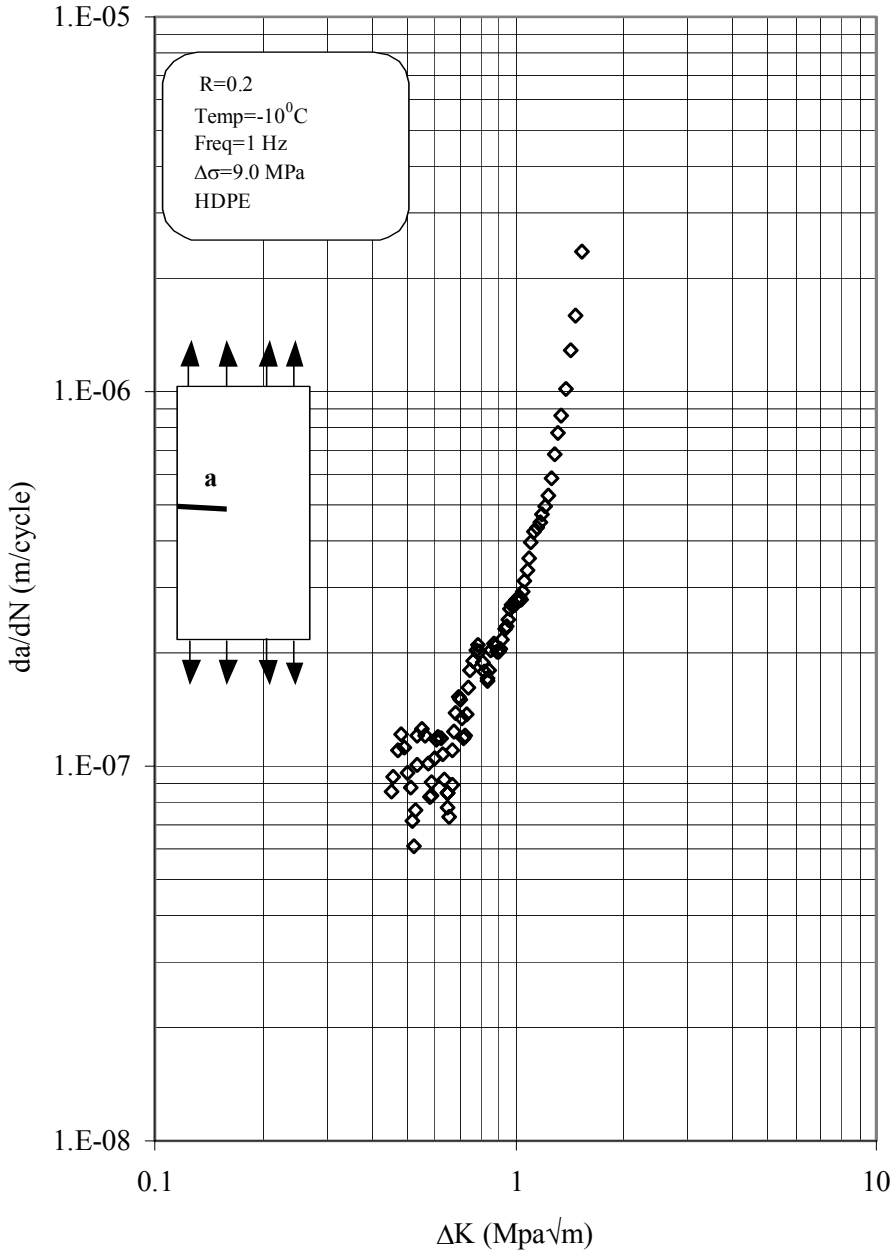

Figure 5.43 da/dN-ΔK curve for HDPE at 1 Hz and -10^o C.

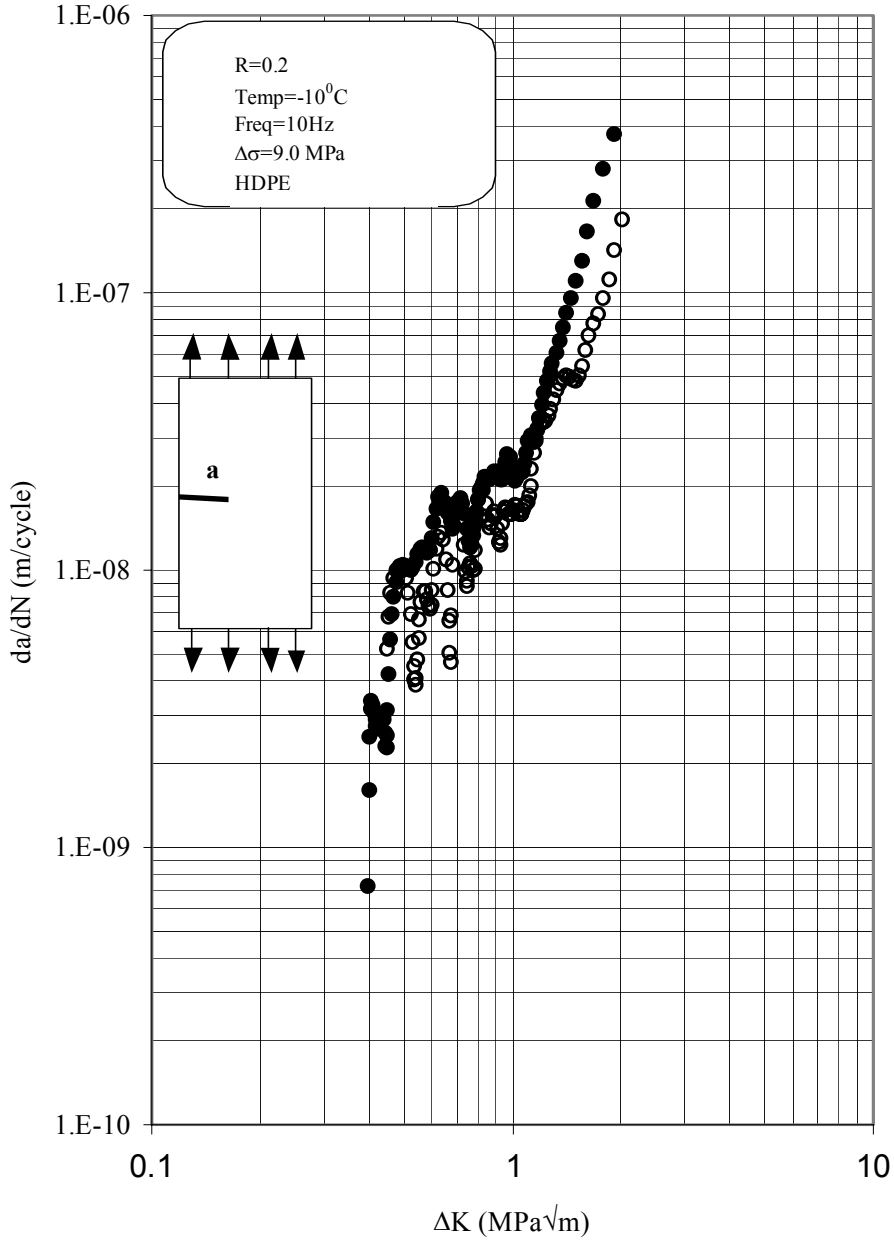

Figure 5.44 da/dN-ΔK curve for HDPE at 10 Hz and -10^o C.

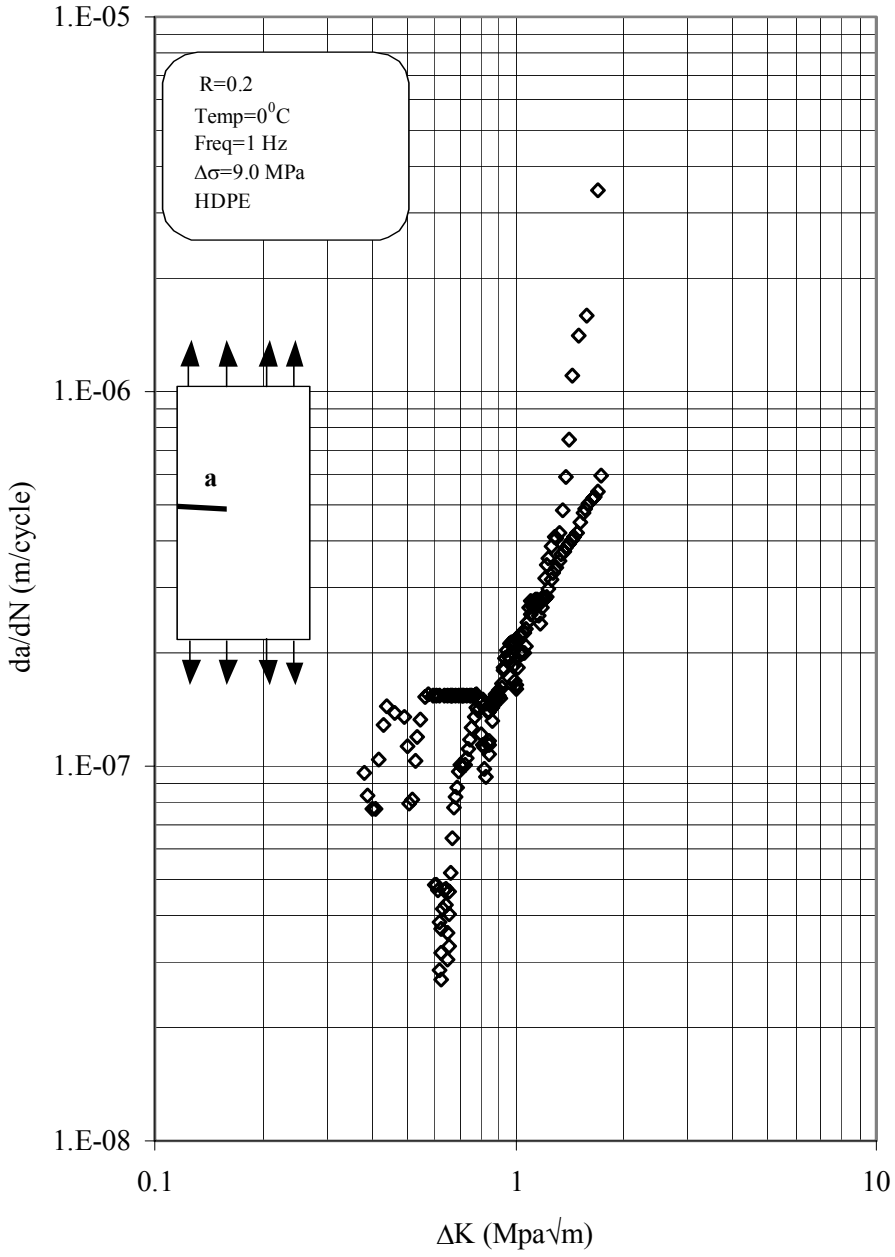

Figure 5.45 da/dN-ΔK curve for HDPE at 1 Hz and 0^o C.

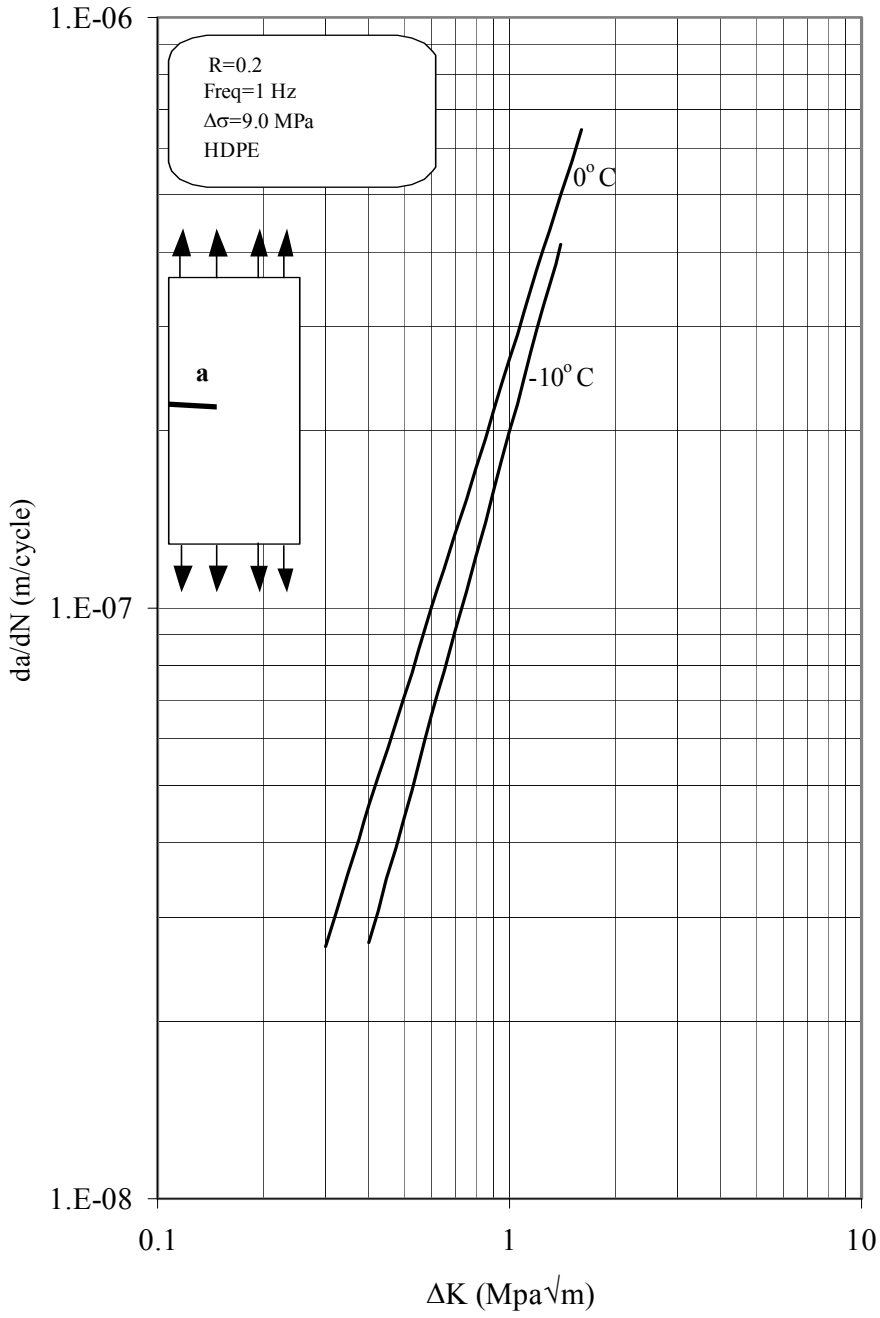

Figure 5.46 Fatigue crack growth rates at different temperatures for HDPE at 1 Hz frequency.

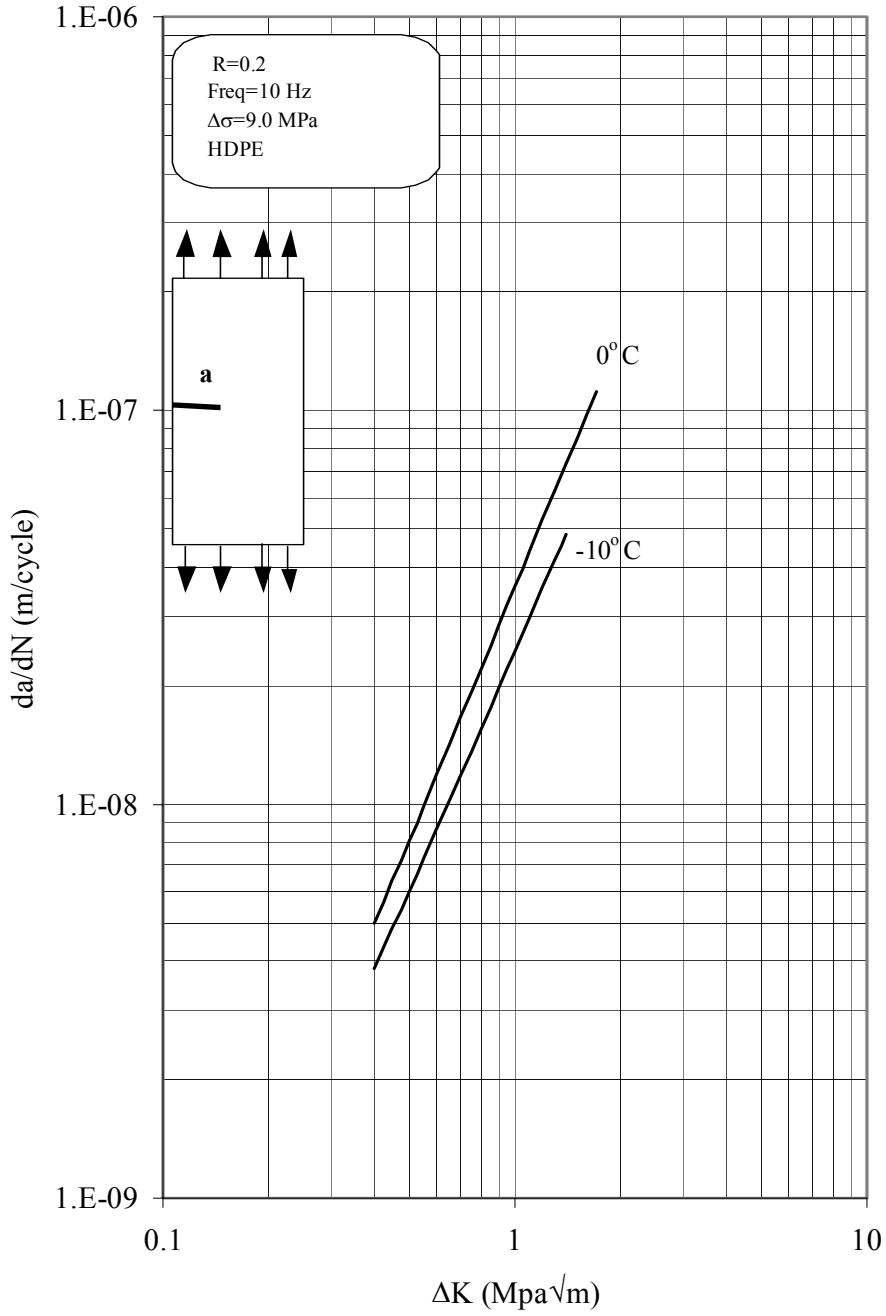

Figure 5.47 Fatigue crack growth rates at different temperatures for HDPE at 10 Hz frequency.

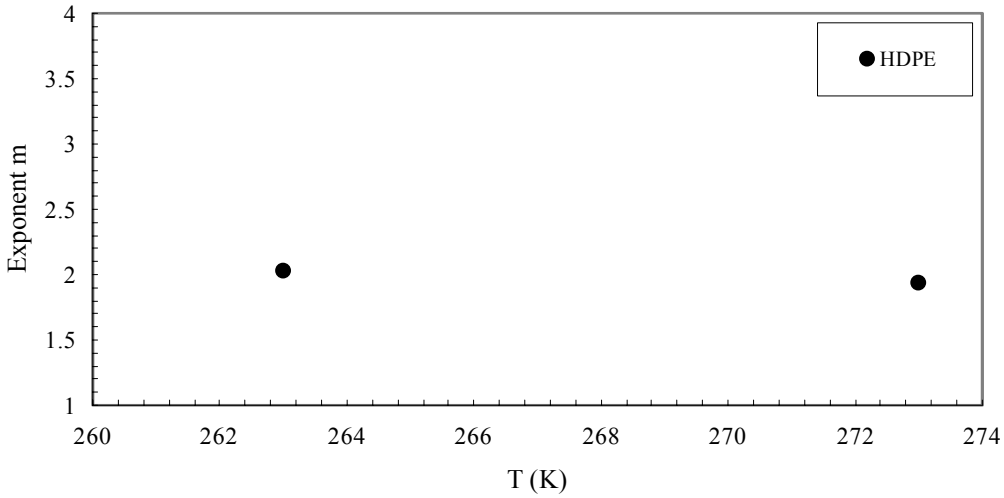

Figure 5.48 Variation of m with temperature for HDPE at 1 Hz frequency.

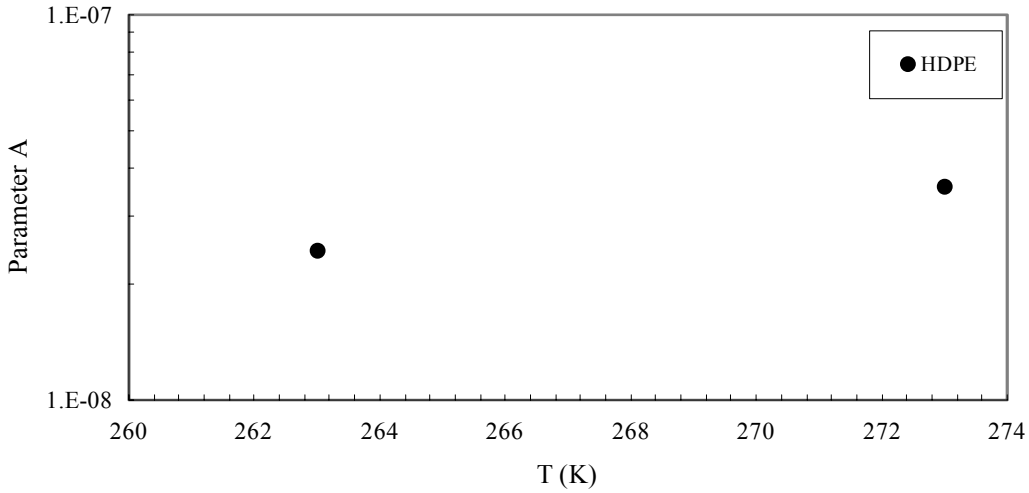

Figure 5.49 Variation of A with temperature for HDPE at 1 Hz frequency.

Dumpleton [50] found that crack growth in these HDPE and PMMA is characterized by crazing along with some deformation mechanisms such as shear bands, wrest bands etc.

5.3.3 Effect of Frequency on FCP rate of CPVC

The effect of test frequency on fatigue crack growth in CPVC is analyzed by using the linear elastic fracture mechanics principles. The effect of frequency on crack growth rate can be better illustrated by using the representative best fit curves on all the test data at each temperature, as shown in figures 5.50 to 5.54.

It has been noticed that the frequency effect on FCP is lower at lower temperatures ranging from no effect at -10^{o} C and 0^{o} C to negligible effect at 23^{o} C. But for high temperatures i.e. 50 and 70^{o} C there is considerable effect of frequency on FCP.

At high temperatures the frequency sensitivity seems to be dependent on the frequency level; being higher in the 0.1-1 Hz decade than in 1-10 Hz range. For ΔK = 2.0MPa$\sqrt{m}$, the frequency sensitivity factor is about 2.7 in the first and 1.7 in the second.

The higher difference in FCP between 0.1 and 1 Hz may be attributed to the interaction of creep with fatigue at 0.1 Hz. Here the creep mechanism is promoted by low frequency, high temperature and high mean stress (R=0.2). Parsons et al. [52] also found that at low enough frequency (0.01 Hz), a fatigue test might behave like a creep test where fracture is completely controlled by a creep process even though the load is cycled, and thus one has to superimpose fatigue and creep components for getting total crack growth.

The results obtained have illustrate a number of important points. First, for a given ΔK, crack growth rate da/dN increases with decreasing frequency for higher

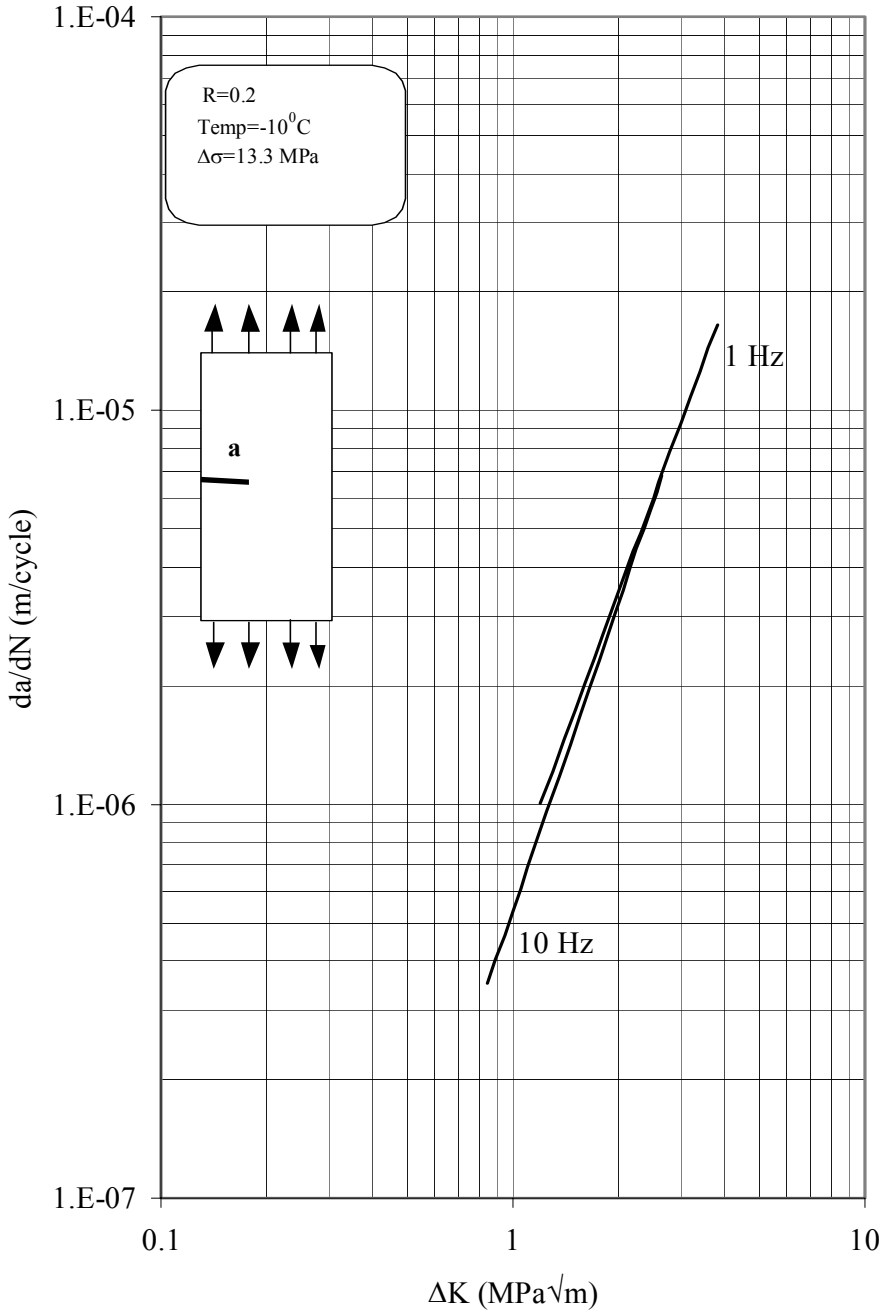

Figure 5.50 da/dN-ΔK curve for CPVC at -10^o C.and different frequencies.

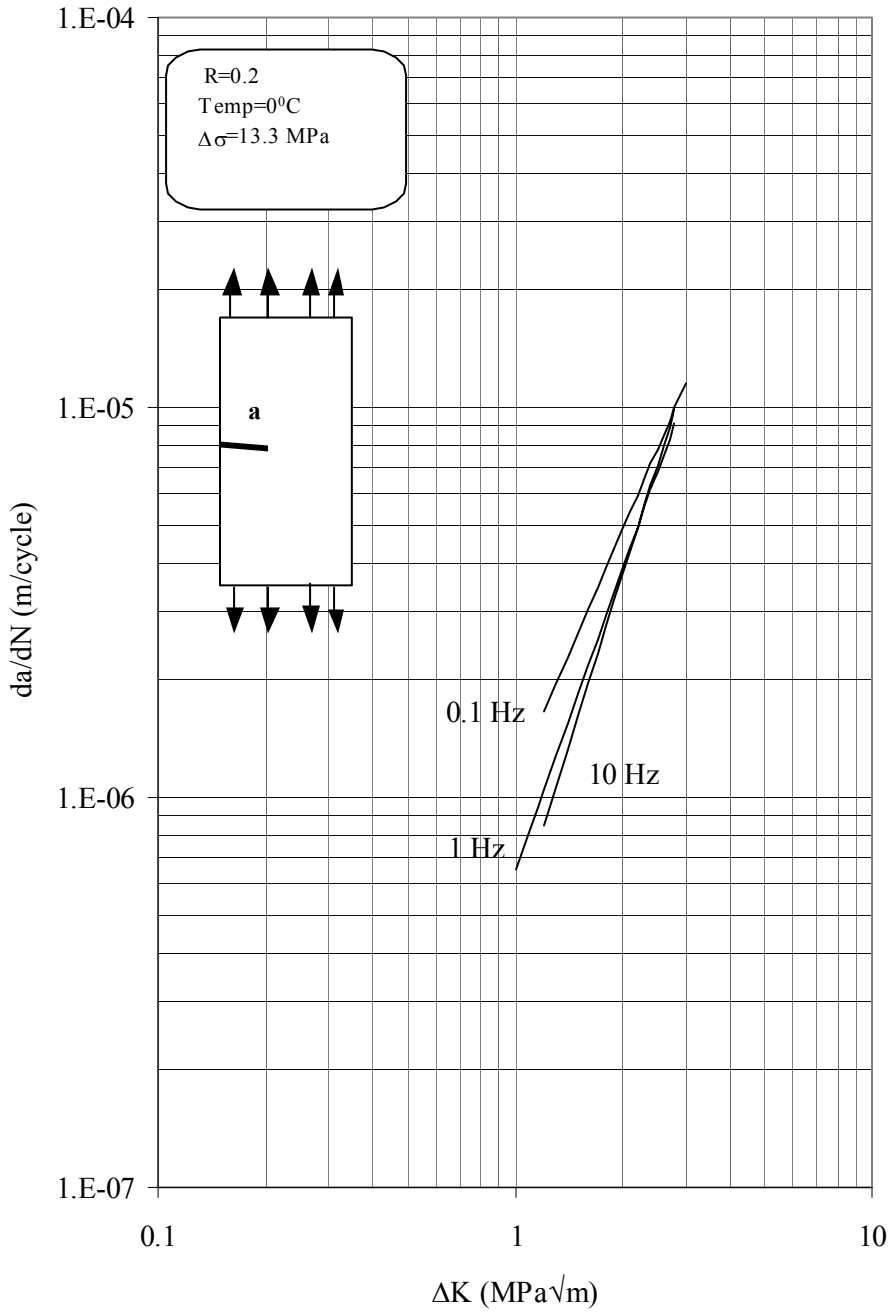

Figure 5.51 da/dN-ΔK curve for CPVC at 0° C.and different frequencies.

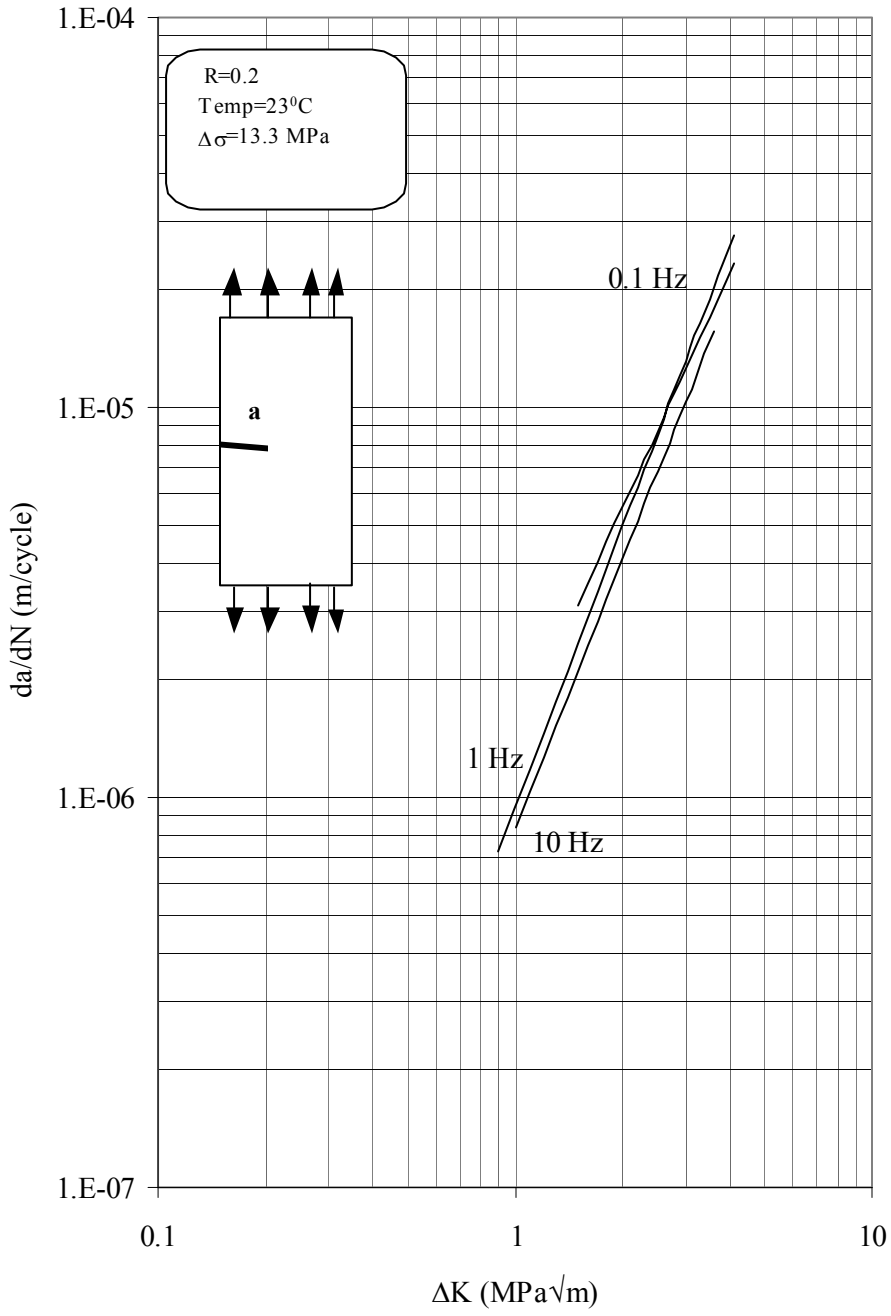

Figure 5.52 da/dN-ΔK curve for CPVC at 23° C.and different frequencies.

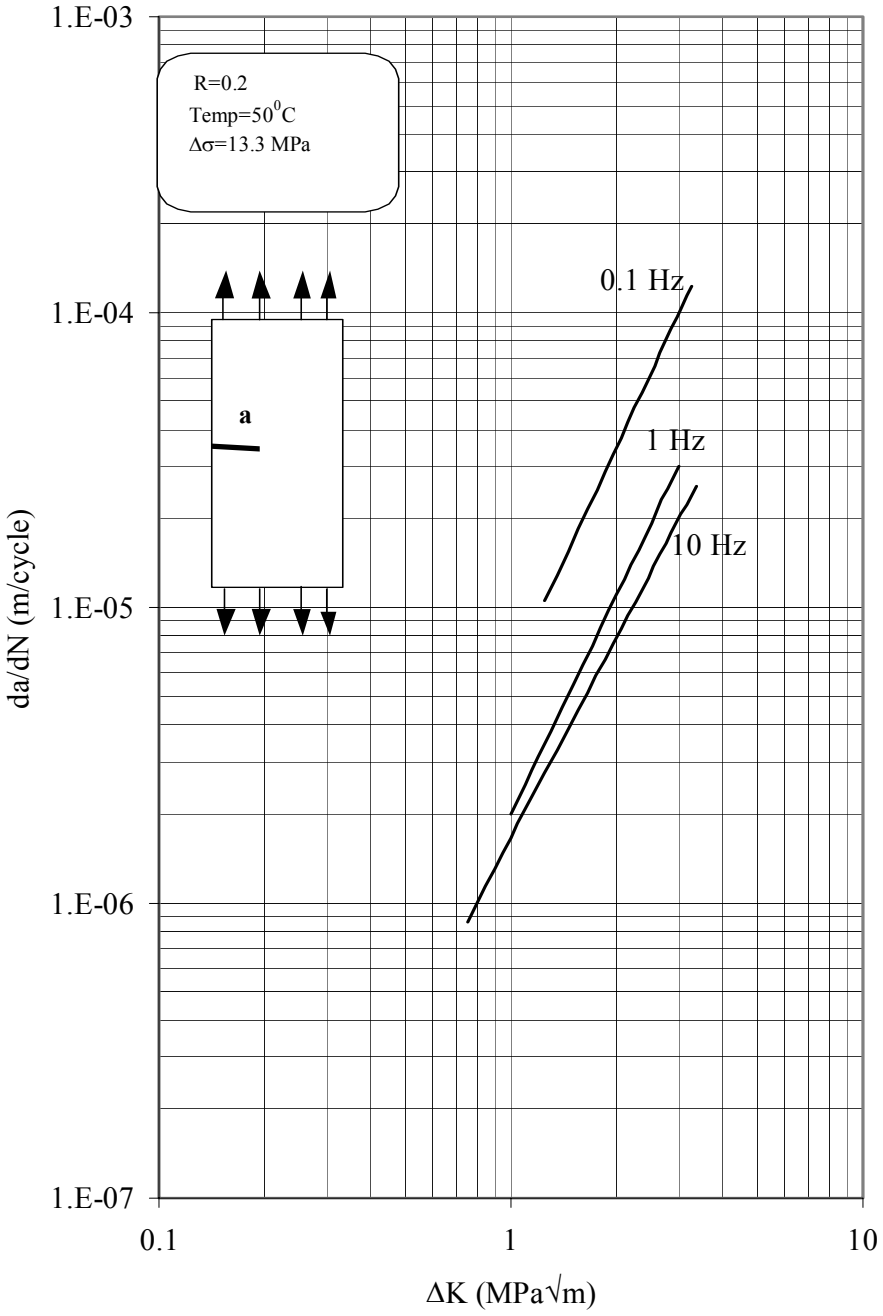

Figure 5.53 da/dN-ΔK curve for CPVC at 50^o C.and different frequencies.

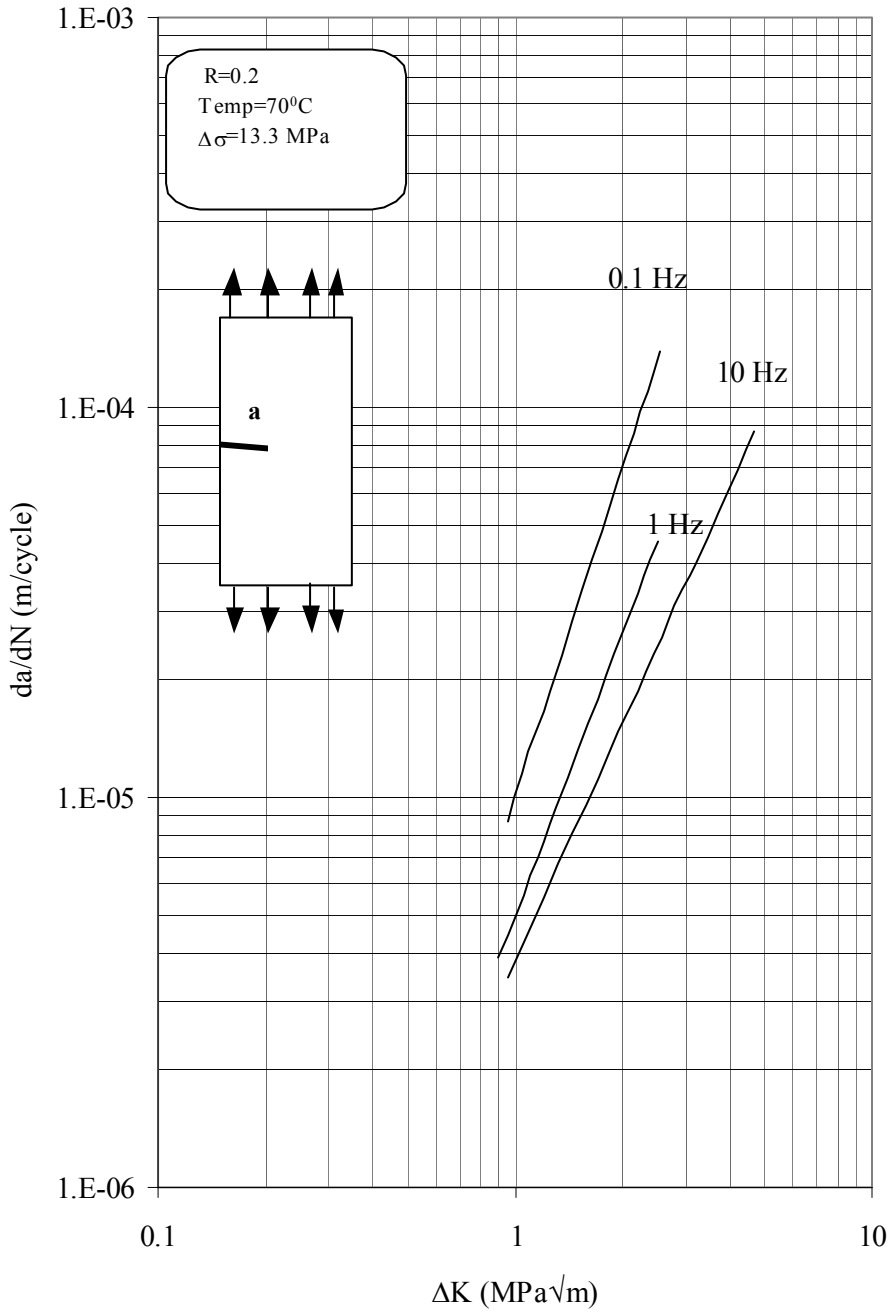

Figure 5.54 da/dN-ΔK curve for CPVC at 70° C.and different frequencies.

temperatures. For example, at $\Delta K = 2.0$ MPa$\sqrt{m}$ and 70^o C, da/dN = 6.5, 2.97 and 1.57 $x10^{-5}$m/cycle for frequency equal to 0.1, 1 and 10 Hz respectively. Also, the intercept A of the fatigue curves changes with frequency. The value of A is varies from $1x10^{-5}$ at 0.1 Hz to $5x10^{-6}$ at 10 Hz for 70^o C. The average values of m and A at all test frequencies for CPVC are given in table 5.1. The variation of m and A with frequency at 50^o C is shown graphically in figures 5.55 and 5.56 respectively. The values of m and A obtained by Kim et al [63] for uPVC are also plotted in these figures for comparison. It has been seen that value of slope m of the fatigue curves remain practically unaffected by variations in the frequency, while A decreases with increasing frequency. A comparison of these parameters for PVC and CPVC show that CPVC has lower crack propagation resistance for the reasons given earlier.

The effect of frequency on FCP is linked with the size of the plastic zone size near the crack tip, and it's variation with frequency result in the decrease or increase of FCP. Fatigue crack propagation in CPVC at high frequencies is also characterized by the localized heating at the crack tip, which causes temperature rise at the tip. In the present investigation an attempt was made to quantify the temperature rise at the crack tip for room temperature (23^o C) using a pair of J type thermocouples. It was found that at a frequency of 1 Hz, the temperature rise was about 4.6^o C, while for 10 Hz it was about 10.2^o C. This temperature rise enhanced yielding processes in the vicinity of the crack tip and lead to an increase in crack tip radius. A larger radius of curvature at the crack tip results in lower effective ΔK, and consequently lower fatigue growth rates.

It should be mentioned however, that this measurement does not represent exactly the temperature rise at the crack tip but that of an area around it. The actual temperature

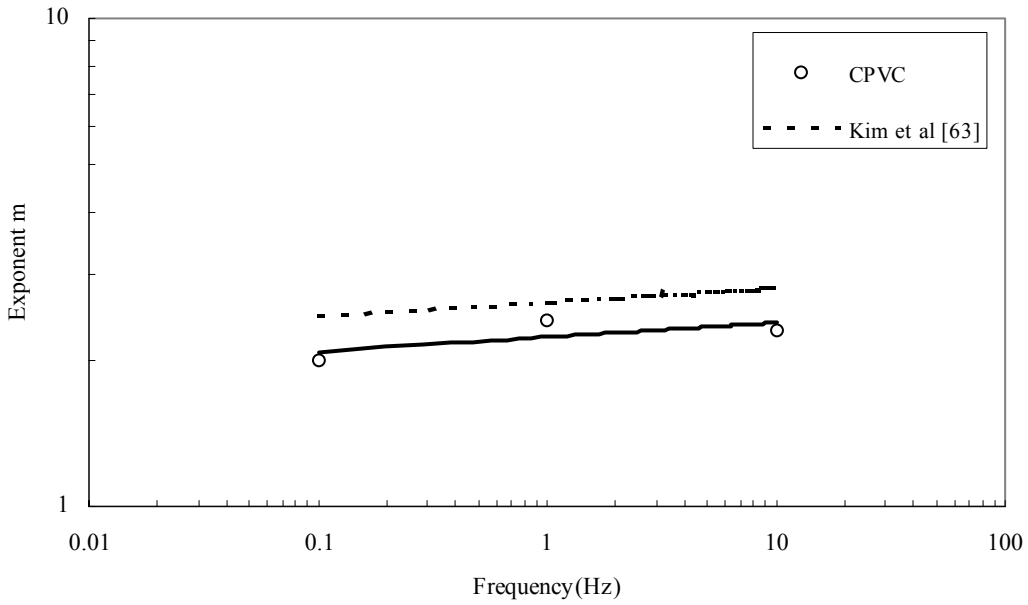

Figure 5.55 Variation of m with frequency for CPVC.

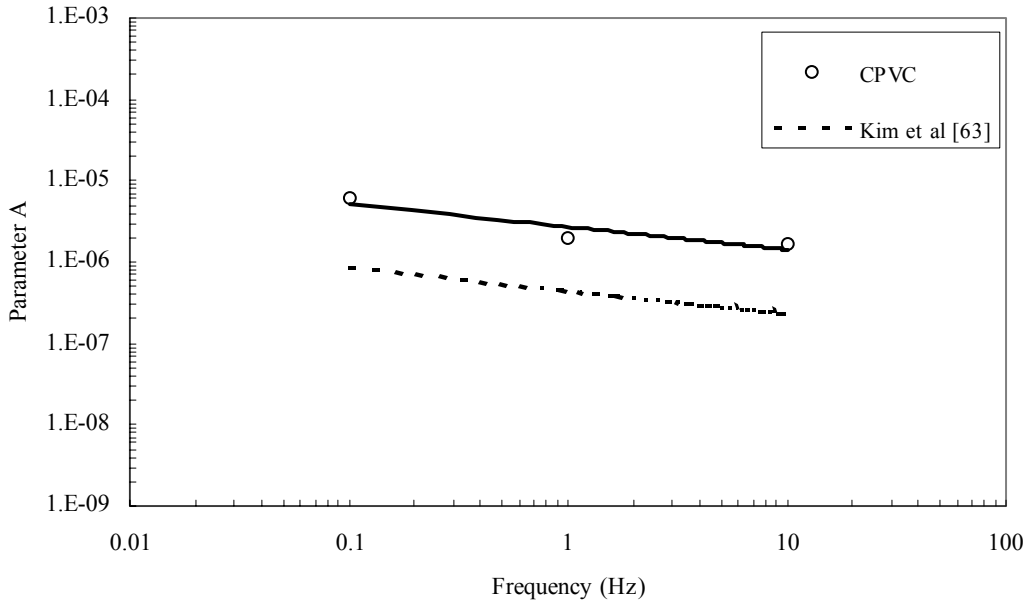

Figure 5.56 Variation of A with frequency for CPVC.

rise may be higher as this heating is known to be confined to the immediate crack tip. It nonetheless gives an indication of a temperature increase associated with higher frequency. For CPVC this temperature rise was insufficient to make a noticeable difference in FCP rate at room temperature , as shown in figure 5.52. The frequency sensitivity factor for ΔK= 2.0 MPa$\sqrt{m}$ at room temperature is of the order of 1.2 compared to 1.7 and 2.7 at 50 and 70^{o} C, respectively.

Our findings of fracture mechanisms at different frequencies for CPVC are similar to that observed by Cheng and manson [60], Kim et al [63]and Allard and others [55].

5.3.4 Effect of Frequency on FCP rate of HDPE

The effect of test frequency on fatigue crack growth in HDPE is analyzed by using the Paris and Erdogan [75] law given by equation 2.7. The effect of frequency on crack growth rate can be better illustrated by using the representative best fit curves on all the test data at each frequency, as shown in figure 5.57 and 5.58.

Results obtained illustrate important points. For example, for a given ΔK, crack growth rate da/dN increases drastically with decreasing frequency for temperatures of -10^{o} C and 0^{o} C, i.e., at ΔK = 1.0 MPa$\sqrt{m}$ and 0^{o} C, da/dN = 3.45 and 20 x10^{-8}m/cycle for frequencies equal to 1 and 10 Hz respectively. Also, the value of intercept A of the fatigue curves changes with frequency, it varies from a value of 2.64x10^{-7} at 1 Hz to 2.44x10^{-8} at 10 Hz for temperature of -10^{o} C. The average values of m and A at all test frequencies for HDPE are given in table 5.2. The variation of m and A with frequency at 0^{o} C is shown graphically in figures 5.59 and 5.60 respectively. It can be seen that the

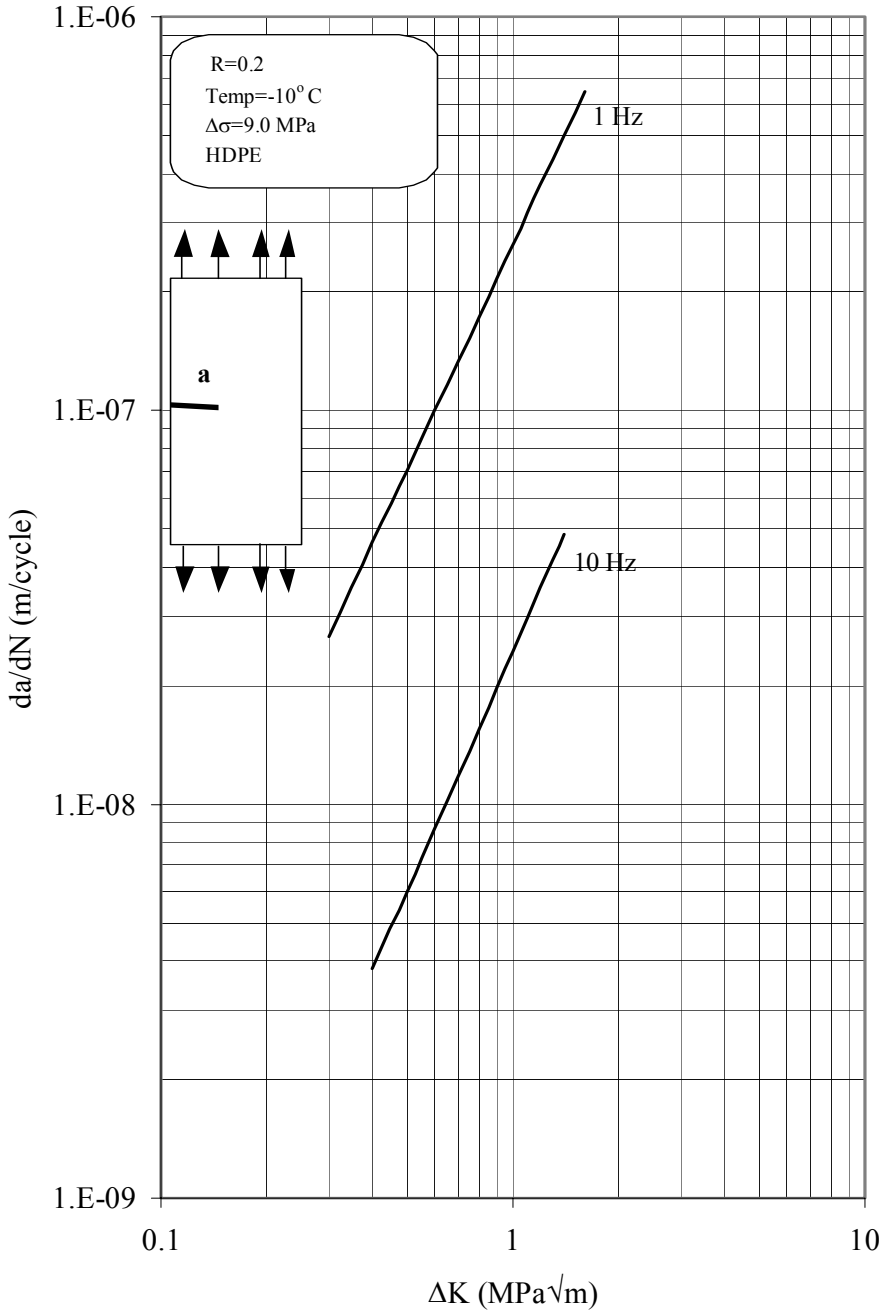

Figure 5.57 da/dN-ΔK curve for HDPE at -10° C and different frequencies.

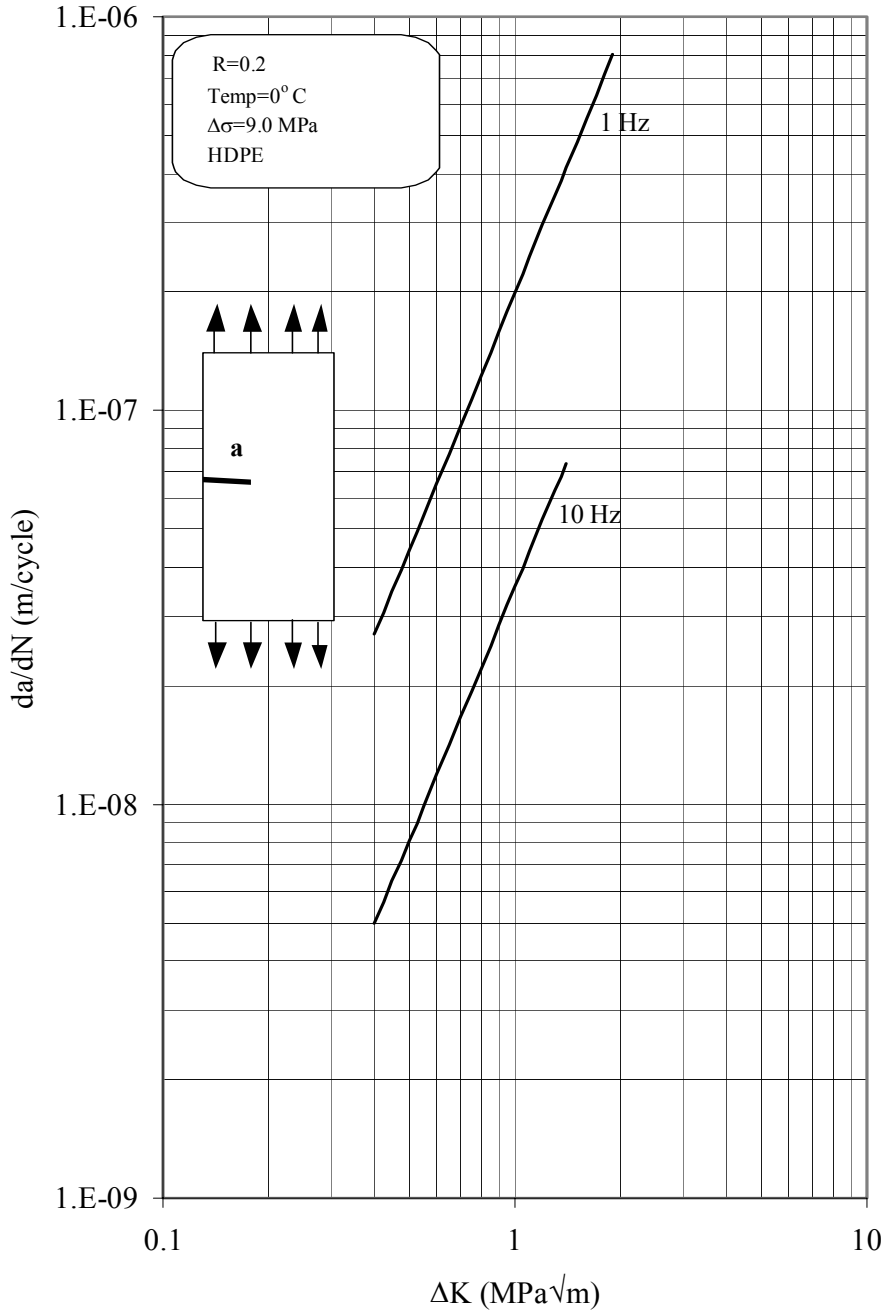

Figure 5.58 da/dN-ΔK curve for HDPE at 0° C and different frequencies.

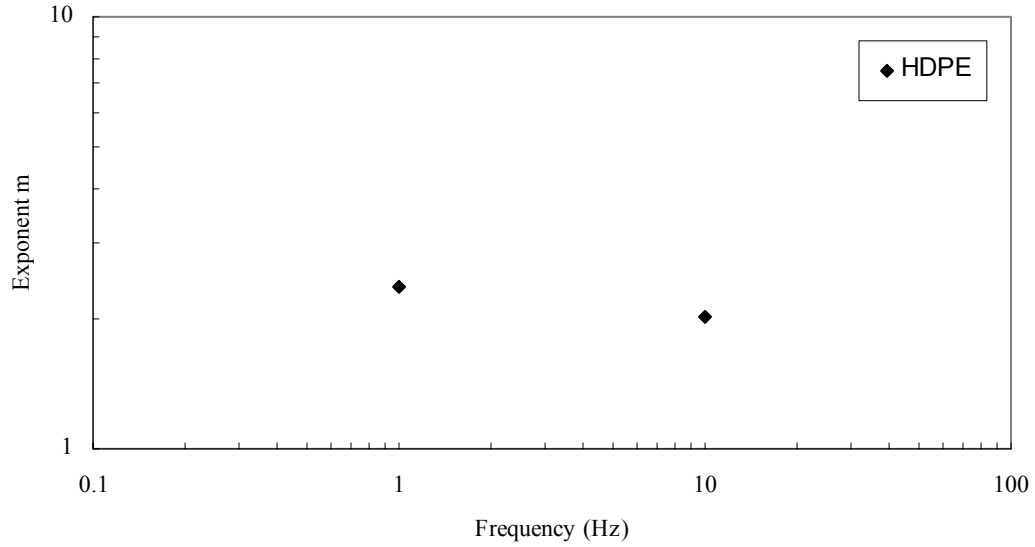

Figure 5.59 Variation of m with frequency for HDPE at 0^{o} C.

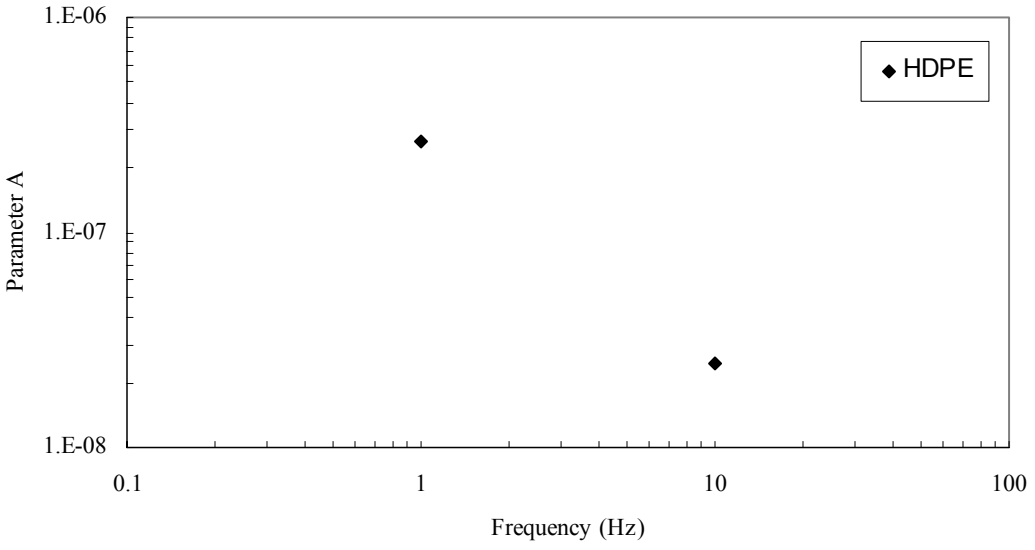

Figure 5.60 Variation of A with frequency for HDPE at 0^{o} C.

frequency affects more intercept A than slope m with the latter remaining atmost equal to 2.0 for both –10 and 0^o C.

The above results show that there is a considerable effect of frequency on FCP at the temperatures of -10^o C and 0^o C. As seen for CPVC the frequency sensitivity factor (FSF) is dependent on temperature being higher at higher temperature; for -10^o C at ΔK = 2.0MPa$\sqrt{m}$ is about 10.0, while for 0^o C it is 5. It should be noted that the glass transition temperature for HDPE is -30^o C and, -10^o C and 0^o C are considered as high temperatures.

Fatigue crack propagation in HDPE is characterized by hysteretic heating. Due to viscoelastic nature of the material, the cycling frequency is a very critical parameter in the resulting FCP rate. High cyclic rates or frequency imposed on the HDPE specimens bring heating that could lead to thermal softening fracture. Since we are using notched specimens, this heating could be confined to crack tip and result in a blunting of the crack tip which reduces both local stress concentration and hence fatigue crack growth.

Deformation response time is also an important factor linked with fatigue crack propagation in HDPE. Frequency-dependent, rate of disentanglement of the molecular motions consisting of chain disentanglements and slippage in the fatigued fibrils also account for part of the frequency effect on fatigue crack growth. Hence, at high frequencies the magnitude of chain entanglements and slippage should be larger over a long period of time (frequency), and as a consequence HDPE show smaller FCP rates at high frequencies.

Our findings of fracture mechanisms at different frequencies for HDPE are similar to that observed by Cheng and manson [60], Kim et al [63] and Allard and others [55].

5.4 Development of da/dN-ΔK Master Curve

From the above discussion it is evident that there is a distinct fatigue crack growth curve at each temperature and frequency for CPVC. And for HDPE there is a distinct fatigue crack growth curve at -10^{o} C and 0^{o} C corresponding to 1 and 10 Hz frequencies. This means that in order to be able to predict fatigue life from the fatigue crack growth rate at a temperature other than studied, FCG tests must be conducted. FCP tests are time consuming and involve high costs especially at low temperatures. If we could however develop a means to predict the FCG properties at the temperature of interest by using the existing FCG data, it can be very beneficial for the designer as well as for the industry.

One good technique to develop the master curve is by using the mechanical properties. This technique has been used by Merah et al [79] to represent the crack propagation rate at different temperatures in terms of the modified ΔK obtained by using the mechanical properties at those temperatures. The authors [79] have applied this method successfully for metallic materials and was later proven to be valid for rigid plastics [53]. In this study, the applicability of this method to CPVC and HDPE is investigated for different frequencies. The impetus behind this investigation stems from the dependence of yield strength on temperature as can be seen in figures 4.1, 4.2, 4.3, 4.4, 4.5 and 4.6. This method uses the dependence of CTOD on the yield stress i.e.,

$$CTOD = \frac{K_I^2}{\sigma_{YS} E} \tag{5.25}$$

From above higher temperatures will result in lower yield stress which causes a higher crack tip opening displacements (CTOD) and hence in lower effective ΔK. The influence of the yield stress on FCG in CPVC and HDPE is examined. In order to

determine the effect of yield stress, da/dN is plotted in terms of the modified stress intensity factor, given as follows:

$$\Delta K_y = \Delta K \frac{(\sigma_{ys})_{RT}}{(\sigma_{ys})_T} \tag{5.26}$$

The indices RT and T indicate the value of the parameter at room temperature and the temperature of interest respectively. The values of σ_{ys} for CPVC at all temperatures of interest are taken from Merah and Irfan [19] (Table 4.1). Figures 5.61, 5.62, 5.63, 5.64 and 5.65 show the da/dN-ΔK master curves of CPVC and HDPE for frequencies of 0.1, 1 10 Hz. The master curves obtained from ΔK_y can be represented by the following equations:

(a) CPVC, 0.1 Hz

$$\frac{da}{dN} = 2.00x10^{-6} \Delta K_y^{2.0} \tag{5.27}$$

(b) CPVC, 1 Hz

$$\frac{da}{dN} = 8.00x10^{-7} \Delta K_y^{2.6} \tag{5.28}$$

(c) CPVC, 10 Hz

$$\frac{da}{dN} = 7.00x10^{-6} \Delta K_y^{2.4} \tag{5.29}$$

(d) HDPE, 1Hz

$$\frac{da}{dN} = 2.46x10^{-7} \Delta K_y^{1.98} \tag{5.30}$$

(e)HDPE, 10 Hz

$$\frac{da}{dN} = 3.75x10^{-8} \Delta K_y^{2.15} \tag{5.31}$$

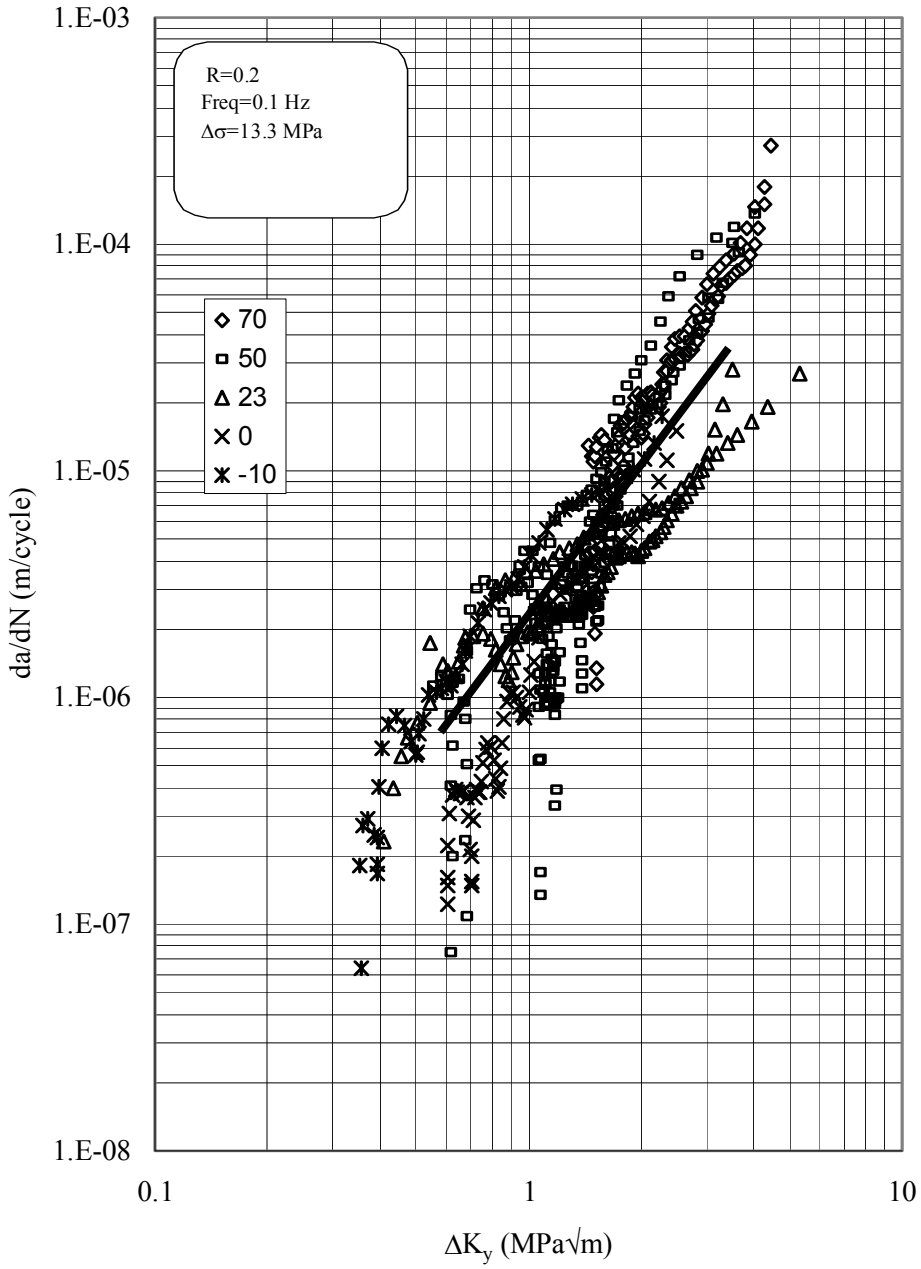

Figure 5.61 Crack propagation in CPVC at different temperatures for 0.1 Hz frequency expressed in terms of modified $\Delta K_{y.}$

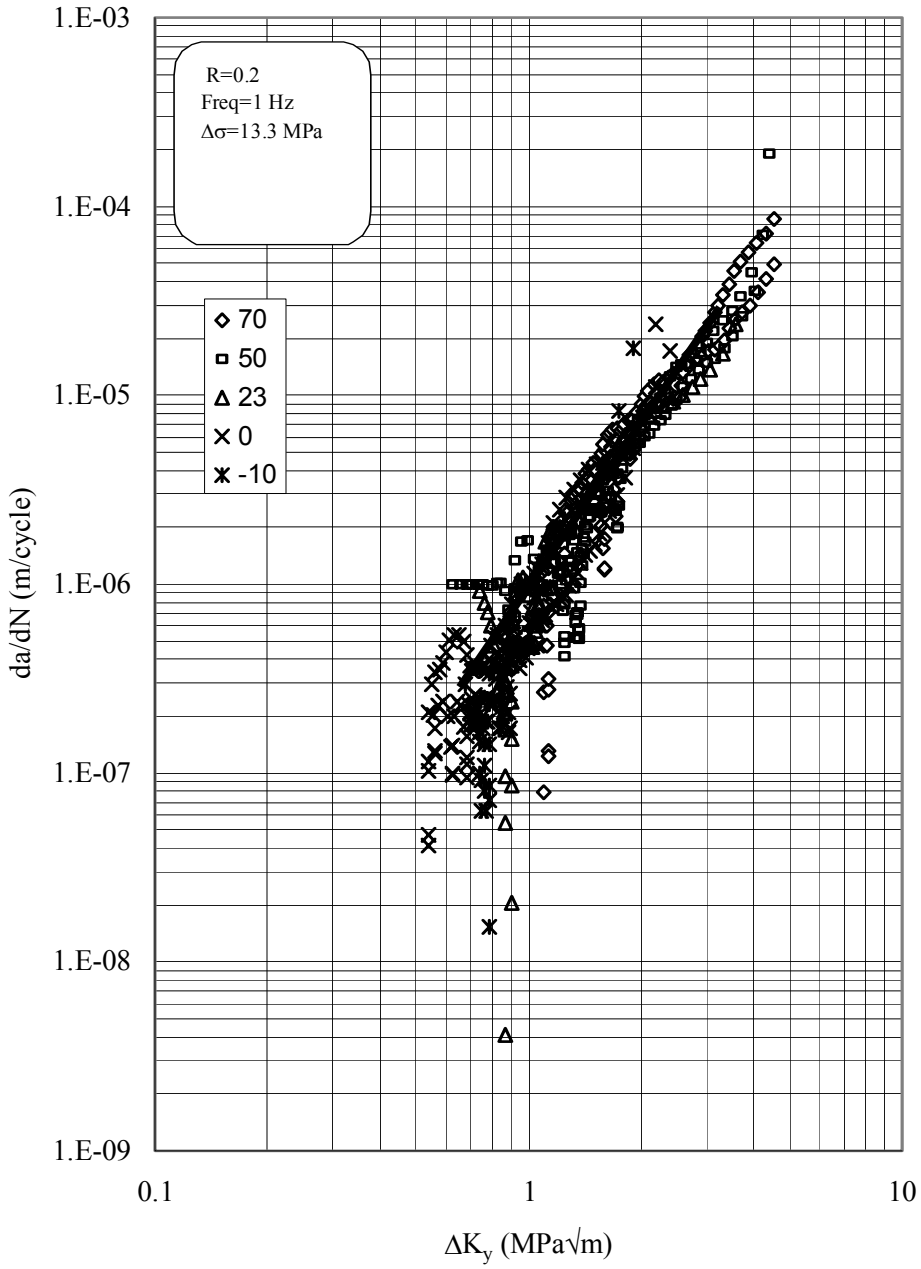

Figure 5.62 Crack propagation in CPVC at different temperatures for 1 Hz frequency expressed in terms of modified $\Delta K_{y.}$

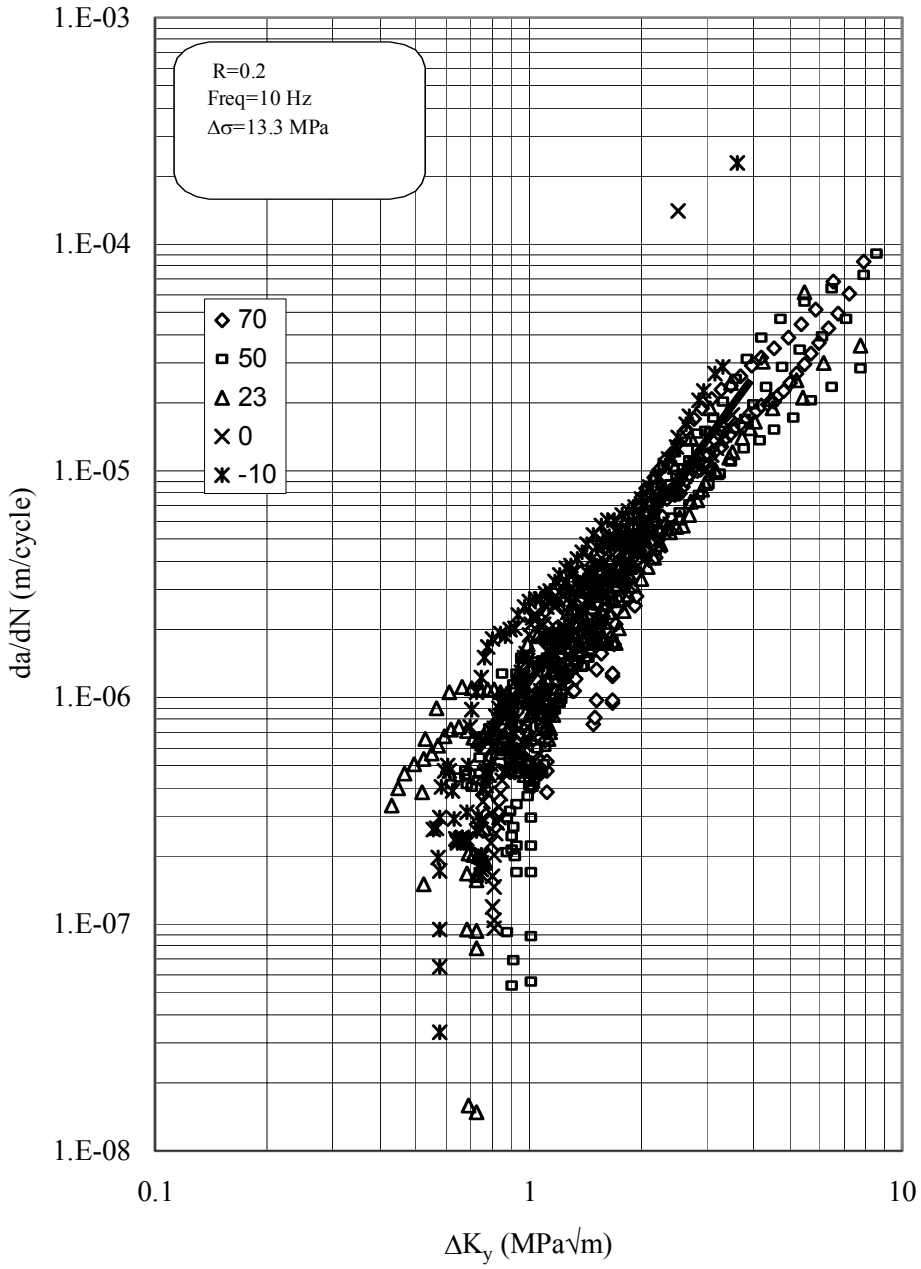

Figure 5.63 Crack propagation in CPVC at different temperatures for 10 Hz frequency expressed in terms of modified $\Delta K_{y.}$

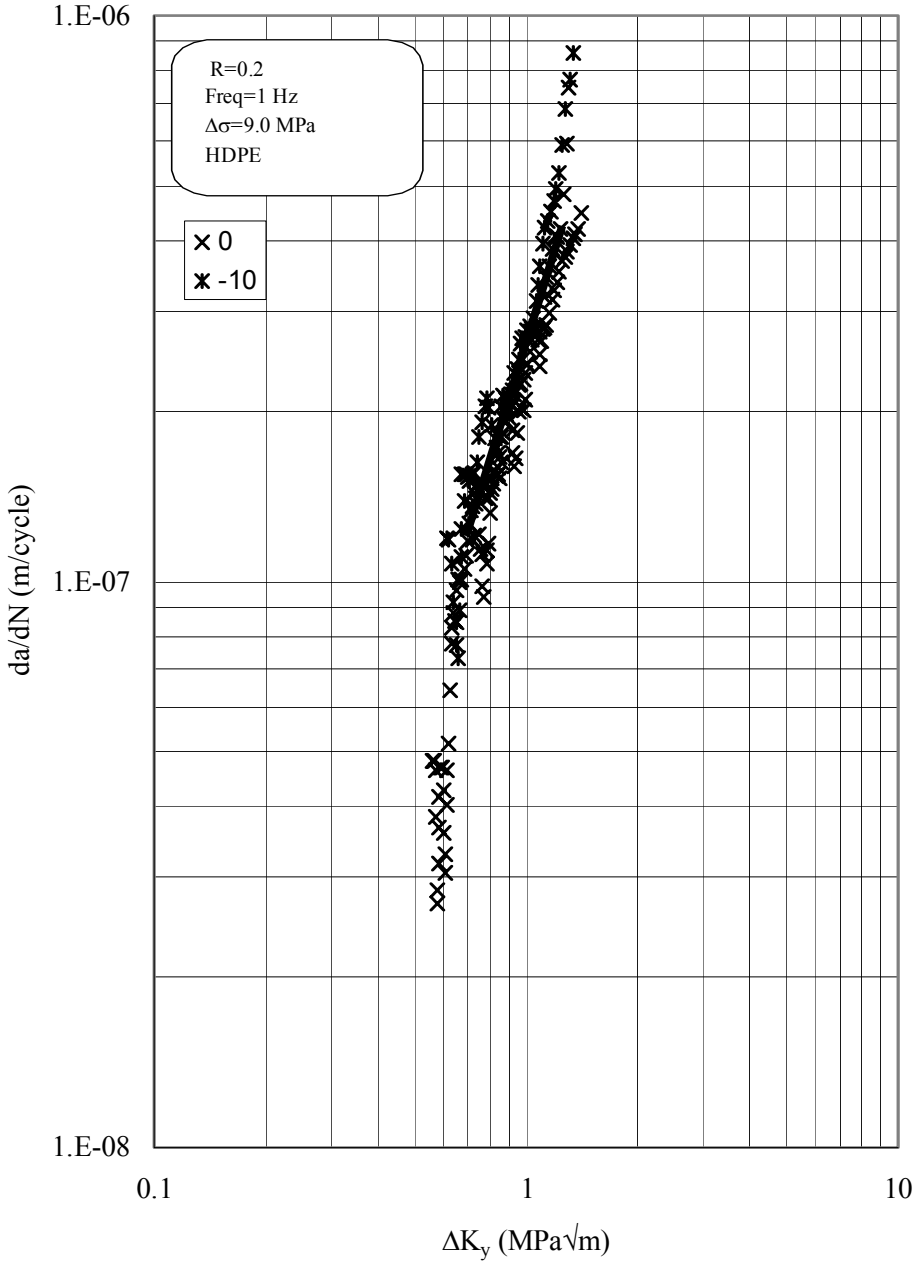

Figure 5.64 Crack propagation in HDPE at different temperatures for 1 Hz frequency expressed in terms of modified $\Delta K_{y.}$

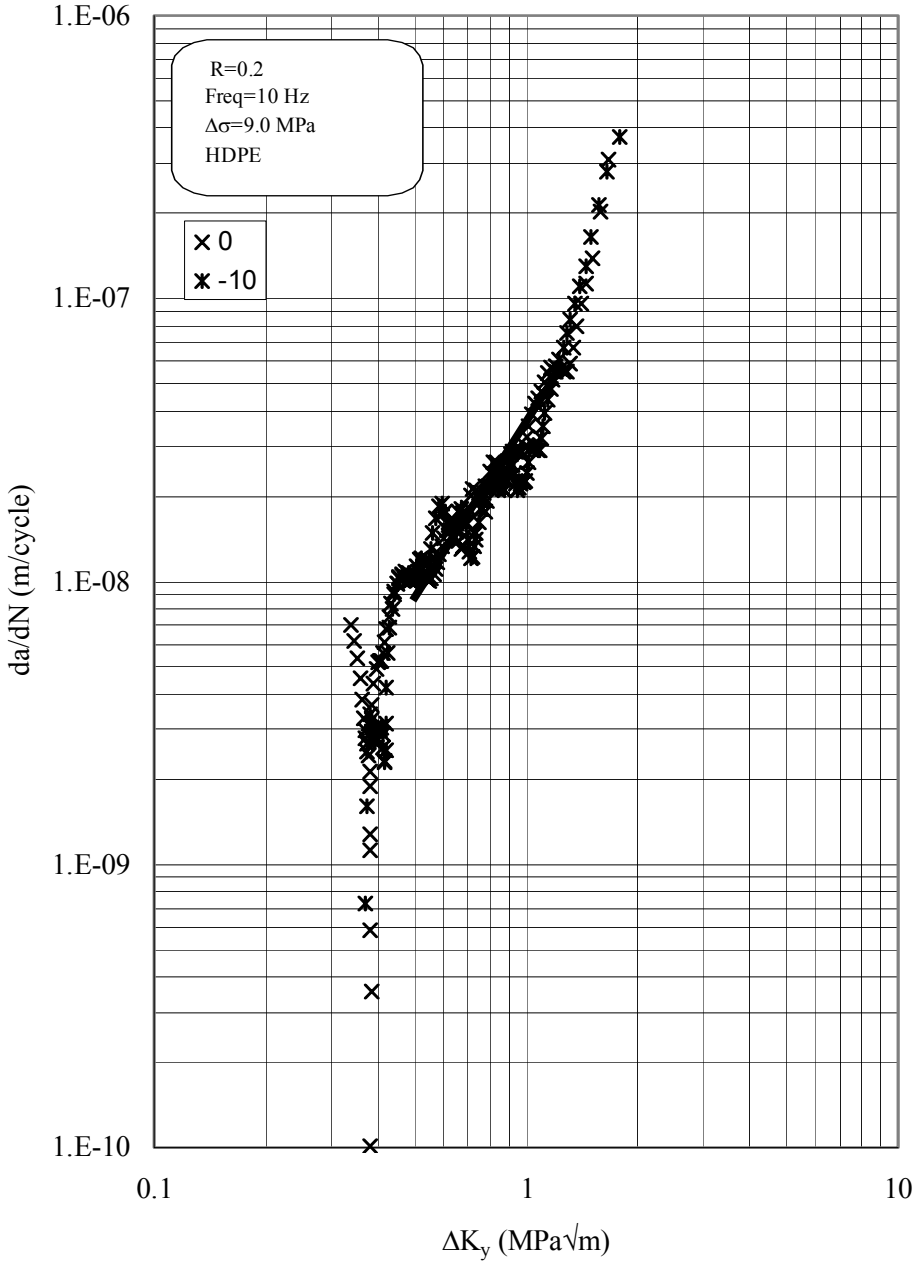

Figure 5.65 Crack propagation in HDPE at different temperatures for 10 Hz frequency expressed in terms of modified $\Delta K_{y.}$

It can be seen that yield stress incorporates the effect of temperature very efficiently. The da/dN-ΔK_y curves for all temperatures of interest lie within a factor of 1.5 from the room temperature curve (except for 0.1 Hz). This may be attributed to the interaction of creep with fatigue at 0.1 Hz. Creep mechanism is promoted by low frequency, high temperature and high mean stress (R=0.2). Thus one has to superimpose fatigue and creep components for getting total crack growth.

5.5 Fractographic Analysis

Most polymers like metals yield at sufficiently high stresses. While metals yield by dislocation motion along slip planes, polymers can exhibit either crazing or shear yielding as they do not contain crystallographic planes, dislocations and grain boundaries.

Crazing is a highly localized deformation that leads to cavitation (voids formation) and strains on the order of 100% [76, 77]. On the macroscopic level, crazing appears as a stress-whitened region, due to low refractive index. The craze zone usually forms perpendicular to the maximum principal normal stress. To quote Kambour [78], "Optimists concentrate on plastic deformation in crazes as a source of toughness or stress relief on polymers, while pessimists focus on crazing as the beginning of brittle fracture.

Shear yielding in polymers resembles plastic flow in metals, at least from a continuum mechanics viewpoint. Molecules slide with respect to one another when subjected to a critical shear stress. Crazing and shear yielding are competing mechanisms; the dominant yielding behavior depends on molecular structure, stress state and temperature. Each yielding mechanism displays a different temperature dependence; thus the dominant mechanism may change with temperature.

It is well established that careful examination of fine scale fracture surface details can provide significant information regarding various fracture processes and phenomena in solids. On the basis of these enlightening information, material and design engineers are better able to improve overall component design through changes in composition and internal microstructure of material. In addition, fractographic investigations often provide useful quantitative information that can be used to analyze the continuum details of fracture processes.

Many distinct fracture surface markings are readily apparent from a macroscopic examination of a component that has been subjected to repeated loadings. First, the fatigue fracture surface is oriented perpendicular to the principal stress direction. Secondly, useful information regarding fatigue process can be obtained by noting changes in the color and texture of polymer fatigue fracture surface. As discussed earlier, the dominant fracture mechanism at high temperature is found to be crazing characterized by rough fatigue fracture surfaces. It has been noticed in present study that transition from craze to shear yielding fracture mechanism is dependent upon temperature only and is independent of frequency. Doll [80] found the similar transitional behavior for PMMA.

In order to investigate these mechanisms in CPVC and HDPE, samples from fracture surfaces were prepared and analyze using Joel JSM scanning electron microscope. Figures 5.66-5.72 show the macrofractographs (magnification = 5x) of CPVC and HDPE tested at different frequencies and temperatures. For CPVC it is observed that the fatigue surface of specimens tested at higher temperatures is rough as

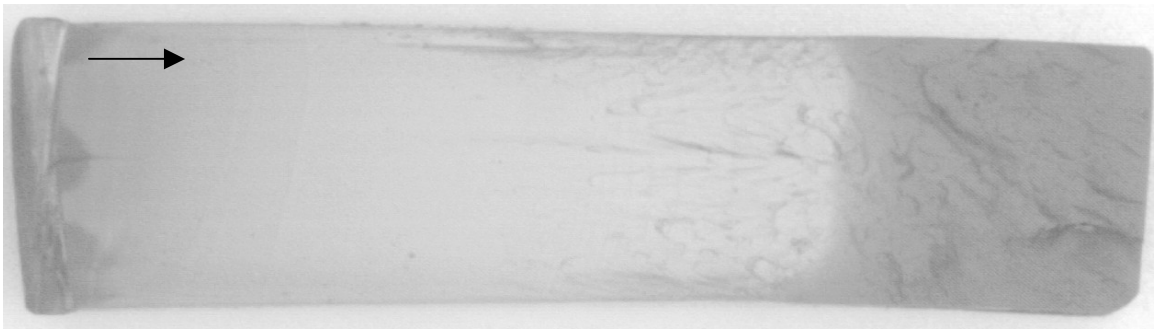

(a) 0.1 Hz

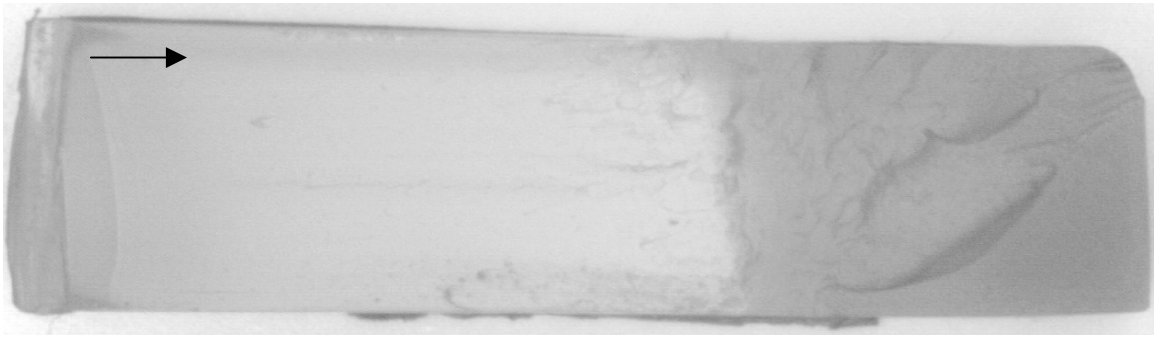

(b) 1 Hz

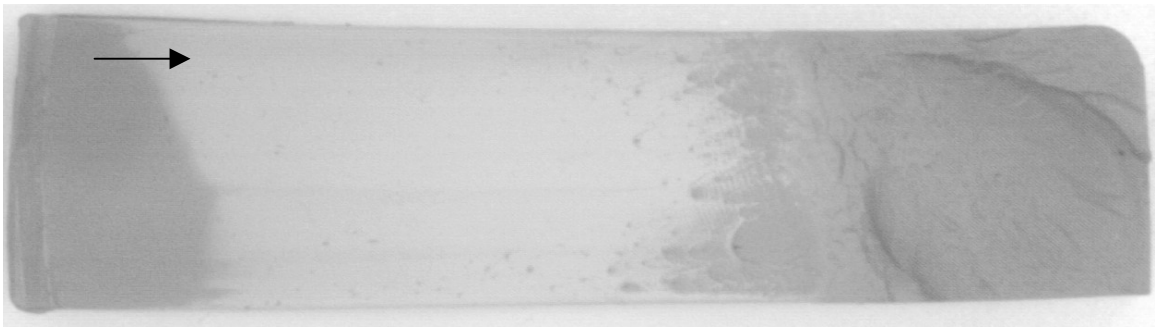

(c) 10 Hz

Figure 5.66 Macrofractographs of CPVC samples at -10^{o} C for different frequencies.

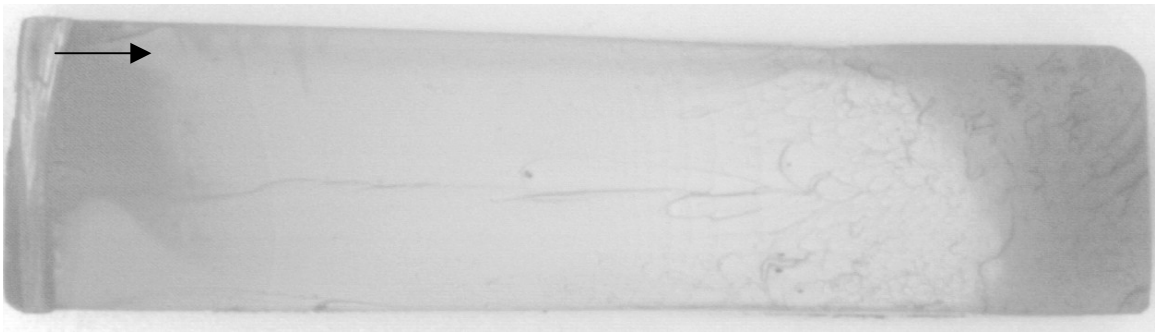

(a) 0.1 Hz

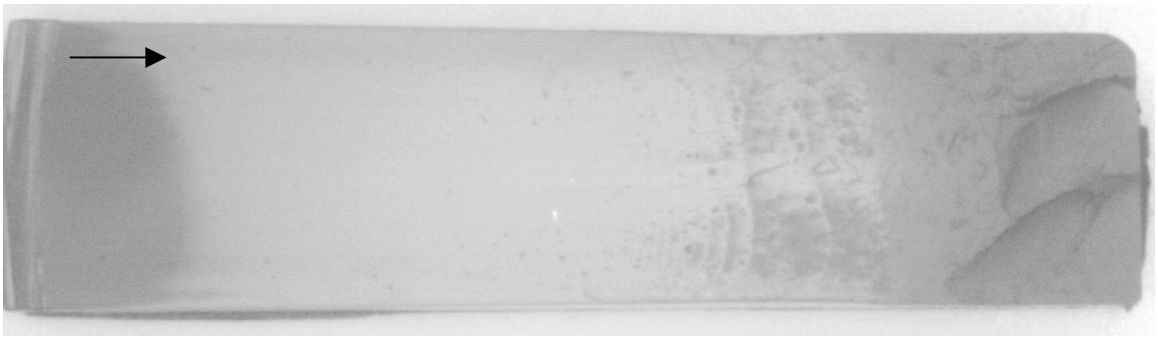

(b) 1 Hz

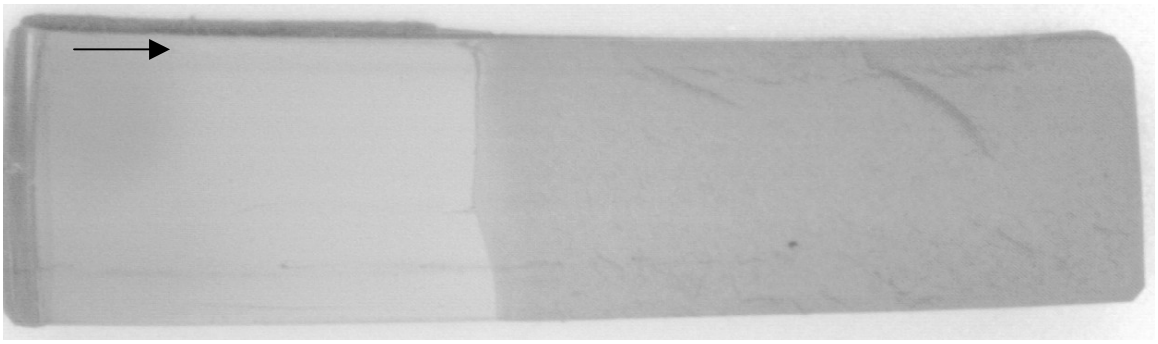

(c) 10 Hz

Figure 5.67 Macrofractographs of CPVC samples at 0^{o} C for different frequencies.

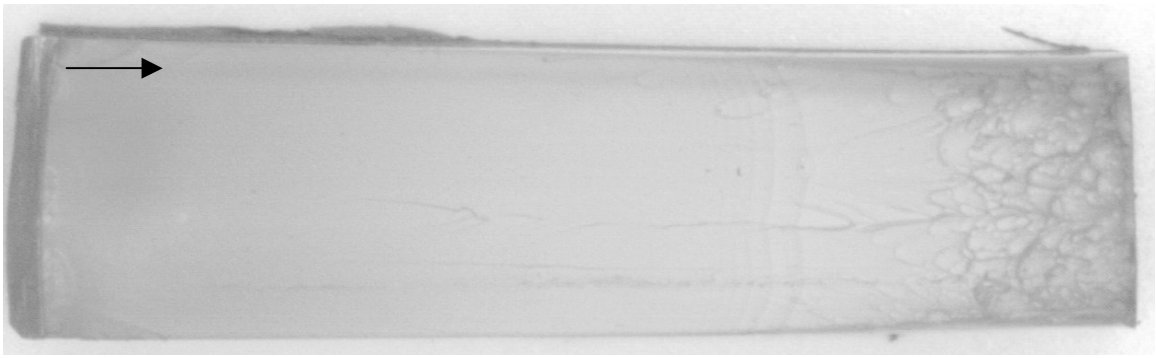

(a) 0.1 Hz

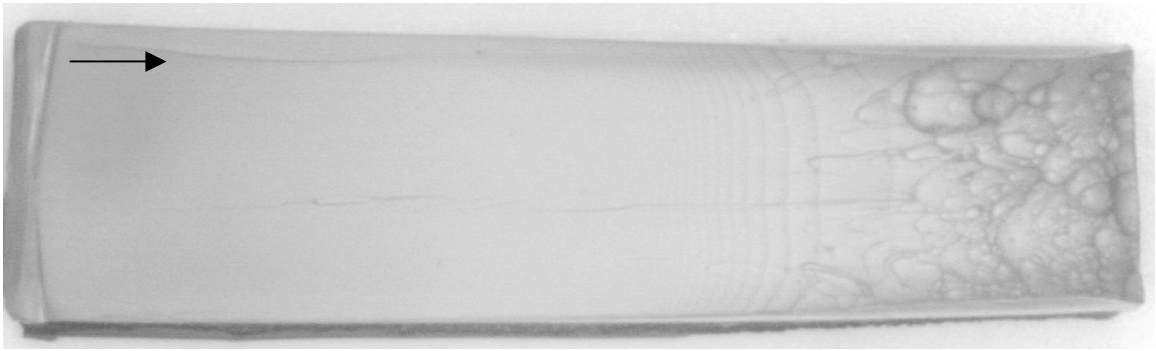

(b) 1 Hz

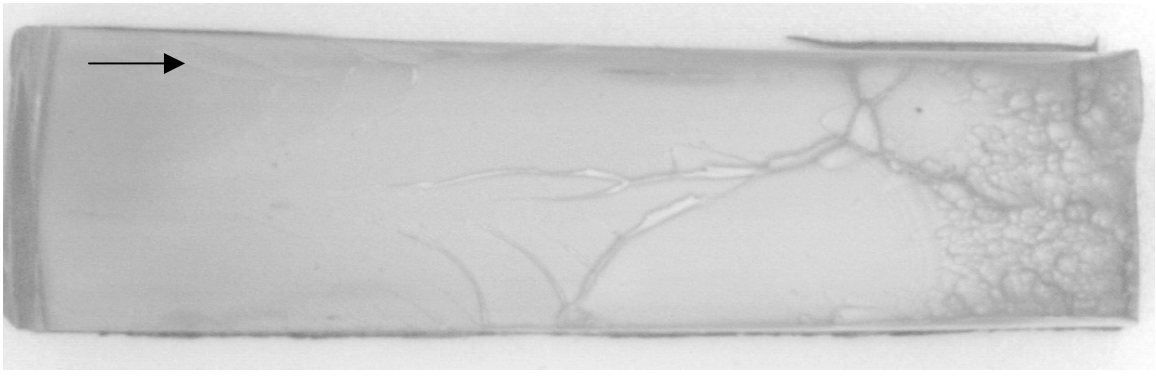

(c) 10 Hz

Figure 5.68 Macrofractographs of CPVC samples at 23^{o} C for different frequencies.

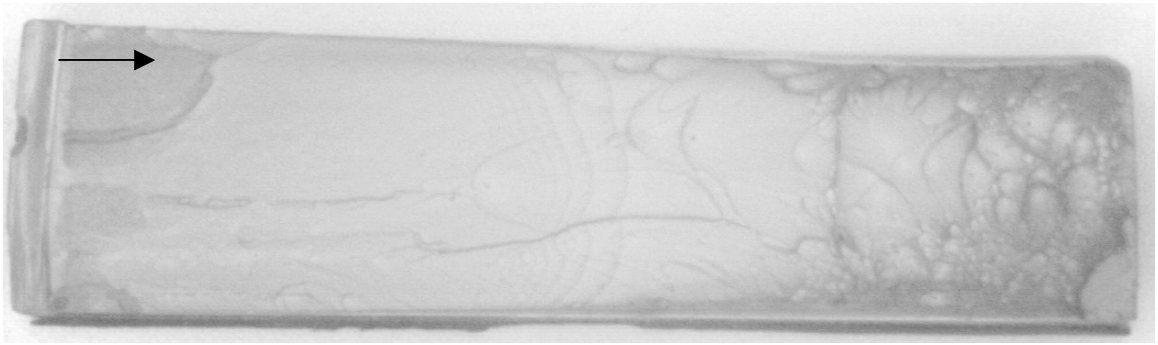

(a) 0.1 Hz

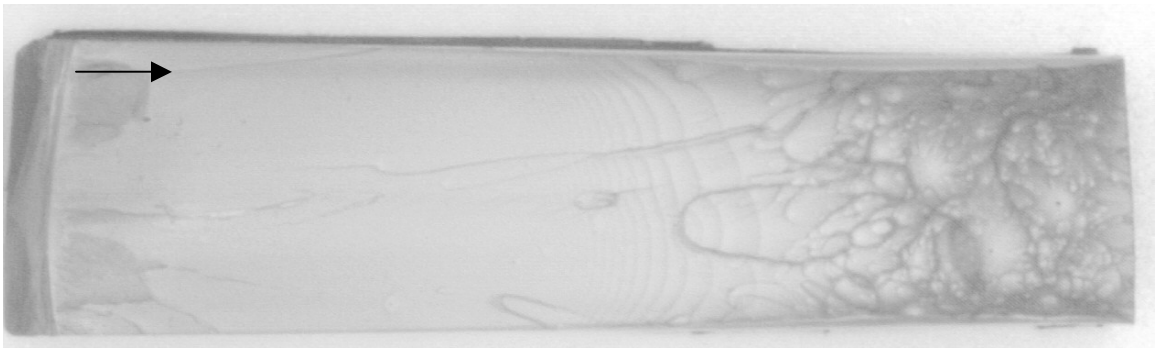

(b) 1 Hz

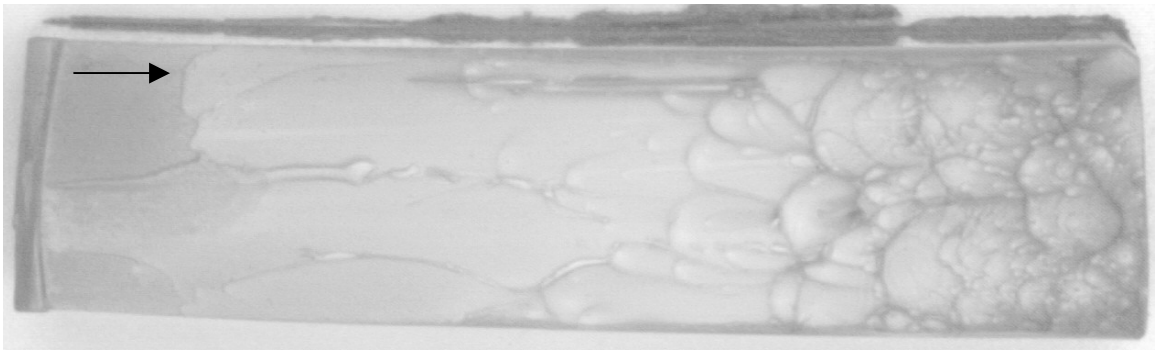

(c) 10 Hz

Figure 5.69 Macrofractographs of CPVC samples at 50^{o} C for different frequencies.

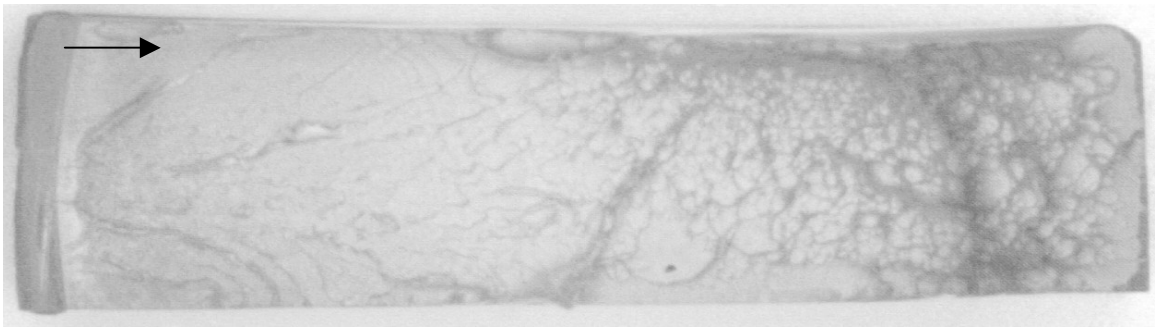

(a) 0.1 Hz

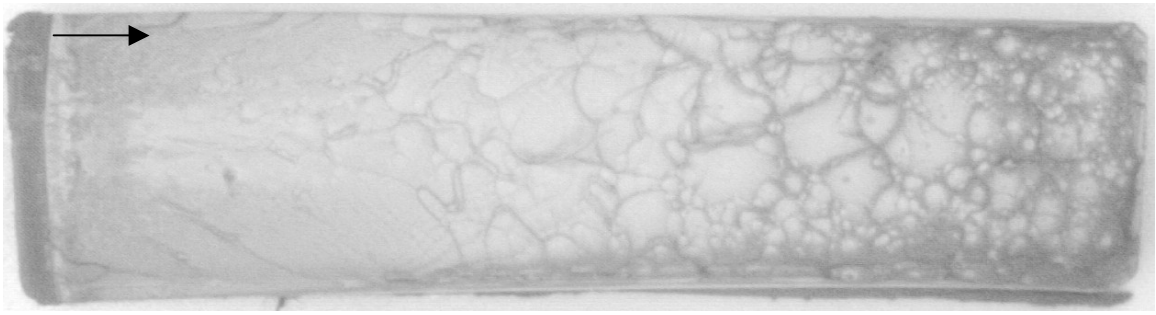

(b) 1 Hz

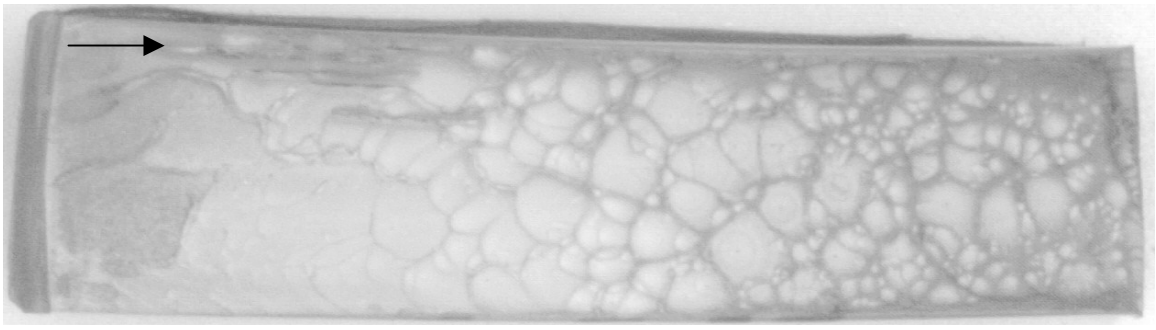

(c) 10 Hz

Figure 5.70 Macrofractographs of CPVC samples at 70^{o} C for different frequencies.

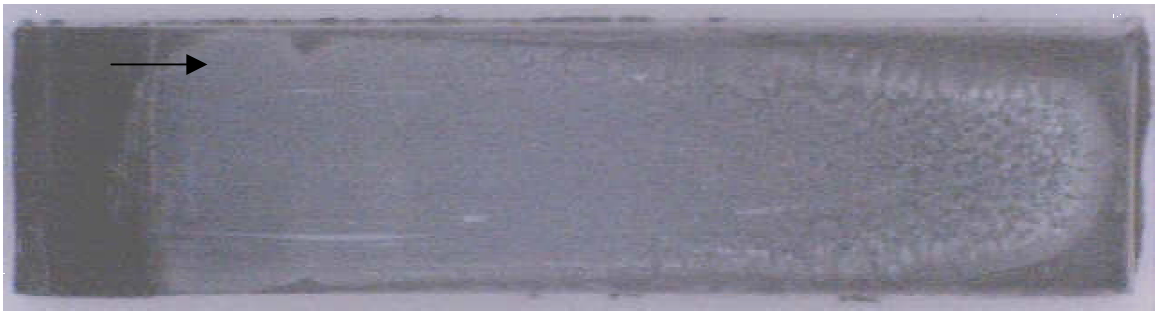

(a) 1 Hz

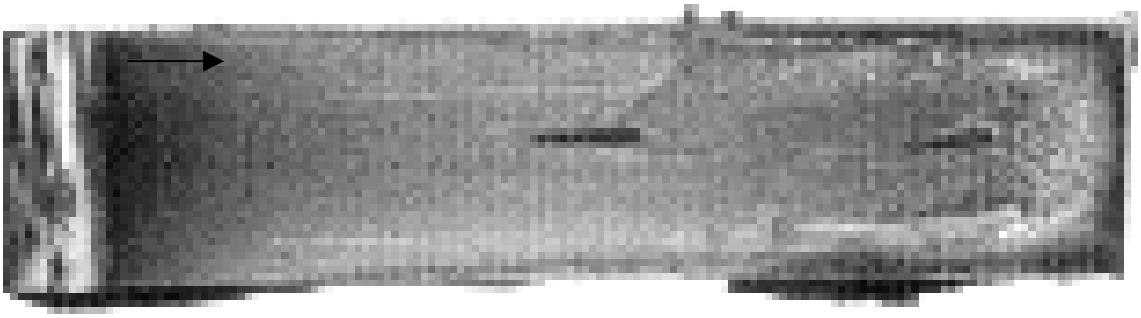

(b) 10 Hz

Figure 5.71 Macrofractographs of HDPE at different frequencies for -10^{o} C temperature.

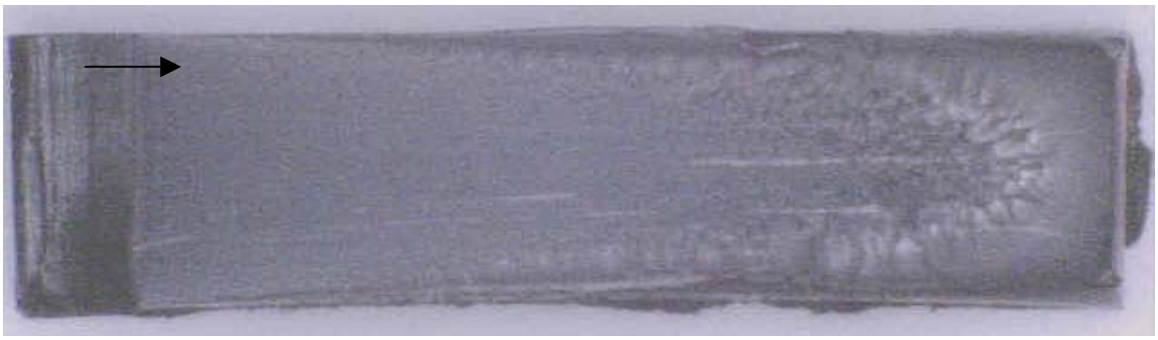

(a) 1 Hz

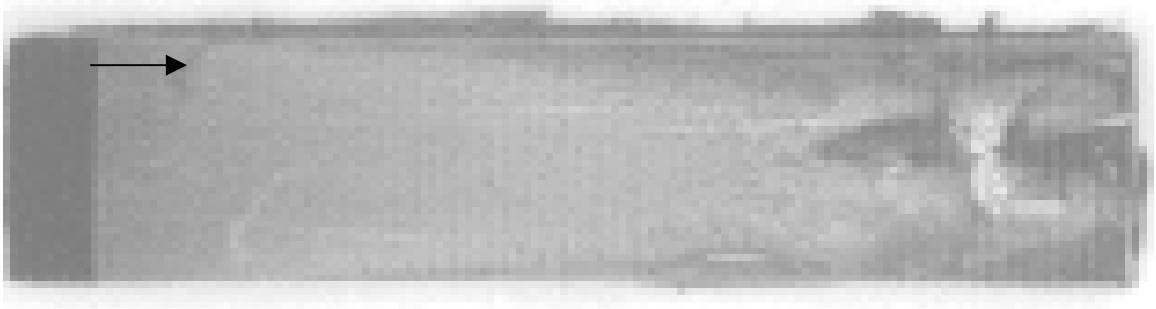

(b) 10 Hz

Figure 5.72 Macrofractographs of HDPE at different frequencies for 0^{o} C temperature.

compared to those tested at low temperatures. The reason for rough surfaces at 50 and 70^{o} C is the presence of larger plastic zones.

SEM fractographs at 100x magnification were taken of CPVC and HDPE specimens at different frequencies and temperatures, at ΔK = 1.0-1.50 MPa$\sqrt{m}$ to see if the above hypothesis is also valid at the micro level. These fractographs are shown in figures 5.73-5.91. It is evident that the fatigue surface at high temperatures is rougher than that at low temperatures. At low temperatures the dominant fatigue mechanism operative is shear yielding. Kim et al [63] and Irfan and Merah [53] have also given similar hypothesis for their fracture surface analysis on uPVC and CPVC respectively.

Fatigue striations are markings corresponding to the successive positions of the advancing crack front as a result of individual load excursions; hence the spacing between each line represents the incremental crack advance during one load excursion. No striations were found on the fatigued surface of any of the specimens even at 1000x magnification. However evidence for discontinuous crack growth (DCG) bands has been found(figure 5.67, 5.68 and 5.69). The presence of DCG bands reflects that crack increments are associated with a large number of loading cycles, usually of the order of hundreds of cycles. The width of the DCG bands increases with crack growth. No DCG bands were observed in HDPE specimens.

DCG's existence found to be affected by both temperature and frequency. They are present at low frequencies of 0.1 and 1 Hz corresponding to temperatures 0, 23, 50 and 70^{o} C (figure 5.67, 5.68 and 5.69). Similar findings were reported by Hertzberg [7] for PVC, where the only mode of fracture at room temperature was observed to be the formation of DCG bands. The existence of DG bands is explained by Doll [80] in terms

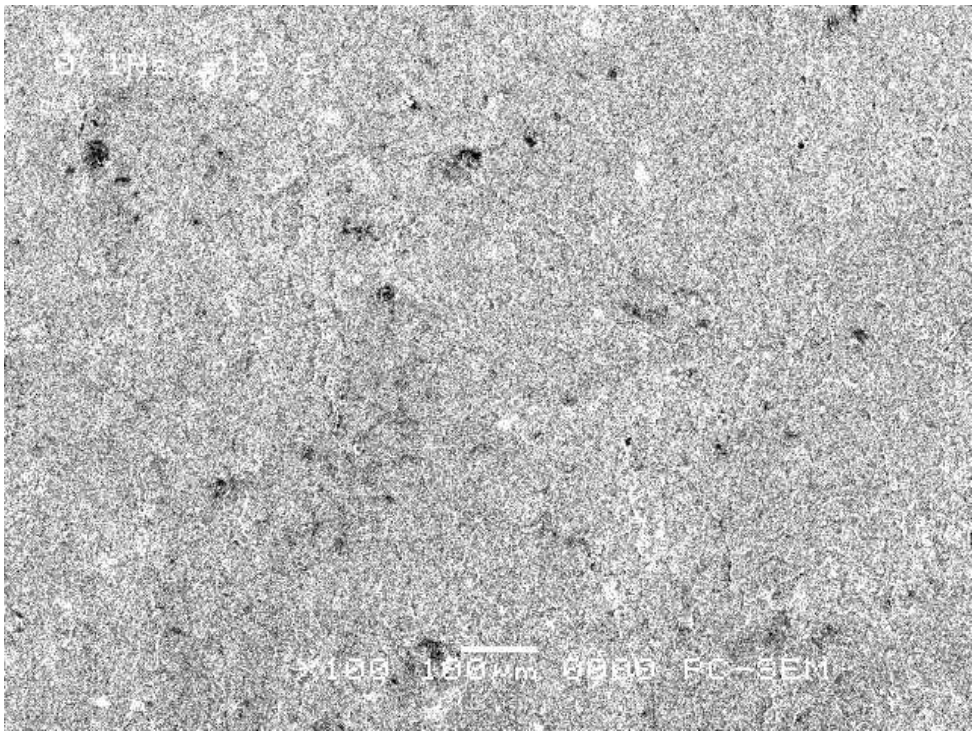

Figure 5.73 SEM fractograph of CPVC at -10° C and 0.1 Hz, ΔK = 1.0 MPa√m
(Magnification = 100x)

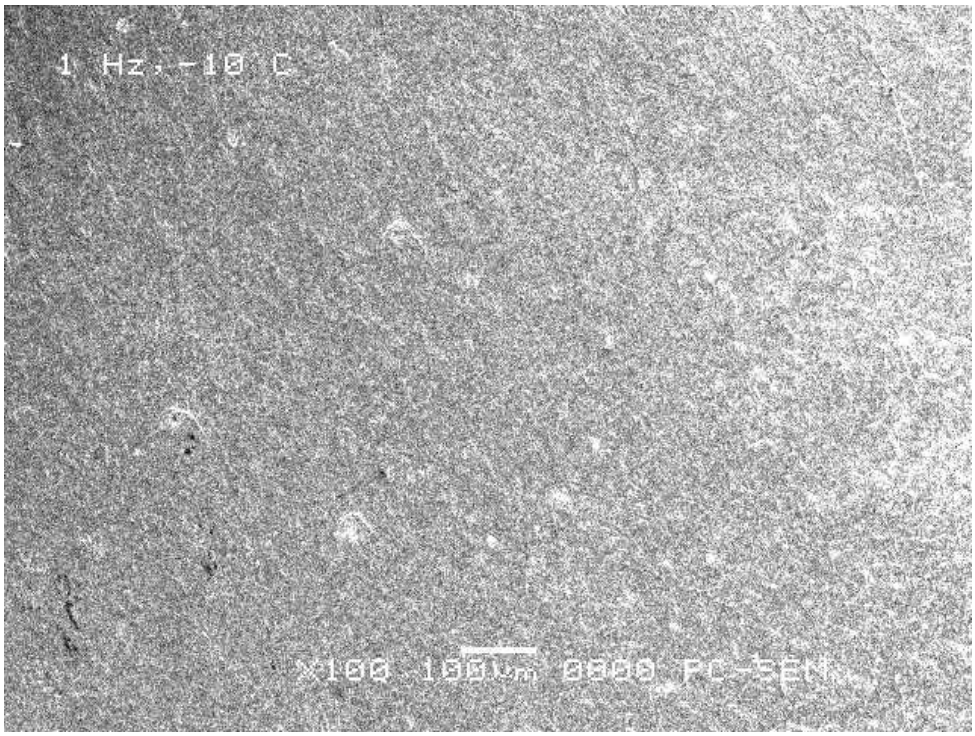

Figure 5.74 SEM fractograph of CPVC at -10° C and 1 Hz, ΔK = 1.0 MPa√m
(Magnification = 100x)

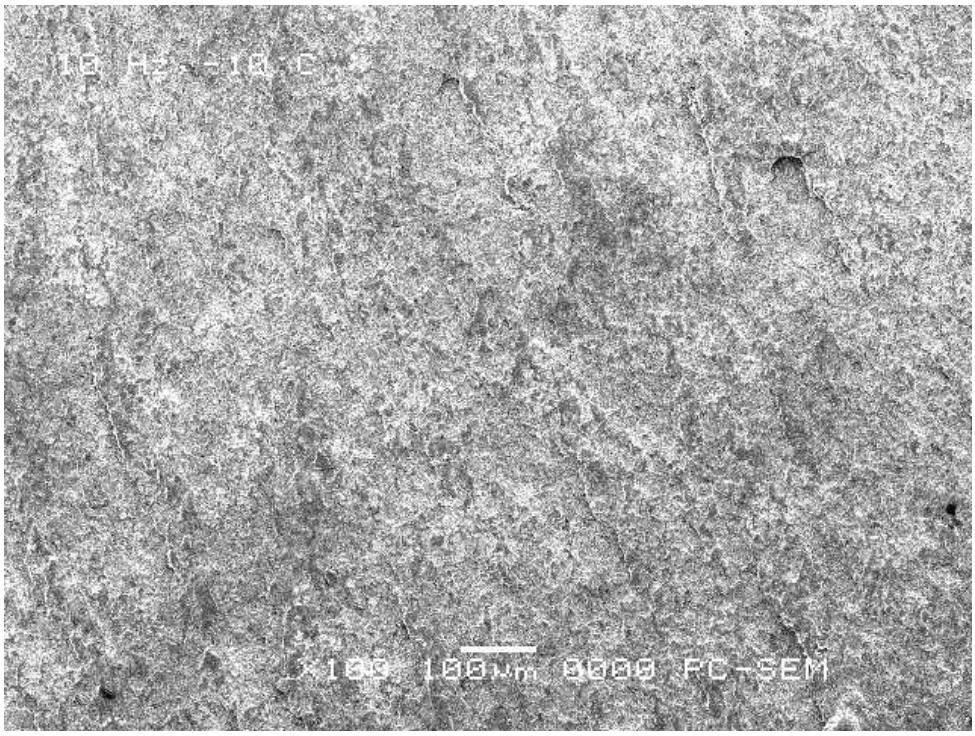

Figure 5.75 SEM fractograph of CPVC at -10° Cand 10 Hz, ΔK = 1.0 MPa√m (Magnification = 100x)

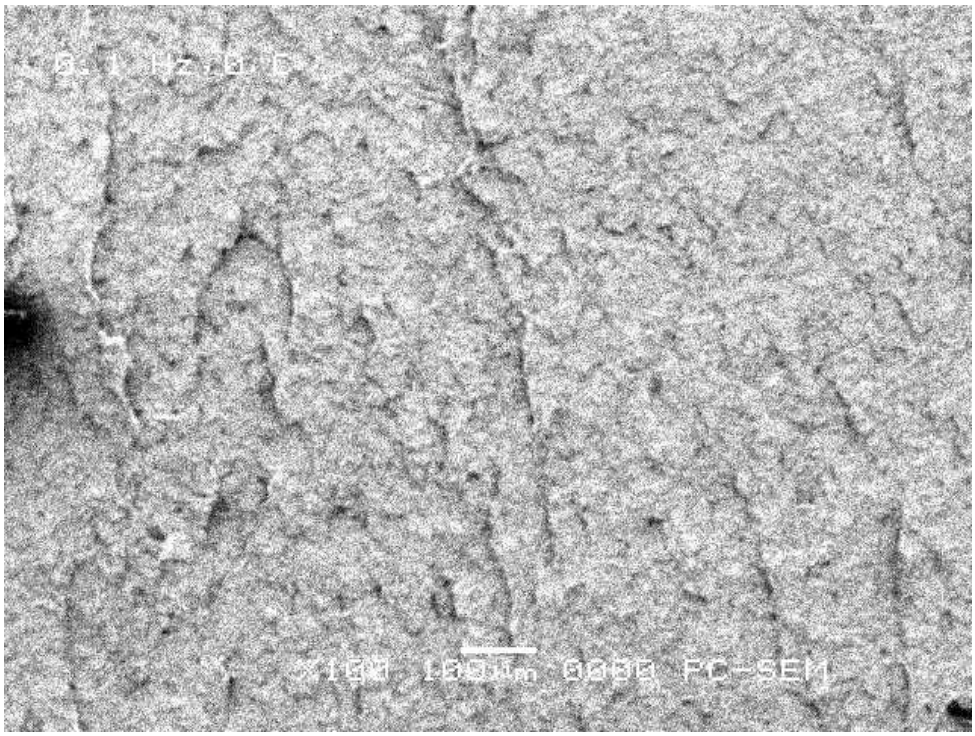

Figure 5.76 SEM fractograph of CPVC at 0° C and 0.1 Hz, ΔK = 1.0 MPa√m (Magnification = 100x)

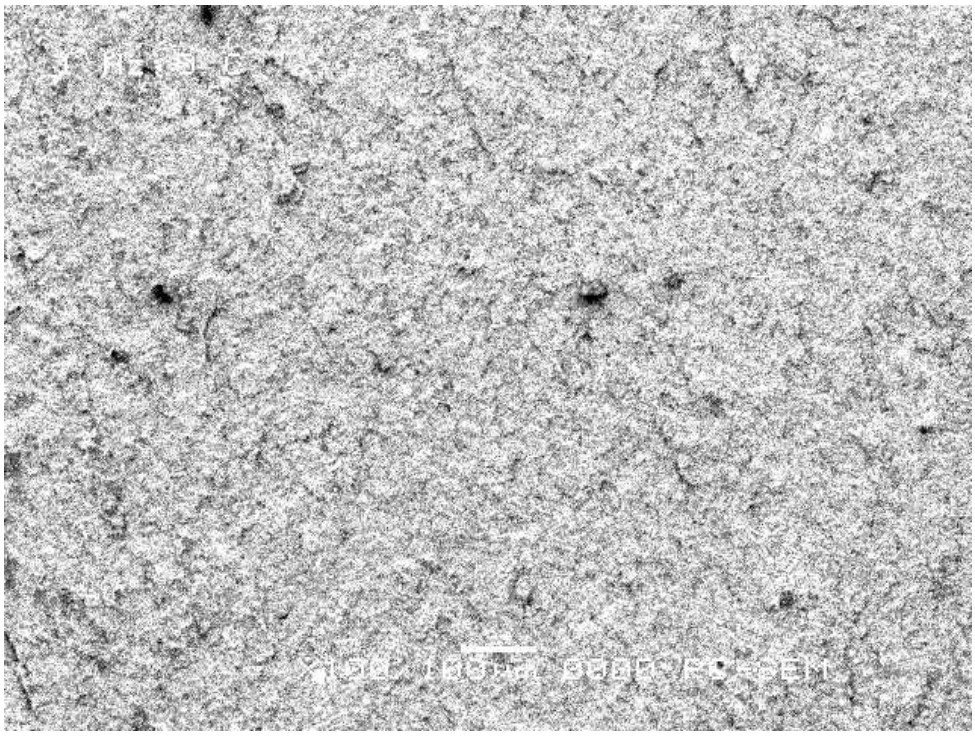

Figure 5.77 SEM fractograph of CPVC at 0° C and 1 Hz, ΔK = 1.0 MPa√m
(Magnification = 100x)

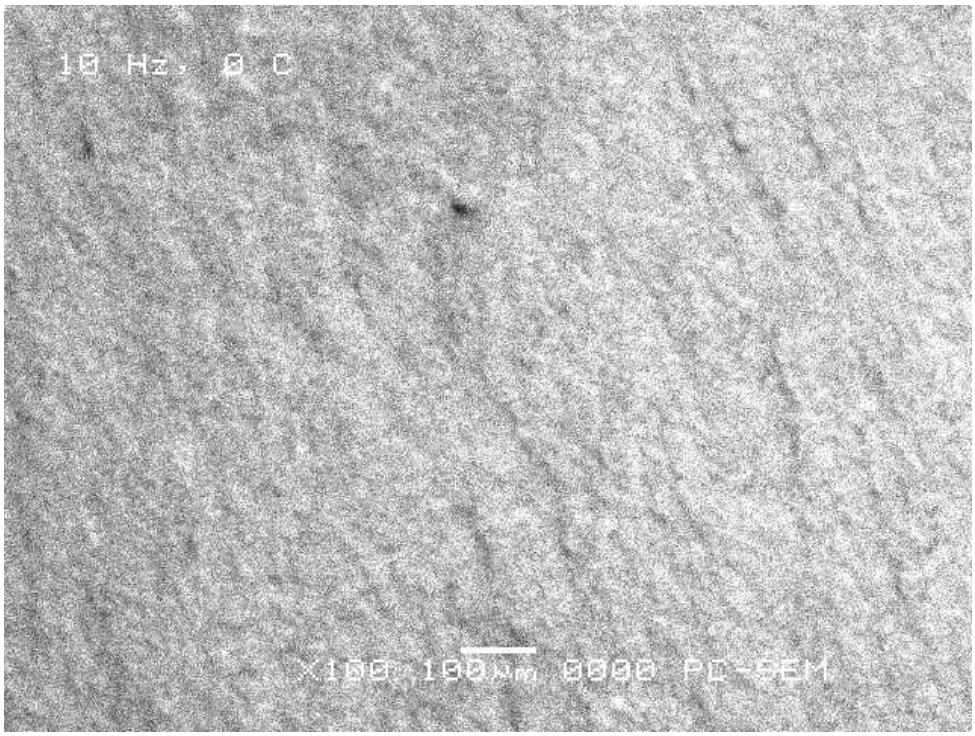

Figure 5.78 SEM fractograph of CPVC at 0° C and 10 Hz, ΔK = 1.0 MPa√m
(Magnification = 100x)

Figure 5.79 SEM fractograph of CPVC at 23° C and 0.1 Hz, ΔK = 1.0 MPa√m
(Magnification = 100x)

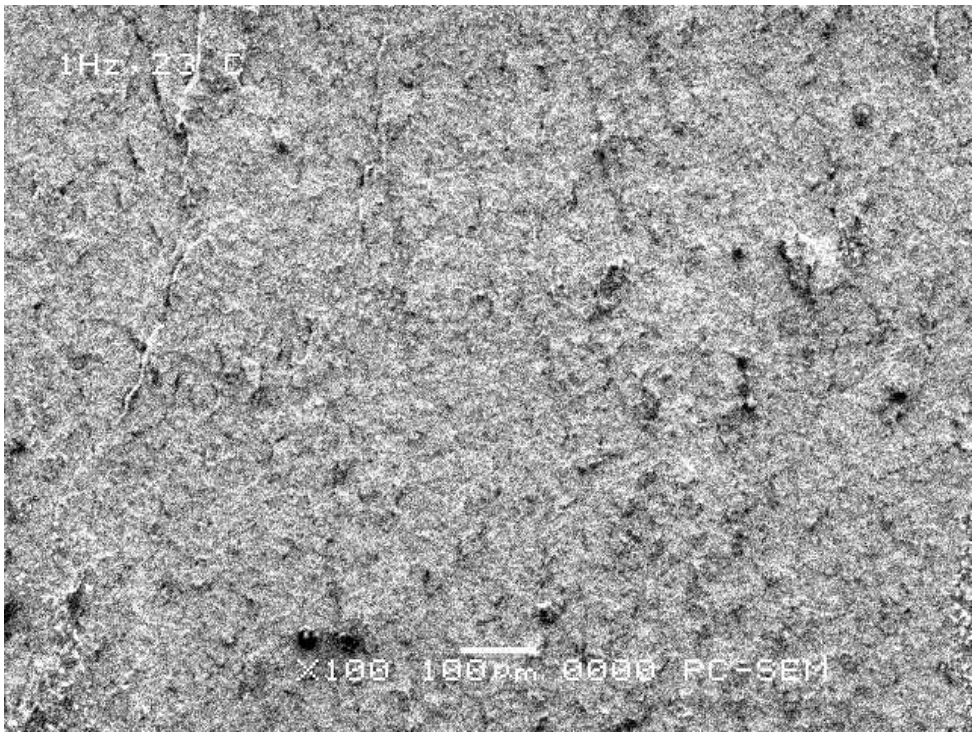

Figure 5.80 SEM fractograph of CPVC at 23° C and 1 Hz, ΔK = 1.0 MPa√m
(Magnification = 100x)

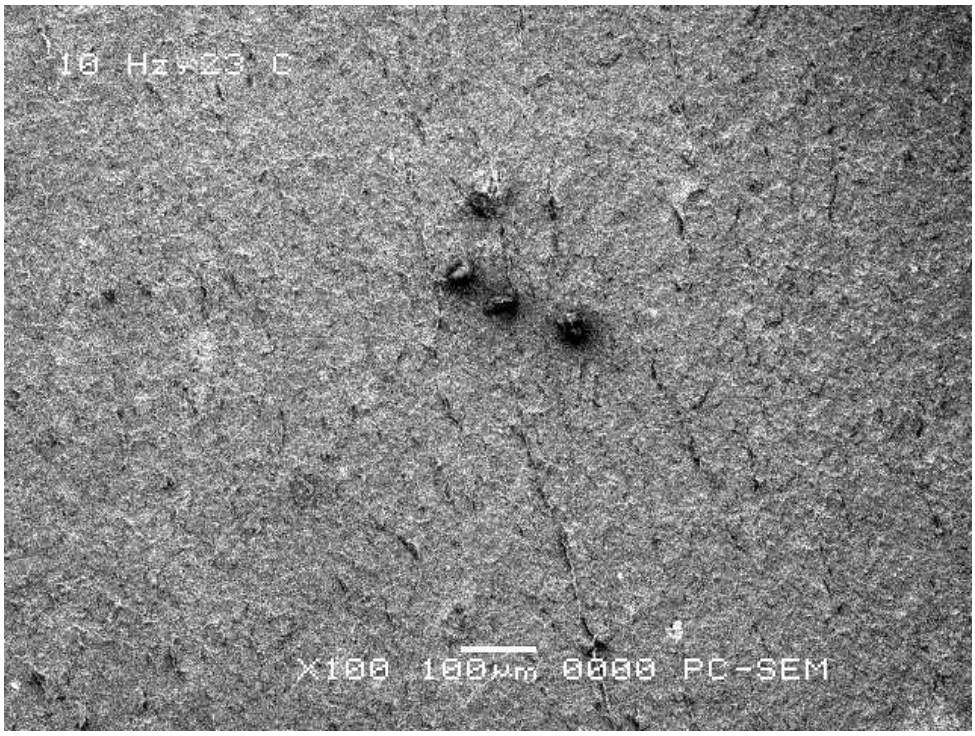

Figure 5.81 SEM fractograph of CPVC at 23° C and 10 Hz, ΔK = 1.0 MPa√m
(Magnification = 100x)

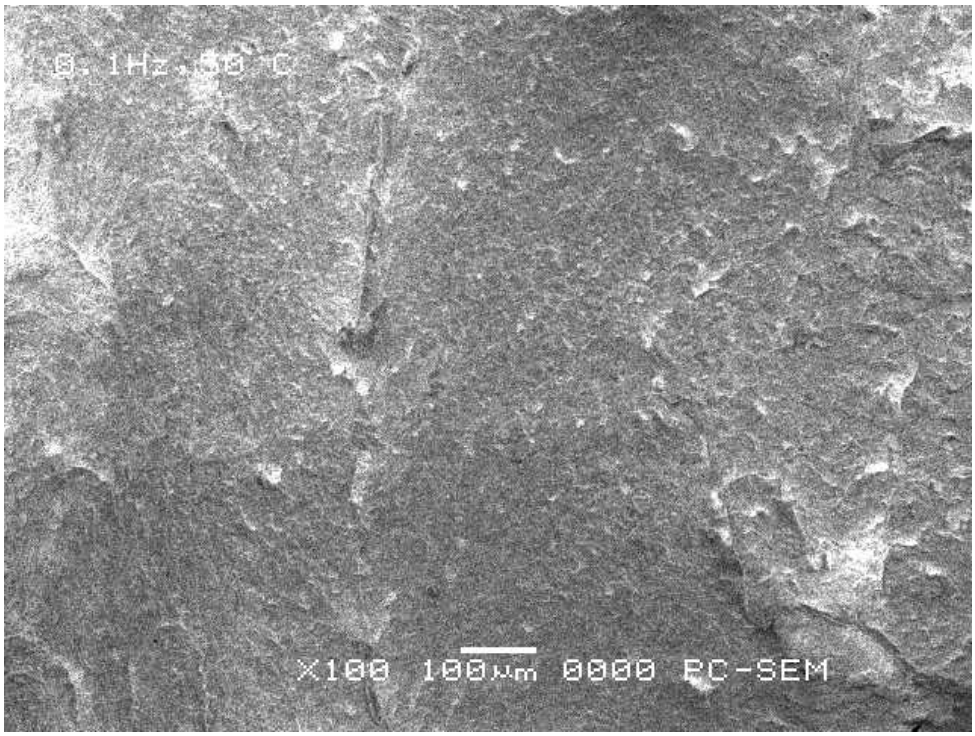

Figure 5.82 SEM fractograph of CPVC at 50° C and 0.1 Hz, ΔK = 1.0 MPa√m
(Magnification = 100x)

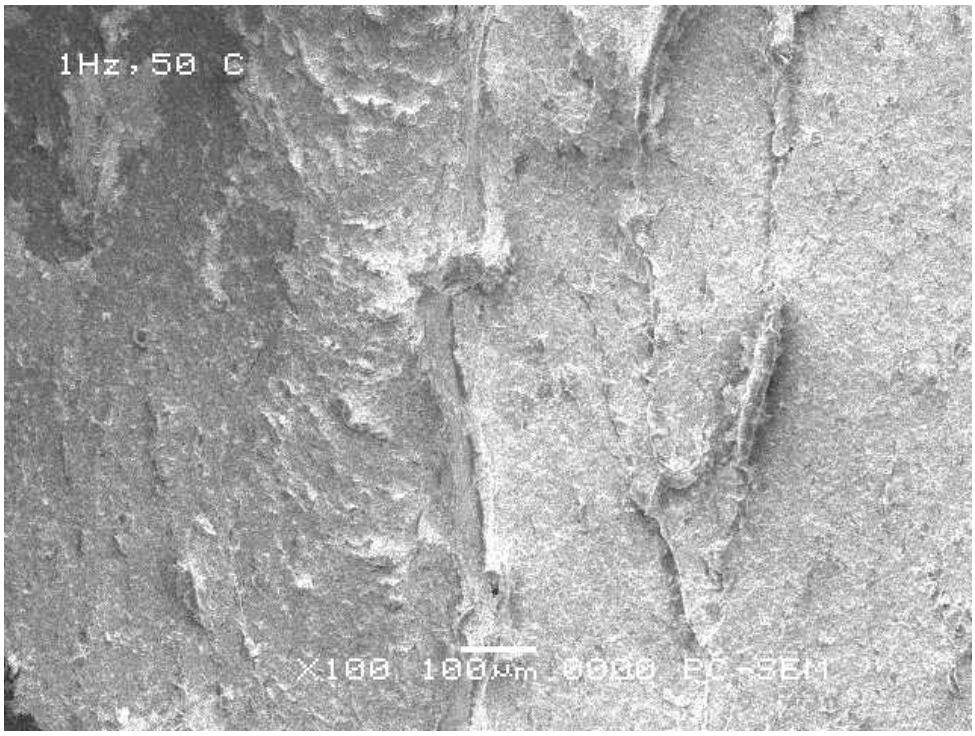

Figure 5.83 SEM fractograph of CPVC at 50° C and 1 Hz, ΔK = 1.0 MPa√m
(Magnification = 100x)

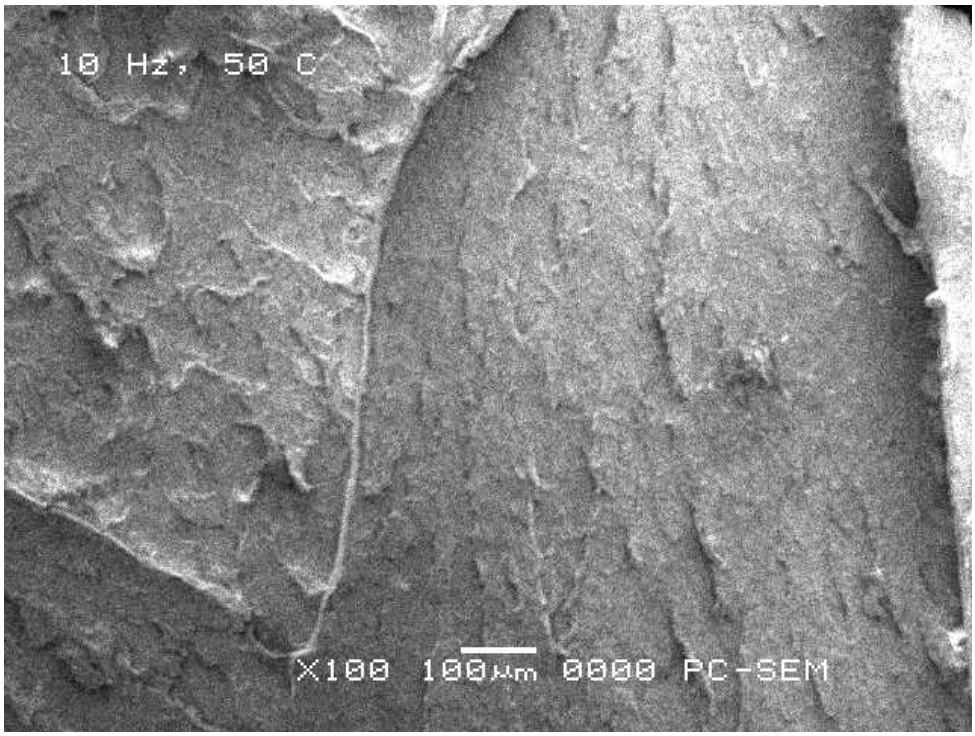

Figure 5.84 SEM fractograph of CPVC at 50° C and 10 Hz, ΔK = 1.0 MPa√m
(Magnification = 100x)

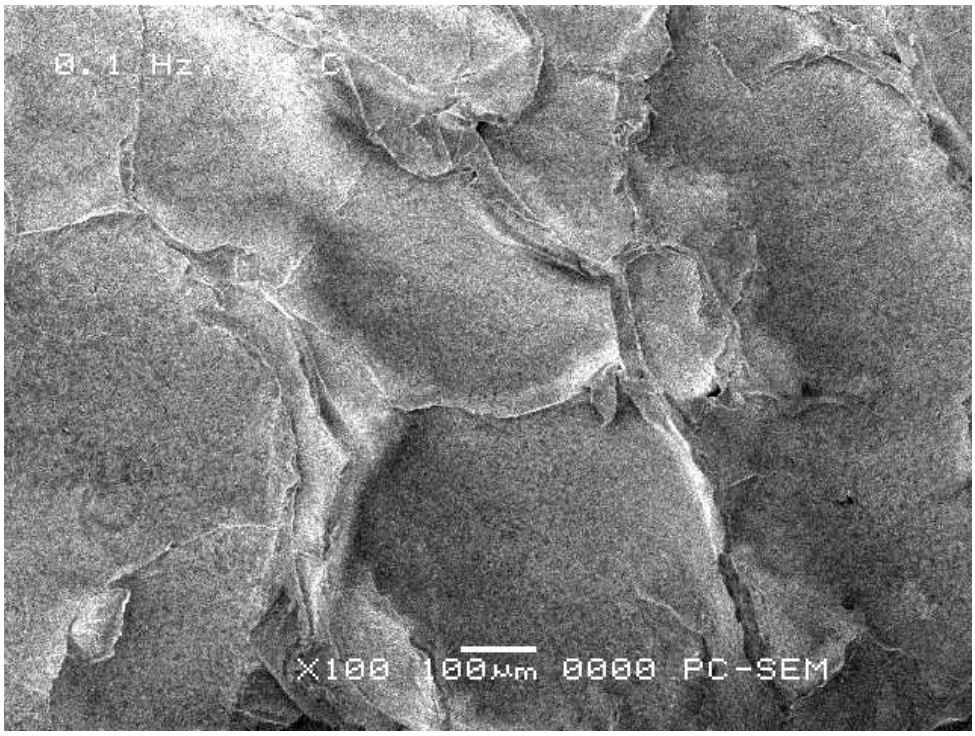

Figure 5.85 SEM fractograph of CPVC at 70° C and 0.1 Hz, ΔK = 1.0 MPa$\sqrt{m}$ (Magnification = 100x)

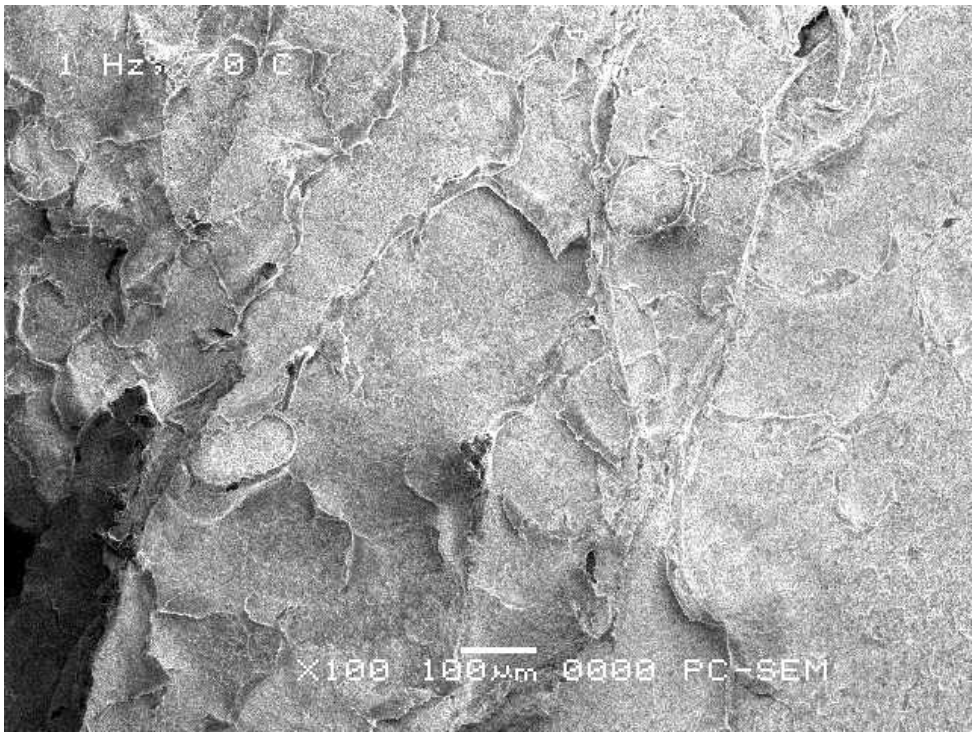

Figure 5.86 SEM fractograph of CPVC at 70° C and 1 Hz, ΔK = 1.0 MPa$\sqrt{m}$ (Magnification = 100x)

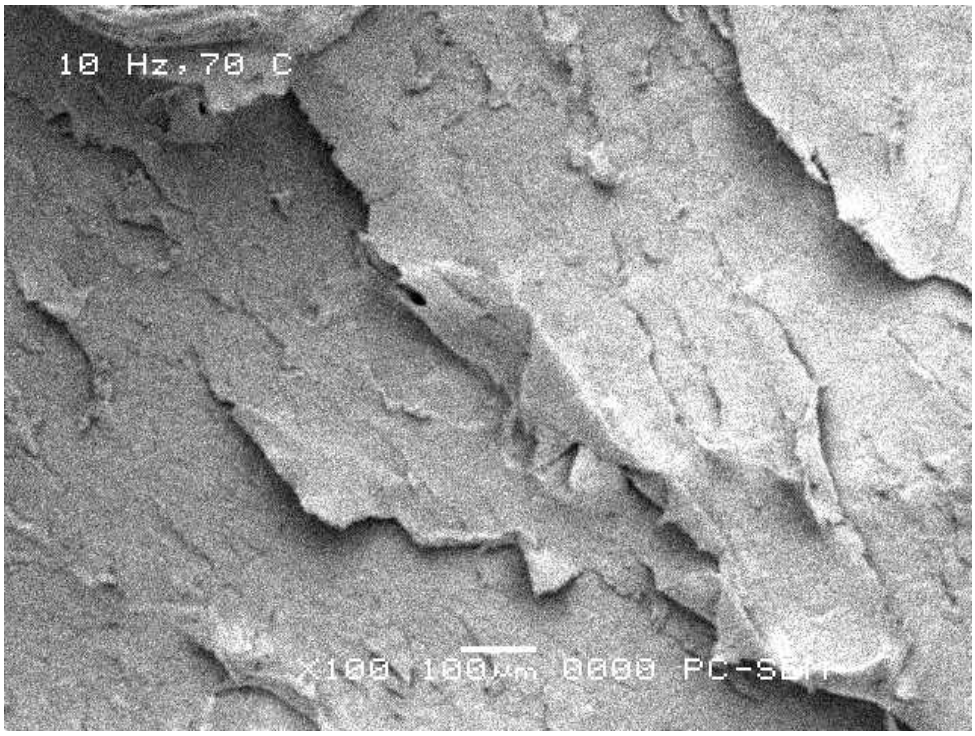

Figure 5.87 SEM fractograph of CPVC at 70° C and 10 Hz, ΔK = 1.0 MPa√m
(Magnification = 100x)

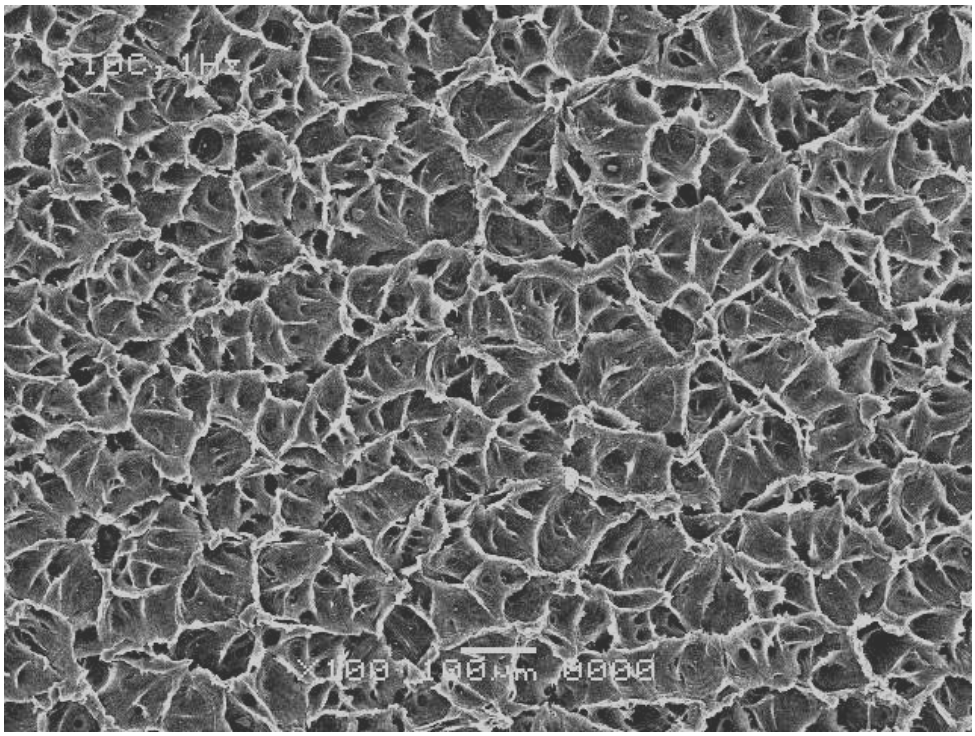

Figure 5.88 SEM fractograph of HDPE at –10° C and 1 Hz, ΔK = 1.0 MPa√m
(Magnification = 100x)

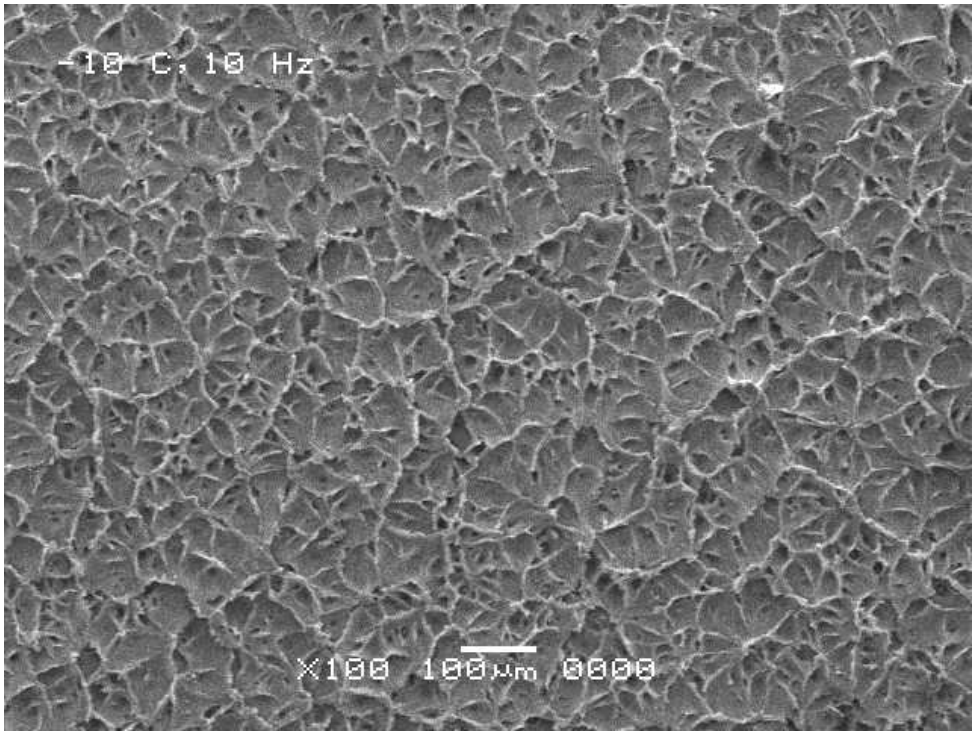

Figure 5.89 SEM fractograph of HDPE at -10° C and 10 Hz, ΔK = 1.0 MPa√m
(Magnification = 100x)

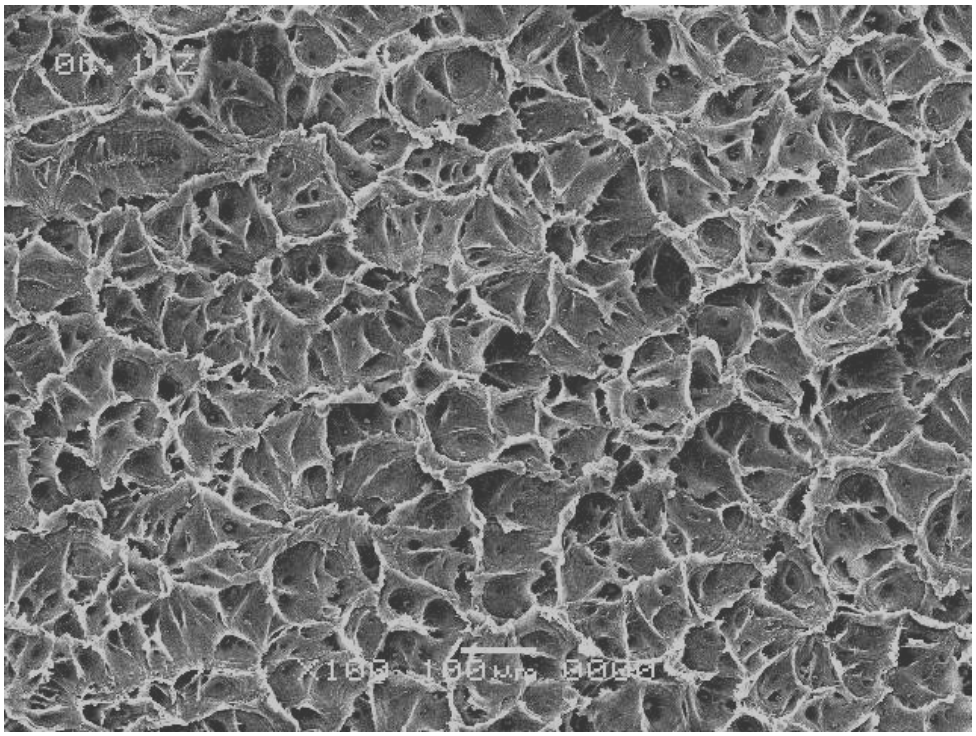

Figure 5.90 SEM fractograph of HDPE at 0° C and 1 Hz, ΔK = 1.0 MPa√m
(Magnification = 100x)

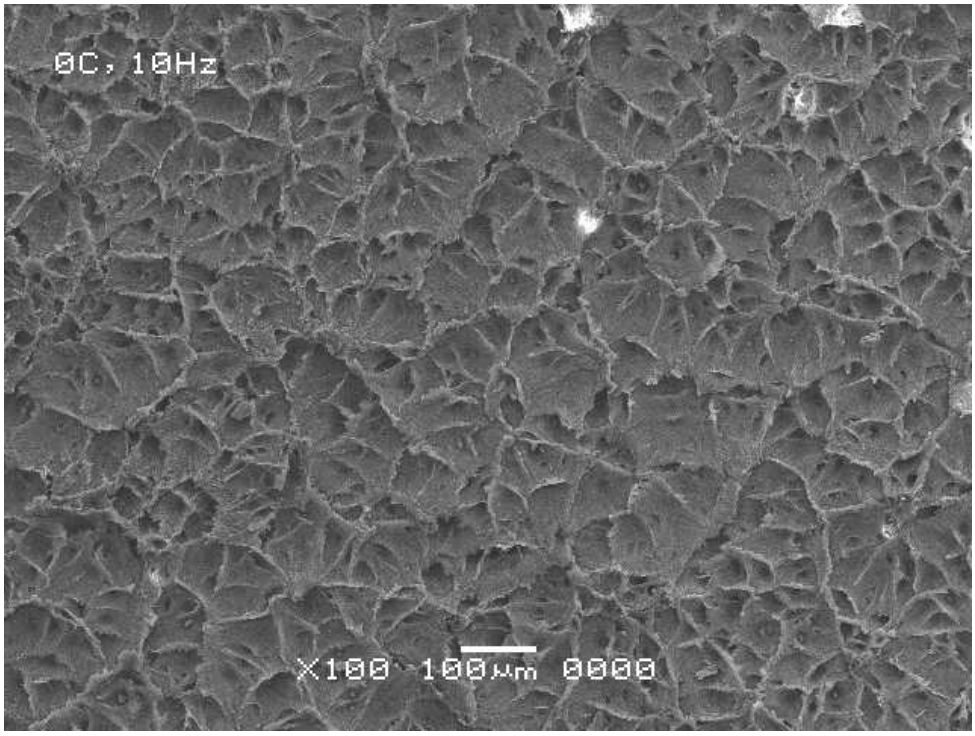

Figure 5.91 SEM fractograph of HDPE at 0^{o} C and 10 Hz, ΔK = 1.0 MPa$\sqrt{m}$ (Magnification = 100x)

of the fibrils of craze that he called “the process of fibril coalescence”. This fundamental process gives rise to the DG growth, and growth of “superfibrils” (due to coalescence) would only occur if the time involved in crack growth was sufficiently high. The present findings of DG bands at lower frequencies is in agreement with this conclusion. Also, the finding of DG bands at high temperatures is also due to the “process of fibril coalescence” as it will be easier if the temperature is sufficiently high. No DCG bands were observed in HDPE specimens.

When the craze fractures, the crack jumps a distance equal to the craze length. Therefore the step length corresponds to the craze length, and the Dugdale model [21] can be the basis for analyzing the fracture surface. From the fracture surfaces in figures 5.67, 5.68 and figure 5.69, it was observed that the step length increased with increasing crack length (i.e. increasing stress intensity factor). According to Dugdale model [21] the increase in the step length was linear with respect to the square of the stress intensity factor (equation 2.14). From the results of monotonic tests we know that yield stress decreases with increase in temperature. From Dugdale model [21] and figures 5.67-5.69, it can be seen that decreasing yield stress with increasing temperature should result in a longer craze and corresponding larger step length.

The discontinuous crack growth process in CPVC at 70^{o} C is shown schematically in figure 5.92 [53]. The band life N^{*} is the number of cycles for craze formation and growth. The craze zone grows continuously with load cycling, though characterized by a decreasing rate with increasing craze length. When some critical condition is satisfied, the crack suddenly strikes through the entire craze before arresting at the craze tip. The craze grows to about 80% of its final equilibrium length within the first 15-20% (equal to

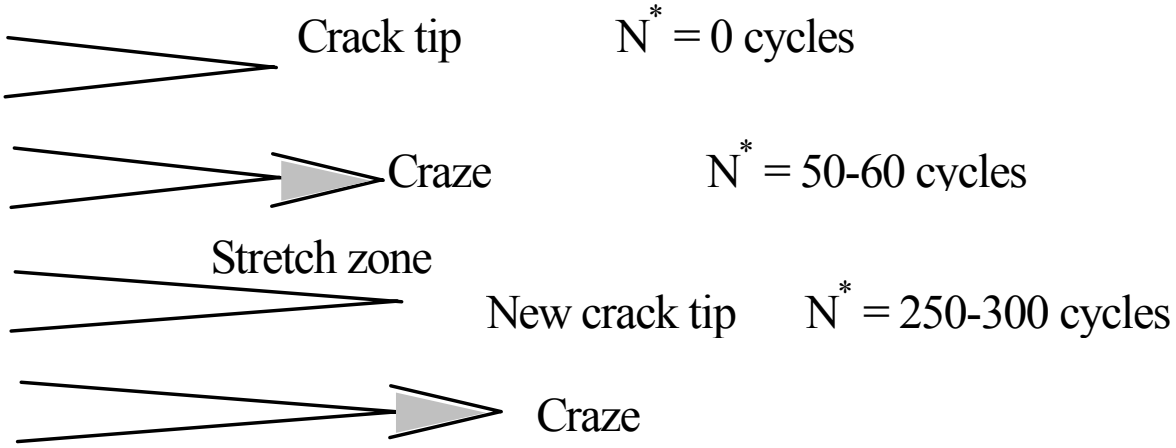

Figure 5.92 Continuous craze growth and discontinuous crack growth model for CPVC at 70° C [53].

about 50-60 cycles) of the band's cyclic life. The equilibrium length is the length where craze does not grow any further but thickens. Gradual thickening of the craze occurs under cyclic loading conditions as the most highly stressed fibrils disentangle and fracture. Little growth then occurs for a substantial portion of the total craze life. Finally, the remaining 15-20% of craze growth occurs during the last 10% of the band's cyclic life.

CHAPTER 6

CONCLUSIONS AND RECOMMENDATIONS

6.1 Conclusions

In this work the effect of frequency on fatigue crack growth properties of CPVC and HDPE was studied at different temperatures. Fatigue crack growth tests were carried out at–10, 0, 23, 50 and 70^{o} C and frequencies equal to 0.1,1 and 10 Hz on CPVC plate specimens prepared from injection molded couplings. Single edge specimens were prepared from HDPE pipes and FCG tests were performed at –10 and 0^{o} C at 0.1, 1 and 10 Hz. Monotonic tests are also performed on HDPE at temperatures –10, 0, 23 and 50^{o} C.

The following conclusions are obtained from the monotonic tests of HDPE.

- The yield stress and elastic modulus decrease linearly with increase in temperature.
- Yield strain for HDPE remains fairly constant for the temperature range studied.
- The Considerable necking is realized at all temperatures for HDPE.
- Load elongation curves for HDPE show yield behavior at all temperatures.

The fatigue crack growth in CPVC and HDPE is analyzed by considering the range of stress intensity factor obtained from linear elastic fracture mechanics concepts. Single edge notch tensile specimens were used. The following conclusions are drawn.

- The crack propagation fatigue lives of both CPVC and HDPE specimens decreased drastically with increase in temperature.
- The fatigue crack growth rate for both CPVC and HDPE increased with increase in temperature; crack propagation resistance reduced with temperature increase. The reduction in fatigue crack resistance is due to the loss of strength in the material. At high temperatures the disentanglement of the molecular chains becomes easier due to the temperature induced molecular vibrations. Whereas at low temperatures the chains are tightly packed and strongly held so it takes a larger number of cycles to disentangle them.
- The fatigue crack growth rate for CPVC and HDPE increased with decrease in frequency; crack propagation resistance reduced with frequency decrease. The effect of frequency on FCP is linked with the size of the plastic zone size near the crack tip, and it's variation with frequency result in the decrease or increase of FCP. Fatigue crack propagation in CPVC at high frequencies is also characterized by the localized heating at the crack tip, which causes temperature rise at the tip.
- The exponent m in the paris power law is found to be constant with temperature, while A increases linearly with increase in temperature, for both CPVC as well as HDPE.
- The exponent m in the paris power law is found to be constant with frequency, while A increases linearly with decrease in frequency, for both CPVC as well as HDPE.
- The effect of temperature on da/dN for CPVC and HDPE at different frequencies is investigated by considering the variation of mechanical properties with

temperature. As higher temperatures will result in lower yield stress which causes a higher crack tip opening displacements (CTOD) and hence in lower effective ΔK. A master curve was developed by using yield stress. All the da/dN-ΔK curves at different temperatures were collapsed on a single curve for a given frequency.

- For CPVC two different fatigue mechanisms were found to be operative in different temperature ranges. At high temperature (23 to 70^{o} C) crazing was found to be the dominant fatigue mechanism while at low temperature (-10 to 0^{o} C) shear yielding was the dominant fatigue mechanism. The transition from one mechanism to the other occurred around 44^{o} C. The results were supported by fractographic analysis.

6.2 Recommendations

Following are some of the recommendations for any future work to be carried out on CPVC and HDPE:

- At low frequencies it is possible that creep contributes to crack propagation. So creep effect should be considered. Other parameters such as J_c (Creep J integral) should be considered .
- Crack tip opening displacement may also be considered.
- Instead of optical technique used for measuring crack some other technique which is accurate and less time consuming should be adopted like compliance or cathetometer or conductive surface grid printed on specimen surface method.
- Due to increase in the frequency there is an increase in the temperature at the crack tip. This crack tip temperature characteristics may be investigated.

- Fracture toughness is an important material property. The effect of temperature on the fracture toughness can be investigated to explain some of the mechanisms observed here.
- Effect of stress ratio and mean stress on fatigue crack growth can be investigated.
- At high temperatures the plastic zones size are considerably large so the LEFM does not remain valid, so elastic plastic fracture mechanics concepts can be used to study crack growth.

REFRENCES:

1. www.csua.berkeley.edu
2. “Modern Plastics Encyclopedia”, 1994, pp57-58.
3. Odian George, “Principles of Polymerization”, Second edition, A wiley Interscience Publication, John Wiley and sons, 1981.
4. Brann Scott and Knight Michelle, “Consider CPVC for Process Applications”, Chemical Engineering Process, Dec 1994, pp36-41.
5. www.epolybags.com
6. www.maropolymeronline.com
7. Hertzberg W.Richard, “Deformation And Fracture Mechanics of Engineering Materials”, John Wiley and sons, 1989.
8. Irfan-ul-Haq, “Crack Propagation in CPVC at Different Temperatures”, M.S. Thesis, KFUPM, December 2000.
9. G.M.Swallowe, “Mechanical Properties and Testing of Polymers an A-Z Reference”, Polymer Science and Technology, 1999.
10. Tordejman P., Tese L., Halary J.L. and Monnerie L., “On the plastic and viscoelastic Behavior of Methylmethacrylate-Based Random Copolymers”, Polymer Engineering and Science, Vol 32, No.17, Mid-Sepetember 1992,pp1204-1208.
11. Bronnikov S.V., Vettegren V.I. and Frenkel S. Ya, “Description of Thermal and Mechanical Properties of Drawn Polymers over a wide temperature Range”, Polymer Engineering and science, Vol3,No. 17, Mid-September 1992,pp1204-1208.
12. Povolo F., Schwartz G. and Hermida E.B, “Stress Relaxation of PVC below the yield point”, Journal of Polymers Science, Vol.64, May 1997,pp1079-1090.
13. Che M., Grellman W., and Seidler Sabine, “Crack Resistance Behavior of Polyvinylchloride”, Journal of polymer Science, Vol 64, No.6, May1997, pp1079-1090.

14. Pal S.N., Ramani A.V. and Subramanium N., “Studies of PVC based Polymer Blends intended for Medical Applications”, Polymer Engineering and Science, Vol32, No.13, July 1992,pp845-853.
15. Han Yuncham, Lach Ralf, Wolfgang Grellman, “Effects of Rubber Content and Temperature on Dynamic Fracture Toughness of ABS Materials”, Journal of Applied Polymers Science, Vol.75, 2000,pp1605-1614.
16. Hitt D.J. and Gilbert M., “Tensile properties of PVC at elevated temperatures”, Materials Science and Technology, Vol 8,Aug 1992,pp 739-744.
17. Lin ye, Chao-Ting Yuan and Yia-Wing Mai, “Effects of Rate and Temperature on Fracture Behavior of TPX Polymer”, Polymer Composites, Vol 19, No.6, Dec 1998,pp830-836.
18. Seitz T., “The Estimation of Mechanical Properties of Polymers from Molecular Structure”, Journal of Applied Polymer Science, Vol49, 1993, pp1331-1351.
19. Merah, N. and Irfan, Haq, “Temperature and Weld Effects on Monotonic Properties of CPVC”, Proceedings of ESDA, Istanbul, Turkey, July 8-11, 2002.
20. Paris, P.C., “The Growth of Fatigue Cracks due to Variations in load”, PhD. Thesis, Lehigh University, 1962.
21. Dugdale D.S., “Yielding in Steel Sheets Containing Slits”, Journal of the Mechanics and Physics of Solids, Vol. 8, pp 100-104.
22. Elber W., “Fatigue Crack Closure Under Cyclic Tension”, Engineering Fracture Mechanics, Vol.2, 1970,pp37-45.
23. Broek David, “Elementary Engineering Fracture Mechanics”, Fourth revised edition, Martinus Nijhoff Publishers, 1986.
24. Broek David, “Fatigue crack growth: effect of sheet thickness”, Aircraft Engineering, Vol.38, No. 11, 1966, pp 31-33.
25. Manson, J.A., “Advances in Fracture Research”, Peragamon Press, Oxford, 1980.
26. Koo, G.P., “Flouropolymers”, High polymers, Vol.25, 1972,pp 507.
27. Meinel, G. and Peterlin, A., Journal of Polymer Science, Polymer letters, Ed.9, 67, 1971.
28. Ramirez A., Ph.D. dissertation, Leigh Univeristy, Bethlehem, PA,1982.

29. Rimnac, C.M., Manson, A., Hertzberg, R.W., Webler, S.M. and Skibo, M.D., Journal of Macromolecular Science, Physics, B19 (3), 351, 1981.
30. Mitchel, J.C., Manson, A. and Hertzberg, R.W., Org. Coatings Plast. Chem.45, 622, 1981.
31. Hertzberg R.W., Manson J.A. and Skibo M.D., Polymer Engineering and Science, Vol.15, 1975,pp252.
32. Hertzberg R.W., Manson J.A. and Skibo M.D., Fracture, Vol.3, 1977,pp1127.
33. Hertzberg R.W., Manson J.A. and Skibo M.D., Polymer, Vol.19, 1978,pp359.
34. Hertzberg R.W., Manson J.A., Donald J.K. and Skibo M.D., Journal of material Science, Vol.14, 1979,pp1754.
35. Hertzberg R.W., Manson J.A. and Phillips J.D., Journal of Material Science, 1988.
36. Hertzberg R.W., Manson J.A. and Skibo M.D., ASTM STP700, 1980,pp 49.
37. Hertzberg R.W., Manson J.A., Hahn M.T., Lang R.W., Michel J.C., Ramirez A., Rimnac C.M. and Webler S.M., "Deformation, Yield and Fracture of Polymers " , Plastics and Rubber Institute, Cambridge, England, 1982,pp19.1.
38. Lang R.W., Unpublished research.
39. Yeh J.T., Lin Y.T., Huang S.S, "Fatigue-fracture mechanism of slowly notch poly(ethyleneterephthalate) polymers", Polymer Bulletin(Berlin), Vol.33, No.3, Aug 1994, pp361-368.
40. Massa F., Piques R., Laurent A., "Rapid Crack Propagation in Polyethylene pipe: Combined Effect of Strain rate and Temperature on Fracture Toughness", Journal of Materials Science, Vol.32, 1997,6583-6587.
41. Zhuang Z., Donoghue P.E., "Determination of Material Fracture Toughness by a Computational/Experimental approach for Rapid Crack Propagation in PE pipe", International Journal of Fracture, Vol.101, 2000, 251-268.
42. Norman B., Xici L., "The Dependence of Rapid Crack Propagation in Polyethylene Pipes on the Plane Stress Fracture Energy of the Resin", Polymer Engineering and Science, Vol.41, No.7, July2001, pp1140-1145.

43. Martin G.C. and Gerberich W.W., “Temperature Effects on Fatigue Crack Growth in Polycarbonate”, Journal of Materials Science, Vol 15, No.7, July 1975, pp500-506.
44. Mai Y.M. and Williams J.G., “Temperature and Environmental effects on the Fatigue Fracture in Polystyrene”, Journal of Materials Science, Vol14, 1979,pp1933-1940.
45. Wann R.J., Martin G.C. and Gerberich W.W., “The Mechanical behavior of Polyarylsulfone”, Polymer Engineering and Science, Vol16, No.9, Sep 1976,pp645-651.
46. Kasakevich, M.; Moet, A.; Chudnovsky, A., “Comparative Crack Layer Analysis of Fatigue and Creep Crack Propagation in HDPE”, Polymer, Vol.31, No.3, March 1990, pp435-439.
47. Kasakevich, M.; Moet, A.; Chudnovsky, A., “Crack Layer Approach to Fatigue Crack Propagation in HDPE”, Journal of Applied Polymer Science, Vol.39, No.2, January 1990, pp395-413.
48. Sehanobish, K.; Chudnovsky, A., Moet, A., “Quasibrittle Crack Propagation in Polyethylene Pipe Material”, Proceedings-Ninth Plastic Fuel Gas Pipe symposium, American Gas Assoc., November 1985,pp291-298.
49. Sehanobish, K.; Chudnovsky, A., Moet, A., “Crack Layer Analysis of Nonmonotonic Fatigue Crack Propagation in HDPE”, Polymer, Vol.28, No.8, July 1987,pp1315-1320.
50. Bucknall, C.B.; Dumpleton, P., “Effects of Loading History On Fatigue Crack Growth in HDPE and PMMA”, Polymer Engineering and Science, Vol.27, No.2, Januray1987.
51. Chudnovsky, A.; Sehanobish, K.; WU, S., “Methodology for Durability Analysis of HDPE pipe”, Journal of Pressure Vessel Technology, Vol.122, No.2, May 2000, pp152-155.
52. Parsons, M.; Stepnov, E.V.; Hiltner, A.; Baer, E., “Effect of Strain Rate on Stepwise Fatigue and Creep Slow Crack Growth in HDPE”, Journal of Materials Science, Vol.35, No.8, 2000, pp1857-1866.

53. Irfan, Haq and Merah, N., " Effect of Temperature on Fatigue Crack Growth in CPVC", Journal of Pressure Vessel Technology, Vol.125, No.1, pp 71-77.
54. Ramsteiner F., Armbrust T., "Fatigue Crack Growth in Polymers", Polymer Testing, Vol.20, 2001,321-327.
55. Allard R.C., Vu-Khanh T. and Chalifoux J.P., "Fatigue Crack propagation in mica-filled Polyfins", Polymer Composites, Vol. 10, No.1, Feb 1989,pp62-68.
56. Hwang J.F., Manson J.A., Hertzberg R.W., Miller G.A., Sperling L.H., "Fatigue Crack Propagation of Rubber-toughened epoxies", Polymer Engineering Science, Vol 29, No.20,Oct 1989, pp1477-1487.
57. Hakeem H. and Culver L., "Environmental Dynamic Fatigue Crack Propagation in HDPE", International Journal of Fatigue, Vol 1, No.1, January1981, pp3-8.
58. Parsons M., Stepnov E., Hiltner A. and Baer E. "Effect of strain rate on stepwise fatigue and creep slow crack growth rate in HDPE", Journal of Materials Science, No.35, 2000, pp1857-1866.
59. Bureau M. and Dickson J. "Comparison of the fatigue propagation behavior of polystyrene and 95/5 PS/HDPE blends", Journal of Materials Science, No.33, 1998, pp1591-1606.
60. Cheng W.M., Manson J.A., Hertzberg R.W., Miller G. A. and Sperling L.H., "The Effects of Temperature and Frequency on the Fatigue Propagation Rate of Poly methymethacrylate", Journal of Material Science, No.25, 1990.
61. Mitchel, J.C., Ph.D Dissertation, Lehigh University, 1984.
62. Kim HS, Wang XM, "Temperature and Frequency Effects on Fatigue Crack Growth of ABS", Journal Of Applied Polymer Science, Vol. 57,1995, pp811-817.
63. Kim HS, Wang XM, "Temperature and Frequency Effects on Fatigue Crack Growth of uPVC", Journal of Materials Science, Vol 29, No.12,1994,pp3209-3214.
64. Radon J. and Culver L., "Fatigue Crack Growth in Polymers I.Effect of Frequency and Temperature", Journal of Polymer Engineering and Science, Vol 15, No.7, July1975, pp500-506.

65. Maddox S.J. and Manteghi S. “The Fatigue Design of uPVC Water Pipe With Consideration of Environmental Effects”, Plastics, Rubber and Composites Processing and Applications”, Vol 17, 1992, pp 5-18.
66. “Standard Test Method for Tensile Properties of Plastics”, ASTM Designation D638 - 94b.
67. “Standard Test Method for Tensile Properties of Plastics”, ASTM Designation D638 - 94b.
68. Ward I.M., “Mechanical Properties of Solid Polymers”, 2nd Edition, Wiley-Interscience Publication, 1983.
69. Argon A.S. and Bessonov M.I., “Plastic Flow in Glassy Polymers’, Polymer Engineering and Science, Vol 17, No. 3, March 1997, pp –174-182.
70. Kitagawa M., “Power Law Relationship Between Yield Stress and Shear Modulus for Glassy Polymers”, Journal of Polymer Science: Polymer Physics Edition”, Vol 15, 1977, pp 1601-1611.
71. Han Y., Yan Y., Binayo Li and Feng Z., “Mechanical Properties of Phenolphthalein Polyether Ketone: Yield Stress, Young’s Modulus and Fracture Toughness”, Journal of Applied Polymer Science, Vol 56, 1995, pp 979-984.
72. www.goodfellow.com
73. Hertzberg R.W., Skibo M.D., and Manson J.A., “Fatigue Crack propagation in Polyacetal”, Journal of Materials Science, Vol 13, 1978, pp 1038-1044.
74. Pecorini T.J. and Hertzberg R.W. “The Fracture Toughness and Fatigue Crack Propagation Behavior of Annealed PET”, Polymer, Vol 34, No. 24, 1993, pp 5053-5062.
75. Paris P.C. and Erdogan F., “A Critical Analysis of Crack Propagation Laws”, Journal of Basic Engineering, Vol85, 1960,pp528-534.
76. Bucknall, C.B., “Toughened Plastics”, Applied Science Publishers, London,1977.
77. Donald, A.M. and Kramer, E.J., “Effect of Molecular Entanglements on Craze Microstructure in Glassy Polymers”, Journal of Polymer Science: Polymer Physics Edition, Vol. 27, 1982,pp889-909.
78. Kambour, R.P., Journal of Polymer Science: D, Vol. 7, No.1, 1973.

79. Merah N., Bui-Quoc T. and Bernard M., “Notch and Temperature Effects on Crack Propagation in SS 304 Under LCF Conditions”, Journal of Pressure Vessel Technology, Vol. 121, Feb 1999, pp 001-007.
80. Doll, W., “Fractography”, A.C. Roulin-Moloney, Ed., Elsevier, London, New York, 1989, p.387.
81. Anderson T.L., “Fracture Mechanics-Fundamentals and Applications”, Second Edition, CRC Press, 1994.

VITAE

NAME: Shiakh Farrukh Saghir
DATE OF BIRTH: 20, April, 1979
PLACE OF BIRTH: New Delhi, INDIA.
ADDRESS: H. No.69/2, Nafis Lane-35,
Zakir Nagar, P. O. Jamia Nagar,
New Delhi-110025.
INDIA.

E-MAIL: farrukhsaghir@hotmail.com
farrukhsaghir@yahoo.com

EDUCATIONAL QUALIFICATION:

M.S ***(Mechanical Engineering)***
January 2004
King Fahd University of Petroleum and Minerals
Dhahran, Saudi Arabia.

B.TECH ***(Mechanical Engineering)***
April 2000
Jamia Millia University
New Delhi, India.